

KATHARINA GALLAS

**FUNCTIONAL MACROMOLECULES FOR
OPTICAL SENSING AND ORGANIC RADICAL
BATTERIES**

DOCTORAL THESIS

DISSERTATION

zur Erlangung des akademischen Grades einer Doktorin der
technischen Wissenschaften an der Technischen Universität Graz

Betreuung: Assoc. Prof. Dipl.-Ing. Dr. techn. Christian Slugovc
Institut für Chemische Technologie von Materialien

Graz, Dezember 2013

Deutsche Fassung:

Beschluss der Curricula-Kommission für Bachelor-, Master- und Diplomstudien vom 10.11.2008

Genehmigung des Senates am 1.12.2008

EIDESSTATTLICHE ERKLÄRUNG

Ich erkläre an Eides statt, dass ich die vorliegende Arbeit selbstständig verfasst, andere als die angegebenen Quellen/Hilfsmittel nicht benutzt, und die den benutzten Quellen wörtlich und inhaltlich entnommenen Stellen als solche kenntlich gemacht habe.

Graz, am

(Unterschrift)

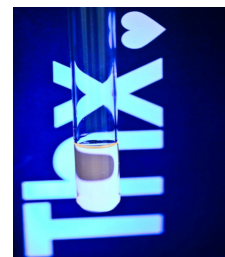
Englische Fassung:

STATUTORY DECLARATION

I declare that I have authored this thesis independently, that I have not used other than the declared sources / resources, and that I have explicitly marked all material which has been quoted either literally or by content from the used sources.

Date

(signature)



Acknowledgement

The last three years of work at the ICTM I met so many people, who helped me, supported and guided me but in particular I wanna thank them for just for being my friends.

At first I would like to express my sincere thanks to Christian Slugovc who gave me the opportunity to accomplish my PhD at this institute and for his support regarding chemical questions, the nice talks we had and for many encouraging mails which made me laugh and generated big smiles 😊.

I also want to thank Franz Stelzer for the support in the ORB project and to Renate Trebizan his good fairy for organization assistance. Furthermore my gratitude goes to Petra Kaschnitz for many NMR measurements, to Josephine Hobisch for the GPC measurements and to Robert Saf for the MS measurements.

Special thanks go out to Astrid Knall. Thank you for, discussing, synthesizing, writing, reading, chatting and just being there when I needed help. I also need to mention David Fast, to whom I owe a real big thank 😊-thank you for being my battery hero 😊

Many thanks go to all my colleagues from the ICTM especially for the coffee and lunch breaks and all the funny times at the university and also amazing times outside the university. Thanks to Verena Schenk for the hours of sudering and drinking hot chocolate when we both were a bit depressed. To our office 05052, many people have come and gone but you are still in my heart. Thanks Flo for the cookies and Gerwin for my always working computer. Thanks to Fradi and Schoko for being my refuge when I needed new inputs. And never to forget thanks to Simone, thank you for just being there, for the cakes and the meals, for the talks and the laughing, for the bad moments which were not that bad with you, for listening to me, for the fun outside the university, for the crazy hours, the cookie eating attacks and just for everything.

Not to forget a special person, thank you Dominik for being my colleague, my friend and my man. Without you I would not have the courage and the ability to survive life. Mit dir ist es endlich, unendlich einfach.

Thanks to my parents and my sister for supporting me with my decisions, with words and deeds and also for their financial support.

But without my horse and my crazy horse riding friends I wouldn't be filled with so much love and happiness because we ride - To fly. To feel. To touch. To breathe. To laugh. To overcome. To relax. To prove them wrong. To belong. To feel strong. To heal. To love. And to be loved back. We ride to LIVE. Every weekend I start living again, thanks for that.

Table of Contents

Acknowledgement	3
Table of Contents	4
Abstract	7
Kurzfassung	8
Water soluble polymers and the LCST effect	9
Introduction	9
Water soluble polymers	9
LCST-effect	9
How to characterize the LCST	10
ROMP	11
Mechanism	11
Advantages and improvements	12
Results and Discussion	13
Monomer and Polymer Syntheses	14
Characterization and analysis	15
The third monomer: An introduction toward carbohydrate chemistry	17
Glycosylation	18
Aza norbornene	20
Amadori-rearrangement	21
Conclusion	23
Experimental	24
Materials	24
Methods	24
Syntheses	25
Perylenes as sensor materials or ROMP as a precision polymerization technique toward molecular probes	31
Introduction	31
Perylenes	31
Syntheses of PDI derivatives	32
π -stacking	35
Synthesis of asymmetric PDIs	36
PET effect	37
Optical pH-sensors	39
Results and Discussion	40
Synthetic strategies for the perylene moiety	40
ROMP in context with the sensor architecture	46
Characterization of the polymer probes	47
PET-behaviour measurements	50
Ascorbic-acid probes	52
LCST-effect in the system	53
Conclusion	55

Experimental	56
Materials	56
Methods	56
Syntheses	56
<i>TPA and Click-Chemistry work together with perylenes</i>	61
Introduction	61
Two Photon Absorption	61
Basics	61
State model	62
Structure of molecules	62
Click-Chemistry	64
Overview	64
Thiol-ene	65
Cu-Catalyzed [3+2] Azide-Alkyne Cycloaddition	66
Results and Discussion	68
Click conditions	70
Characterization of the products with different methods	71
Conclusion	79
Experimental	80
Materials	80
Methods	80
Alkynes, Thiols and Click-Reactions	83
<i>Triphenylamine Studies; Literature, Syntheses and Computational work</i>	89
Introduction	89
Amine-oxide	89
Results and Discussion	92
<i>Organic Radical Batteries</i>	97
Introduction	97
Organic Molecular Radicals	97
Nitroxides	98
Transfer rates and electron hopping	99
Comparison with other battery systems	100
State of the Art	102
Toward flexible Batteries – NEC	103
Tetramethyl- <i>p</i> -phenylenediamine (TMPD)	104
Cyclic Voltammetry	105
Results and Discussion	106
First steps and overview	106
C-N bond formation	109
Buchwald-Hartwig reaction	109
Catalyst systems	110
Ligands (BINAP and DPPF)	114
Base (NaO- <i>t</i> -Bu and cesium carbonate)	114
Reductive amination	115
Direct or stepwise formation	116
Polymer Limitations	118

Guey-Sheng Polymer, a working system	118
Poly(amine-imide)s	119
C-rate	119
Our system	120
Norbornene-systems	122
Monomer 1, a photochromic derivative? Analysis and characterization	123
Electrochemical measurements	127
TEMPO	131
Different characterization-methods through the example of the polynorbornene with TEMPO-radicals	132
Mass spectrometry	132
ESR	132
GPC	134
Magnetic susceptibility	134
IR-spectroscopy and cyclic voltammetry	135
Conclusion	135
Experimental	136
Materials	136
Methods	136
Syntheses	137
Appendix	153
Abbreviations	153
List of Figures	155
List of Schemes	158
List of Tables	159

Abstract

This work is subdivided into four different chapters in which ring opening metathesis polymerization (ROMP) is used for different applications.

The first chapter deals with the synthesis of water soluble molecules featuring a lower critical solution temperature (LCST). Furthermore, the possibility of tuning this effect by copolymerization of functionalized oligo(ethylene oxide) monomers with mannose or alkyl amino hydrochloride bearing monomers indifferent polymer architectures is studied.

In the second chapter optical pH- and redox-sensors were realized with the obtained know-how from chapter one. The so called PET-effect (photoinduced electron transfer) is used to design a fluorophore-spacer-receptor system and synthesize it by means of ROMP. Thereby, a modular approach towards water soluble pH-sensors became available. The living characteristics of ROMP allowed for the preparation of precisely designed block copolymers which were found to have a better quenching efficiency and thus, improved sensitivity. The modular concept was then extended to a redox-sensor system allowing for the quantification of ascorbic acid in water. Furthermore, another strategy, for the conjugation of the dyes, based on click chemistry, was elaborated.

The third chapter focuses on the oxidation of triphenylamine. In particular the possibility of synthesizing triphenylamine-*N*-oxides was investigated. Literature research, synthetic work with analytical methods and computational studies should give an overall picture of this question.

In chapter four research on organic radical batteries based on the *N,N,N',N'*-tetramethyl-*p*-phenylenediamine or so called Wurster blue structure and other stable organic radicals is presented. This project, which was cooperation between the Polymer Competence Center in Leoben (PCCL), Varta Micro Innovation (VMI) and the Institute of Chemistry and Technology of Materials at TU Graz (ICTM), was focused on the synthesis as well as the characterization and application of stable polymerized organic radicals as active material in radical batteries.

Kurzfassung

Diese Arbeit ist in vier verschiedene Kapitel, in denen Ring Öffnende Metathese Polymerisation (ROMP) für verschiedene Anwendungen verwendet wird, unterteilt.

Das erste Kapitel beschäftigt sich mit der Synthese wasserlöslicher Moleküle, die eine untere kritische Lösungstemperatur (LCST) besitzen. Außerdem wird die Möglichkeit untersucht, diesen Effekt mittels Copolymerisation von Monomeren mit Oligo(Ethylenoxid)-Substituenten und anderen Monomeren mit Mannose oder Alkylamino Hydrochlorid Einheiten zu verändern. Unterschiedliche Polymer Strukturen wurden zu diesem Zweck hergestellt und untersucht.

Das Wissen und die Erfahrungen aus Kapitel 1 wurden dazu genutzt, um im zweiten Teil optische pH- und Redox-Sensoren herzustellen. Der so genannte PET-Effekt (Photoinduced electron transfer) wird verwendet, um Sensoren am Beispiel eines Fluorophor-Spacer-Rezeptor-Systems zu entwickeln. Die Synthese erfolgt hier wiederum mittels Ring Öffnender Metathese Polymerisation. Dabei wurde ein modulares Konzept für wasserlösliche pH-Sensoren entwickelt. Die Eigenschaften dieser lebenden Polymerisationsmethode führten zur Herstellung genau definierter Blockcopolymerer. Dieser Polymeraufbau weist eine bessere Quenching-Effizienz und somit eine verbesserte Empfindlichkeit des Sensors auf. Auf Grund des modularen Aufbaus konnte das Sensor System einfach zu einem Redox-Sensor System abgewandelt werden, das die Quantifizierung von Ascorbinsäure in Wasser erlaubt. Darüber hinaus wurde ein weiterer Ansatz, der sich mit der Konjugation von Farbstoffen mittels Klick-Chemie beschäftigt, erarbeitet.

Im dritten Kapitel wird auf die Oxidation von Triphenylamin eingegangen. Insbesondere geht es hier darum, eine synthetische Methode für die Herstellung von Triphenylamin-*N*-Oxiden zu finden. Eine ausführliche Literaturrecherche sollte synthetisches Arbeiten, sowie Analysen und theoretische Studien verbinden, um einen guten Gesamtüberblick über die Oxidation von Triphenylamin zu geben.

Kapitel 4 behandelt organische Radikalbatterien, die auf der Basis von *N,N,N',N'*-Tetramethyl-*p*-Phenylendiamin (Wurster Blau Struktur), hergestellt und charakterisiert wurden. In diesem Projekt, das die Zusammenarbeit zwischen dem Polymer Competence Center Leoben (PCCL), der Varta Micro Innovation (VMI) und dem Institut für chemische Technologie von Materialien an der TU Graz (ICTM) war, wurde die Synthese, sowie die Charakterisierung und Anwendung von diversen stabilen Radikal-Polymeren als Aktivmaterial in Batterien erforscht.

Chapter 1

Water soluble polymers and the LCST effect

Introduction

Water soluble polymers

The demand for new and well defined water soluble polymers has gained more and more interest because of their broad variety of applications in fields like bioseparation, gene and protein-therapy, diagnostics, sensor applications or controlled release of bioactive agents.^{1,2} Water soluble polymers can be received from synthetic e.g. polyvinyl alcohol (partially de-esterified PVAc) or cationic polyelectrolytes and natural sources e.g. starch and its components amylose, cellulose, or different polysaccharides. Basically water soluble polymers are highly hydrophilic as a result of the presence of oxygen and nitrogen atoms: hydroxyl, carboxylic acid, sulfonate, phosphate, amino-, imino-groups etc. Their properties in solution are complex: e.g. the solubilities of PAA and polyacrylamide increase with temperature, but others such as PEO, PPO and polymethacrylic acid precipitate at higher temperatures. Where there are ionic groups, the solution properties are pH dependent. Polyanions are used to precipitate organic wastes and also to remove phosphates, also water soluble polymers have been used by oil industry as lubricants in drilling muds. Other applications are in food industry as gelling agents in ice cream (carboxymethyl cellulose, carrageenans, guar gum) or in pharmaceuticals as suspension agents for insoluble drugs, in cosmetics, hair care products and so on.

LCST-effect

An approach towards the release of substances is to make use of phase separation driven by increasing temperature. This effect is called the lower critical solution temperature (LCST)³ which is a feature of among others, polymers bearing oligo(ethylene oxide) groups in the side chain.⁴ The IUPAC defines this effect as the critical temperature below which the components of a mixture are miscible for all compositions.⁵ The phase behaviour of polymer solutions is an important property involved in the development and design of most polymer related processes. Partially

¹ Langer, R.; Tirell, D.A. *Nature*, **2004**, *428*, 487-492.

² Klok, H.A. *J. Polym. Sci. Part A: Polym. Chem.*, **2005**, *43*, 1-17.

³ Kohori, F.; Yokoyama, M.; Sakai, K.; Okano, T. *J. Control Release*, **2002**, *78*, 155-163.

⁴ Lutz, J.F.; *J. Polym. Sci. Part A: Polym. Chem.*, **2008**, *46*, 3459-3470.

⁵ "IUPAC Compendium of Chemical Terminology", Retrieved **2009-03-05**

miscible polymer solutions often exhibit two solubility boundaries, the upper critical solution temperature (UCST) and the lower critical solution temperature, which both depend on the molar mass and the pressure.⁶

The LCST is largely independent from the molecular weight and the macromolecular architecture and is enthalpy driven. Below the LCST ether-water hydrogen bonds are formed because of the favourable ΔG^{EX} ($\Delta G^{\text{EX}} = G(\text{solution}) - [G(\text{solvent}) + G(\text{ideal gas solute})]$), consistent with the solubility of PEO in water. By increasing the temperature above the LCST the ether-water interactions become unfavourable compared with water-water hydrogen bonding.⁷ The entropy augments by the break-up of ether-water hydrogen bonds is more efficient than the enthalpic effects going along with the break-up of the aforementioned bonding.⁸

Polymers prepared from *endo,exo*-bicyclo[2.2.1]hept-5-ene-2,3-dicarboxylic-acid, bis[2-[2-(2-ethoxyethoxy)ethoxy] ethyl] ester show satisfactory water solubility and a LCST of about 25°C. Another prominent polymer is poly (*N*-isopropylacrylamide), which shows a LCST at about 33°C and also systems like triethylamine in water or the nicotine water system posses a lower critical solution temperature.⁹

How to characterize the LCST

There are some approaches to predict the LCST, but most need experimental data and a solid theoretical background which results in a limited predictive ability.¹⁰ Another system only depends on the solvent and the polymer structures,¹¹ but a more useful method is the quantitative structure-activity/property relationship (QSAR/QSPR) for polymers and solutions. More recently QSPR models for the prediction of the θ using molecular (electronic, physicochemical, etc.) descriptors have been published.¹²

To characterize the LCST effect, a differential turbidity measurement cell (DTM) was used. The DTM cell is a heat and cool able copper pipe in which a test tube with the polymers in aqueous solution with a concentration of 5 mg mL⁻¹ was placed. The temperature is measured against time and a light source and a photo diode are sensing the differential transmission.

⁶ Charlet, G.; Delmas, G. *Polymer*, **1981**, *22*, 1181–1189.

⁷ Bauer, T.; Slugovc, C. *J. Polym. Sci. Part A: Polym. Chem.*, **2010**, *48*, 2098-2108.

⁸ Smith, G.D.; Bedrov, D. *J. Phys. Chem. B*, **2003**, *107*, 3095-3097.

⁹ White, M.A. *Properties of Materials* (Oxford University Press **1999**) p. 175.

¹⁰ Sanchez, I.C.; Stone, M.T. *Polymer Blends Volume 1: Formulation*. Edited by Paul, D.R.; Bucknall, C.B. **2000** John Wiley & Sons, Inc.

¹¹ Liu, H.; Zhong, C. *Eur. Polym. J.*, **2005**, *41*, 139–147.

¹² Liu, H.; Zhong, C. *Ind. Eng. Chem. Res.*, **2005**, *4*, 634–638.

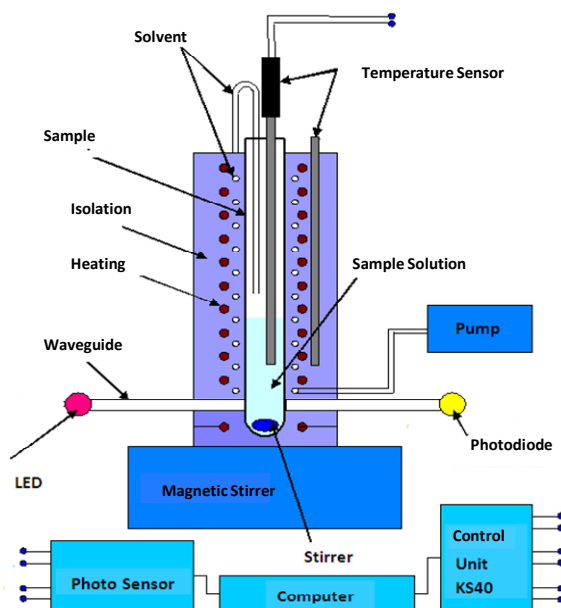


Figure 1: Set-up of a differential turbidity cell¹³

ROMP

Mechanism

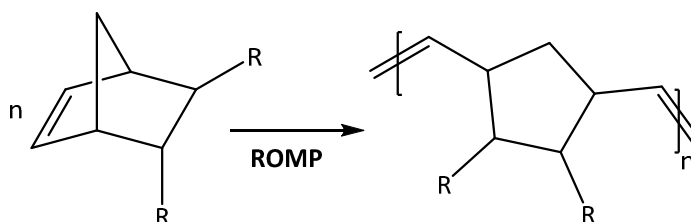


Figure 2: Schematic ROMP

ROMP is a chain growth polymerization method which enables the synthesis of well defined specialty polymers.¹⁴ Fehler! Textmarke nicht definiert.¹⁵ The three step polymerization reaction including initiation, propagation and termination is shown in Figure 3. It starts with the coordination of the monomer to the metal center of the catalyst. Through a [2+2]-cycloaddition a four-membered metalla-cyclobutane intermediate is formed. This step is followed by a subsequent cyclo-revision forming a new metal-alkylidene species. These steps are repeated until the polymerization stops e.g. by full consumption of the monomer.

¹³ Gallas, K.; Wrodnigg, T.M.; Slugovc, C. "Water-soluble polymers prepared by Ring opening metathesis polymerization", EPF **2011**.

¹⁴ Leitgeb, A.; Wappel, J.; Slugovc, C. *Polymer*, **2010**, *51*, 2927-2946.

¹⁵ Sutthasupa, S.; Shiotsuki, M.; Sanda, F. *Polymer Journal*, **2010**, *42*, 905-915.

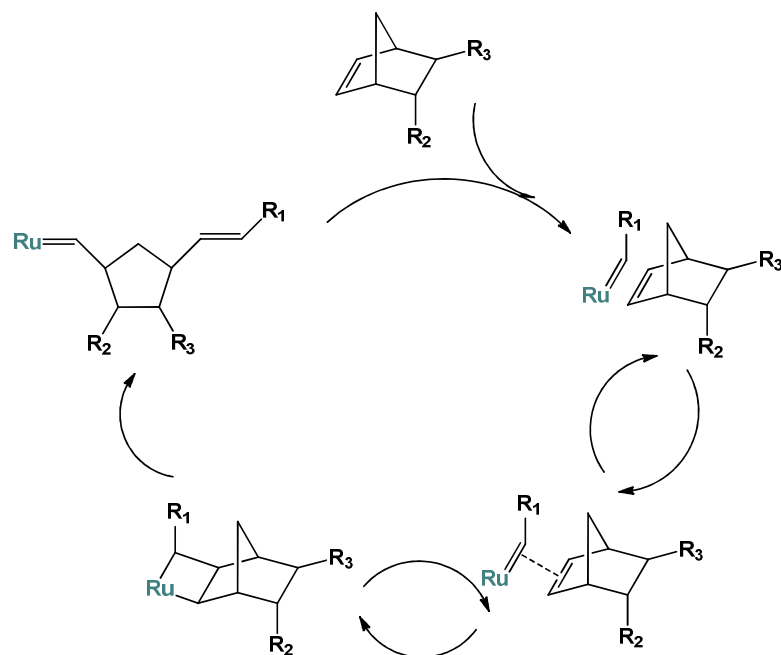


Figure 3: The ROMP mechanism at the example of a norbornene¹⁶

For ending the reaction a terminating agent like ethyl vinyl ether is added which leads to the formation of a less active Fischer-Carbene complex an inactive Fischer Carbene. This termination step removes the metal from the end of the polymer chain and allows for attaching specific end-groups to the polymer chain.¹⁷

Advantages and improvements

The great advantage of ROMP over other polymerization methods is the possibility of living polymerization.¹⁸ Living polymerization means a reaction without side reactions, i.e. intermolecular or intramolecular (backbiting) chain transfer, and yields polymers with narrow molecular weight distributions and predictable molecular weights.^{19,20} With this method, not only defined homopolymers, but also well defined block and graft-copolymers are accessible. When using such a polymerization method not only the initiator and the monomer have to be considered, also other parameters like the solvent, temperature, concentration etc. have a great influence.²¹ In the beginning of olefin metathesis the catalyst systems were cheap and often used in industrial applications but however limited by a low functional group tolerance.²² The “Grubbs

¹⁶ Wappel, J. *Contributions to the Chemistry of Halide exchanged Olefin Metathesis Catalysts, Doctoral Thesis, 2013.*

¹⁷ Gestwicki, J.E.; Cairo, C.W.; Mann, D.A.; Owen, R.M.; Kiessling L.L. *Analytical Biochemistry*, **2002**, *305*, 149.

¹⁸ a) Szwarc, M. *Nature*, **1956**, *178*, 1168-1169. b) Darling, T.R.; Davis, T.P.; Gridnec, A.A.; Haddleton, D.M.; Ittel, S.D. *J. Polym. Sci. Part A: Polym. Chem.* **2000**, *38*, 1706-1708.

¹⁹ Bielawski, C.W.; Grubbs, R.H. *Prog. Polym. Sci.* **2007**, *32*, 1-29.

²⁰ Alb, A.M.; Enohnyaket, P.; Craymer, J.F.; Eren, T.; Coughlin, E.B.; Reed, W.F. *Macromolecules*, **2007**, *40*, 444-451.

²¹ Slugovc, C. *Macromol. Rapid Commun.* **2004**, *25*, 1283-1297.

²² Trimmer, M.S. “*Handbook of Metathesis*”, Grubbs, R.H., Ed Wiley-VCH, Weinheim **2003**, *3*, 407.

1st generation initiator” solved this problem but lacks from other limitations. However, the “2nd generation Grubbs catalyst” and the Hoveyda type initiators become better and better in functional group tolerance, activity and narrow molecular weight distributions, nowadays for every problem there is a initiator solution.²¹ Besides that there are a huge variety of monomers have been successfully polymerized using ROMP.²³ Typical monomer classes include norbornenes, norbornadienes, 7-oxonorbornenes and a lot of other strained cyclic olefins like azanorbornenes,²⁴ cyclobutenes,²⁵ and cyclooctadienes²⁶ just to mention a few. For advanced functional polymer preparation, norbornene derivatives are doubtless the preferred monomers.²¹ Another great advantage of ROMP is, that it can also be carried out in many different media either in bulk, in solution or in a heterogeneous system.²⁷ Various solvents such as benzene, toluene, dichloromethane, acetone, alcohols, water and many others, have been used for different monomers.²⁸ Several factors affect the solvent choice. The most important one is that initiator, monomer and the polymer are soluble in the used solvent.²¹ The reaction rate of such polymerizations increase with increasing temperature due to increase of both the propagation and the initiation rate constant. At higher temperatures and prolonged reaction time secondary metathesis reactions like backbiting become more important.²⁹ Furthermore ROMP has been already very well studied for obtaining complex polymer structures like different block and random copolymers.^{30 31} Polymers consisting of various blocks bearing different functional moieties will self assemble under selective conditions to give supramolecular structures such as micelles, liquid crystals or semi crystalline materials.¹⁴

ROMP is promoted for its versatility, functional-group tolerance and “livingness” and it is particularly used for the synthesis of functional polymers realizing tailor made complex materials.²¹

Results and Discussion

The idea behind this part of my work was to tune the LCST temperature of a known oligoethyleneglycol-polymer by copolymerization with other water soluble monomers. For a second monomer a also known amino functionalized norbornene-derivative was used. It was only used in its deprotonated form as an antimicrobial active agent. In addition the synthesis of a new carbohydrate based monomer should be realized.

²³ Fürstner, A. “Alkene Metathesis in Organic Synthesis”, Ed. Springer, **1998**, Berlin.

²⁴ Schitter, R.M.E.; Jocham, D.; Saf, R.; Mirtl, C.; Stelzer, F.; Hummel, K. *J. Mol. Catal. A*, **1998**, *133*, 75.

²⁵ Weck, M.; Mohr, B.; Maughon, B.R.; Grubbs, R.H. *Macromolecules*, **1997**, *30*, 6430.

²⁶ Bielawski, C.W.; Benitez, D.; Grubbs, R.H. *J. Am. Chem. Soc.*, **2003**, *125*, 8424.

²⁷ Lee, B.S.; Mahajan, B.; Clapham, B.; Janda, K.D. *J. Org. Chem.*, **2004**, *69*, 3319.

²⁸ Mecking, S.; Held, S.; Bauers, F.M. *Angew. Chem. Int. Ed.* **2002**, *114*, 564.

²⁹ Wright, D.L.; Schulte, J.P.; Page, M.A. *Org. Lett.*, **2000**, *2*, 1847.

³⁰ Chen, B.; Metera, K.; Sleiman, H.F. *Macromolecules*, **2005**, *38*, 1084-1090.

³¹ Sandholzer, M.; Bichler, S.; Stelzer, F.; Slugovc, C. *J. Polym. Sci. Part A: Polym. Chem.* **2008**, *46*, 3648-3660.

Therefore common synthetic approaches like *O*-glycolsylation and the Amadori rearrangement were expected to be useful.

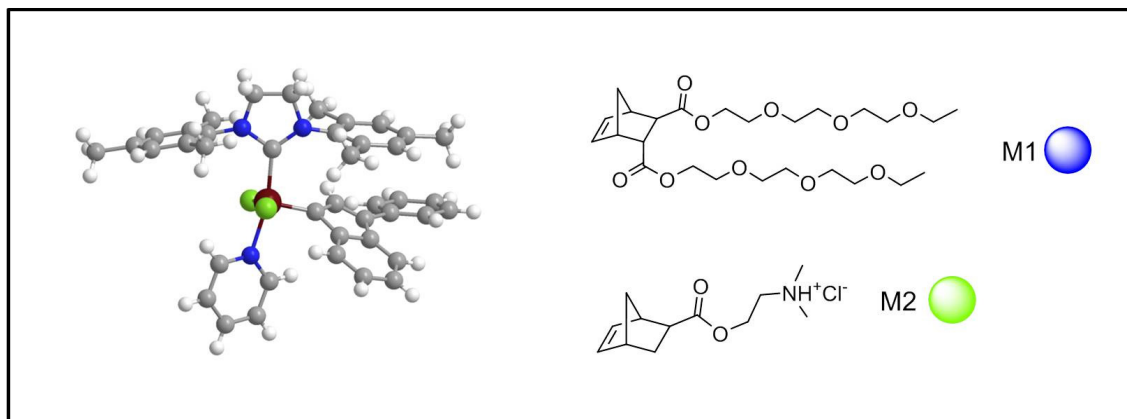


Figure 4: ROMP catalyst **M31** and monomers

Monomer and Polymer Syntheses

Monomer 1, a oligo(ethylene glycol) ester of a norbornene, has a known LCST of about 25°C. It is soluble in water but on the other hand it is also possible to use organic solvents for polymerization or synthetic reasons. The already known synthesis of the disubstituted norbornene derivative was performed via esterification of commercially available *endo,exo*-5-norbornene-2,3-dicarbonyl chloride with [tri(ethylene glycol)monoethyl]ether by nucleophilic catalysis with DMAP and pyridine.⁷

Monomer 2 was prepared by a [4+2] cycloaddition reaction of the corresponding acrylate derivative with cyclopentadiene, the isomers were not separated and the synthesis was performed according to literature.³² The polymerization in both cases was performed with the “Grubbs 3rd generation initiator” **M31** [(H₂IMes)(py)Cl₂Ru(3-phenylindenylid-1-ene)] (H₂IMes = N,N-bis(mesityl)-4,5-dihydroimidazol-2-yl, py = pyridine), which is not sensitive to water, air or functional groups.³³ Monomer 2 was obtained as hydrochloride, currently in literature only a polymerization of the deprotonated monomer is known.³⁴

For a better water-solubility the 2-(dimethylamino)ethyl-bicyclo[2.2.1]hept-5-ene-2-carboxylate dihydrochloride was not deprotonated, but in this form polymerization in dichloromethane with the initiator **M31** was not possible due to the limited solubility of the monomer. A test series with different solvents and solvent-mixtures was performed. The “Grubbs 3rd generation initiator” was used in all experiments due to its high functional group tolerance and the stability in solvents like methanol. Different

³² Gstrein, X. „*Neue antimikrobielle Polymere durch ringöffnende Metathesepolymerisation*“, diploma thesis, **2007**.

³³ Burtscher, D.; Lexer, C.; Mereiter, K.; Winde, R.; Karch, R.; Slugovc, C. *J. Polym. Sci. Part A: Polym. Chem.* **2008**, *46*, 4630 – 4635.

³⁴ Kreuzwiesner, E.; Noormofidi, N.; Wiesbrock, F.; Kern, W.; Rametsteiner, K.; Stelzer, F.; Slugovc, C. *J. Polym. Sci. Part A: Polym. Chem.* **2010**, *48*, 4504-4514.

dichloromethane/methanol and dichloromethane/nitromethane mixtures were tested in advance as best alternatives. In Table 1 some of the results are listed and the DCM/MeOH 1:1 mixture was identified as the most promising one. As required for ROMP all components of the polymerization reaction are soluble in this solvent mixture and also the molecular weight distribution and the reaction time was the best of all experiments. The good polymerization effort is also proven by a linear progression of the increase of the number molecular weights with monomer feed.

Table 1: Solvents, M_n and PDI for the hydrochloride of monomer 2

monomer eq.	solvent	M_n [g/mol]	PDI	Yield
300	CH ₂ Cl ₂	81,300	2.1	96
300	CH ₂ Cl ₂ /MeOH 1:1	65,800	1.2	95
300	CH ₂ Cl ₂ /MeNO ₂ 4:1	66,000	1.2	98
200	CH ₂ Cl ₂ /MeOH 1:1	56,400	1.2	89
100	CH ₂ Cl ₂ /MeOH 1:1	30,800	1.2	95
100	CH ₂ Cl ₂ /MeNO ₂ 4:1	31,200	1.2	98

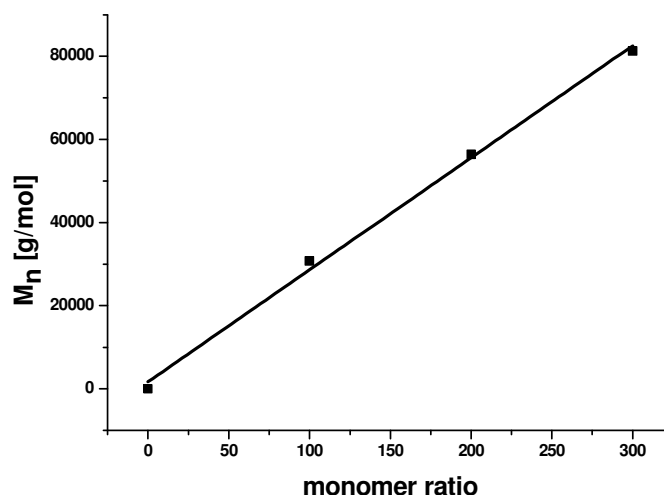


Figure 5: Linear polymerization rate in the CH₂Cl₂/MeOH solvent

Characterization and analysis

The characterization of the obtained polymers was done by ¹H-NMR spectroscopy and of course by GPC. Exemplarily, the ¹H-NMR spectrum for **poly2-300** in MeOD is shown in Figure 6. Some of the obtained GPC values are listed in Table 1, the PDIs were all around 1.2 and also the experimental derived M_n compare well with the calculated data.

For this work random copolymers consisting of different ratios of the oligo ethylene glycol unit and the amine unit were prepared. The properties of these copolymers were compared with those of the homo-polymers, especially with those bearing oligo-(ethylene oxide) groups.

Polymerizations of all polymers were performed with high yields and molecular weights are in the expected range. The polymerization time necessary for complete conversion checked by TLC varied from 2-4h, depending on the amount of **M1** in the copolymers. The conversion of **poly-2** was completed in about 30 minutes. The moderate yield of homo-polymer **poly-1** derived from the product loss during diligent purification of the polymer by repeated precipitation. Especially this polymer was hard to precipitate

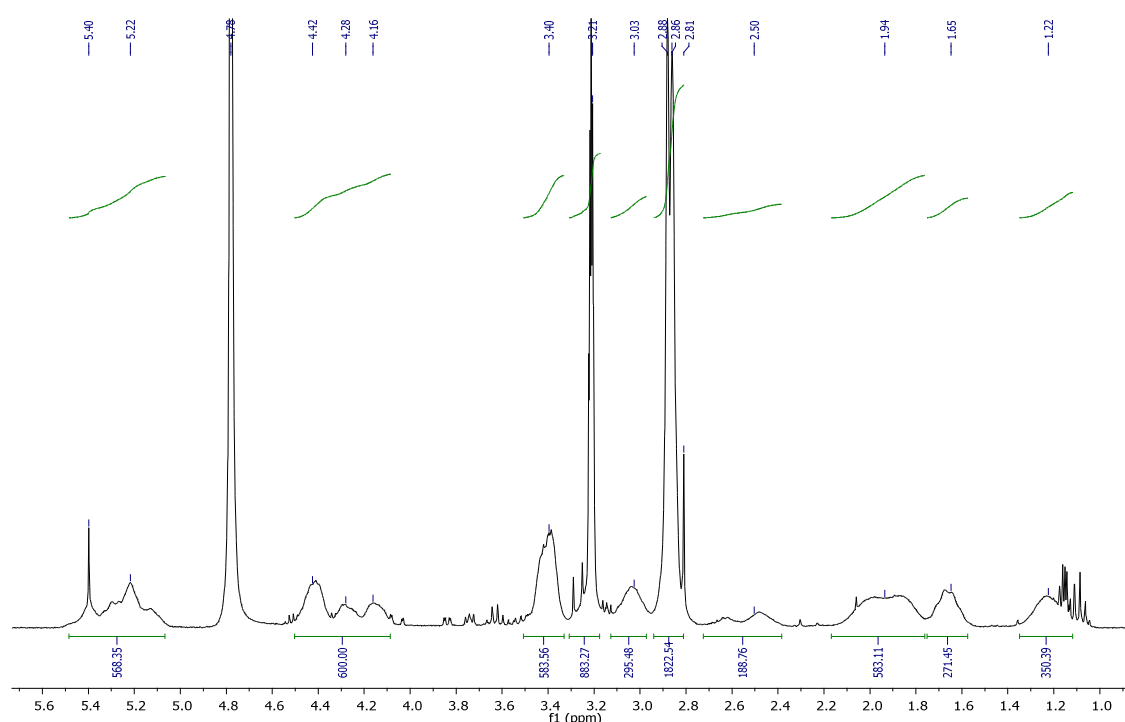


Figure 6: $^1\text{H-NMR}$ of poly2-300

Further on, The water solubility of the polymers was also investigated. All the polymers possess a very good to good water solubility of about 10 to 25 g/L. The solubility decreases with the increasing amount of the ethylene glycol unit. Besides also the time for complete dissolving in the water depends on the polymer architecture. For the homo-polymers **poly1-100** the oligoethylene glycol polymer was dissolved at 20°C in 30 minutes whereas **poly2-100** the amine polymer only had to be stirred for about one minute till complete dissolution occurred.

Only **poly-1** showed a LCST effect in neat water which was expected due to former data.⁷ All the copolymers did not show any effect in neat water as protonation of the amines provided a much better water solubility. By increasing the pH-value with a base, the partial deprotonation of the amino groups restored a LCST effect in the

copolymers. The influence of the basic conditions decreased after full deprotonation of the amines. In this connection one guess was that the higher the amount of the amine part in the copolymer is, the lower the change in the lower critical solution temperature is. In this context only the influence of the ionic strength by increasing the amount of base increases the clouding effect in the test tubes. In Figure 7 the lower critical solution temperatures at different pH values are given, the values vary between 20 and 25 degrees centigrade with a higher value of about 30 and some lower values of around 12 degrees centigrade. Figure 7 and Table 2 summarize the results.

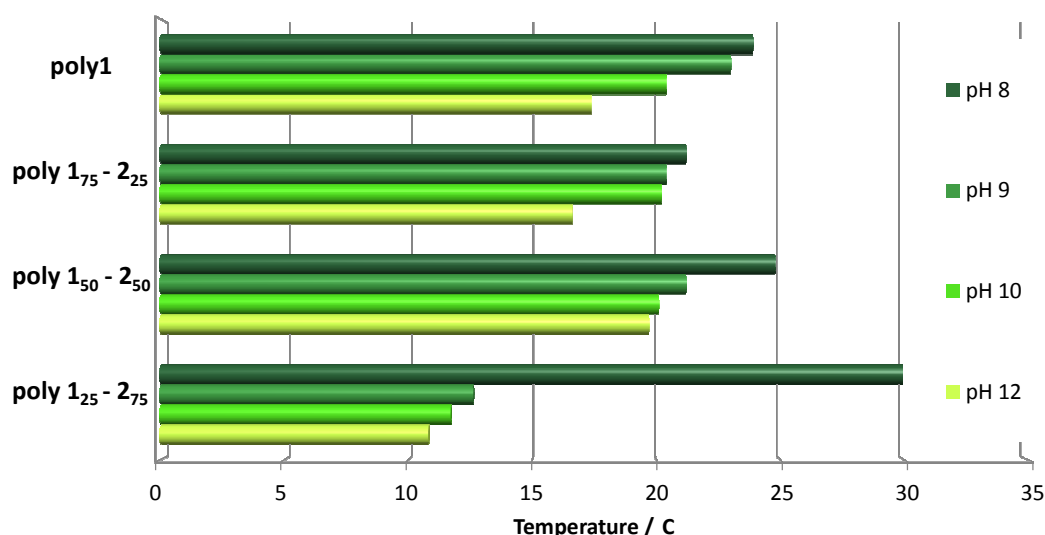


Figure 7: Lower critical solution temperatures at different pH-values with different polymer architectures

Table 2: Polymer characterization of different random copolymers

polymer	LCST [$^{\circ}\text{C}\pm 0.5$]	M_n [g/mol]	PDI	Yield [%]
	pH = 8			
poly-1 ^a	23.9	47,000	1.2	55
poly1 ₇₅ -2 ₂₅ ^a	21.2	45,000	1.3	88
poly1 ₅₀ -2 ₅₀ ^b	24.8	38,000	1.4	95
poly1 ₂₅ -2 ₇₅ ^b	31.5	34,000	1.3	90
poly-2 ^b	precipitates	33,000	1.4	98

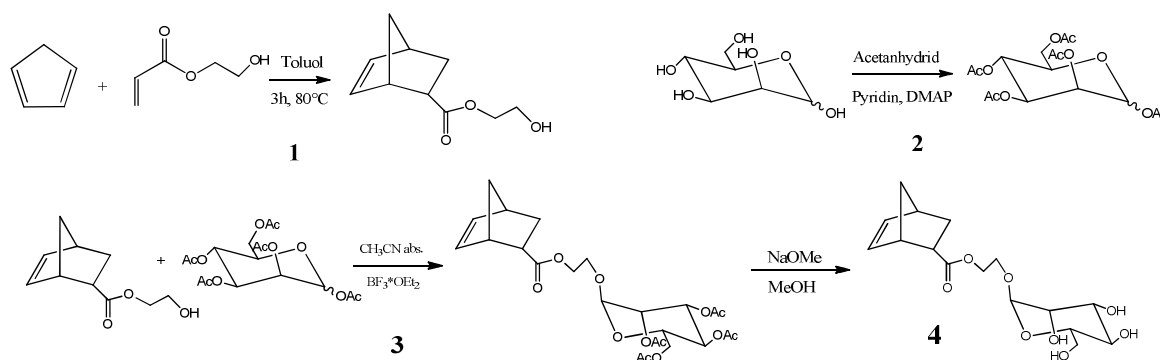
^a determined in THF; ^b determined in CHCl_3 ; Et_3N :i-PrOH 94:4:2

The third monomer: An introduction toward carbohydrate chemistry

The two up to now used monomers were readily available start materials for the tuning of the LCST because there were already investigations done in our group with

the oligoglycol-unit and the amine-unit was used in its deprotonated form as an antimicrobial compound. So the syntheses are already known and both are easy to synthesize. The next step or idea here was due to my former work with carbohydrates, to realize a sugar monomer, as third building block and study the LCST of their of their presumably water soluble polymers.

The requirements for such a carbohydrate monomer are an easy and cheap synthesis which is not too time consuming and is also working in good yields. The synthesis plan shown in Scheme 1 fulfills these requirements



Scheme 1: Scheme of the mannose-monomer preparation³⁵

In the last step, the removal of the protecting acetyl group, it was not considered that when the ester cleavage is performed under basic or acidic conditions, also the ester group at the norbornene breaks down.³⁶

Glycosylation

The most important step of the monomer preparation was the *O*-glycosylation step, between the norbornene and the carbohydrate.

In a glycosylation reaction a glycosyl donor (carbohydrate) is attached to a glycosyl acceptor (a hydroxyl or other functional group). In biology the concept of glycosylation refers to enzymatic processes that attach glycans to organic molecules. The carbohydrate chains attached to the target proteins serve various functions.³⁷ For instance, some proteins do not fold correctly unless they are glycosylated first.³⁸ The reaction product here is a glycoside or, in the case of proteins a peptidoglycane. There are five classes of glycans. The *N*-linked glycans are attached to nitrogen, which requires the participation of the lipid dolichol phosphate. *O*-linked glycans are attached on the hydroxy groups of the aminoacids or the oxygens of the lipids. Phospho-glycans are linked through a phosphate of a phospho-serine. *C*-linked glycans are a very rare form where a sugar is added to a carbon on the tryptophan side

³⁵ Obata, M.; Shimizu, M.; Ohta, T.; Matsushige, A.; Iwai, K.; Hirohara, S.; Tanihara, M. *Polym. Chem.*, **2011**, DOI: 10.1039/COPY00326C.

³⁶ Carlise, J.R.; Kriegel, R.M.; Rees, W.S.; Weck, M. *J. Org. Chem.*, **2005**, *70*, 5550-5560.

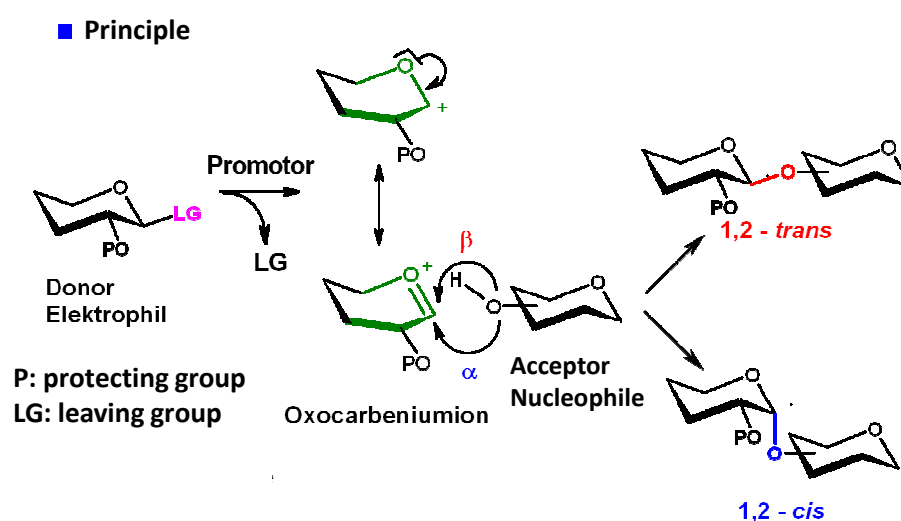
³⁷ Drickamer, K.; Taylor, M.E. (*Introduction to Glycobiology* (2nd Ed.). Oxford University Press, **2006**.)

³⁸ Varki, A. (*Essentials of Glycobiology* (2nd Ed.). Cold Spring Harbor Laboratories Press, **2009**.)

chain and as last the glypiation, which is the addition of a GPI anchor that links proteins to lipids through glycan linkages.³⁹

A similar reaction to the glycosylation is the glycation, where an amine reacts with a reducing sugar which is explained in the next chapter of the Amadori-reaction.

In Scheme 2 the principle of an *O*-glycosylation reaction is represented with the rearrangement of the sugar molecule and the effect of the promoter onto the reaction. Also the most common leaving groups and activators are shown for different kind of structures. As always in sugar chemistry also the effect of α or β position of the C-1-group has to be considered for the expected type of bond linkage. β gives a 1,2 trans-linkage and α gives a 1,2 cis-linkage of the two binding sites.



Leaving group	Activator	Comments
LG = OAc	$\text{BF}_3 \cdot \text{Et}_2\text{O}$, SnCl_4 , TMSOTf	not for complex structures
LG = Br	AgCO_4 , AgOTf, $\text{Hg}(\text{CN})_2$	most frequently used
LG = Cl	AgOTf, $\text{Hg}(\text{CN})_2$, BgBr ₂	more stable than glycosylbromide

Scheme 2: *O*-Glycosylation with different leaving groups and activators⁴⁰

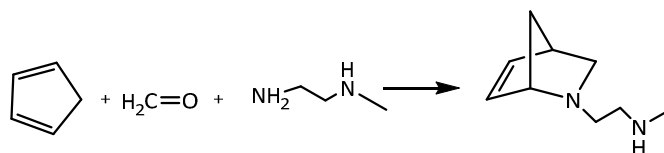
Due to the problem with the ester cleavage of the norbornene and the sugar part during elimination of the acetyl protecting groups a further plan has to be made. The linkage between the molecules is weak when we do *O*-glycosylation reactions and so as second idea for the synthesis of the sugar monomer a path through two fields I already worked with was considered. Thereby a more stable linkage like an amide bond should be introduced.

³⁹ Wikipedia, <http://en.wikipedia.org/wiki/Glycosylation>, 2013.

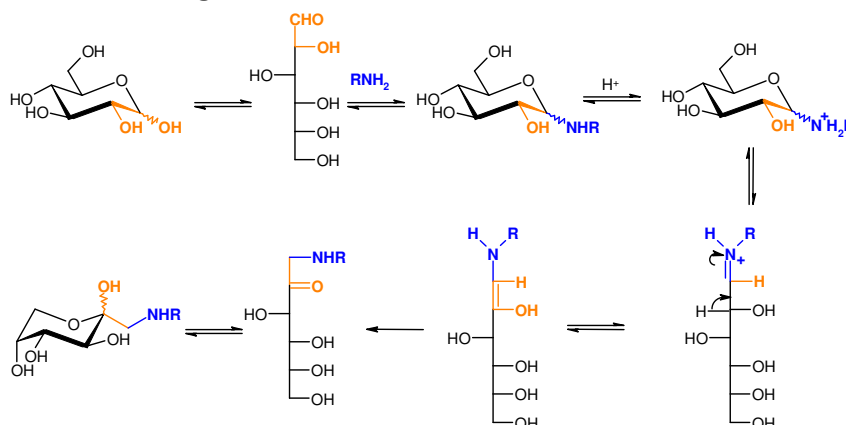
⁴⁰ Van den Stehen, P.; Rudd, P.M.; Dwek, R.A.; Opdenakker, G. *Crit. Rev. Biochem. Mol. Biol.*, **1998**, *33*, 151-208.

The first step is the synthesis of an aza norbornene and the second step is a subsequent Amadori reaction. Both reactions should work without protecting groups or complicated purification steps and at least the aza norbornene has been synthesized before without further purification.

1.step: Building of an aza-norbornene



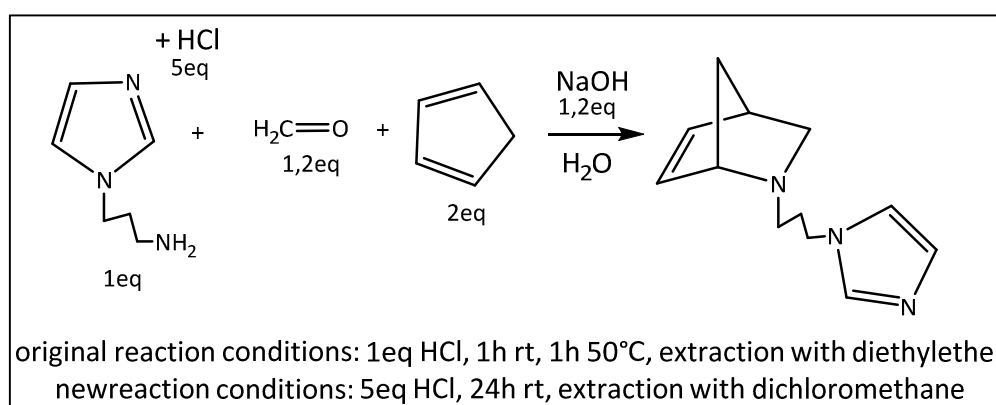
2.step: Amadori-rearrangement



Scheme 3: Aza norbornene building and subsequent Amadori-rearrangement

Aza norbornene

The reaction conditions for the synthesis of the aza norbornene were elaborated in a similar reaction. The conditions are originally derived from Larsen et al. and modified for an easier work up.⁴¹



Scheme 4: Reaction scheme of the original aza norbornene reaction with the improved reaction conditions

⁴¹ Larsen, S.D.; Grieco, P.A. *J. Am. Chem. Soc.*, **1985**, *107*, 1768-1769.

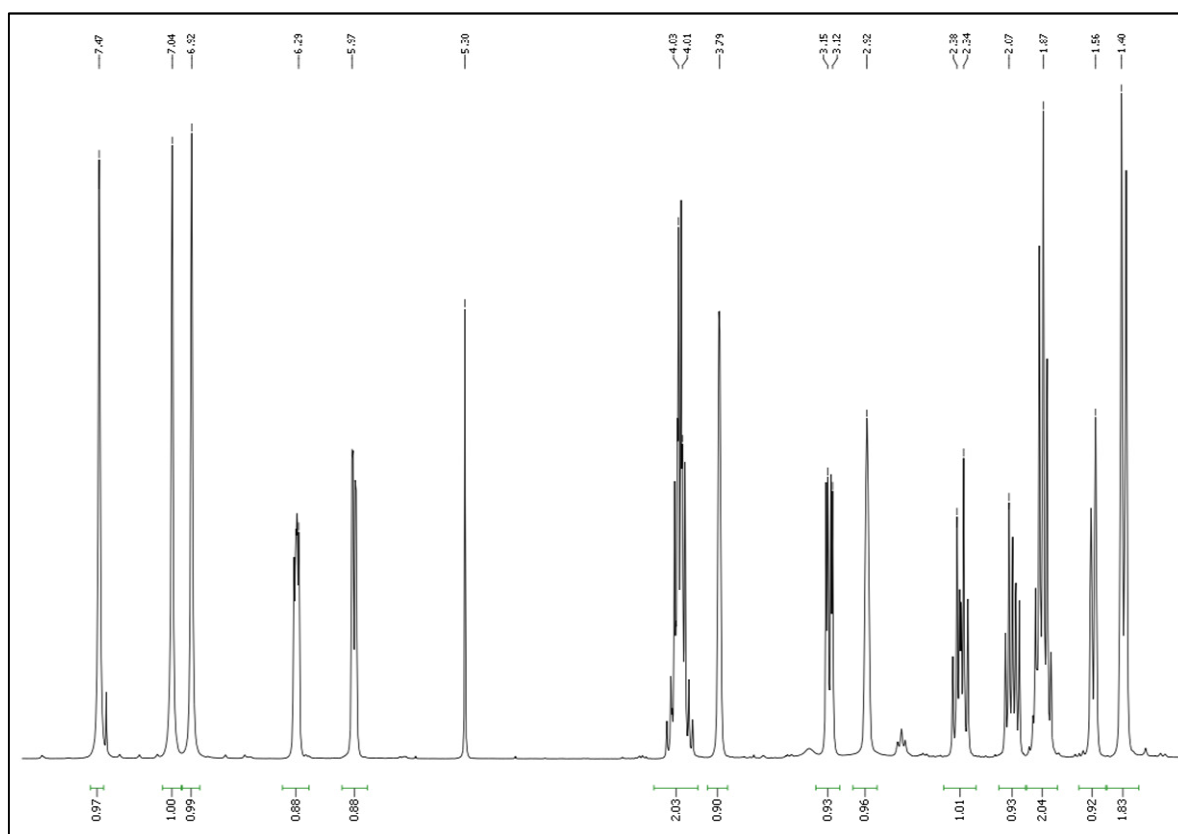


Figure 8: NMR of the aza norbornene product without further purification. Nearly no side products are visible

Amadori-rearrangement

The Amadori rearrangement is a reaction between α -hydroxy-aldehydes and amines. It leads to glycosylamines and in the subsequent rearrangement to 1-deoxy-ketosamines, the so called Amadori-rearrangement products. This reaction is also the first step in the Maillard-reaction cascade, the non enzymatic browning of food. It goes back to Mario Amadori, who observed the reaction products between D-glucose and *p*-fenetidin in 1925.⁴²

Kuhn and Weygand⁴³ described the mechanism of this reaction in 1937, which is still valid today.

The mechanism shown in Scheme 3 as second step starts with the building of an *N*-glycoside between the anomeric position of an aldose (glucose) and an amine group, which after protonation leads to a ring opening reaction and the formation of a Schiff base. Through the enamin-aldimin tautomerism we have equilibrium with the enol-form. The enol is stabilized by building a 1-amino-1-deoxy-hexose which closes the ring and leads to the reaction product. The loss of the proton at C-2 of the Schiff base is the rate determining step.

⁴² Amadori, M. *Atti R. Accad. Lincei*, **1925**, 2, 337-342.

⁴³ Kuhn, R.; Weygand, F. *Ber.*, **1937**, 70, 769-772.

In 1940 also Weygand discovered the catalytic improvement of acids, to ensure better yields and purer products.⁴⁴ The components for this reaction are very variable for example the synthesis of Amadori-products with carbohydrates and polyvinylamine,⁴⁵ the reaction of α -hydroxycarbonyl compound with aromatic^{46a} or aliphatic amines,^{46b} the Amadori-rearrangement in pyridin⁴⁷ or starting from 2-amino-2-deoxy-D-hexoses and ascorbic acid.⁴⁸ Amadori-compounds generated in vivo are glycation products, which are associated with diabetes or the Alzheimer disease.⁴⁹ Amadori-products are preliminary stages of Maillard-products and they are mostly colored (yellow to black), with intensively smelling and tasting aromas like pyrroles, imines, furans, imidazoles and their polymerization products.^{50 51 52} In food, there are many of these compounds, which are important for the aroma or conservation;⁵³ however degradation of the Amadori products leads to aromatic heterocycles which have carcinogenic or mutagenic effects.⁵⁴

Although the Amadori-rearrangement is a very useful chemical reaction, you are confronted with some synthetic problems like low yields or that at high temperatures the Amadori-products enter the Maillard reaction cascade. Besides that, due to reversibility the glycosylamine is able to isomerize to the 1-aminoketose or hydrolyse to the starting compound. Furthermore the purification with chromatographic methods is complicated because of the reaction mixtures with nearly the same R_f values.

As mentioned before the *O*-glycosylation pathway failed because of the deprotection step, till this point it was an easy, reproducible and cheap way to synthesize the monomer. The second guess with the aza norbornene seemed to be much more complicated in the end. Unfortunately the Amadori rearrangement did not work out with the norbornene counterpart. Here changes in the reaction conditions and adaptations have to be done. For sure is that also this way does not fulfill the

⁴⁴ Weygand, F. Ber., **1940**, 73, 1259-1278.

⁴⁵ Micheel, F.; Büning, R. Chem. Ber., **1957**, 90, 1606-1611.

⁴⁶ a) Heyns, K.; Stumme, W. Chem. Ber., **1956**, 89, 2833-2844, b) Heyns, K.; Stumme, W.; Chem. Ber., **1956**, 89, 2844-2853.

⁴⁷ Rosen, L.; Woods, J.W.; Pigman, W. Chem. Ber., **1957**, 90, 1038-1046.

⁴⁸ Klemer, A.; Funcke, W. Liebigs Ann. Chem., **1979**, 1682-1688.

⁴⁹ a) Mossine, V.V.; Glinsky, G.V.; Feather, M.S. Carb. Res., **1994**, 262, 257-270 b) Day, J.F.; Thorpe, R.; Baynest, J.W. J. Biol. Chem., **1979**, 254, 595-597.

⁵⁰ Hodge, J.E. Agric. Food Chem., **1953**, 1, 928-943.

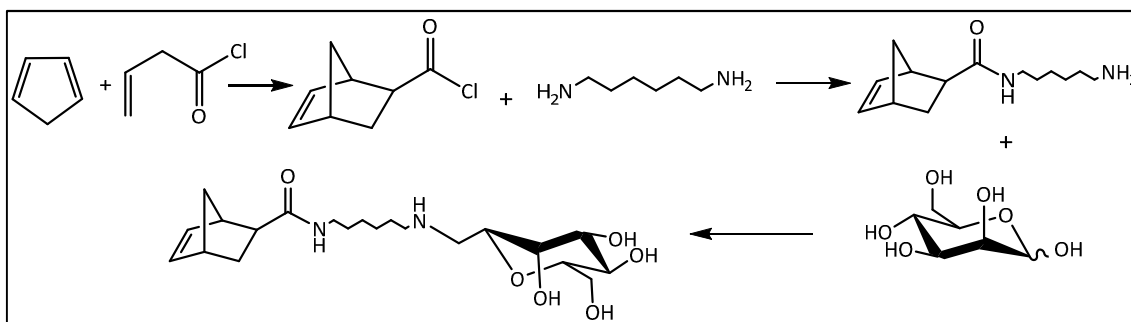
⁵¹ Smith, M.A.; Taneda, S.; Richey, P.L.; Miyata S.; Yan, S.D.; Stern, D.; Syre, L.M.; Monnier, V.M.; Perry, G. Proc. Natl. Acad. Sci. U.S.A., **1994**, 91, 5710-5714.

⁵² Reynolds, T.M. Adv. Food. Res., **1963**, 12, 1-52.

⁵³ Mills, F.D.; Hodge, J.E.; Carbohydr. Res., **1976**, 51, 9-21.

⁵⁴ a) Ohgaki, H.; Kusama, K.; Matsukura, N.; Marino, K.; Hasegawa, H.; Sato, S.; Takayama, S.; Sugimura, T. Carcinogenesis, **1984**, 5, 921. b) Yamaizumi, Z.; Shiomi, T.; Kasai, H.; Nishimura, S.; Takahashi, Y.; Nagao, M.; Sugimura, T. Cancer Letter, **1980**, 9, 75-83.

requirements. The very complicated NMRs with multiple product mixtures are hard to interpret and require further investigations.



Scheme 5: Different approach to the third monomer based on a carbohydrate structure with a more stable amide bond and the involvement of the Amadori rearrangement

Furthermore, a third synthetic strategy was evolved with the more stable amide bond between the spacer and the norbornene. Therefore the whole structure should be more consistent against hydrolysis. Due to the avoidance of protecting group strategies again the Amadori rearrangement was used to combine the sugar moiety with the polymerizable part. The establishment of the monomer was successful but the polymerization under common polymerization properties did not work. For lack of time no further investigations were made on this product

Conclusion

Polymers with content of **M1** and **M2** could be prepared in a controlled manner and combine satisfactory water solubility with the occurrence of an LCST-effect. The LCST of these polymers has a good tuning potential within the change of pH conditions and also the amount of the two polymers. Considering all these parameters the LCST is between 12 to 31 degrees centigrade. The ionic strength has also an influence on the decreasing temperature because **poly-1** showed this effect without any deprotonation. The possibility to tune the LCST to higher temperatures of particularly 37°C should work out by decreasing the amounts of **poly-2** in the copolymers.

As second or experimental more challenging part the synthesis of a third monomer based on a carbohydrate structure was considered. The sugar molecule should be linked to the norbornene backbone to integrate it as third part with the ROMP technique to obtain different block and random copolymer architectures.

As mentioned in the results and discussion part the *O*-glycosylation step could not be performed without further decomposition of the molecule at the ester bond.

The aza norbornene strategy gave too complicated structures and no well purified aza norbornene with the general reaction conditions could be obtained. As third synthetic pathway a norbornene part with an amide bond was synthesized. This bond should be much more stable to hydrolysis and pH-changes. Also the Amadori rearrangement

could be performed successful but the subsequent polymerization with Grubbs catalyst did not work. The amide bond interferes with the ROMP reaction and due to other projects unfortunately no third polymer for further copolymer investigations could be obtained.

Experimental

Materials

M31 ([1,3-bis(2,4,6-trimethylphenyl)-2-imidazolidinylidene]dichloro(3-phenyl-1H-inden-1-ylidene)(pyridyl)ruthenium(II) was obtained from UMICORE AG&Co.KG. (\pm)*endo,exo*-2-(tert-butylamino)ethyl bicyclo[2.2.1]-hept-5-ene-2-carboxylate hydrochloride⁵⁵ (**2**) was provided by Aglycon (Austria). (\pm)*endo,exo* -bicyclo[2.2.1]hept-5-ene-2,3-dicarboxylic acid,bis[2-[2-(2-ethoxyethoxy)ethoxy]ethyl]ester (**1**) was prepared according to a previously published procedure.⁵⁶ Other materials were obtained from commercial sources (Aldrich, Fluka or Lancaster).

Methods

Polydispersity indices (PDI) and molecular weight data were determined by gel permeation chromatography (GPC) using THF as eluent, if not stated otherwise. The device setup comprises a Merck Hitachi L6000 pump (delivery volume 1 mL/min), separation columns from Polymer Standards Service (5 μ m grade size) and a refractive index detector from Wyatt Technology. For calibration polystyrene standards from Polymer Standards Service were used. NMR spectroscopy (¹H, ¹³C, COSY, HSQC and HMBC) was done on a Bruker Avance 300 MHz spectrometer (75 MHz for ¹³C). Deuterated solvents were obtained from Cambridge Isotope Laboratories Inc. For FT-IR spectroscopy a Bruker ALPHA FT-IR Spectrometer was used. Measurements were performed in ATR mode. Electron impact (EI, 70 eV) mass spectra were recorded on a Waters GCT Premier equipped with direct insertion (DI). MALDI-TOF mass spectrometry was performed on a Micromass ToFSpec 2E Time-of-Flight Mass Spectrometer using DCTB as a matrix. The identification of the cloud point was done with a DTM cell (Figure 1). In a heat and cool able copper pipe a test tube with an aqueous polymer solution was placed. Two drill holes in an arrangement of 180° were made next to the bottom. In the first one, a light source (white light emitting diode, 3.6 V, 20 mA, 1000 mcd) and in the second one a photo diode (BPW 34, 500-10.000 nm, 0.62 AW⁻¹) for sensing the differential transmission was placed. On the shell of the copper pipe, a heating element (heating cable 50 W, using a PTFE isolation, Horst GmbH, Lorsch, Germany) for linear heating, was placed, using a KS 40 controller (Prozeß und Maschinen-Automation GmbH, Kassel, Germany). Furthermore, the

⁵⁵ Kreuzwiesner, E.; Noormofidi, N.; Wiesbrock, F.; Kern, W.; Rametsteiner, K.; Stelzer, F.; Slugovc, C. *J. Polym. Sci. Part A: Polym. Chem.*, **2010**, *20*, 4504.

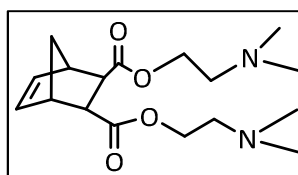
⁵⁶ Sandholzer, M.; Fritz-Popowski, G.; Slugovc, C. *J. Polym. Sci. A Polym. Chem.*, **2008**, *46*, 401.

temperatures down to 10°C were achieved by cooling coils, which are placed on the outside of the copper pipe.⁷

Syntheses

***endo,exo*-Bicyclo[2.2.1]hept-5-ene-2,3-dicarboxylicacid,bis-dimethylaminoethanol**

The whole synthesis was performed under inert atmosphere of nitrogen. In a three-neck-bottom flask the *trans*-5-norbornene-2,3-dicarbonyl-chloride (1.5 mL, 9.31 mmol, 1 eq) was dissolved in dichloromethane (dry, 35 mL). Under ice-cooling the dimethylaminoethanol (3.0 mL, 20.6 mol, 2.1 eq) was added drop wise and the DMAP (56 mg, 0.46 mmol, 0.05 eq) was added afterwards. Then the pyridine (1.9 mL, 23.27 mmol, 2.5 eq) was added drop wise and the reaction was allowed to get to room-temperature. The reaction was stirred for about 24 hours at room temperature. The reaction got orange and the solid was filtered and the filtrate was extracted five times with HCl (2M). During this procedure the-product is formed and nothing is in the organic phase, so you have to neutralize it with NaHCO₃ and extract it with dichloromethane. The organic phase was dried with Na₂SO₄, filtered and the solvent was removed. The crude product was dissolved in dichloromethane and purified by flash column chromatography, DCM/MeOH 10:1 +1% ammonia.TLC: DCM/MeOH 20:1. The final product was dried in vacuum. Yield: 2.4g of a light yellow oily product (80%).

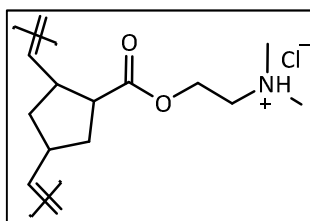


¹H-NMR (δ , 20 °C, CDCl₃, 300.36 MHz): 6.25 (s, 1H, nb⁶), 6.01 (s, 1H, nb⁵), 4.19 (t, 2H, O-CH₃), 4.12 (t, 2H, O-CH₃), 3.40 (t, 1H, nb), 3.26 (s, 1H, nb), 3.11 (s, 1H, nb), 2.70 (d, 1H, nb), 2.52 (q, 4H, 2xCH₃-N), 2.26 (s, 6H, 4xCH₃), 1.59 (d, 1H, nb⁷), 1.41 (d, 1H, nb⁷)

¹³C-NMR (δ , 20 °C, CDCl₃, 75.53 MHz): 174.12, 172.88, 137.37, 134.84, 62.56, 62.41, 57.59, 57.54, 47.66, 47.58, 47.03, 46.92, 45.59

Polymerization of (\pm)*endo,exo*-2-(*tert*-butylamino)ethyl-bicyclo[2.2.1]-hept-5-ene-2-carboxylate hydrochloride

A Schlenk tube was evacuated and the monomer (100 mg, 0.41 mmol, 300 eq) was dissolved in 5 ml of a 0.1M solution of DCM/MeOH (1:1). The catalyst M31 (1.02 mg, 1.4*10⁻⁶ mmol, 1 eq) was dissolved in 0.1 ml solvent mixture and added at once to the stirred solution. The mixture changed the color from red to yellow and after 20 to 30 minutes reaction-time it was stopped with 150 μ L ethyl vinyl ether. The solvent was nearly removed and the rest solution was precipitated in cold ether. The ether was decanted and the product was dissolved again in DCM/MeOH (1:1) and then dried on the vacuum line.

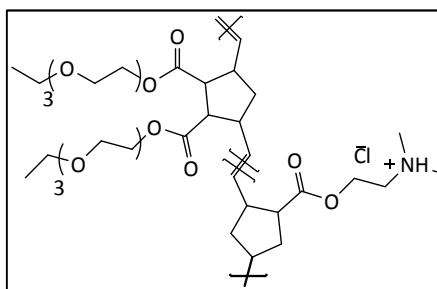


$^1\text{H-NMR}$ (δ , 20 °C, CDCl_3 , 300.36 MHz): 6.15, 5.88 (dd, 2H, nb^{5,6}) 4.07 (t, 2H, COOCH_2), 3.16, 2.92, 2.85 (bs, m, bs, 3H, nb^{1,2,4}), 2.48 (t, 2H, CH_2N), 2.23 (s, 6H, $\text{N}(\text{CH}_3)_2$), 1.84 (m, 1H, nb³), 1.36 (m, 2H, nb^{3,7}), 1.21 (d, 1H, nb⁷) only signals for the endo isomer are given, characteristic signals of the exo isomer: 6.10 (m, 2H, nb^{5,6}), 4,14 (m, 2H, COOCH_2). Endo/exo = 90:10.

GPC: M_n = 33,000; PDI = 1.4; solvent: CHCl_3 : Et_3N : $i\text{-PrOH}$ 94:4:2

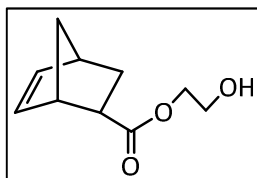
Random Copolymer Synthesis

All copolymers were synthesized as random copolymers. (\pm)*endo,exo*-2-(*tert*-butylamino) ethyl-bicyclo[2.2.1]-hept-5-ene-2-carboxylate hydrochloride and (\pm)*endo,exo*-bicyclo[2.2.1]hept-5-ene-2,3-dicarboxylic acid, bis[2-[2-(2-ethoxyethoxy) ethoxy]ethyl]ester were dissolved together in varying amounts between 10 and 90 percent each dissolved in DCM/MeOH and the initiator M31 was then added in one portion to the reaction mixture. After the needed reaction time between 30 minutes and 4 hours the reaction was stopped with an excess of ethyl vinyl ether. The solvent was nearly removed and the rest was added drop wise to chilled *n*-pentane for precipitation. The product was dried under vacuum.



endo,exo-Bicyclo[2.2.1]hept-5-ene-2,3-dicarboxylic acid-1-ethanol

Freshly distilled cyclopentadiene (1.2 mL, 14.5 mmol, 3 eq) and 2-hydroxyethylacrylate (0.57 mL, 4.96 mmol, 1 eq) were dissolved in toluene (20 mL). The reaction was refluxed and stirred for three hours. After that it was cooled down to room temperature and the solvent was removed. The crude product (2.2 g) was dissolved in cyclohexane and purified by flash column chromatography (CH/EA 20:1 with a gradient to EA). TLC: CH/EA 3:1. Yield: 0.7g (55.6%) oily product.

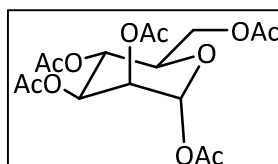


$^1\text{H-NMR}$ (δ , 20 °C, CDCl_3 , 300.36 MHz): 6.22 (m, 1H, nb⁶), 5.93 (m, 1H, nb⁵), 4.17 (q, 2H, O-CH₃), 3.80 (q, 2H, CH₃-OH), 3.22 (bs, 1H, OH), 3.00 (q, 1H, nb), 2.92 (s, 1H, nb) 1.99-1.91 (m, 2H, nb) 1.46-1.40 (m, 2H, nb), 1.28 (d, 1H, nb). Only signals for the endo isomer are given, characteristic signals of the exo isomer: 6.15, 4.23, 3.83, 3.05, 1.88, 1.39, 1.25. Endo/exo = 60:40.

$^{13}\text{C-NMR}$ (δ , 20 °C, CDCl_3 , 75.53 MHz): 175.36, 138.07, 132.35, 66.07, 61.57, 49.81, 45.96, 43.40, 42.68, 29.43. exo: 176.96, 138.28, 135.65, 66.23, 61.54, 46.85, 46.47, 43.19, 41.78, 31.06

1,2,3,4,6-Pentakis-O-acetyl-D-mannopyranoside

D-Mannose (1 g, 5.55 mmol, 1 eq) was dissolved in 15 mL of pyridine and under ice cooling acetic anhydride (6.3 mL, 66.67mmol, 12 eq) was added drop wise. The reaction was stirred for 5 hours at room temperature and the progress was controlled via TLC in CH/EA 1:1. The reaction was quenched with methanol and the pyridine was removed under reduced pressure. The mixture was extracted with ethyl acetate and HCL and in the second step with NaHCO₃. The organic phase was dried, the solvent was removed and the product was dried under vacuum. Yield: 2.1 g white solid (98%)



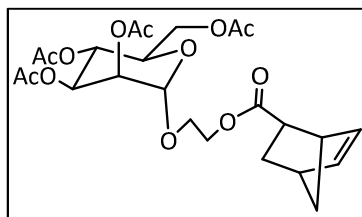
$^1\text{H-NMR}$ (δ , 20 °C, CDCl_3 , 300.36 MHz): 6.00 (s, 1H), 5.30 (t, 2H), 5.19 (s, 1H), 4.20 (q, 1H), 4.04 (d, 1H), 3.98 (s, 1H), 2.10 (d, 6H, 2xCH₃), 2.02 (s, 3H, CH₃), 1.98 (s, 3H, CH₃), 1.93 (s, 3H, CH₃)

$^{13}\text{C-NMR}$ (δ , 20 °C, CDCl_3 , 75.53 MHz): 169.56, 168.93, 168.69, 168.50, 167.03, 89.58, 69.59, 67.73, 67.32, 64.51, 61.07, 19.82, 19.73, 19.67, 19.63, 19.60

2-(Acetoxymethyl)-6-(2-((bicyclo[2.2.1]hept-5-ene-2-carbonyl)oxy)ethoxy)-tetrahydro-2H-pyran-3,4,5-triyl triacetate

The whole reaction was performed under nitrogen atmosphere in a dry flask. The mannose (0.6 g, 1.53 mmol, 1 eq) and the *endo,exo*-bicyclo[2.2.1]hept-5-ene-2,3-dicarboxylic acid-1-ethanol (0.42 g, 2.31 mmol, 1.5 eq) were dissolved in acetonitrile (dry, 10mL). The mixture was cooled and BF₃·OEt₂ (1 mL, 8.10 mmol, 5 eq) was added drop wise till the reaction got dark-orange. The reaction was stirred for 36 hours and the progress controlled via TLC in CH/EA 1:1. For the work up the reaction was cooled

again and dichloromethane was added and extracted with NaHCO_3 . It was dried with Na_2SO_4 , filtered and the solvent was removed. The crude product (1 g) was dissolved in cyclohexane and purified by flash column chromatography (CH/EA 5:1→2:1) TLC CH/EA 1:1.

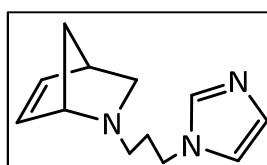


$^1\text{H-NMR}$ (δ , 20 °C, CDCl_3 , 300.36 MHz): 6.19 (s, 1H, nb⁵), 6.07 (s, 1H), 5.92 (s, 1H, nb⁶), 5.34-5.25 (m, 3H), 4.86 (s, 1H), 4.32-3.99 (m, 6H), 3.20 (s, 1H, nb), 2.92 (s, 1H, nb), 2.16 (d, 3H, CH_3), 2.08 (d, 3H, CH_3), 2.03 (d, 3H, CH_3), 1.98 (d, 3H, CH_3), 0.89 (d, 2H, nb⁷)

$^{13}\text{C-NMR}$ (δ , 20 °C, CDCl_3 , 75.53 MHz): 174.55, 170.6, 169.98, 169.82, 169.68, 137.87 (nb⁵), 132.38 (nb⁶), 97.59 (C1), 70.59, 68.73, 68.57, 66.14, 62.85, 62.08, 49.55 (nb⁷), 45.69, 43.29, 42.51, 30.35 (CH_3), 29.23 (nb³), 20.26, 20.75, 20.67

2-(3-(1H-Imidazol-1-yl)-propyl)-2-azabicyclo[2.2.1]hept-5-ene

1-Amino-3-propylimidazol (4.77 mL, 0.039 mol, 1 eq) was dissolved in about 100 mL of H_2O dest. and protonated with HCl (6 mL, 0.19 mol, 5 eq)(not really acidic, but a bit more than neutral). Furthermore, 37 % formaldehyde (1.32 mL, 0.047 mol, 1.2 eq) was adjoined and after that the freshly distilled cyclopentadiene (19.3 mL, 0.24 mol, 6 eq) was added in small amounts of 2 mL. The flask was closed with a septum because of the volatile cyclopentadiene and stirred for 18 hours at room temperature. The reaction was controlled via TLC in DCM/MeOH 5:1. For the purification dichloromethane was added and extracted one time so that the cyclopentadiene is in the organic phase. Then NaOH was added to the water to make it basic and extracted again with dichloromethane. After that the organic phase was dried, filtered and the solvent was removed. If it was not just the product after these steps you can stir it again with cyclopentadiene and formaldehyde to obtain a purer product.

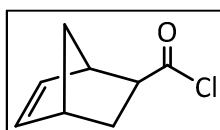


$^1\text{H-NMR}$ (δ , 20 °C, CDCl_3 , 300.36 MHz): 7.44 (s, 1H, N-CH-N), 7.02 (s, 1H, N-CH-CH), 6.89 (s, 1H, N-CH-CH), 6.28 (dd, 1H, nb⁵), 5.93 (dd, 1H, nb⁶), 4.08-3.91 (m, 2H, $\text{CH}_2\text{-N}^{\text{tri}}$), 3.77 (s, 1H, nb¹), 3.11 (dd, 1H, nb⁷), 2.90 (s, 1H, nb⁴), 2.34 (dt, 1H, nb³), 2.04 (q, 1H, nb³), 1.85 (q, 2H, $\text{CH}_2\text{-CH}_2\text{-CH}_2$), 1.54 (d, 1H, $\text{CH}_2\text{-CH}_2\text{-CH}_2$), 1.41-1.34 (m, 2H, $\text{CH}_2\text{-CH}_2\text{-CH}_2$, nb⁷)

$^{13}\text{C-NMR}$ (δ , 20 °C, CDCl_3 , 75.53 MHz): 137.29 (N-CH-N), 136.18 (nb), 130.43 (nb), 129.30 (CH-N-CH), 118.84 (CH-N-CH-CH), 64.63 (nb¹), 52.40 (nb⁷), 51.34 (CH₂-CH₂-CH₂), 48.22 (CH₂-CH₂-CH₂), 44.80 (nb³), 43.73 (nb⁴), 30.37 (CH₂-CH₂-CH₂)

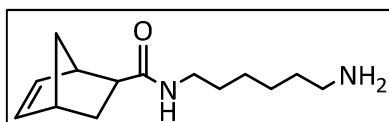
Bicyclo[2.2.1]hept-5-ene-2-carbonyl chloride

In a three-neck-round-bottom flask CP (5.5 mL, 0.066 mol, 3 eq) was provided in dichloromethane (30 mL, dry). The whole reaction was performed under nitrogen atmosphere. The acryloylchloride (1.79 mL, 0.022 mol, 1 eq) was added drop wise under cooling conditions. Afterwards the reaction was stirred for one hour at room temperature and the solution was in situ used for the next reaction step. TLC in CH/EA 1:1.



***N*-(6-Aminoethyl)bicyclo[2.2.1]hept-5-ene-2-carboxamide**

The hexamethylenediamine (5.9 g, 0.051 mol, 2.3 eq) was dissolved in dichloromethane (30 mL) and under cooling conditions the in situ reaction of bicyclo[2.2.1]hept-5-ene-2-carbonyl chloride was added drop wise. A white solid was formed and the whole reaction was stirred for three hours. The remaining solvent was removed and the dry product was dissolved in ethyl acetate and two times extracted with NaOH. Afterwards it was dried, filtered and the solvent was removed. TLC: CH/EA 1:1.

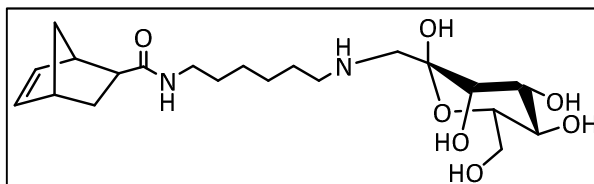


$^1\text{H-NMR}$ (δ , 20 °C, CDCl_3 , 300.36 MHz): 6.20 (q, 1H, nb), 5.94 (q, 1H, nb), 5.59 (s, 1H, NH), 3.17 (q, 2H), 3.11 (s, 1H), 2.87 (s, 1H), 2.84 (q, 1H), 2.66 (t, 2H), 1.51-1.25 (m, 14H)

$^{13}\text{C-NMR}$ (δ , 20 °C, CDCl_3 , 75.53 MHz): 174.07 (C=O), 137.71 (nb), 132.27 (nb), 50.04 (nb), 46.22 (nb), 44.82 (nb), 42.72 (nb), 42.21, 38.88, 33.82, 29.87, 29.57, 26.78, 25.96

(6-Desoxy-manno-hexose)-1-methylamino)hexyl)bicyclo[2.2.1]hept-5-ene-2-carboxamide

The D-mannose (0.4 g, 2.22 mmol, 1 eq) and the *N*-(6-aminoethyl)bicyclo[2.2.1]hept-5-ene-2-carboxamide (0.64 g, 2.7 mmol, 1.2 eq) were added to ethanol (15 mL) with a few drops of H₂O dest. for a better solubility. Then acetic acid (0.2 mL, 2.7 mmol, 1.2 eq) was added drop wise and the reaction mixture was stirred for three days at 40°C. TLC: DCM/MeOH 10:1. The solvent was removed and a column chromatography was performed with 1.25 g crude product in a CH/EA (10:1-2:1) mixture.



¹H-NMR (δ, 20 °C, CDCl₃, 300.36 MHz): 6.02 (q, 1H, nb), 5.72 (q, 1H, nb), 3.96-3.40 (m, 4H), 3.17 (s, 1H), 2.98 (m, 5H), 2.80-2.69 (m, 4H), 1.78-1.68 (m, 2H), 1.52 (q, 2H), 1.36 (q, 4H), 1.32-1.15 (m, 10H)

¹³C-NMR (δ, 20 °C, CDCl₃, 75.53 MHz): 176.61 (C=O), 138.59 (nb⁵), 133.05 (nb⁶), 96.95 (C-1), 84.30 (C-5), 71.38, 71.12, 70.59 (C-2, C-3, C-4), 64.74 (CH₂-C-5), 54.51 (NH-CH₂-C1), 50.58 (NH-CH₂-chain), 47.68, 45.41, 44.03, 40.70, 40.24, 30.33, 30.15, 28.54, 27.38, 27.06

Chapter 2

Perylenes as sensor materials or ROMP as a precision polymerization technique toward molecular probes

Introduction

Perylenes

To start this chapter, I first want to clarify the definition of the used perylenes. Perylene-3,4,9,10-tetracarboxdiimides or perylene-3,4,9,10-tetracarboxylic bisimide, are two different names, which are used equally in literature and the abbreviations are then PDI or PBI. However, in this thesis –the more commonly used term diimide will be used which is also in accordance with IUPAC.

The perylene ring system is planar, symmetrical to inversion and can be elongated to poly(peri-naphthalenes), which represents the so called rylene dyes from which perylene is the smallest and most important homolog.⁵⁷ The primary starting material for synthesizing symmetrical or unsymmetrical PDI derivatives, is PTCDA (*cf.* Figure 9). For many applications the unsymmetrical PDI derivatives, with different substituents at the imide position, are more useful because their solubility is better than that of symmetrical diimides. The symmetrical dyes with no substituents at the bay area are often insoluble due to π -stacking of the molecules.

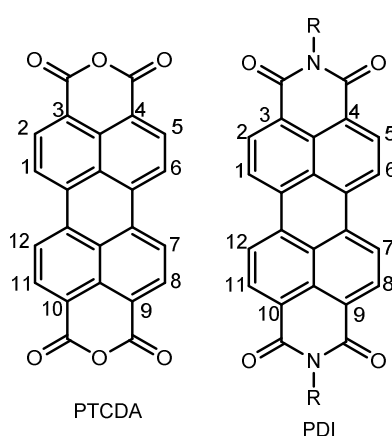


Figure 9: Starting materials for perylene syntheses

⁵⁷ Schmidt, C.D.; Hirsch, A. *Ideas in Chemistry and Molecular Sciences: Advances in Synthetic Chemistry*, Edt. Bruno Pignataro, 2010, Wiley VCH.

PDI is a widely known dye class, and was first prepared in 1912.⁵⁸ Due to their great thermal stability, chemical inertness and strong electron-accepting character,⁵⁹ in combination with their photochemical stability, perylene-3,4,9,10-tetracarboxylic acid diimide derivatives have been extensively studied as industrial colorants, as dyes (soluble) and pigments (insoluble).⁶⁰ More advanced applications in various optical and electronic include devices such as n-type semiconductors in organic field effect transistors (OFETs)⁶¹ fluorescent solar collectors,⁶² optical switches,⁶³ dye lasers or in automotive industry. In analytical chemistry they are often used for high sensitive detection schemes because of their high absorption coefficients, strong fluorescence with visible ranges and high photostability.⁶⁴ The practical use of PDIs is often inhibited by their insolubility, particularly in polar solvents, but it can be taken advantage for some unique applications – such as incorporation of PDI in hydrophobic sensor membranes.⁶⁵ There is also a great demand of solubilization of PBI dyes in aqueous solution in their monomeric form because of their good fluorescent properties. For example, the high hydrophobicity of PBI might inhibit their contribution to biological analysis.⁶⁶

Syntheses of PDI derivatives

PDI derivatives can be obtained by a condensation reaction between PTCDA and alkyl amines normally in high yield.⁶⁷

⁵⁸Kardos, M. DR P276357. DR P276357, 1913.

⁵⁹Würthner, F. *Chem. Commun.*, **2004**, 1564–1579.

⁶⁰Langhals, H. *Heterocycles*, **1995**, *40*, 477–500.

⁶¹Ahrens, M. J.; Fuller, M. J.; Wasielewski M.R. *Chem. Mater.*, **2003**, *15*, 2684–2686.

⁶²Langhals, H. *Nachrichten aus Chemie*, **1980**, *28*, 716.

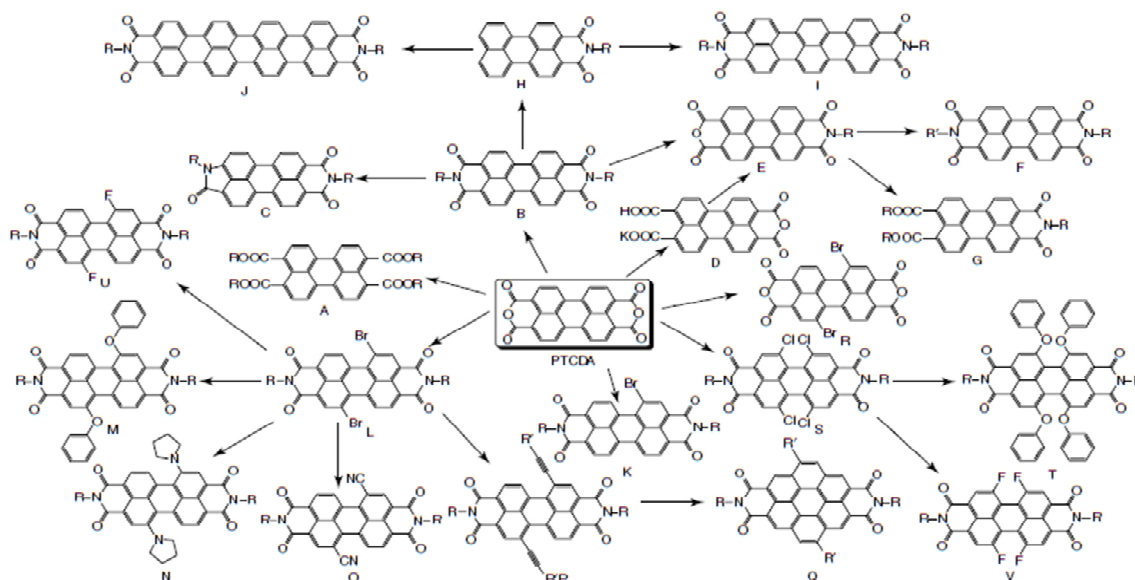
⁶³O’Neil, M.P.; Niemczyk, M.P.; Svec, W.A.; Wasielewski, M.R. *Science*, **1992**, *63*, 257.

⁶⁴Langhals, H. *Color Chemistry. Synthesis, Properties and Applications of Organic Dyes and Pigments*. 3rd revised edition, by Heinrich Zollinger, **2004**, 43.

⁶⁵Neelakandan, P.P.; Pan, Z.; Hariharan, M.; Zheng, Y.; Weissman, H.; Rybtchinski, B.; Lewis, F.D., *J. Am. Chem. Soc.*, **2010**, *132*, 15808-15813.

⁶⁶Soh, N., Ueda, T. *Talanta*, **2011**, *85*, 1233-1237.

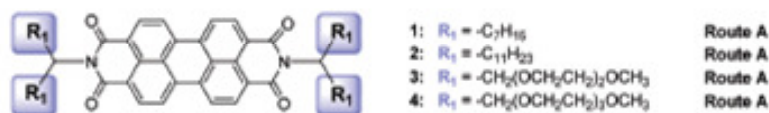
⁶⁷Nguyen, D.C.; Keller, R.A.; Jett, J.H.; Martin, J. C. *Anal. Chem.*, **1987**, *59*, 2158.



Scheme 6: Possible reactions of perylene-3,4,9,10-tetracarboxylic acid dianhydride (PTCDA)⁵⁷

Although pigment industry requires insoluble and high melting PDI based materials the current work for different chemical and analytical applications requires PDIs with reasonable solubility in common solvents. In the 1990s Langhals and co-workers first described organosoluble symmetrical PDIs with branched alkyl or aryl substituents like so called swallow tail substituents or *ortho* substituted *N*-aryl groups⁶⁸, which are effective solubilizing groups, in the imide positions.

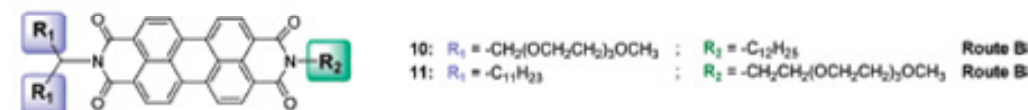
Type I: symmetrically *N*-substituted PBIs (2 x swallowtail)



Type II: unsymmetrically *N*-substituted PBIs (2 x swallowtail)



Type III: unsymmetrically *N*-substituted PBIs (swallowtail + linear)



Scheme 7: Overview of symmetrically and asymmetrically *N*-substituted perylene bisimides (PBIs) classified according to the nature of respective substituents⁶⁹

⁶⁸ Rademacher, A.; Märkle, S.; Langhals, H. *Chem. Ber.*, **1982**, *115*, 2927–2934.

⁶⁹ Wicklein, A.; Lang, A.; Muth, M.; Thelakkat, M. *J. Am. Chem. Soc.*, **2009**, *131*, 14442–14453.

Scheme 7 is taken from the work of Wicklein et al. who wanted to introduce liquid crystallinity by avoiding substitution at bay positions to maintain the planarity and strong π - π interactions, which favor intermolecular order and charge carrier transport. Oligoethylenglycolether swallow tail moieties facilitate thermotropic liquid crystalline behavior in most cases and unsymmetrical substitution allows the tuning of the mesophase width. The strong degree of crystallinity was weakened here by the approach of swallow tail substitution.

In 1985 Langhals reported PDIs which are substituted with 2,6-diisopropylphenyl and 2,5-di-tert-butylphenyl and are highly soluble in common organic solvents and display a bright color with strong fluorescence.⁷⁰ Such bulky groups are limiting the face to face π - π stacking because they are forced out of the plane of the PDI chromophore.⁷¹ However substituents in both positions affect solubility and aggregation behavior but variation of substituents at the imide position only shows limited effects on the optical and redox properties at molecular level.⁷² Based on this knowledge, solubility, aggregation and molecular packing in the solid state can be tuned independently of the molecular electronic properties.

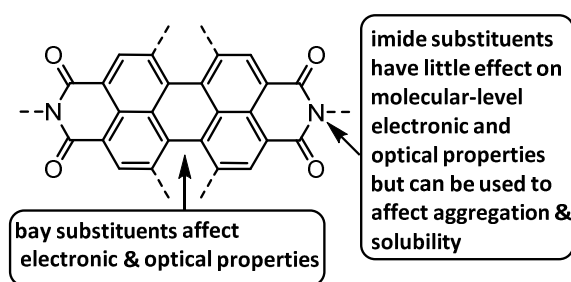


Figure 10: Effects of imide and bay substituents⁷²

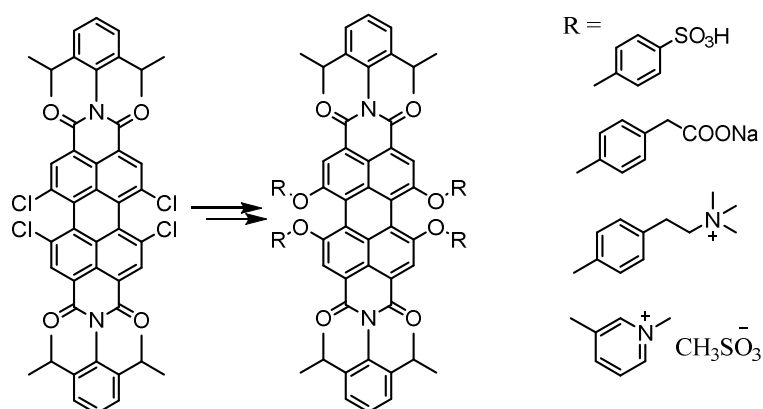
As water is a cheap, nonpolluting, easily available solvent, it should be also aspired to create water-soluble building blocks for industrial applications.⁵⁷ To achieve water soluble perylene dyes, the bay position is functionalized with sulfonic acid groups, poly(ethylene oxide) or quaternized amines to prevent aggregation which was introduced by Müllen and co-workers but also these water-soluble derivatives tend to aggregate in aqueous solution which causes fluorescence quenching.⁷³

⁷⁰ Langhals, H. *Chem. Ber.*, **1985**, *118*, 4641.

⁷¹ Wescott, L.D.; Mattern, D.L. *J. Org. Chem.*, **2003**, *68*, 10058–10066.

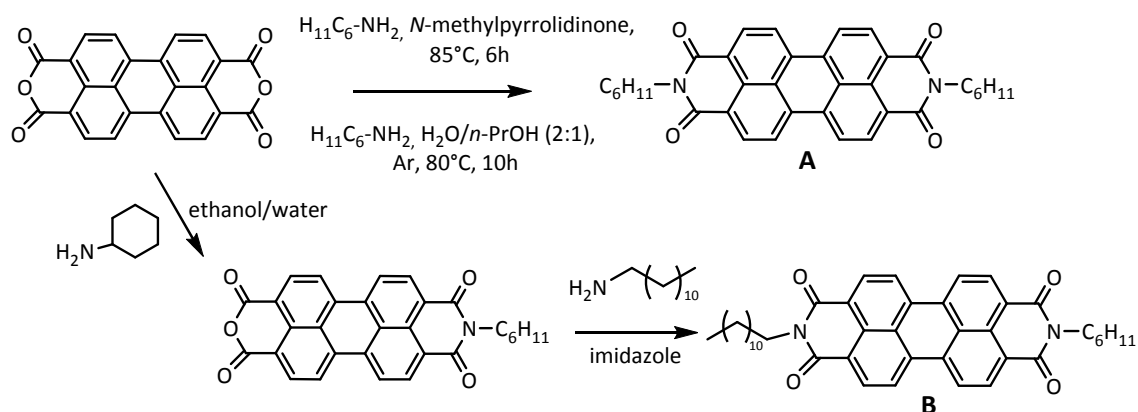
⁷² Huang, C.; Barlow, S.; Marder, S.R. *J. Org. Chem.*, **2011**, *76*, 2386–2407.

⁷³ Schmidt-Mende, L.; Fechtenkotter, A.; Müllen, K.; Moons, E.; Friend, R.H.; MacKenzie, J.D. *Science*, **2001**, *293*, 1119.



Scheme 8: Synthesis of water-soluble perylene diimides bearing polar substituents in the bay region⁷³

Long chained alkyl groups lead to a decreased solubility but a secondary alkyl rest with two chains leads to an increasing solubility. The long alkyl chains lead to lower solubility which decreases from hexyl to dodecyl with a factor 3 and also the aliphatic groups are more photo stable than aryl groups. Cyclic groups therefore lead to a good solubility in organic solvents.⁷⁴ As shown in Scheme 9 there are different synthetic routes for getting a mono- or di-cyclohexyl substituted perylene derivative. Cycloalkanes represent a special class of side-chains that possess a crossed orientation with the perylene plane at about 90°, thus enforcing rotated stacking between the molecular planes so as to minimize the steric hindrance caused by the cycloalkane rings.⁷⁵



Scheme 9: Cyclohexyl as solubilizing group^{76 77}

II-stacking

Aryl or similar groups at the bay positions are forced out of the PDI plane by steric interactions. Furthermore also smaller substituents such as bromo or chloro can lead to twisting of the two naphthalene half units in PDIs. If particularly bulky imide

⁷⁴ Demmig, S.; Langhals, H.; *Chem. Ber.*, **1988**, *121*, 225-230.

⁷⁵ Che, Y.; Yang, X.; Balakrishnan, K.; Zuo, J.; Zang, L. *Chem. Mater.*, **2009**, *21*, 2930-2934.

⁷⁶ Würthner, F.; Stepanenko, V.; Chen, Z.; Saha-Möllner, C.R.; Kocher, N.; Stalke, D. *J. Org. Chem.*, **2004**, *69*, 7933-7939.

⁷⁷ Huang, H.; Che, Y.; Zang, L. *Tetrahedron Lett.*, **2010**, *51*, 6651-6653.

substituents are used, the parallel stacking of PDI can be completely avoided due to the steric hindrance to give perylene dyes instead of perylene pigments.⁷⁸ Both effects disrupt π - π stacking and bulky groups at the bay area can increase the solubility in several orders of magnitude.⁷⁹ However this ability of the perylenes is a useful electronic property because they crystallize in tightly packed one dimensional π - π stacks. The small distance of only 3.2 Å facilitates π -orbital, overlap and therefore it is regarded as the “archetype molecular semiconductor”.⁸⁰

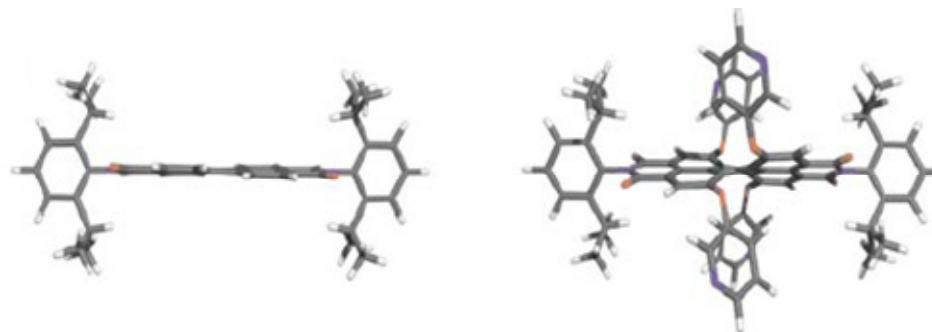


Figure 11: Three-dimensional structure of PDI with no substituents attached at the bay region (planar) on the left and three-dimensional structure with four substituents attached at the bay region (twisted scaffold)⁸¹

Synthesis of asymmetric PDIs

Synthesis of unsymmetrical substituted PDIs is more difficult because of differences in reactivity of the amines with PTCDA, and the dominant species are always the two symmetrical PDIs. One method is a partial hydrolysis of symmetrical PDIs by partial saponification with conc. sulphuric acid at high temperatures or under strong basic conditions with KOH in *t*-BuOH. An alternative route is to use the imide anhydride as building block, in which the anhydride is used for condensation methods with amines, whereas the imide offers possibility for introduction of a *N*-substituent via nucleophilic substitution. Another practical approach was described by Tam-Chan and co-workers namely partial hydrolysis of PTCDA to a mixed anhydride-dicarboxylate salt followed by successive imidization reactions.^{82 83 84} In literature the most common way to synthesize perylene derivatives is condensation of primary amines with PTCDA in molten imidazole with zinc acetate. This way offers high yields but only symmetrically substituted products. Also limited amounts of one amine offers the disubstituted product and the educt.

⁷⁸ Rademacher, A.; Maerkle, S.; Langhals, H. *Chem. Berich.* **1982**, *115*, 2927.

⁷⁹ Würthner, F.; Sautter, A.; Schilling, J. *J. Org. Chem.*, **2002**, *67*, 3037–3044.

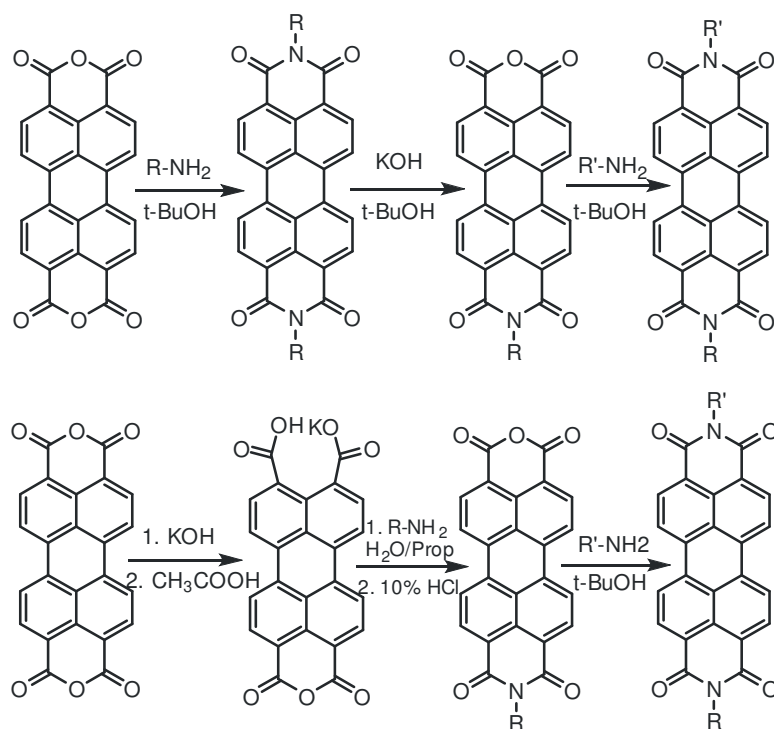
⁸⁰ Würthner, F.; Chen, Z.; Dehm, V.; Stepanenko, V. *Chem. Commun.*, **2006**, *11*, 1188–1190.

⁸¹ Kohl, C.; Weil, T.; Qu, J.; Müllen, K. *Chem. Eur. J.*, **2004**, *10*, 5297–5310.

⁸² Iverson, I.K.; Tam-Chang, S.-W. *J. Am. Chem. Soc.*, **1999**, *121*, 5801–5802.

⁸³ Lindner, S. M.; Kaufmann, N.; Thelakkat, M. *Org. Electr.*, **2007**, *8*, 69–75.

⁸⁴ Sommer, M.; Lang, A. S.; Thelakkat, M. *Angew. Chem. Int. Ed.*, **2008**, *47*, 7901–7904.



Scheme 10: Syntheses of asymmetric perylenes

Tröster et al. used the not very soluble potassium salt of PTCDA (Scheme 10) which is produced by adjusting the pH-value via acetic acid and potassium hydroxide to the right color.⁸⁵ The salt is condensed with aliphatic primary amines which are not too hydrophobic. A synthesis with sterically hindered or hydrophobic amines is not possible. A partial saponification by Nagao and Misono⁸⁶ is performed with sulphuric acid at high temperatures, aromatic rests get sulfonated and the imide is not splitted. Under basic conditions a partial saponification with KOH is possible.

These procedures are all multistage reactions with complex and difficult purification steps, the synthetic work is “dirty” and really time consuming with often not really high yields and despite the aliphatic or aromatic rests the solubility of the perylene is still not very high.

PET effect

Photoinduced electron transfer can be described most simply as the movement of an electron, caused by the absorption of light, from an electron-rich species (donor) to an electron deficient species (acceptor). The first law of photochemistry tells us that $D + A \rightarrow D^+ + A^-$ a photoinduced process must be initiated by the absorption of light.⁸⁷

⁸⁵ Tröster, H. *Dyes Pigm.*, **1983**, 4, 171.

⁸⁶ Nagao, Y.; Misono, T. *Dyes Pigm.* **1984**, 5, 171.

⁸⁷ Fox, M.A. *Photochem. and Photobiol.*, **1990**, 52, 617-627.

A single simple picture encapsulates the design of fluorescent PET-sensors. The fluorophore-spacer-receptor format is a rational combination of three components. The rationale is contained in Figure 12.⁸⁸

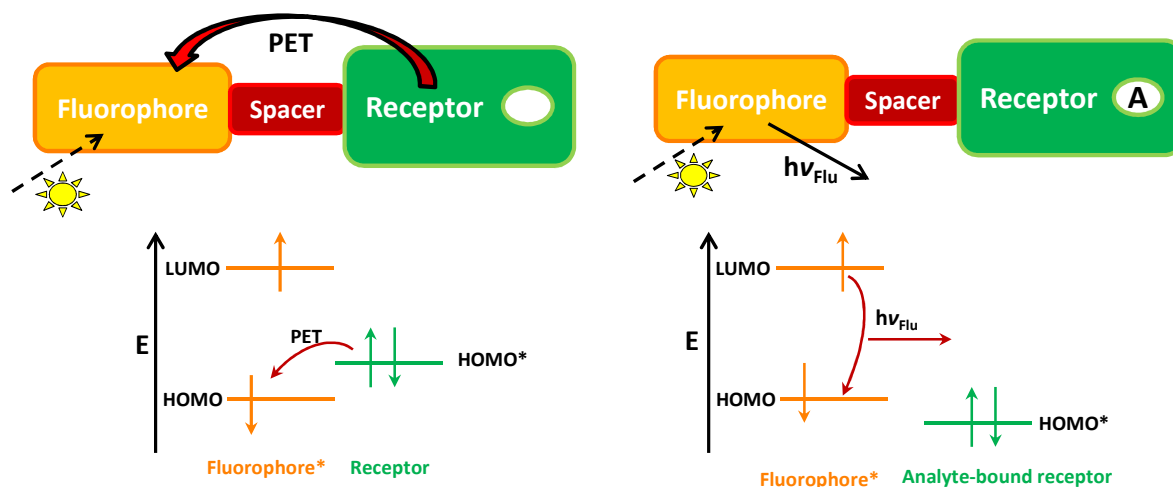


Figure 12: PET sensor concept with molecular orbital scheme⁸⁸

Via molecular orbital energy diagrams in the off state the bracketing of the receptor HOMO by the frontier orbitals of the fluorophore is noted. In the on state there is a stabilization of the analyte-bound receptor's HOMO to lie below the fluorophore's HOMO. In the fluorophore-spacer-receptor scheme the electron transfer from the analyte free receptor to the fluorophore and therefore PET quenching can be seen. When an analyte is bound to the receptor the electron transfer is blocked and fluorescence can be seen. Each of the three components within this sensor format deserves the designer's attention. The analyte to be sensed determines the choice of the receptor. The reciprocal of the binding constant for the receptor analyte interaction determines the median analyte concentration to be sensed.^{89,88} Also the selectivity and possible interferences have to be considered. However, the supramolecular nature of the system can be best preserved by interposing spacer between the original units.⁸⁹

The spacer concept was really interesting and important in our case. In a normal system the ease of sensor synthesis dictates the choice of spacer but the more fundamental determinant is that the spacer must be short enough to permit reasonably fast PET rates in the off state of the sensor.⁹⁰ Also the fluorophore-receptor interaction must be able to transcend the spacer, which PET fits well because it is an enduringly long-range process.⁹¹ Even virtual spacers can be used provided that other means, such as sterically-induced orthogonalization, maintains the separation between

⁸⁸ Silva, A.P.D.; Moody, T.S.; Wright, G.D. *Analyst*, **2009**, *134*, 2385-2393.

⁸⁹ Lehn, J.-M., *Supramolecular Chemistry*, VCH Weinheim, **1995**.

⁹⁰ Closs, G.L.; Miller, J.R. *Science*, **1988**, *240*, 440-447.

⁹¹ Paddon-Row, M.N. *Acc. Chem. Res.*, **1994**, *27*, 18-28.

the fluorophore and the receptor.⁹² The spacer is important to obtain a difference in the fluorescence quantum yields as Onoda et al. showed. A too short spacer between fluorophore and receptor gives no differences between the fluorescence quantum yields in the on and off state of the sensor.⁹³ The idea behind this sensor system is that in ideal cases, the UV-Vis absorption spectra should remain virtually untouched by the analyte, as do the emission spectra except as mentioned before their quantum yields.⁹⁴ Failure to meet these high standards is usually due to lumophore-receptor interactions (other than PET) crossing the spacer.⁹⁵

Optical pH-sensors

Optical pH-sensors based on fluorescence are attractive because real-time measurement can be performed in a virtually contactless way. Moreover, optical sensors are in contrast to electrochemical pH-sensors not sensitive to electromagnetic interferences and can feature higher sensitivity within their dynamic range.⁹⁶ However, most optical sensors suffer from drawbacks like their limited photostability, sometimes moderate brightness and cross sensitivity to ionic strength. A problem here can also be the different spectral properties in the protonated and deprotonated state because the protonizable function is located within the chromophore. PET probes are attractive because they possess fluorescence switch on/off character and therefore a high sensitivity. The process is a redox reaction that can be found within the same molecule but in most cases is not integrated into it.⁹⁷

The pH-sensitivity can be achieved as mentioned before via the photoinduced electron transfer, which has been reported for pH,⁹⁸ but also for cations⁹⁹ and anions,¹⁰⁰ thiols¹⁰¹ and others. In our system a fluorescent moiety is combined with an amine with a free electron pair as electron donor, which quenches the excited state of a fluorophore by electron transfer. Modulating the oxidation potential of the PET acceptor, e.g. in a signaling event, such as protonation or binding of an analyte, suppresses the PET process, which has emission increase as a consequence.¹⁰² An advantage of PET based systems is their modularity,¹⁰³ it is possible to select

⁹² Jonker, S.A.; Ariese, F.; Verhoeven, J.W. *Rec. Trav. Chem. Pays Bas*, **1989**, *108*, 109-115.

⁹³ Onoda, M.; Uchiyama, S.; Santa, T.; Imai, K. *Luminescence*, **2002**, *17*, 11-14.

⁹⁴ Silva, A.P.D.; Silva, S.A.D. *J. Chem. Soc. Chem. Commun.*, **1986**, 1709.

⁹⁵ Silva, A.P.D.; Gunaratne, H.Q.N.; Habib-Jiwan, J.-L.; McCoy, C.P.; Rice, T.E.; Soumillion, J.P. *Angew. Chem. Int. Ed.*, **1995**, *34*, 1728.

⁹⁶ Aigner, D.; Borisov, S. M.; Klimant, I. *Anal. Bioanal. Chem.*, **2011**, *400*, 2475-2485.

⁹⁷ Bissel, R.A.; Silva, A.P.D.; Gunarante, H.Q.N.; Lynch, P.L.M.; Maguire, G.E.M.; Sandanayake, K.R.A.S. *Chem. Soc. Rev.*, **1992**, *21*, 187-195.

⁹⁸ Niu, C.G.; Zeng, G.M.; Chen, L.X.; Shen, G.L.; Yu, R.Q. *Analyst*, **2004**, *129*, 20-24.

⁹⁹ Hennrich, G.; Sonnenschein, H.; Resch-Genger, U. *J. Am. Chem. Soc.*, **1999**, *121*, 5073-5074.

¹⁰⁰ Gunnlaugsson, T.; Davis, A.P.; Hussey, G.M.; Tierney, J.; Glynn, M. *Org. Biomol. Chem.*, **2004**, *2*, 1856-1863.

¹⁰¹ Yi, L.; Li, H.; Sun, L.; Liu, L.; Zhang, K.; Xi, Z. *Angew. Chem. Int. Ed.*, **2009**, *22*, 4034-4037.

¹⁰² Gallas, K.; Knall, A.C.; Scheicher, S.R.; Fast, D.E.; Saf, R.; Slugovc, C. *Macromol. Phys. Chem.*, **2013**,

DOI: 10.1002/macp.201300561.

¹⁰³ Silva, A.P.D.; Gunnlaugsson, T.; Rice, T.E. *Analyst*, **1996**, *121*, 1759-1762.

fluorophore and receptor independently because the spectral properties are at the chromophore part, while the proton affinity lies within the amino functionality (fluorophore-spacer-receptor).⁸⁸ In such a system the combination of different PET-based pH indicators is easy since several with different pK_a values possess virtually identical spectral properties.

A similar concept relies on the well-known circumstance that paramagnetic nitroxide radicals quench fluorescence.¹⁰⁴ This led to the development of profluorescent nitroxides,¹⁰⁵ which can be “switched on”, once the paramagnetic nitroxides are converted into diamagnetic species. This has been used for the detection of e.g. hydroxyl radicals,¹⁰⁶ to study radical formation in polymers,¹⁰⁷ and to selectively detect reducing agents such as glutathione or antioxidants.¹⁰⁸

Results and Discussion

In our contribution, we present a modular approach towards polymeric pH-sensors by combining a perylene-derived monomer with pH-sensitive comonomers. An additional feature is added by copolymerization of monomers bearing oligo(ethylene oxide). Such materials undergo phase separation driven by increasing temperature,⁷ called LCST (lower critical solution temperature) effect.¹⁰⁹

Synthetic strategies for the perylene moiety

The commercially available 1,6,7,12-tetrachloroperylene-3,4,9,10-tetracarboxylic bisanhydride (TCP) was chosen as a starting material for our work due to the chloro substituents at the bay position which increase solubility compared with unsubstituted perylenes. The bay substitution does not affect significantly the spectral properties and also offers the possibility to tune the absorption wavelength and improve photostability.

¹⁰⁴ a) Colvin, M.T.; Giacobbe, E.M.; Cohen, B.; Miura, T.; Scott, A.M.; Wasielewski, M.R. *J. Phys. Chem. A* **2010**, *114*, 1741; b) Zhu, P.; Clamme, J.P.; Deniz, A.A. *Biophys. J.* **2005**, *89*, L37.

¹⁰⁵ Blinco, J.P.; Fairfull-Smith, K.E.; Morrow, B.J.; Bottle, S. E. *Aust. J. Chem.* **2011**, *64*, 373.

¹⁰⁶ Maki, T.; Soh, N.; Fukaminato, T.; Nakajima, H.; Nakano, K.; Imato, T. *Anal. Chim. Acta*, **2009**, *639*, 78.

¹⁰⁷ Blinco, J.P.; Keddie, D.J.; Wade, T.; Barker, P.J.; George, G.A.; Bottle, S.E. *Polym. Degrad. Stab.* **2008**, *93*, 1613.

¹⁰⁸ Pei, D.; Hong, J.; Lin, F.; Shi, Z.; Chen, Z.; Nie, H.; Guo, X. *Chem. Commun.*, **2011**, *47*, 9492.

¹⁰⁹ Gallas, K., Green, J., Knall, A.C., Slugovc, C. Polymer Preprint, ACS Philadelphia **2012**, *pH-sensitive, perylene-based, water soluble copolymers*.

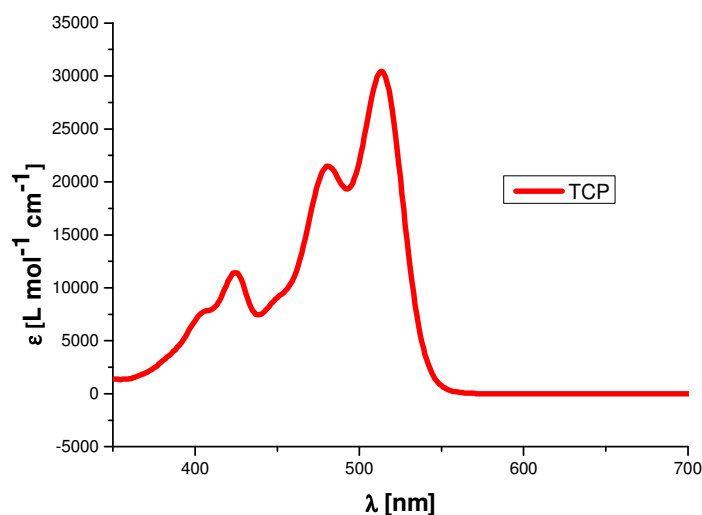
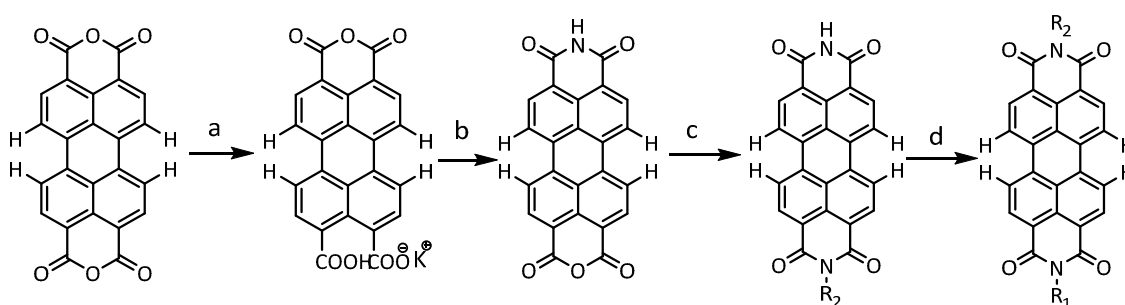


Figure 13: UV-Vis spectrum of tetrachloroperylene

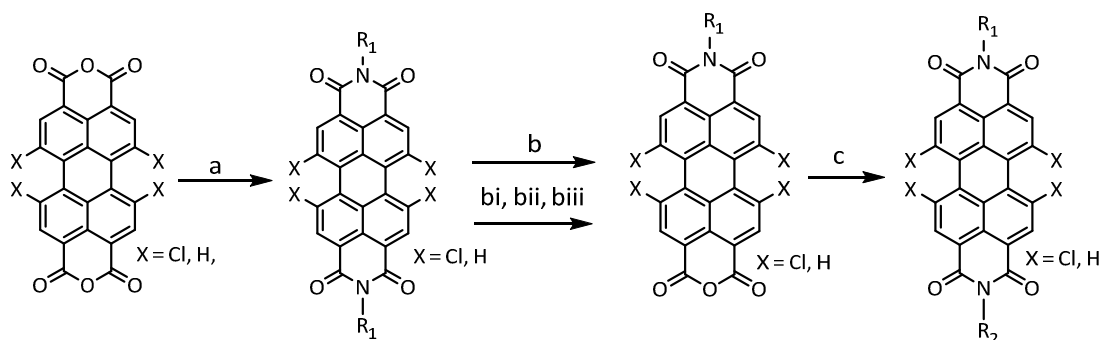
The chloro substituents lead to a twisting of the naphthalene units in the PDI, reduce stacking and so also the solubility of the molecule is increased.

In literature mostly PTCDA is chosen as starting material for perylene syntheses. As mentioned in the introduction chapter, there are many different ways to obtain symmetrical or unsymmetrical molecules. We also tried different synthetic possibilities to obtain the shortest route with the highest product yield.



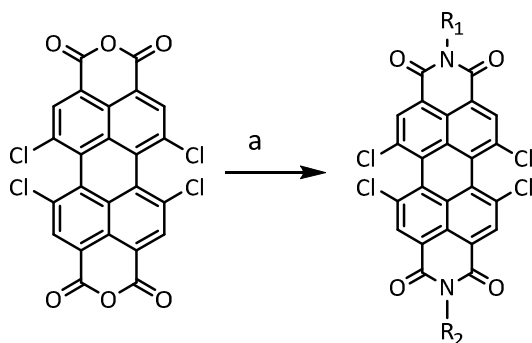
Scheme 11: “Bad” synthetic route to asymmetric perylene derivatives, time consuming, bad yields

- a)⁸⁵KOH, H₂O, reflux, 1h, centrifugation b)¹¹¹ NH₃, K₂CO₃, KOH, H₂O, time-consuming purification c) imidazole, 1.2eq amine-1, 2h, 110°C d)⁶⁹ DMF, KI, K₂CO₃, amine-2
- not possible with tetrachloro-substrate
- overall yield 5%
- the product structure is not proven, no clear NMR



Scheme 12: “Good” synthetic route to asymmetric perylene derivatives, not time consuming but bad yield

- a)¹¹⁰ toluene, 110°C, 2eq amine, ~12h, easy purification with DCM b)¹¹¹ *tert*-butanol, 20eq KOH, CH₃COOH/HCl, column chromatography c) imidazole, 1.2eq amine, 2h, 130°C
- different way for b: bi) 1eq diimid : 400eq KOH in isopropyl-alcohol; bii) 1eq diimid : 50eq KOH in isopropylalcohol; biii) 1eq diimid : 5eq KOH in *tert*-butanol
- overall yield about 8%
- NMR only with impurities, product structure not proven



Scheme 13: Best synthetic route to asymmetric perylene derivatives with good yields and easy purification

- a)¹¹² toluene, amines 1.2eq : 1.2eq, 110°C, 12h, column chromatography
- overall yield 30%
- structure NMR proven

Due to their high degree of functionality perylenes offer possibilities for chemical modifications. However, the preparation of asymmetrically substituted perylene derivatives remains challenging requiring either multi-step transformations via imide-

¹¹⁰ Langhals, H. *Helvetica Chimica Acta*, **2005**, *88*, 1309 – 1343.

¹¹¹ Kaiser, H.; Lindner, J.; Langhals, H. *Chem.Ber.*, **1991**, *191*, 529 -535.

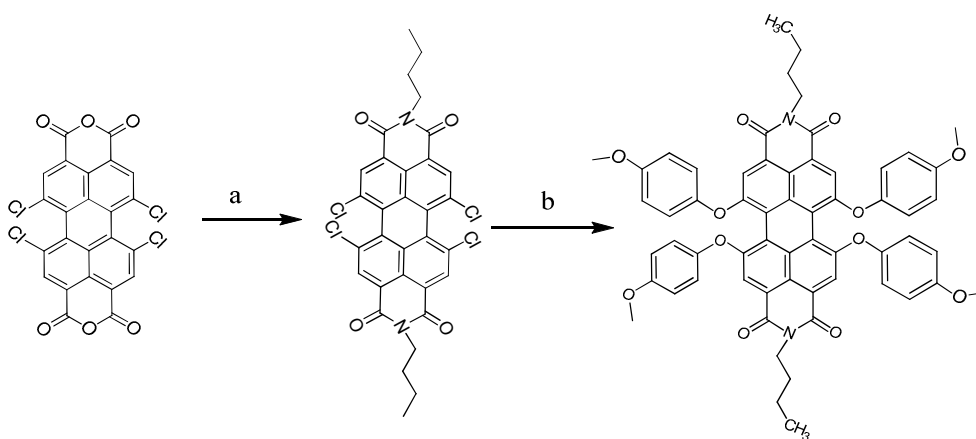
¹¹² Leroy-Lhez, S.; Baffreau, J.; Perrin, L.; Levillain, E.; Allain, M.; Blesa, M.; Hudhomme, P. *J. Org. Chem.*, **2005**, *70*, 6313-6320.

anhydride intermediates or preparation of a statistical mixture with subsequent purification steps.⁶⁹ As shown in the Scheme 11 and Scheme 12 and also described in the introduction, the preparation of an unsymmetrical perylene was at first obtained with the most common methods described in literature. The syntheses are really time-consuming and the characterization during the synthetic work via TLC is insufficient, for proof of conversion. It is sometimes a more alchemistic way of work and also the purification is non-satisfying, due to bad filtration and solubilization properties of the intermediates. Solid phase reactions with imidazole are normally very promising but with the small amounts of educts, which were used due to the costs of the perylene educts and the many different ideas, it was not possible to get a promising product and also the purification methods were not good enough to obtain a pure product.

So a different approach called the mixed amine approach was used, therefore the tetrachlorosubstituted perylene derivative was used as educt. The TCP was treated with an equimolar amount of *n*-butylamine and ethanolamine in this case. A general overview of this method with the reaction conditions is given in Scheme 13. Due to the theoretical composition of AA/AB/BB which leads to a ratio of 25:50:25, the possible yield here is 50%, in our case it was about 35-40% which is much better than in all the other synthetic cases, which have also more steps and worse purification possibilities.¹¹² This method was used in this publication for every preparation of an unsymmetrical perylene.

PET functionalities were attached at the imide position because due to nodes in the molecular orbitals located at the nitrogen atoms, spectral properties are not influenced by imide substituents.¹¹³ In unsymmetrically substituted PDI dyes, one imide position can be used to incorporate a PET acceptor to render the molecule pH sensitive whereas the second position can be occupied by a group which enhances solubility and provides sufficient lipophilicity, like an aliphatic chain. However it was also found that the reaction with aliphatic amines was easier than with aromatic amines. However, there were also approaches of substituting the bay area, because of better solubility and also to maybe have a different UV-Vis absorption. In Scheme 14 the mixed amine approach with *n*-butylamine and a further substitution of the bay area is shown.

¹¹³ Langhals, H.; Demmig, S.; Huber, H. *Spectrochim. Acta Mol. Spectros.* **1988**, *44*, 1189-1193.



Scheme 14: Synthetic route to bay-position substituted perylenes (special case for *n*-butylamine)

- a) mixed amine approach with *n*-butylamine, b)⁹⁶ 4eq *p*-methoxyphenol, K₂CO₃, NMP, 170°C, 12h
- yield: 10%, NMR good
- bathochromic shift in the UV-Vis spectrum compared to TCP

The expected improvement in the solubility of the molecule are not given, furthermore the yield is not good and also the strong bathochromic shift shown in the UV-Vis spectrum of the *p*-methoxyphenol substituted perylene seemed to be not that promising. Therefore bay-area substitutions were not pursued as a synthetic strategy.

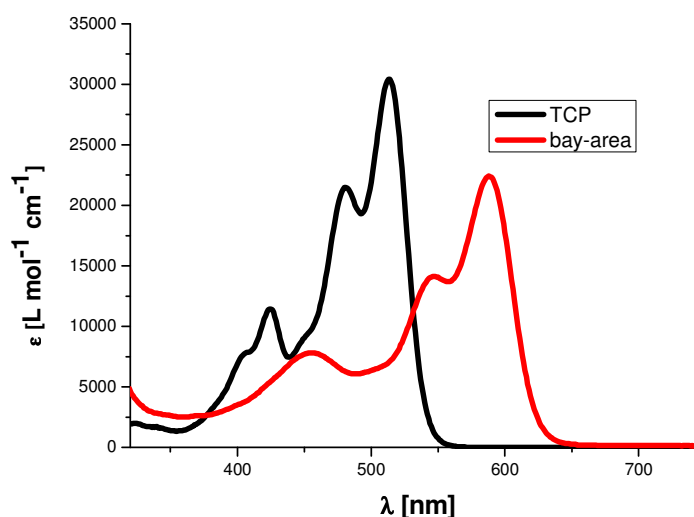
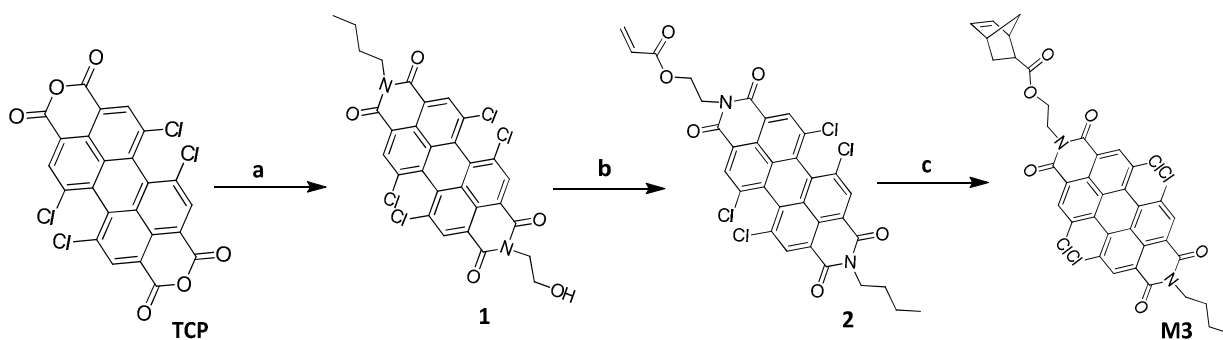


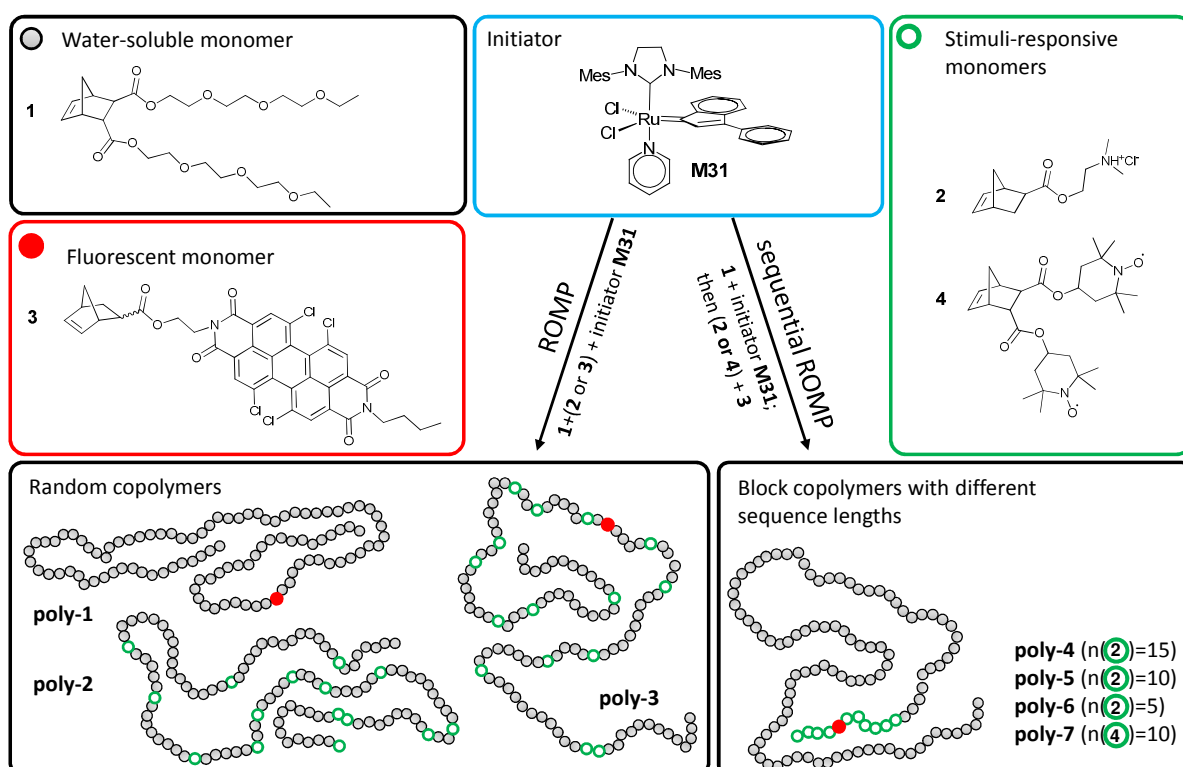
Figure 14: UV-Vis spectrum of the substituted bay area derivative. Replacement of the chlorine atoms led to a strong bathochromic shift.

For the norbornene derivative now all the chemical improvements were tested and the synthesis in Scheme 15 was chosen to be the best alternative for a fast and cheap reaction path with good overall yields and the expected spectral properties.

Scheme 15: Synthesis of the perylene-based monomer **M3**.

- a) ethanolamine, *n*-butylamine (1equiv. each), toluene, 80°C, 12 h b) acryloyl chloride, Et₃N, CH₂Cl₂, rt, 2h c) 1.1 equiv. cyclopentadiene (Diels-Alder), CH₂Cl₂, rt, 48h

After using the mixed amine approach the resulting statistical mixture of **2** and the respective symmetrical by-products were purified using flash chromatography. Subsequent esterification with acryloyl chloride followed by a Diels-Alder cycloaddition of cyclopentadiene led to the functional monomer **M3**. The norbornyl moiety makes this compound polymerizable via ROMP (ring-opening metathesis polymerization). Thus, a variety of polymer architectures can be achieved while allowing precise placement of the dye molecules at specific regions in the polymer chain. In this work it was attempted to combine water-soluble (**M1**) with pH-sensitive (**M2**) and fluorescent (**M3**) molecules as different homo, random and block copolymers.

Scheme 16: Synthesis of the different polymer architectures¹⁰²

In this case the pH-sensitive moiety should be variable to get different sensing molecules.¹⁰⁹ The commonly applied fluorophore-spacer-receptor setup¹¹⁴ has the drawback that for each acceptor-fluorophore combination, a sensor dye has to be prepared individually. As mentioned before, the intermolecular PET is, due to the large distance, considered rather inefficient, the modularity of this approach is however intriguing since a large number of combinatorial probes¹¹⁵ can be accessed from several simple compounds. By copolymerization, however, the advantages of both approaches can be combined to obtain efficient probes on a modular basis.

Evolving from copolymerizable PET probes,^{104b} Zhou et al. presented pH-responsive block copolymers derived from a polyethylene glycol macro-initiator and different PET acceptor groups and rhodamine as fluorophore and hypothesized that a block copolymer architecture is favourable because of micellization of the probes.¹¹⁶ Xu et al. used a perylene bisimide-based initiator for the preparation of polymeric, water-soluble pH-sensitive polymers¹¹⁷ to determine the CO₂ concentration in aqueous samples.

ROMP in context with the sensor architecture

Living polymerisation characteristics together with a huge number of available monomeric building blocks and initiators constitute a ring opening metathesis polymerisation (ROMP) toolbox¹⁴ which has been previously shown to enable the preparation of complex macromolecular architectures.¹¹⁸ Thereby, a large repertory of different fluorescent and phosphorescent dyes has become available.¹¹⁹ The high functional group tolerance of ROMP allowed us to combine different responsive units bearing paramagnetic TEMPO groups or PET acceptors with a perylene bisimide-derived fluorescent monomer and oligo(ethylenglycol)-functionalised comonomers to make the resulting functional co-polymers water-soluble. These polymers were then used for the detection of pH and ascorbic acid concentrations in aqueous solution. In previous publications, *endo*-norbornene dicarboxylic acid anhydride was used as starting material¹²⁰ which led to a mixture of *endo,endo*, *endo,exo* and *exo,exo*-

¹¹⁴ Daffy, L.M.; de Silva, A.P.; Gunaratne, H.Q.N.; Huber, C.; Lynch, P.L.M.; Werner, T.; Wolfbeis, O.S. *Chem. Eur. J.*, **1998**, *4*, 1810.

¹¹⁵ Vendrell, M.; Zhai, D.; Er, J.C.; Chang, Y.T. *Chem. Rev.*, **2012**, *112*, 4391.

¹¹⁶ Zhou, K.; Wang, Y.; Huang, X.; Luby-Phelps, K.; Sumer, B.D.; Gao, J. *Angew. Chem. Int. Ed.*, **2011**, *50*, 6109.

¹¹⁷ Xu, L.Q.; Zhang, B.; Sun, M.; Hong, L.; Neoh, K.G.; Kang, E.T.; Fu, G.D. *J. Mater. Chem. A*, **2013**, *1*, 1207.

¹¹⁸ a) Noormofidi, N.; Slugovc, C. *Eur. Polym. J.*, **2010**, *46*, 594. b) Sankaran, N.B.; Rys, A.Z.; Nassif, R.; Nayak, M.K.; Metera, K.; Chen, B.; Bazzi, H.S.; Sleiman, H.F. *Macromolecules*, **2010**, *43*, 5530.

¹¹⁹ a) Knall, A.C.; Schinagl, C.; Pein, A.; Noormofidi, N.; Saf, R.; Slugovc, C. *Macromol. Chem. Phys.* **2012**, *213*, 2618. b) Sandholzer, M.; Lex, A.; Trimmel, G.; Saf, R.; Stelzer, F.; Slugovc, C. *J. Polym. Sci. A Polym. Chem.*, **2007**, *45*, 1336. c) Niedermair, F.; Sandholzer, M.; Kremser, G.; Slugovc, C. *Organometallics*, **2009**, *28*, 2888. d) Niedermair, F.; Stubenrauch, K.; Trimmel, G.; Slugovc, C. *J. Mater. Chem.*, **2011**, *21*, 15183. e) Sandholzer, M. Slugovc, C. *Macromol. Chem. Phys.*, **2009**, *210*, 651.

¹²⁰ Tanyeli, C.; Gümüş, A. *Tetrahedron Lett.*, **2003**, *44*, 1639.

product. Due to the reactivity differences of diastereomers in ROMP,¹²¹ ill-defined polymers with a broad molecular weight distribution were obtained. Therefore, **4** was prepared in diastereopure form from (\pm)-(endo,exo)-bicyclo[2.2.1]hept-5-ene-2,3-dicarbonyl dichloride and 4-hydroxy-TEMPO.

For polymer synthesis the synthesized norbornene derivatives **1-4** were polymerized via ROMP using **M31** as initiator (*cf.* Scheme 16).^{102 122} The desired polymer constitutions (*cf.* Table 1) were achieved by applying appropriate monomer to initiator ratios. For the random copolymers, a solution of **M31** was added to a mixture of the respective monomers in dichloromethane. In the case of **poly-3**, a methanol/dichloromethane mixture (1:1) had to be used as solvent due to insufficient solubility of **2** in pure dichloromethane. For the preparation of block copolymers, the glycol-functionalized norbornene derivative **1** was dissolved in dry dichloromethane and then **M31** was added. After full consumption of **1** (as detected by TLC), a mixture of **3** and **2** or **4**, respectively, was added. The polymerization time necessary for complete conversion (checked by TLC) varied from 15 minutes to one hour depending on the monomer. Then, the polymerizations were terminated with an excess of ethyl vinyl ether and the polymers were purified by precipitation into cold *n*-pentane.¹⁰²

Characterization of the polymer probes

For confirmation of successful incorporation of all the monomers the obtained polymers were characterized by ¹H-NMR, UV-Vis, FT-IR spectroscopy and gel permeation chromatography. Due to a different coiling behavior, caused by the hydrophilic and hydrophobic nature of the monomers, they seem to have a brush like structure, a comparison with the polystyrene standards used for calibration led to significantly lower M_n values than calculated. This was observed in a previous work.¹²³ A narrow monodisperse size distribution can be concluded which proves a living polymerization. Other polymerization techniques such as controlled radical polymerization or group transfer polymerizations interfere with the monomer bearing nitroxyl groups, unless they were protected with suitable groups.¹⁰²

Table 3: GPC Data

	constitution	yield (%)	M_n /kDa	PDI
poly-1 ^a	(1 ₁₀₀ :3 ₁)	82	27,000	1.1
poly-2 ^a	(1 ₁₀₀ :2 ₁₅)	64	28,000	1.1
poly-3 ^b	(1 ₅₀ :2 ₅₀ :3 ₁)	95	24,000	1.9

¹²¹ Nishihara, Y.; Inoue, Y.; Nakayama, Y.; Shiono, T.; Takagi, K. *Macromolecules*, **2006**, *39*, 7458.

¹²² Burtcher, D.; Lexner, C.; Mereiter, K.; Winde, R.; Karch, R.; Slugovc, C. *J. Polym. Sci. Part A: Polym. Chem.*, **2008**, *46*, 4630.

¹²³ Sandholzer, M.; Lex, A.; Trimmel, G.; Saf, R.; Stelzer, F.; Slugovc, C. *J. Polym. Sci. A: Polym. Chem.*, **2008**, *45*, 1336.

poly-4 ^b	(1 ₁₀₀ :2 ₁₅ :3 ₁)	82	43,000	1.4
poly-5 ^a	(1 ₁₀₀)-(2 ₁₅ :3 ₁)	87	23,000	1.1
poly-6 ^a	(1 ₁₀₀)-(2 ₁₀ :3 ₁)	98	19,500	1.2
poly-7 ^a	(1 ₁₀₀)-(2 ₅ :3 ₁)	98	19,000	1.2
poly-8 ^a	(1 ₁₀₀)-(4 ₁₀ :3 ₁)	98	22,000	1.1

^a Determined in THF, ^b determined in CHCl₃: Et₃N:i-PrOH 94:4:2

In all polymer architectures only a small amount of monomer **3** is incorporated, which results in extremely weak NMR-peaks for the aromatic protons at 8.62 and the CH₃ group at 0.93ppm. These peaks were absent in D₂O, most probably to micellization in the aqueous solution. To be sure that the incorporation of the fluorescence part was successful it was also proven via UV-Vis spectroscopy.

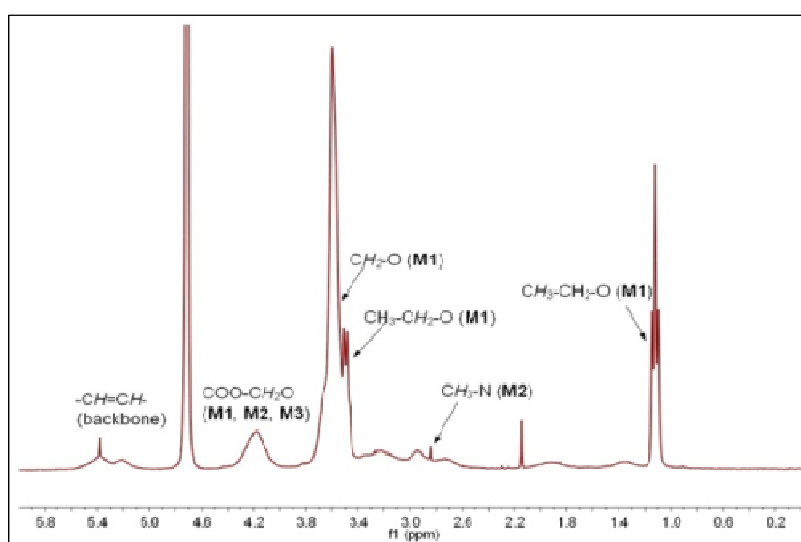


Figure 15: NMR spectrum of the M3 copolymer in D₂O

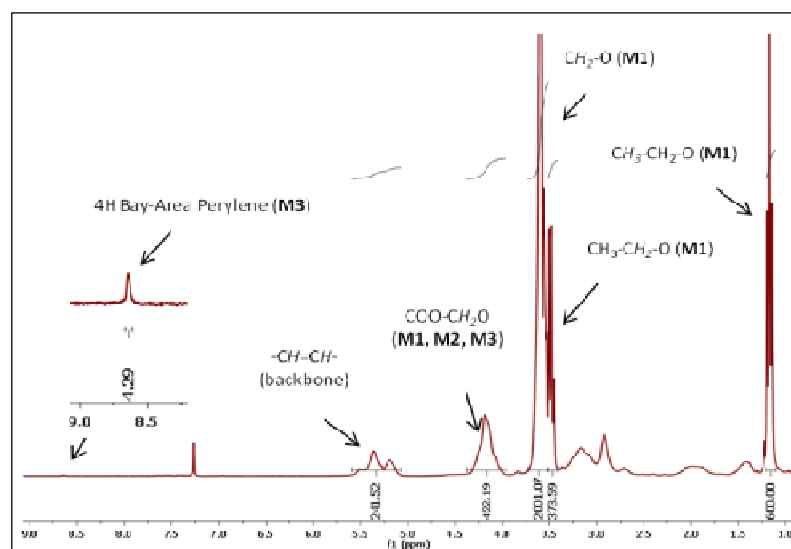


Figure 16: NMR spectrum of the M3 copolymer in CDCl₃, with the perylene peaks

The UV-Vis spectra of the tetrachlorperylene educt, the perylene-norbornene monomer **M3** and the co-polymer are very consistent. As it is shown in Figure 17 there are no shifts or other peaks, only small differences in the intensity.

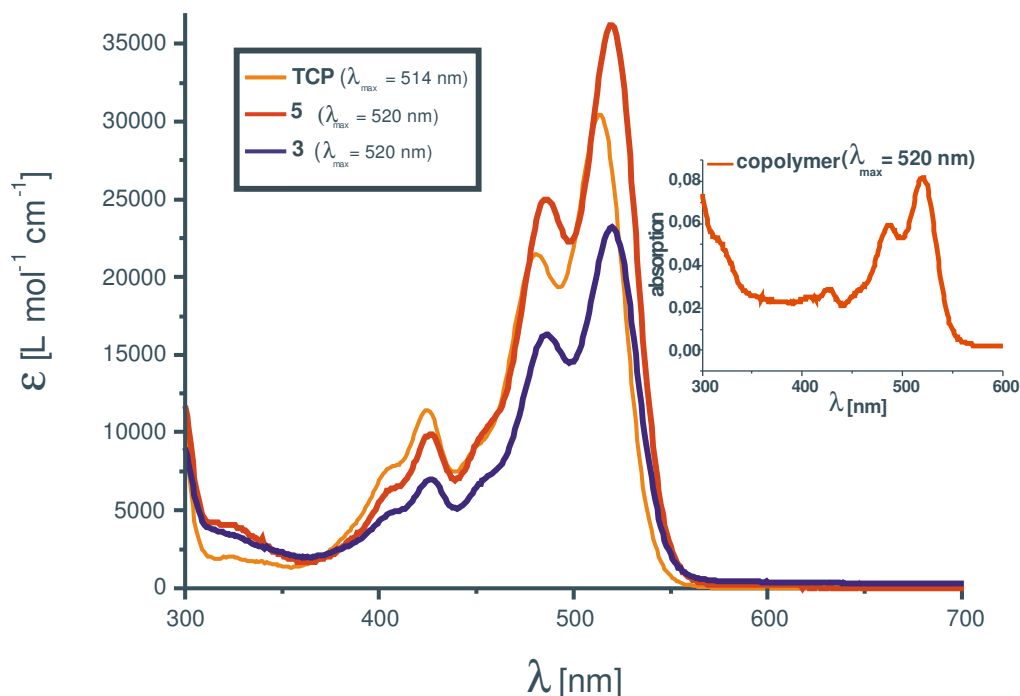


Figure 17: UV-Vis spectrum of TCP, 5, 3 (in chloroform $c = \text{ca. } 10^{-5} \text{ M}$) and poly-1 (with fluorescence spectroscopy; $c = 0.2 \text{ mg mL}^{-1}$, inset)

The photoluminescence measurements showed that the molar extinction coefficient of the bis(*n*-butyl) substituted symmetrical byproduct of **5** was about $3.6 \cdot 10^{-4} \text{ mol}^{-1} \text{ cm}^{-1}$ which matches well with the analogous *n*-pentyl substituted perylene bisimide.¹¹² Also, our obtained fluorescence spectra were consistent with the literature.¹²⁴

The PET efficiency was determined by measuring the fluorescence intensity with a concentration of $c_{(\text{polymer})} = 0.5 \text{ mg mL}^{-1}$ and wavelengths of $\lambda_{\text{exc}} = 518 \text{ nm}$ for the extinction and $\lambda_{\text{em}} = 540 \text{ nm}$ for the emission. Solutions of **poly-4**, **poly-5**, **poly-6** and **poly-7** as well as a blend of **poly-1** and **poly-2** were measured at different pH values. These measurements gave sigmoidally shaped curves which allowed us to determine the apparent $\text{p}K_{\text{a}}$. In table to the results of the $\text{p}K_{\text{a,app}}$ and PET efficiency of functional copolymers **poly-1/poly-2** and **poly-4 – poly-7** were summarized.¹⁰²

Table 4: $\text{p}K_{\text{a,app}}$ and PET efficiency

sample number	$\text{p}K_{\text{a,app}}$	PET efficiency
poly-1/poly-2 (blend)	n.d.	0.99
poly-5	6.4	5.1
poly-6	6.75	4.0

¹²⁴ Aigner, D.; Borisov, S.M.; Petritsch, P.; Klimant, I. *Chem. Commun.*, **2013**, 49, 2139.

poly-7	6.9	2.0
poly-4	7	2.2

$pK_{a,app}$ is the pH at which 50% of maximum intensity is observed; PET efficiency is $I_{(unquenched)}/I_{(quenched)}$

The different observed $pK_{a,app}$ values for **poly-4** – **poly-7** can be explained by the different ratio of **2** and **3** in the polymer chains. **poly-5** has a higher number of quenchers in proximity to the fluorophore-bearing repeating unit. Therefore, a lower pH value needs to be reached in order to have all amine units present in the protonated and therefore, non-quenching state which is reflected in a lower $pK_{a,app}$ value. Furthermore, **poly-7** and the random copolymer **poly-4** showed a similar $pK_{a,app}$ together with the overall lowest PET efficiency of all copolymers.¹⁰²

PET-behaviour measurements

One important question was if the monomers **2** and **3** have to be located at the same polymer chain, which is confirmed by the measurement of the blend **poly-1/poly-2** which is showing no pH dependent change in luminescence at all. Now the second question was if it does not matter where or how far the building blocks are away from each other. Here the block polymers **poly-5** - **poly-7** showed stronger response because **2** and **3** are side by side in the polymer. The random copolymer **poly-4** tended to show not that strong response to the different pH-values. Both of these findings are straightforwardly rationalised by the distance dependence of PET processes.¹²⁵

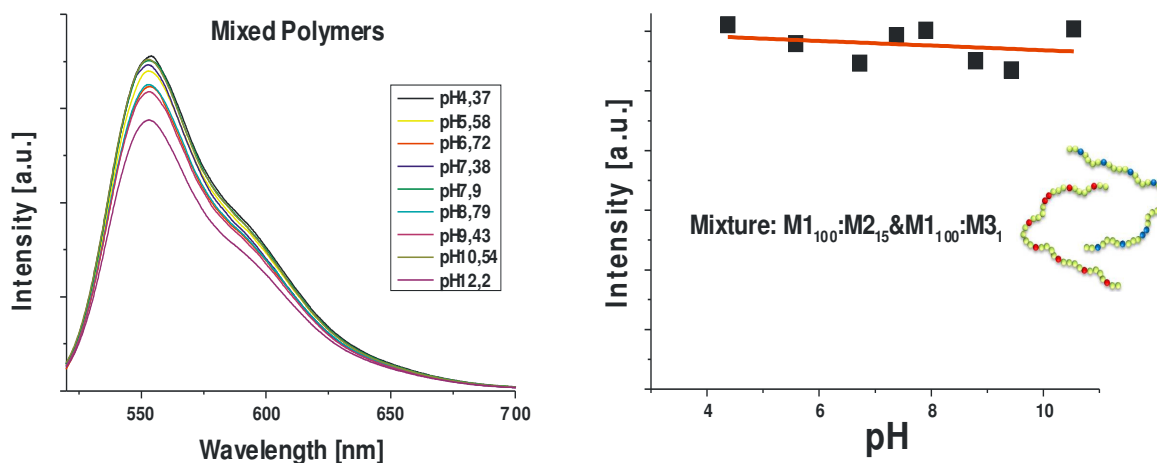


Figure 18: Sigmoidal curve and PET measurements at different pH-values for the polymer blend

¹²⁵ a) Staab, H.A.; Hauck R.; Popp, B. *Eur. J. Org. Chem.*, **1998**, 631. b) Smitha, M.A.; Prasad E.; Gopidas, K.R. *J. Am. Chem. Soc.*, **2001**, 123, 1159.

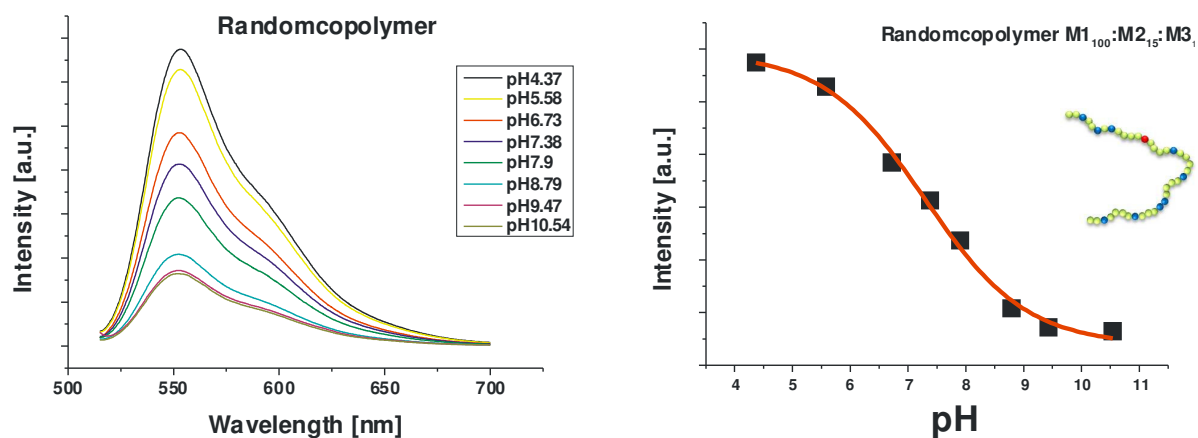


Figure 19: Sigmoidal curve and PET measurements at different pH-values for a random copolymer

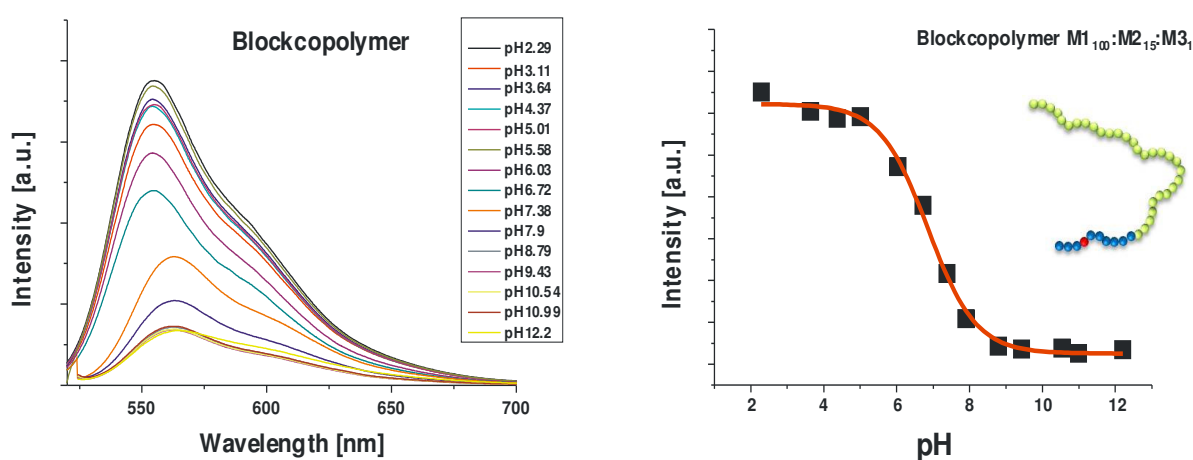


Figure 20: Sigmoidal curve and PET measurements at different pH-values for a block copolymers

Figure 21 is a direct comparison between the blend system, the random copolymer and three different block copolymers. The fluorescence intensity is plotted as a function of the pH and then normalized. Again the blend system (white) showed no pH dependent change in the luminescence, the block copolymers **poly-5** and **poly-6** exhibit a higher PET efficiency than **poly-4**. These results can be explained by the distance dependence of PET processes. The different pK_a values result from the different ratios of **M1** and **M2** in the polymer chains. Furthermore **poly-7** and the random copolymer showed a similar pK_a and the overall lowest PET efficiencies, the block length of only five repeating units of **M2** is too short to benefit from the block copolymer architecture.

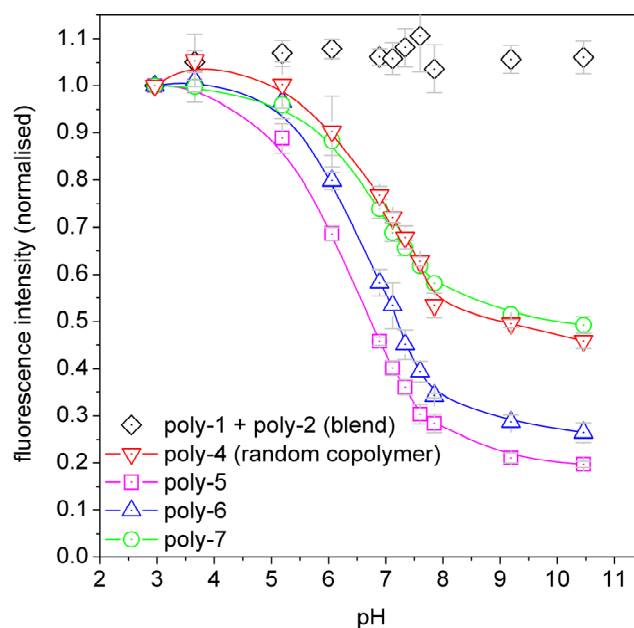


Figure 21: Fluorescence intensity as a function of pH (normalized, $c(\text{polymer})=0.5 \text{ mg mL}^{-1}$)¹⁰²

Ascorbic-acid probes

For the tests with **poly-8**, the polymer with the nitroxide units, aqueous solutions of **poly-8** were added to solutions containing different concentration levels of ascorbic acid ($c(\text{polymer})=0.5 \text{ mg mL}^{-1}$). For the detection of ascorbic acid the same measuring setup as for the pH-measurements was used and the fluorescence intensity was monitored over 35 minutes in 60 second intervals ($\lambda_{\text{exc}}=518 \text{ nm}$, $\lambda_{\text{em}}=540 \text{ nm}$). In Figure 22 the fluorescence intensity of **poly-8** solutions, depending on the ascorbic acid concentration is applied. In contrast to the results presented by Ishii et al.¹²⁶ no gradual luminescence increase over time was noted. Indeed, the fluorescence intensity reached its maximum already after one minute with photobleaching being observed after this point. However, like already observed therein, the luminescence intensity was not reduced when oxidating agents (*meta*-chloroperbenzoic acid or hydrogen peroxide) were added. Between a concentration of 0 and 20 mmol of ascorbic acid a strong increase in luminescence intensity can be established with a linear range between 0 and 1 mmol and a detection level of 0.1 mmol. These results are comparable with previous systems.^{7 126} The quenching of perylenebisimide-linked nitroxides was successfully used for the detection of hydroxyl radicals but THF had to be used as a co-solvent due to the lipophilicity of the probes,¹²⁷ which is unfavorable in biological applications. Contrarily, our system works in aqueous solution.¹⁰²

¹²⁶ Ishii, K.; Kubo, K.; Sakurada, T.; Komori, K.; Sakai, Y. *Chem. Commun.*, **2011**, 47, 4932.

¹²⁷ Silva, A.P.D.; Gunnlaugsson, T.; Rice, T.E. *Analyst*, **1996**, 121, 1759-1762.

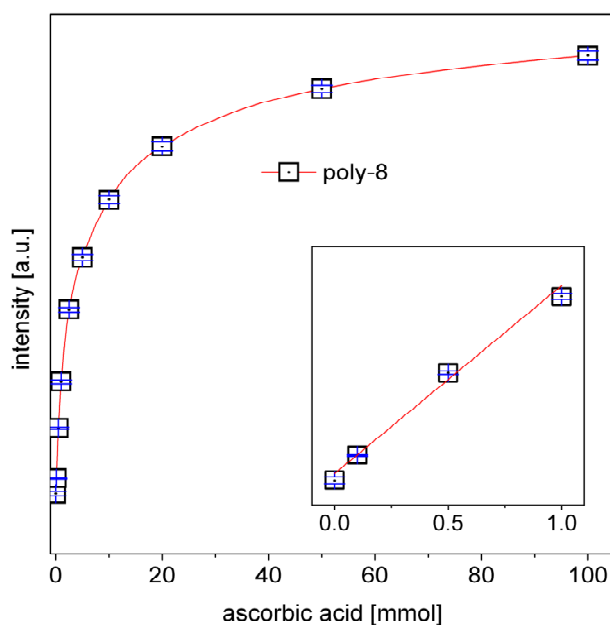


Figure 22: Fluorescence intensity of poly-8 as a function of ascorbic acid concentration (inset: linear range, $c(\text{polymer})=0.5 \text{ mg mL}^{-1}$)¹⁰²

LCST-effect in the system

Due to the reason that the homo-polymers of **1** show a pH-dependent LCST (lower critical solution temperature) effect at about 25°C,⁷ there was some clouding of the polymer solutions at higher temperatures and pH-values. (More detailed information about the LCST effect are in Chapter 1 *cf.* LCST effect)

Therefore, the LCST of **poly-1 and poly-3 - poly-5** was determined using a differential turbidity measurement cell as previously described⁷ and were performed at a polymer concentration of 4 mg mL⁻¹ in buffer solutions. All polymers except **poly-2** (25°C) showed LCST values between 27°C and 30°C.

Table 5: LCST temperatures at different pH-values

sample number	constitution	Temp. at pH 14 ^a	Temp. at pH 10 ^a	Temp. at pH 5 ^a
poly-1	(1 ₁₀₀ :3 ₁)	22.4	24.8	25.1
poly-2	(1 ₁₀₀ :2 ₁₅)	17.3	22.3	26.4
poly-3	(1 ₅₀ :2 ₅₀ :3 ₁)	20.5	20.3	n.p.
poly-4	(1 ₁₀₀ :2 ₁₅ :3 ₁)	23.0	25.2	n.p.
poly-5	(1 ₁₀₀)-(2 ₁₅ :3 ₁)	22.6	25.2	28.2
poly-6	(1 ₁₀₀)-(2 ₁₀ :3 ₁)	23.1	26.4	27.3
poly-7	(1 ₁₀₀)-(2 ₅ :3 ₁)	21.1	24.4	27.6

^a ± 1°C

At a pH of 5, the random copolymers **poly-3** and **poly-4** did not precipitate at all, while **poly-1** showed a LCST of 25°C and **poly-5** a LCST of 28°C. This can be ascribed to the random distribution of the protonated comonomer **2** in **poly-3** and **poly-4** resulting in too short glycol monomer sequence lengths for precipitation. At a more alkaline pH of 10, all samples had an LCST of 25 +/-1°C, the only exception being **poly-3** (20°C). This can be explained by a higher number of pH-sensitive groups and consequent enhanced precipitation. In a strongly alkaline environment (pH>14), all polymers showed LCST temperatures of around 21°C. Overall, no significant difference in LCST behavior between block copolymer and random copolymers was noted, only the sample **poly-3** containing a higher co-monomer content of **2** showed lower LCST values at higher pH, as expected.¹⁰² This effect could be used for heat-driven precipitation and recovery of polymeric molecular probes¹²⁸ or dually sensitive systems.¹²⁹

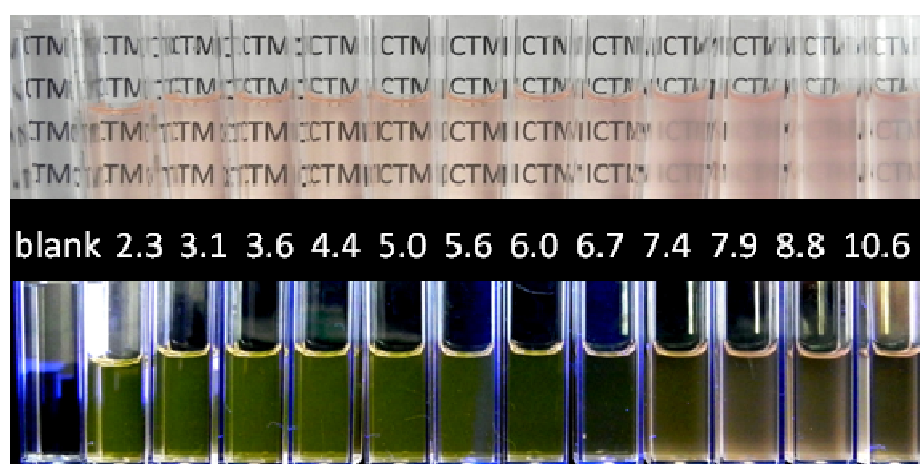


Figure 23: LCST effect in perylene PET probes at different pH-values

¹²⁸ Mackenzie, K.J.; Francis, M.B. *J. Am. Chem. Soc.*, **2013**, *135*, 293.

¹²⁹ Liu, G.; Zhou, W.; Zhang, J.; Zhao, P. *J. Polym. Sci. A Polym. Chem.*, **2012**, *50*, 2219.

Conclusion

In this chapter, PET probes and profluorescent nitroxides were disassembled into their functional compartments and recombined, together with oligo(ethyleneglycol)-bearing monomers to yield functional, water-soluble, copolymers using ROMP. The high functional group tolerance of ROMP allowed, simply by replacing the stimuli-responsive monomer **2** with nitroxide monomer **4**, to also prepare profluorescent polymers which were able to detect ascorbic acid in water. The living characteristics allowed the precise preparation of block copolymers which were found to have a better quenching efficiency and thus, improved sensitivity. The materials could be successfully used to detect near-physiological pH and 0.1 mM ascorbic acid in aqueous solution. Thereby, not only the ability of ROMP to incorporate different detection schemes into functional copolymers could be demonstrated, but also the sensitivity and $pK_{a,app}$ could be tuned using different donor-acceptor ratios. Therefore, ROMP is a suitable approach towards combinatorial synthesis and optimization of molecular probes, screening of different fluorophore-acceptor combinations, and polymeric sensors with tailorable properties such as bioavailability or pharmacokinetics.¹⁰²

Via ring-opening metathesis polymerization, functional copolymers containing perylenes were obtained. The synthesis of the perylene monomer emerged to be the most difficult part of that work. Therefore many different synthetic approaches were tested and the most promising one was sorted to get easy accessible perylene probes. The monomer was successful incorporated in the polymers and this incorporation of **M3** was proven via UV-Vis spectroscopy. The obtained copolymers were found to be pH-sensitive and also showed pH-dependant LCST behavior. Future endeavor in our group will be directed towards more detailed characterization of the photo physical properties of the obtained materials. Furthermore, variations in polymer design and incorporation of other pH-sensitive co-monomers will be conducted.

Experimental

Materials

1,6,7,12-Tetrachloroperylene-3,4:9,10-tetracarboxylic bisanhydride (**TCP**, technical grade) was purchased from Beijing Wenhaiyang Industry and Trading Co. Ltd. Initiator **M31** ([1,3-bis(2,4,6-trimethylphenyl)-2-imidazolidinylidene]dichloro(3-phenyl-1H-inden-1-ylidene)(pyridyl)ruthenium(II)) was obtained from UMICORE AG&Co.KG. (\pm)*endo,exo*-2-(tert-butylamino)ethyl bicyclo[2.2.1]-hept-5-ene-2-carboxylate hydrochloride ¹³⁰ (**2**) was provided by Aglycon (Austria). (\pm)*endo,exo* - bicyclo[2.2.1]hept-5-ene-2,3-dicarboxylic acid,bis[2-[2-(2-ethoxyethoxy) ethoxy] ethyl] ester (**1**) was prepared according to a previously published procedure.¹³¹ Other materials were obtained from commercial sources (Aldrich, Fluka or Lancaster). All reactions were performed under an inert atmosphere of nitrogen using Schlenk techniques.

Methods

Polydispersity indices (PDI) and molecular weight data were determined by gel permeation chromatography (GPC) using THF as eluent, if not stated otherwise. The device setup comprises a Merck Hitachi L6000 pump (delivery volume 1 mL/min), separation columns from Polymer Standards Service (5 μ m grade size) and a refractive index detector from Wyatt Technology. For calibration polystyrene standards from Polymer Standards Service were used. NMR spectroscopy (¹H, ¹³C, COSY, HSQC and HMBC) was done on a Bruker Avance 300 MHz spectrometer (75 MHz for ¹³C). Deuterated solvents were obtained from Cambridge Isotope Laboratories Inc. For FT-IR spectroscopy a Bruker ALPHA FT-IR Spectrometer was used. Measurements were performed in ATR mode. UV/VIS absorption spectra were recorded with a Cary 50 UV/VIS Spectrophotometer from Varian. Electron impact (EI, 70 eV) mass spectra were recorded on a Waters GCT Premier equipped with direct insertion (DI). MALDI-TOF mass spectrometry was performed on a Micromass ToFSpec 2E Time-of-Flight Mass Spectrometer using DCTB as a matrix. Fluorescence spectroscopy was performed in 0.01 mM buffer solutions ($c_{\text{polymer}} = 0.5 \text{ mg mL}^{-1}$) in a plate reader (Tecan Infinite M200 Pro) at 25°C using 96 well plates (costar, Corning Incorporated).

Syntheses

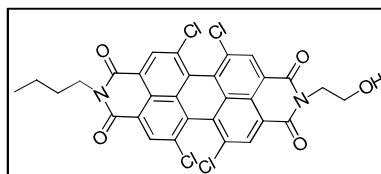
***N*-Butyl-*N'*-2'-hydroxyethyl-1,6,7,12-tetrachloroperylene-3,4:9,10-bis(dicarboximide) (5)**

Ethanolamine (68 μ L, 1.13 mmol, 1.2 eq) and butylamine (112 μ L, 1.13 mmol, 1.2 eq) were dissolved in 2 mL dry toluene in a Schlenk tube and TCP (0.5 g, 9.43 mmol, 7 eq)

¹³⁰ Kreuzwiesner, E.; Noormofidi, N.; Wiesbrock, F.; Kern, W.; Rametsteiner, K.; Stelzer, F.; Slugovc, C. *J. Polym. Sci. Part A: Polym. Chem.*, **2010**, *20*, 4504.

¹³¹ Sandholzer, M.; Fritz-Popowski, G.; Slugovc, C. *J. Polym. Sci. A Polym. Chem.*, **2008**, *46*, 401.

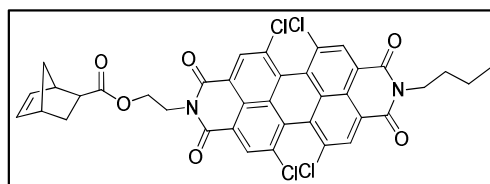
was added afterwards. The mixture was heated to 110°C for 12 h and the conversion was monitored via TLC (DCM/MeOH 20:1, detection UV-Vis, R_f : 0.7). For work up, the reaction mixture was diluted with DCM (6 ml) and filtered through a paper filter, then, the solid residue was washed with DCM. The solvents were removed under reduced pressure and the product was purified using column chromatography (silica, DCM). Yield: 117 mg (20%), red powder.



$^1\text{H-NMR}$: (δ , 20°C, ppm, CDCl_3 , 300.36 MHz): 8.68 (s, 2H, per) 8.66 (s, 2H, per), 4.48 (t, 2H, CH_2), 4.20 (t, 2H, CH_2), 3.99 (t, 2H, CH_2), 1.72 (m, 2H), 1.7 (bs, OH) 1.45 (m, 2H), 0.98 (t, 3H, CH_3).

***N*-butyl-*N'*-(2'-ethyl(bicyclo[2.2.1]hept-5-ene-2-carboxylate))-1,6,7,12-tetrachloroperylene-3,4:9,10-bis(dicarboximide), (3 mixture of *endo*- end *exo*-derivative)**

5 (110 mg, 0.18 mmol, 1eq) was dissolved in dry DCM (8 mL) in a Schlenk tube and triethylamine (70 μL , 0.49 mmol, 3 eq) and acryloyl chloride (50 μL , 0.67 mmol, 4 eq) were added. After full conversion, which was monitored via TLC (cyclohexane/ethyl acetate 5:1, detection UV-Vis, R_f : 0.55), cyclopentadiene (0.3 mL, 3.69 mmol, 20 eq) was added and the reaction mixture was stirred for four days at room temperature. For work up the organic layer was washed three times with HCl (2M) and three times with NaHCO_3 (saturated solution), dried over Na_2SO_4 and the solvent was removed under reduced pressure. The crude product was purified using column chromatography (silica, DCM). Yield: 120 mg (92%), red powder.



$^1\text{H-NMR}$: (δ , 20°C, ppm, CDCl_3 , 300.36 MHz): 8.69 (s, 2H, per) 8.68 (s, 2H, per) 6.10 (d, 1H, nb⁶), 5.86 (d, 1H, nb⁵), 4.49 (t, 2H, CH_2), 4.42-4.31 (m, 2H, CH_2), 4.21 (t, 2H, CH_2), 3.10(bs, 1H, nb³), 2.92-2.86 (m, 2H, nb^{1,4}), 1.88 (t, 1H, nb^{2a}), 1.70 (t, 2H), 1.47-1.22 (m, 5H), 0.97 (t, 3H, CH_3). Only signals for the *endo*-isomer are given; characteristic signals of the *exo*-isomer: 6.20 (d, 1H, nb⁶), 5.78 (d, 1H, nb⁵) *endo:exo* = 80:20 (4:1)

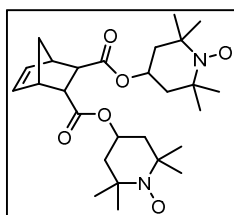
$^{13}\text{C-NMR}$: (δ , 20°C, ppm, CDCl_3 , 75.53 MHz): 174.90, 162.43, 162.36, 138.22(nb⁵), 135.60 (2C, per), 135.49 (2C, per), 133.15 (2C, per), 133.07 (2C, per) 132.56 (nb⁶), 131.62 (2C, per), 131.57 (2C, per), 128.94 (2C, per), 128.64 (2C, per), 123.46 (2C, per), 123.10 (2C, per), 61.45, 49.75, 45.73, 45.35, 43.16, 42.63 (nb²), 40.87, 39.97, 30.30,

29.49, 20.45, 13.95 (1C, CH₃). Characteristic signals of the *exo*-isomer: 137.87 (nb⁵), 132.52 (nb⁶), 41.74 (nb²)

MALDI-TOF-MS for [C₃₈H₂₆Cl₄N₂O₆Na]⁺ [M+Na]⁺ calcd 769.0443, found 769.0521.

***±endo,exo*-Bicyclo[2.2.1]hept-5-ene-2,3-dicarboxylic acid bis[4-(2,2,6,6-tetramethylpiperidine-1-oxy)] ester (4)**

1.79 g (8.16 mmol, 1eq) of bicyclo[2.2.1]hept-5-ene-2,3-dicarbonyl dichloride were dissolved in 50 mL of dry DCM. This solution was cooled to 0°C and 50 mg of DMAP (4-dimethylaminopyridine, 0.408mmol, 0.05eq) were added. Subsequently, 4-hydroxy-TEMPO (2.95 g, 17.13mmol, 2eq) was added portion wise, followed by drop wise addition of 1.6 mL of pyridine (dissolved in 25 mL of dry DCM). Then, the ice bath was removed and the reaction mixture was stirred for 12 h. TLC (DCM/MeOH 10:1, UV-Vis, KMnO₄ staining, R_f: 0.8) proved full conversion. The reaction was worked up by extraction with 50 mL HCl (2M), 50 mL NaHCO₃ sat. and 50 mL of brine. The organic layer was dried over Na₂SO₄. After evaporation of the solvent, the raw product was purified using column chromatography (silica, DCM with 10% methanol as eluent).Yield 3.8 g (95%), light orange powder.

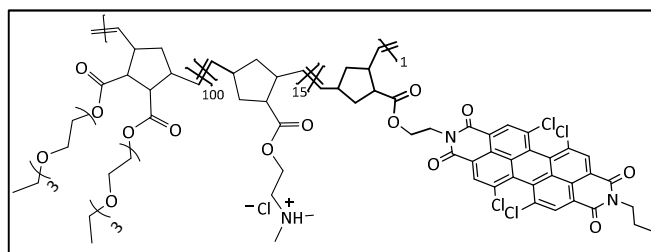


IR: 2971 (m), 2935 (m), 2871 (s), 1719 (s, v C=O), 1462 (m), 1364 (m), 1303 (m), 1262 (m), 1241 (m), 1172 (s), 1111 (m); no NMR possible‡

HRMS (EI) for C₂₇H₄₂N₂O₆ [M⁺] calculated 490.3043; found 490.3058.

Random copolymer synthesis (1₁₀₀:2₁₅:3₁, poly-4)

To a solution of **1** (151 mg, 0.3 mmol, 100 eq), **2** (11 mg, 0.04 mmol, 15 eq) and **3** (2.3 mg, 0.003 mmol, 1 eq) in dry DCM (3.5 mL) a solution of initiator **M31** (2.3 mg, 0.003 mmol, 1 eq) in dry DCM was added. After consumption of the monomers, monitored by TLC (DCM/MeOH 2:1; detection: 2% KMnO₄ solution) the reaction was terminated with ethyl vinyl ether (100 μL, excess) and stirred for 15 minutes at room temperature. The polymer was purified by repeated precipitation of the polymer into cold *n*-pentane (80 mL) and dried *in vacuo*. Yield: 134 mg (82%), red gluey polymer.



$^1\text{H-NMR}$: (δ , 20°C, ppm, CDCl_3 , 300.36 MHz): 5.58-5.18 (bt, 2.25H, CH=CH), 4.34-4.02(bs, 4.14 H, COOCH_2), , 3.71-3.59 (m, OCH_2 , (1)), 3.59-3.45 (q, $\text{O-CH}_2\text{CH}_3$, (1)), 3.37-3.04 (m, CH_2N , $\text{N}(\text{CH}_3)_2$, cp^1 , cp^2 (1); cp^1 (2, 3)), 3.00-2.82 (m, cp^5 ; cp^3 (1)), 2.20-1.81(m, cp^{4a} (1)), 1.55-1.30 (m, cp^2 (2, 3); cp^{4b} (1)) 1.14 (t, 6H, OCH_2CH_3). Characteristic perylene signals: 8.65, 0.98 (t, CH_3)

$M_n = 43 \text{ kDa}^{-1}$, $\text{PDI} = 1.4$.

IR: 3490 (w, b), 2971 (w) 2866 (m), 1728 (s, v C=O), 1452 (s), 1447 (m), 1352 (m), 1171 (m), 1105 (s), 1043 (m).

Block copolymer synthesis (1_{100} -(2_{15} : 3_1), poly-5)

151 mg (0.300 mmol, 100 eq) of **1** was dissolved in dry DCM in a Schlenk tube and 2.45 mg (0.003 mmol, 1 eq) of the initiator **M31** was added and stirred at room temperature. After full consumption of the monomer was determined by TLC (DCM/MeOH 2:1; detection: 2% KMnO_4 solution), a mixture of 11.04 mg (0.045 mmol, 15 eq) of **2** and 2.24 mg (0.003 mmol, 1 eq) of **3** dissolved in dry DCM was added to the reaction mixture. After full turnover was detected, ethyl vinyl ether (100 μL) was added. The copolymer was purified by repeated precipitation of DCM solutions into chilled *n*-pentane and dried *in vacuo*. Yield: 143 mg (87%), red gluey polymer.

$^1\text{H-NMR}$: (δ , 20°C, ppm, CDCl_3 , 300.36 MHz): 5.47-5.16 (bt, 2.25H, CH=CH), 4.36-3.92 (m, 4.14 H, COOCH_2), 3.71-3.49 (m, OCH_2 , (1)), 3.49-3.42 (q, $\text{O-CH}_2\text{CH}_3$, (1)), 3.29-2.98 (m, CH_2N , $\text{N}(\text{CH}_3)_2$, cp^1 , cp^2 (1); cp^1 (2, 3)) 2.96-2.78 (m, cp^5 ; cp^3 (1)), 2.73-2.59 (cp^3 (2, 3)), 2.12-1.72 (m, cp^{4a} (1)), 1.56-1.26 (m, cp^2 (2, 3); cp^{4b} (1)), 1.14 (t, 6H, OCH_2CH_3). Characteristic perylene signals: 8.62 (s), 0.93 (t, CH_3)

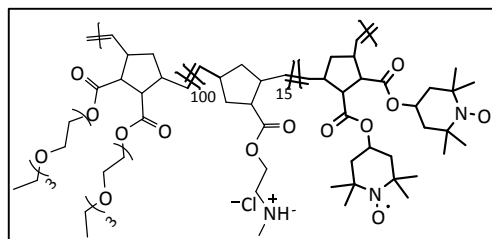
$M_n = 23 \text{ kDa}$, $\text{PDI} = 1.1$.

IR: 2970 (w), 2866 (m), 1728 (s, v C=O), 1450 (m), 1349 (m), 1171 (m), 1105 (s), 1043 (m)

Block copolymer synthesis (1_{100} -(4_{10} : 3_1), poly-8)

To a solution of **1** (151 mg, 0.3 mmol) dissolved in dry DCM in a Schlenk tube the initiator **M31** (2.3 mg, 0.003 mmol) in dry DCM was added and stirred at room temperature. After full consumption of the monomer, a mixture of **4** (15mg, 0.03 mmol) and **3** (2.3 mg, 0.003 mmol) in dry DCM (3 mL) was added. After consumption of the monomers (3 h), monitored by TLC (DCM/MeOH 2:1; detection: 2% KMnO_4

solution) the reaction was terminated with ethyl vinyl ether (100 μ L, excess) and stirred for 15 minutes at room temperature. The polymer was purified by repeated precipitation in chilled *n*-pentane (80 mL) and dried *in vacuo*. Yield: 165 mg (98%), red gluey polymer.



No NMR possible, due to the paramagnetic nature of the TEMPO-monomer, which is influencing the whole polymer.

Mn = 22 kDa, **PDI** = 1.1

IR: 2974 (w), 2869 (m), 1728 (s, $\nu_{C=O}$), 1452 (m), 1349 (m), 1275 (m), 1261 (m), 1171 (m), 1105 (s), 1043 (m)

Chapter 2, Part 2

TPA and Click-Chemistry work together with perylenes

Introduction

Two Photon Absorption

Basics

Also Part 2 of this chapter is connected to the area of sensor materials, especially perylenes. Here the focus is on surface-grafting of sensor molecules via TPA.

TPA –Two photon absorption is the virtually simultaneous absorption of two photons from the same molecule. The photons can have identical or different frequencies to excite the molecule and in this excited state the molecule can undergo a chemical reaction to form a covalent bond.¹³² TPA is a nonlinear optical process and it is quadratically dependent on intensity of the incident radiation, which opens a possibility of spatial localization.¹³³ For such techniques you need information about the energetic position of the electronic states of an organic molecule, therefore a large variety of optical spectroscopy techniques are available. A Jablonski diagram shows the electronic states of a molecule and the transitions between.

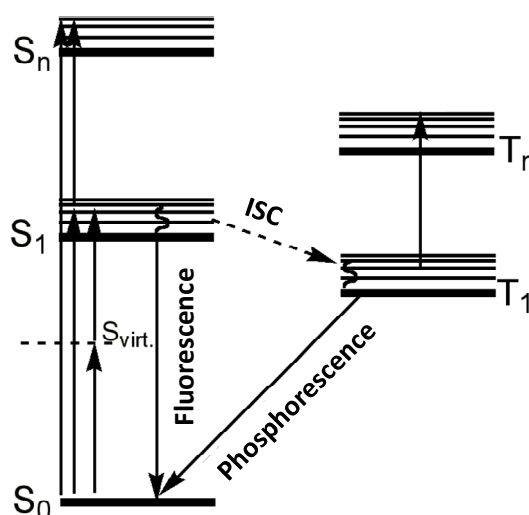


Figure 24: Jablonski diagram

¹³² Göppert-Mayer, M. *Annalen der Physik*, **1931**, 3, 273-294.

¹³³ Masunov, A.E.; Mikhailov, I.A. *Eur. J. Chem.*, **2010**, 2, 142-161.

State model

In contrast to single molecular actions, with TPA an excited state can be reached by using photons with half of the energy or twice the wavelength that is required. If TPA is described with a state model, it must be distinguished between centrosymmetric and non centrosymmetric chromophores. In this work only centrosymmetric molecules were used, so this process is reported in detail.¹³⁴ In centrosymmetric molecules all static dipole moments are zero and because of that the three energy levels (energetic states) have alternating symmetries. For the ground state (g) and the final state (f) the wave functions are even, this means symmetric in relation to the inversion center, but the wave function of the intermediate state (i) is odd. One photon transitions are allowed for the ground to the intermediate state and back and for the intermediate to the final state and back. The situation for two photon transitions is different, here the optical frequency (ν) is out of resonance but creates a non-stationary state which is a superposition or mixture of the ground and the intermediate state which only exists for about 5 fs. This virtual state has a frequency difference from the intermediate which corresponds to the energy $\Delta = E_{gi} - h\nu$. Due to the transient occurrence of the intermediate state with uneven parity in this overlay, a second photon of frequency (ν) can induce the transition of the electric dipole to the final state with even parity.¹³⁴ So in TPA the transition from the ground to the final state is allowed while in OPA it would be forbidden.

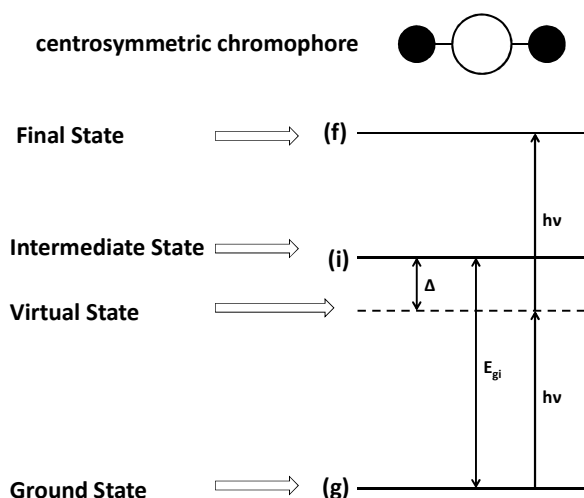


Figure 25: Energy diagram for the essential states in centrosymmetric chromophores.¹³⁵

Structure of molecules

Not all molecules are applicable for the use as TPA chromophores. They need to have a high symmetry in the ground as well as in the excited state and should have an extensive π -system to allow a sufficiently large polarization of the molecule.¹³⁵ As

¹³⁴ Wohlmuth, D. master thesis, „About the synthesis of fluorophores for grafting via two or multiphoton absorption”, **2012**.

¹³⁵ Pawlicki, M.; Collins, H.A.; Denning, R.G.; Anderson, H.L. *Angew. Chem. Int. Ed.*, **2009**, *121*, 3292-3316.

shown in Figure 26, electron withdrawing (A) and electron donating groups (D) should be bound in a symmetrical way, so that a well polarizable chromophore is formed. Two well suited structural motifs of TPA chromophores are the [D-A-D] and [A-D-A] motif.¹³⁶

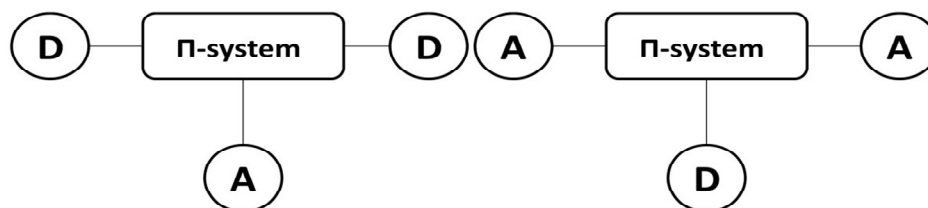
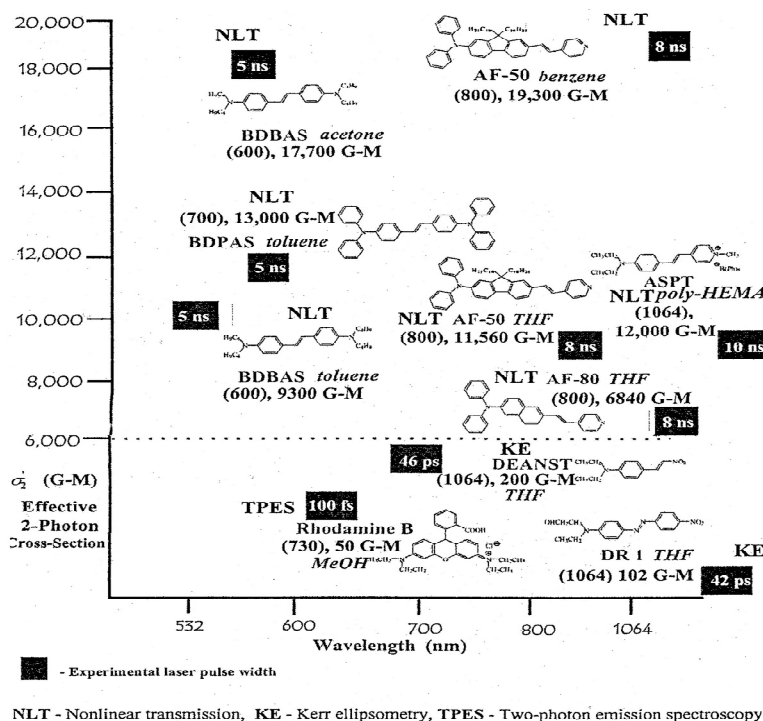


Figure 26: Two concepts for the design of TPA molecules according to Marder et al.¹³⁶

The Beer-Lambert law for one-photon absorption changes from $I(x) = I_0 e^{-\alpha cx}$ to $I(x) = \frac{I_0}{1 + \beta cx I_0}$ for TPA with residual light intensity as a function of path length or cross section x as a function of concentration c and the initial light intensity I_0 . The absorption coefficient α now becomes the TPA cross section β .¹³⁷ The molecular two-photon cross-section is usually expressed in the units of Goepfert-Mayer (GM) where 1 GM is $10^{-50} \text{ cm}^4 \text{ s photon}^{-1}$.¹³⁸ The units in GM come from the areas of the photons (each in cm^2) and the time in which they have to arrive to be able to act together. The scaling factor is introduced to get convenient values for cross sections of the measured dyes.



¹³⁶ Ibot, M.; Beljonne, D.; Bredas, J.L.; Ehrlich, J.E.; Fu, J.Y.; Heikal, A.A.; Hess, S.E.; Kogej, T.; Levin, M.; Marder, S.R.; McCord-Maughon, D.; Perry, J.W.; Rockel, H.; Rumi, M.; Subramaniam, G.; Webb, W.W.; Wu, X.L.; Xu, C. *Science*, **1998**, *28*, 1653–1656.

¹³⁷ http://en.wikipedia.org/wiki/Two-photon_absorption, **September 2013**.

¹³⁸ PowerPoint presentation @ chem.ucsb.edu www.chem.ucsb.edu/~ocf/lecture_ford.ppt Link, **2013**.

Figure 27: Application of the TPA cross-section for the excitation wavelength for some chromophores, indicating the structure and measurement conditions¹³⁹

Click-Chemistry

Overview

Principles of click chemistry are based on nature's astonishing structural and functional diversity. Click chemistry is not a single specific reaction, it was meant to mimic nature, by joining small modular units to a big molecule. The idea relies on a calculation of Guida, who mentioned it is possible to make a pool of drug candidates at 10^{63} , based on the presumption that a candidate consists of fewer than 30 non-hydrogen atoms, weighs less than 500 Da, is made up of atoms of H, C, N, O, P, S, Cl, Br, is stable at room temperature and does not react with oxygen and water.¹⁴⁰ Sharpless et al. described in 2001 the principles of click-chemistry and their characteristics or criteria a reaction needs to fulfill. The most important things are that these reactions must be carried out under simple conditions, be modular, give very high chemical yields and generate only inoffensive byproducts.¹⁴¹ As organic solvent water is preferred and an ideal click reaction exhibits a large thermodynamic driving force (> 84 kJ/mol) to favor a reaction with a single reaction product. Such reactions are observed in breaking of strained ring-systems or a carbon-heteroatom bond formation. In literature there are a lot of examples for such click reactions given in Table 6.

Table 6: Different types of click reactions¹⁴²

	reagent A	reagent B	mechanism
1	azide	alkyne	Cu-catalyzed [3+2] azide-alkyne cycloaddition (CuAAC)
2	azide	cyclooctyne	strain-promoted [3+2] azide-alkyne cycloaddition (SPAAC)
3	azide	activated alkyne	[3+2] Huisgen cycloaddition
4	azide	electron deficient alkyne	[3+2] cycloaddition
5	azide	aryne	[3+2] cycloaddition
6	tetrazine	alkene	Diels–Alder [4+2] cycloaddition with inverse electron demand
7	tetrazole	alkene	1,3-dipolar cycloaddition
8	dithioester	diene	hetero-Diels–Alder cycloaddition

¹³⁹ Marder, S.R. *Chem. Commun.*, **2006**, 131–134.

¹⁴⁰ Guida W.C. *Med. Res. Rev.*, **1996**, *16*, 3–50.

¹⁴¹ Kolb, H.C.; Finn M.G.; Sharpless K.B. *Angew. Chem. Int. Ed.*, **2001**, *40*, 2004–2021.

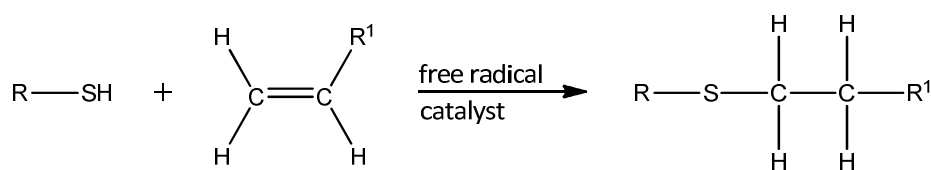
¹⁴² Remzi Becer, C.; Hoogenboom, R.; Schubert, U.S. *Angew. Chem. Int. Ed.*; **2009**, *48*, 4900 – 4908.

9	anthracene	maleimide	[4+2] Diels–Alder reaction
10	thiol	alkene	radical addition (thio click)
11	thiol	enone	Michael addition
12	thiol	maleimide	Michael addition
13	thiol	<i>para</i> -fluoro	nucleophilic substitution
14	amine	<i>para</i> -fluoro	nucleophilic substitution

Thiol-ene

The concept to couple thiols with a carbon-carbon double bond (an “ene”) is a well known reaction but only recently the potential as click reaction was recognized.¹⁴³

What makes that reaction so widely useable are following attributes: such reactions can proceed under a variety of conditions, such as a radical pathway,¹⁴⁴ via catalytic processes mediated by nucleophiles,¹⁴⁵ acid/base catalysis¹⁴⁶ or without a catalyst in highly polar solvents such as water or dimethyl formamide¹⁴⁷ or finally via supramolecular catalysis.¹⁴⁸ Secondly, due to that diversity of mechanisms, a high number of “enes” serve as suitable substrates; depending on the desired product, activated and non-activated species as well as multiple-substituted olefinic double bonds can be employed.¹⁴⁹ There is almost an unlimited range of thiols and the reactivity of the reaction depends on the chosen mechanism and the nature of the “ene”. Either the free-radical addition of thiols and “enes” of both kinds, electron rich and electron poor, or the base catalyzed nucleophilic Michael addition, which needs electron poor substrates, can be performed.



Scheme 17: Thiol-ene reaction either with a free radical or the catalyzed thiol-Michael addition, which both lead to the same endproduct¹⁴¹

For the free radical thiol-ene reaction a series of the two substrates containing molecules have been ranked according to their relative reactivity. Norbornenes and

¹⁴³ Hoyle, C.E.; Bowman, C.N. *Angew. Chem. Int. Ed.*, **2010**, *122*, 1584-1617.

¹⁴⁴ Hoyle, C.E.; Lee, T.Y.; Roper, T. *J. Polym. Sci. Part A: Polym. Chem.* **2004**, *42*, 5301-5338.

¹⁴⁵ Sanui, K.; Ogata, N. *Bull. Chem. Soc. Jpn.*, **1967**, *40*, 1727.

¹⁴⁶ Li, M.; De, P.; Gondi, S. R.; Sumerlin, B. S. *J. Polym. Sci. Part A: Polym. Chem.*, **2008**, *46*, 5093–5100.

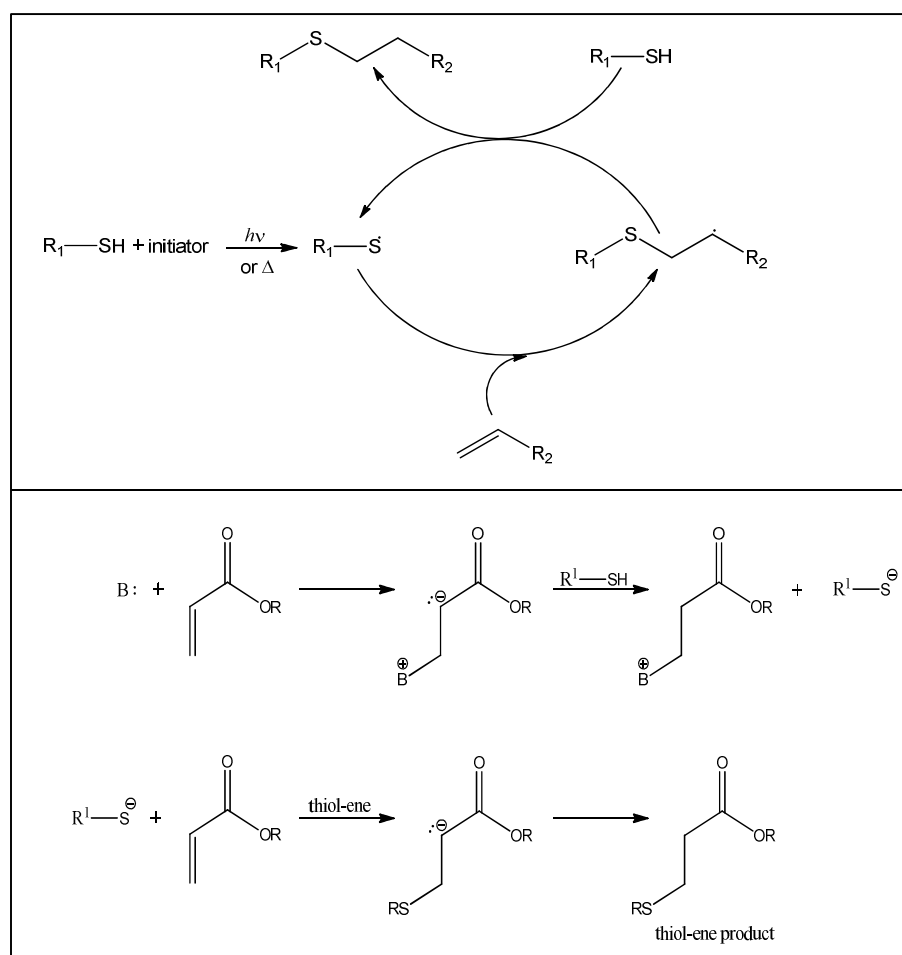
¹⁴⁷ a) Kakwere, H.; Perrier, S. *J. Am. Chem. Soc.*, **2009**, *131*, 1889-1895. b) Tolstyka, Z.P.; Kopping, J.T.;

Maynard, H.D. *Macromolecules*, **2008**, *41*, 599.

¹⁴⁸ Krishnaveni, N.S.; Surendra, K.; Rao, R. *Chem. Comm.*, **2005**, 669-671.

¹⁴⁹ Kienberger, J. Doctoral Thesis, „Antibacterial Equipment of Polyolefins via Thiol-ene Chemistry”, **2013**.

vinyl ethers are the most reactive ones, because they have a high electron density at the carbon-carbon double bond. However in case of strained or non-conjugated double bonds the addition of a thiyl radical is comparatively rapid.¹⁵⁰ The addition of the thiol to the alkene double bond is exothermic and reaction enthalpies ranges from $-10.5 \text{ kcal mol}^{-1}$ (for electron-rich double bonds e.g. vinyl ether) to $-22.6 \text{ kcal mol}^{-1}$ (for the electron-poor double bonds e.g. *N*-alkyl maleimide).¹⁵¹ Under radical conditions, the reaction proceeds via a chain process and is initiated by thermal or photochemical initiation, here a thiyl radical RS and side products are formed.



Scheme 18: Mechanism of the radical thiol-ene coupling at the above picture¹⁵² and of the thiol-Michael addition¹⁴³

The so called thiol-Michael addition is a key reaction in biosynthesis and mostly base catalyzed but there are also reaction conditions where it is catalyzed with metals.¹⁵³ The mechanism of this reaction is similar to the one of the free radical reaction but instead of radicals anions are used (*cf.* Scheme 18).

Cu-Catalyzed [3+2] Azide-Alkyne Cycloaddition

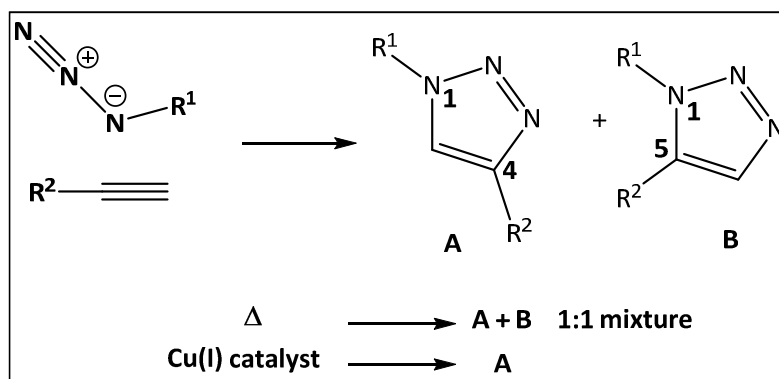
¹⁵⁰ Hoyle, C.E.; Lee, T.Y.; Roper, T. *J. Polym. Sci.*, **2004**; *42*; 5301-5338.

¹⁵¹ Kunz, D. *Chem. Unserer Zeit*; **2009**; *43*; 224-230.

¹⁵² Kade, M.J.; Burke, D.J.; Hawker, C.J. *J. Polym. Sci. Part A: Polym. Chem.*, **2010**, *48*, 743-750.

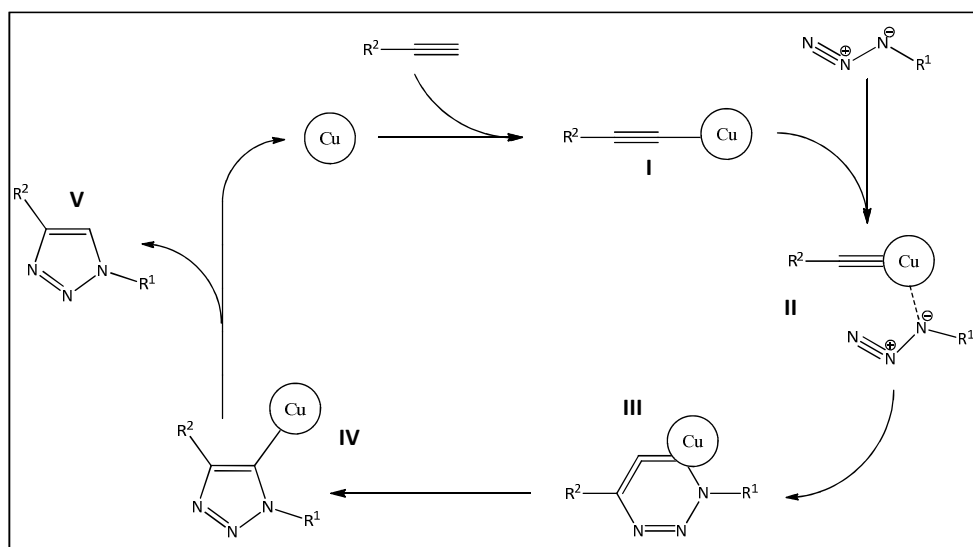
¹⁵³ Movassagh, B.; Shaygana, P. *Arkivoc.*, **2006**; *12*; 130-137.

During their work, Sharpless and co-workers have identified a number of reactions that meet the criteria for click chemistry, arguably the most powerful of which discovered to date is the Cu(I)-catalyzed variant of the Huisgen 1,3-dipolar cycloaddition.¹⁵⁴ Alkynes and azides are both known for their chemical stability, which is directly responsible for their slow cycloaddition which generally requires elevated temperatures and long reaction times.¹⁵⁵ In 2001 Sharpless¹⁴¹ and Meldal¹⁵⁶ independently described the advantages of Cu(I)-catalyzed synthesis, which dramatically improves regioselectivity to afford the 1,4-regioisomer exclusively and increases the reaction rate up to 10^7 times.¹⁵⁷



Scheme 19: Products of thermal and catalyzed 1,3-cycloaddition

Although the thermal dipolar cycloaddition of azides and alkynes occurs through a concerted mechanism, DFT calculations indicate that this is strongly disfavored relative to a stepwise mechanism.¹⁵⁴



Scheme 20: Early proposed mechanism for the CuAAC¹³⁴

¹⁵⁴ Bock, V.D.; Hiemstra, H.; van Maarseveen, J.H. *Eur. J. Org. Chem.* **2006**, *1*, 51–68.

¹⁵⁵ Katritzky, A.R.; Singh, S.K. *J. Org. Chem.*, **2002**, *67*, 9077–9079.

¹⁵⁶ Tornøe, C.W.; Christensen, C.; Meldal, M. *J. Org. Chem.*, **2002**, *67*, 3057–3064.

¹⁵⁷ Appukkuttan, P.; Dehaen, W.; Fokin, V.V.; van der Eycken, E. *Org. Lett.*, **2004**, *6*, 4223–4225.

This type of reaction should be called a copper (I) catalyzed azide alkyne cycloaddition. Formally it is not a 1,3-dipolar Huisgen cycloaddition because the triazole is formed from a terminal alkyne and an azide. It is possible to perform the reaction with commercially available copper (I) sources like the iodide or the bromide but it has to be considered that an in situ produced species out of copper (II) sulfate and a reducing agent like sodium ascorbate is much more reactive. Copper (I) is also not very stable in water so for improving the reaction stabilizing ligands are used. As it can be seen in Scheme 20 the reaction starts via the formation of a copper acetylide, this complex is not formed in the case of an internal acetylene which has a lack of reactivity towards Cu(I)salts. The second step is the activation of the azide which takes place by the coordination with copper to form a complex. Before the next step, an endothermic formation of a six-membered metallacycle, takes place, both reaction components get bound to the copper ion. The next step is the formation of a triazole copper derivative which finally releases triazole. The copper (I) species generated in situ forms a π -complex with the triple bond of a terminal alkyne. In the presence of a base, the terminal hydrogen, being the most acidic one, is deprotonated first to give a Cu acetylide intermediate. It has been suggested that the transition state involves two copper atoms. One copper atom is bonded to the acetylide while the other Cu atom serves to activate the azide. The metal center coordinates with the electrons on the nitrogen atom. The azide and the acetylide are not coordinated to the same Cu atom in this case. The ligands employed are labile and are weakly coordinating. The azide displaces one ligand to generate a copper-azide-acetylide complex. At this point cyclization takes place. This is followed by protonation; the source of proton being the hydrogen which was pulled off from the terminal acetylene by the base. The product is formed by dissociation and the catalyst ligand complex is regenerated for further reaction cycles. The reaction is assisted by the copper, which, when coordinated with the acetylide lowers the pK_a of the alkyne C-H by up to 9.8 units. Thus under certain conditions, the reaction may be carried out even in the absence of a base. In the uncatalysed reaction the alkyne remains a poor electrophile. Thus high energy barriers lead to slow reaction rates.¹⁵⁴

Results and Discussion

For this work the TPA active molecule 2,6-bis(4-azidobenzylidene)-4-methylcyclohexanone (BAC-M) was chosen and the focus was emphasized on functionalization of this molecule via thiol-ene and Cu-catalyzed [3+2] azide alkyne cycloaddition reactions.¹³⁴

In cooperation with the Technical University in Vienna the aim of this work was the functionalization of the polymer cross linking agent BAC-M with two different dyes. The work with the 5-(dimethylamino)naphthalene-1-sulfonyl chloride (dansyl) was the main issue of a master thesis made by Dominik Wohlmuth¹³⁴ and the other part with

the 1,6,7,12-tetrachloroperylene-3,4,9,10-tetracarboxylic acid dianhydride (perylene) is mentioned here.

The results are listed in a comparative way and documented by pictures. The dansyl and the perylene dyes have to be functionalized with different alkyne and thiol groups for the later use in click reactions. The derivatization of the dansyl dye was really easy and fast and so it was used for tests with different click-conditions and reactions like the thiol-ene, the Michael addition and the azide alkyne CuAAC reaction. These model reactions performed on the BAC-M and resembling dansyl molecules demonstrated that the use of the CuAAC reaction is most suitable for our needs.

For the asymmetric functionalization of the perylene dye the knowledge of the chapter "Synthesis of asymmetric PDIs" could be used to realize the idea of a molecule which is soluble, asymmetric with an alkyne or thiol functionality and easy to synthesize. As mentioned before, normally the preparation of an asymmetrically perylene is not that easy but treating the TCP with an equimolar amount of 2-ethyl-hexylamine and propargylamine or 2-aminoethanethiol leads to a three compound mixture and an overall yield of about 35-45% can be obtained. This method was used for every preparation of an unsymmetrical perylene.¹¹² In Figure 28 the spectra of the perylene substituted with propargylamine and with cysteamine can be seen, both are recorded in CDCl₃ and show all peaks in correct ratio.

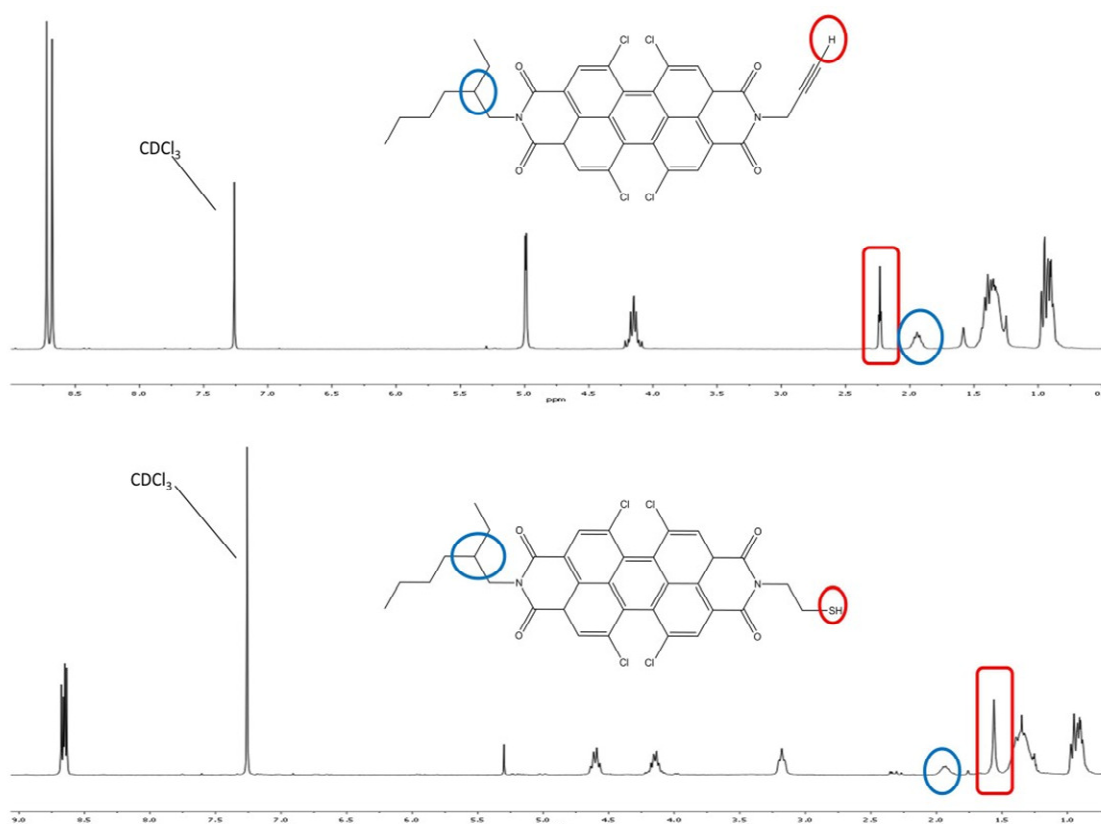


Figure 28: Spectra of the two functionalized perylenes for click-reactions¹³⁴

For the copper-catalyzed 1,3-dipolar cycloaddition two approaches were pursued to functionalize the BAC-M. At first it was assumed that the BAC-M is grafted onto the polymer matrix and there are some residual azide groups. This model action was performed with the dansyl derivative. However, according to the results of Ovsianikov et al.¹⁵⁸ there are no more azide groups left after grafting of the BAC-M. Hence, this option was discarded. The second option was to label the molecule before grafting on the polymer matrix. Therefore one azide functionality has to stay unfunctionalized. So the focus was on the preparation of mono-functionalized BAC-M but for characterization and comparison with the dansyl dye also the di-functionalized molecule was synthesized.

Click conditions

In general, the copper(I)-catalyzed 1,3-dipolar cycloaddition is known as a mild reaction that does not require much specific precautions. It usually proceeds to completion in 6-36 hours at ambient temperatures in water with a variety of organic co-solvents, such as *tert*-butanol, ethanol, DMSO, THF or CH₃CN.¹⁵⁹ A few papers recently reported that the addition of ligand, a copper(I) stabilizer, enhanced the catalytic activity of copper(I), improved reaction yields and reduced reaction times.¹⁶⁰ Although dichloromethane has been employed as solvent in ligand-mediated copper(I) catalyzed 1,3-dipolar cycloaddition, it was used for organic ligand which accelerated the reaction rate, not as a co-solvent.¹⁶¹ Herein, we tested also the application of dichloromethane as a co-solvent in a ligand free reaction.¹⁵⁹

The most common experimental procedure involves the in situ generation of Cu(I) by reducing CuSO₄ with sodium ascorbate in aqueous media.¹⁶² In our reactions we tested Cu turning/CuSO₄ combinations,¹⁶³ and Cu(I) salts¹⁶⁴ with different solvent and temperature conditions. The turnover to the di-substituted BAC-M could be obtained under nearly all conditions but the challenging part was the mono-substitution of the molecule. Therefore a great excess of the BAC-M educt was used but with some of the solvent/catalyst combinations this synthetic approach did not work. For the perylene-norbornene and the dansyl-alkyne Cu(I) in dichloromethane was filtered as the best combination. Both educts were not soluble in water and therefore an organic solvent had to be used. Dichloromethane was the compromise among water and DMF. Water could not be used due to the bad solubility and DMF could not be removed during purification. For accelerating the reaction progress the reaction mixture can be heated at the beginning. For work up we used a chromatographic method which is not

¹⁵⁸ Ovsianikov, A.; Li, Z.; Torgersen, J.; Stampfl, J.; Liska, R. *Adv. Funct. Mater.*, **2012**, *22*, 3429-3433.

¹⁵⁹ Lee, B.Y.; Park, S.R.; Jeon, H.B.; Kim, K.S. *Tetrahedron Lett.*, **2006**, *47*, 5105-5109.

¹⁶⁰ Chan, T. R.; Hilgraf, R.; Sharpless, K.B.; Fokin, V.V. *Org. Lett.*, **2004**, *6*, 2853.

¹⁶¹ Meng, J.C.; Fokin, V.V.; Finn, M.G. *Tetrahedron Lett.*, **2005**, *46*, 4543.

¹⁶² Rostovtsev, V.V.; Green, L.G.; Fokin, V.V.; Sharpless, K.B., *Angew. Chem. Int. Ed.*, **2002**, *41*, 2596-2599.

¹⁶³ Brik, A.; Muldoon, J.; Lin, Y.C.; Elder, J.H.; Goodsell, D.S.; Olson, A.J.; Fokin, V.V.; Sharpless, K.B.;

Wong, C.H. *ChemBioChem*, **2003**, *4*, 1246-1248.

¹⁶⁴ Tornøe, C.W.; Christense, C.; Meldal, M. *J. Org. Chem.*, **2002**, *67*, 3057-3064.

common for click reactions. In the ideal case the product precipitates in the solvent and can be filtered. A filtration can be used for the double substituted product but to separate the BAC-M from the mono-substituted product a column chromatography is necessary to eliminate the educt. To perform comparative measurements of the TPA cross section BAC-M substituted with an alkyne chain and with a alcohol were needed. Unfortunately, for these two reactions it was not possible to obtain the product in a mono substituted form. Hence, we had to test again click reaction conditions.

Reaction conditions for the test reaction of BAC-M with 5-hexyn-1-ol were chosen according to Chrominski et al.¹⁶⁵

Table 7: Different reaction conditions for test-reaction of BAC-M with 5-hexyn-1-ol

reaction	catalyst	solvent	time [h]	yield [%]	mono/di [%]
1	CuSO ₄ /Na ascorbate	DMF	24	85	0/100
2	CuSO ₄ /Na ascorbate/TBTA	DMF	2	30	50/50
3	CuSO ₄ /Na ascorbate/TBTA	CH ₂ Cl ₂	24	70	80/20
4	CuI/TBTA	DMF	24	40	0/100
5	CuI/TBTA	H ₂ O/ <i>t</i> -BuOH	24	80	60/40
6	CuI	CH ₂ Cl ₂	48	0	-
7	CuOAc	H ₂ O	5	0	-

Reactions 3 and 5 were chosen to be the best ones. The optimized reaction conditions under adapting the reaction time and the work up conditions are *tert*-BuOH/H₂O 1:1 with copper iodide at room temperature stirring for about 24 hours. For synthesizing the disubstituted product also other reactions and shorter reaction times are possible.

The alkyne substituted BAC-M could not be synthesized with neither of these reaction conditions. As mentioned before we tried now to use dichloromethane as the co solvent in a ligand free reaction. A DCM/H₂O mixture seemed to be very favorable for the substrates, because the BAC-M is slightly soluble in both solvents, the alkyne is soluble in the organic phase and the copper catalyst system is soluble in the water. The substrates were treated with CuSO₄*H₂O (5 mol%) and sodium ascorbate (15 mol%) in DCM/H₂O (1:1).¹⁵⁹

Characterization of the products with different methods

¹⁶⁵ Chrominski, M.; Gryko, D. *Chem. Eur. J.*, **2013**, *19*, 5141-5148.

In Figure 29 the ^1H -spectrum of the mono-functionalized BAC-M with the perylene is presented. As proof for the coupling a new peak at 8.16 ppm appears which is the hydrogen atom in the triazole ring. The three important peaks are marked with colors and the others are just integrated and named.

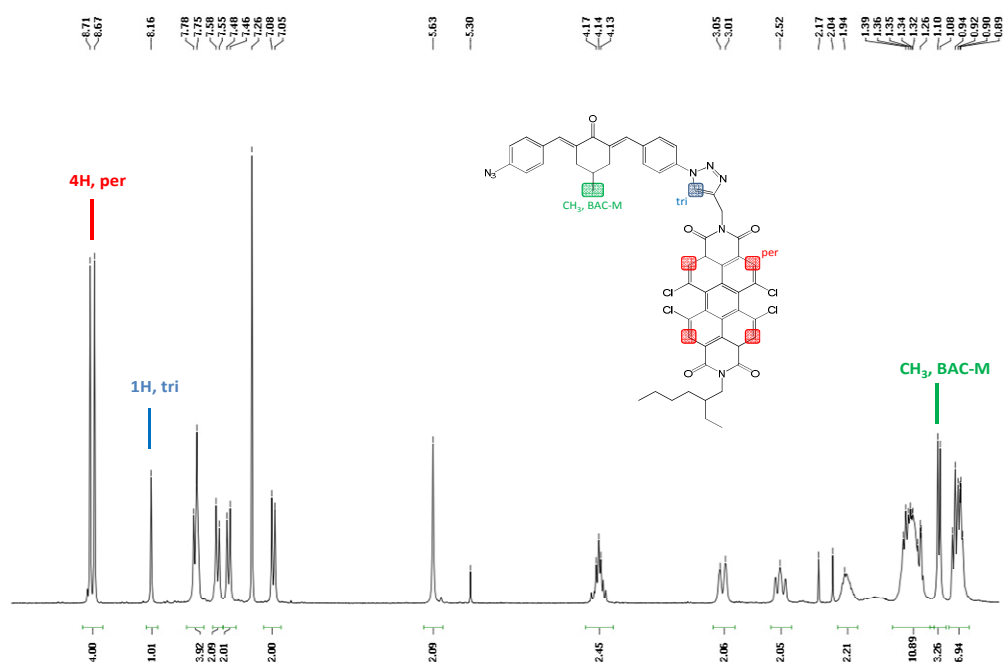


Figure 29: ^1H -NMR of the mono-substituted BAC-M¹³⁴

No ^1H NMR spectrum of the di-substituted perylene derivative could be recorded due to the bad solubility of the molecule in the deuterated solvent.

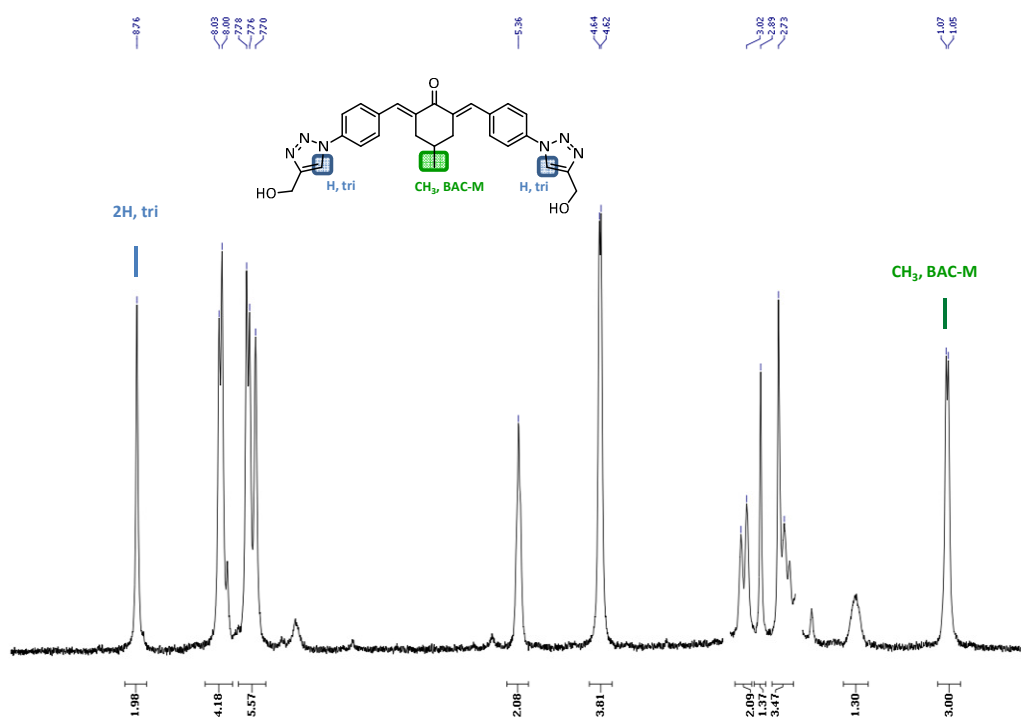


Figure 30: ^1H -NMR of the di-substituted BAC-M

As comparison or to see the clear difference in the spectrum of a double substituted species, in Figure 30 the di-substituted BAC-M with a propargylalcohol substituent and its characteristic peaks is shown. This di-substituted product has also not the best solubility characteristics but is soluble in deuterated DMSO in contrast to the perylene derivative, which is in its double substituted form insoluble in any solvent.

As second proof for the substitution level FT-IR measurements were used as supplement to the NMR-spectroscopy. With this method it is possible to detect the free azide groups and to determine the amount of azides in the molecule. Spectra were recorded both in solution and as solid products. However, the best method was to combine the solid product and Nujol (a paraffin oil) in a mortar and make a mull which is directly placed on the spectrometer.¹³⁴ Figure 31 shows the spectra of the mono and the difunctionalized BAC-M, the characteristic azide peak arise at 2117 cm^{-1} . As mentioned before it was not possible to record a NMR spectrum of the di-functionalized product of the perylene and also the dansyl compounds. The FT-IR showed the difference between the amounts of azide in the molecule, in the mono substituted blue line the peak is much higher than the peak at the red line. But it seems like, that also in the disubstituted product some free azides are left. Insufficient purification due to the bad solubility characteristics might be the reason for that.

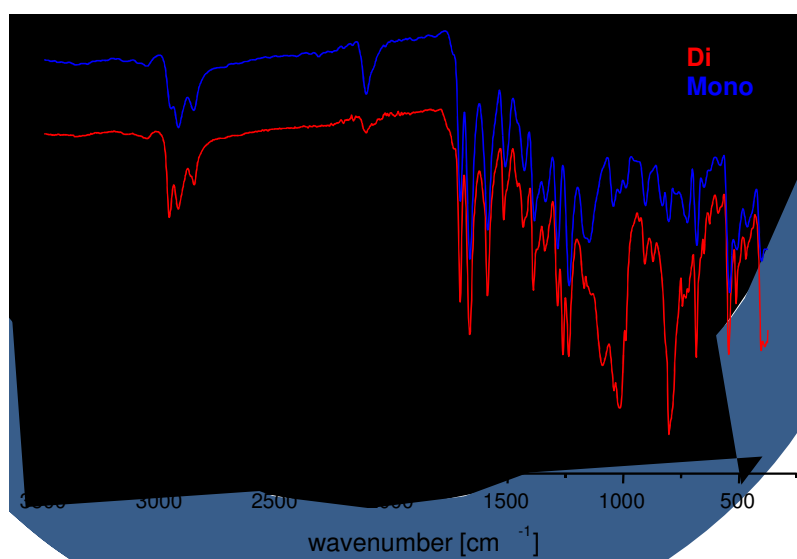


Figure 31: FT-IR spectra of the two functionalized BAC-M perylene derivatives¹³⁴

For completion of the characterization, the optical properties of our substances were also measured. The UV-Vis spectra were measured in dichloromethane as solvent with a concentration of $3 \cdot 10^{-3}$ g/mL in a quartz cuvette with an excitation range from 300 nm to 600 nm.

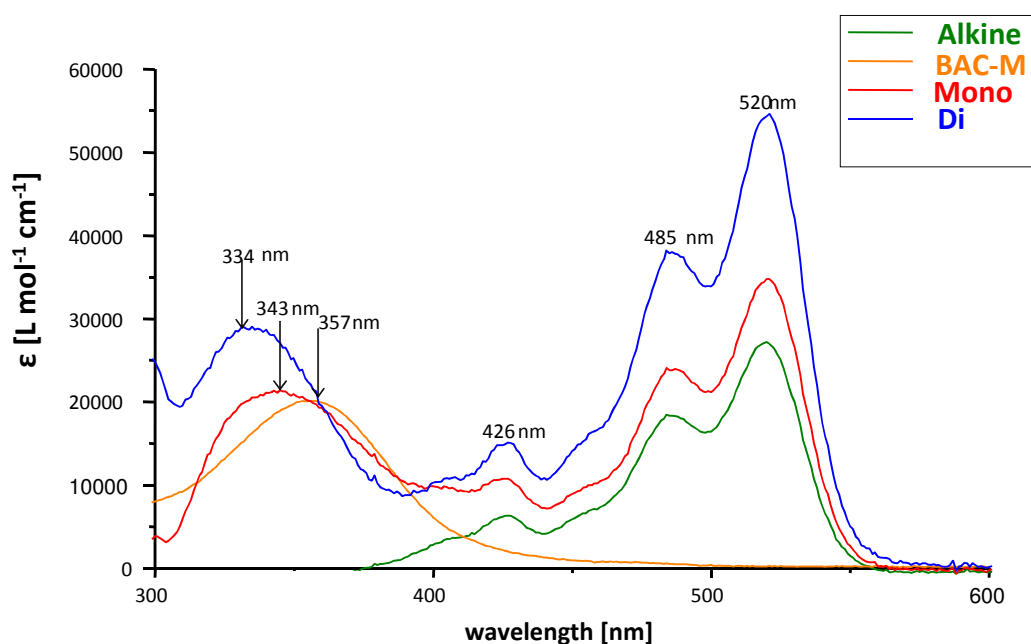


Figure 32: UV-Vis spectra of the BAC-M, perylene-alkyne and the mono- and di-functionalized derivatives¹³⁴

The UV-Vis spectra showed a maximum around 350 nm for the BAC-M unit. Due to functionalization, the pure BAC-M molecule the maximum got a hypsochromic shift to about 335 nm in the disubstituted form. The same results could be obtained with the dansyl derivative. The maxima of the perylene functionality, which are around 520 nm and 485 nm could be conserved in the perylene alkyne and also in the mono and di-substituted BAC-M derivative. Only the ratio of the perylene peak to the BAC-M peak slightly changed. For the di-functionalized product it is 2:1 but for the mono it is 1.5:1.¹³⁴

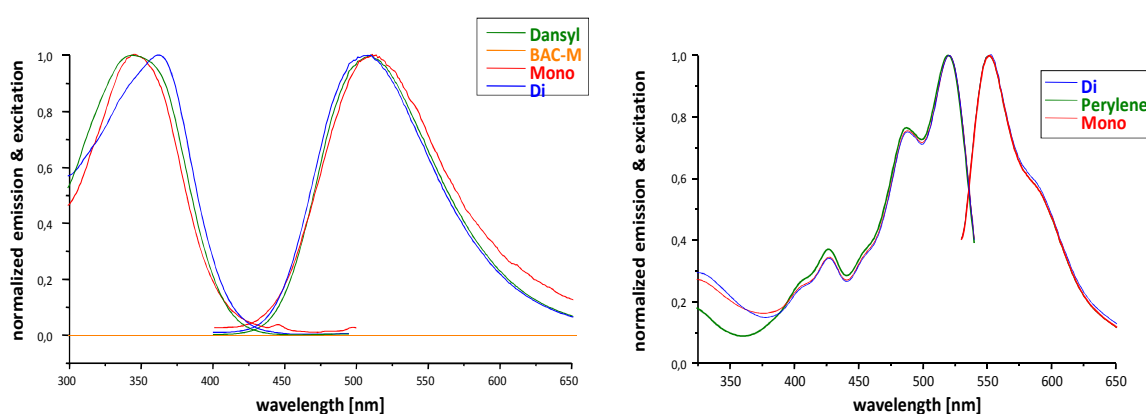


Figure 33: Fluorescence spectra of the perylene and the dansyl derivatives¹³⁴

The fluorescence spectra were also measured in dichloromethane but with a lower concentration of about $3 \cdot 10^{-4}$ g/mL. Excitation and emission spectra were recorded at different wavelengths depending on depending on the substituents. All derivatives and

the functionalized cross linking agents showed nice curves with a good response (cf. Figure 33) except for the BAC-M itself (yellow line). In the excitation of the di-functionalized dansyl derivative a hyperchromic shift is visible but all the other recorded spectra show absolutely no difference.

The grafting experiments were performed in collaboration with TU Vienna. For preparation a 2 weight% solution of the mono-substituted dansyl and perylene derivatives was made in toluene. One important thing was to prevent exposure to light, so brown glass vials were used or the normal vials were wrapped with aluminum-foil. As next step a commercially available hydrogel (poly(ethylene glycol) (PEG) based matrix) pellet was placed in the solution for about one hour to expand. We also made solutions with 1 weight% and 5 weight% and left the pellets from 15 minutes to two hours in the solution to find the best conditions due to different molecular weight of the substances and also to the different solubility characteristics.

After this treatment the pellet was placed in the sample holder of the TPA-laser inscribing system which is described in the experimental part. The multiphoton interaction is highly localized; the process of BAC-M immobilization on the PEG matrix is restricted to a limited volume. By moving the laser focus within the sample, 3D patterns of immobilized molecules can be recorded.¹⁵⁸ The inscribed structures in our case were small squares which have a line distance of about 0.5 μm . The resulting small squares in a square or rectangular form have a dimension of 50x50x40 μm . The mechanism of the multiphoton grafting process could be expected to follow the single photon grafting principle.¹⁶⁶ The interaction between the chromophore (BAC-M) and the focused laser beam takes place via multi photon absorption (MPA).

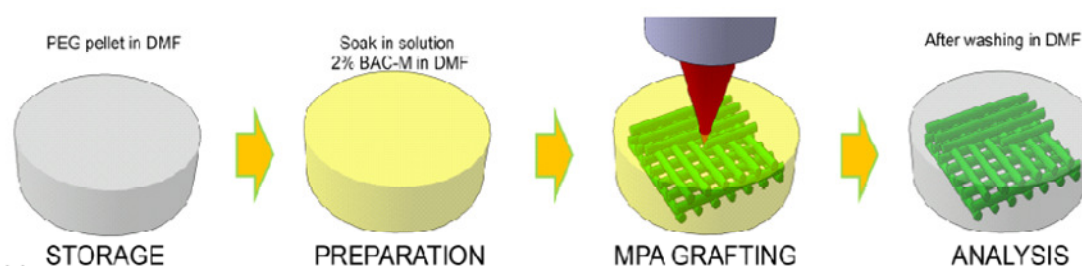
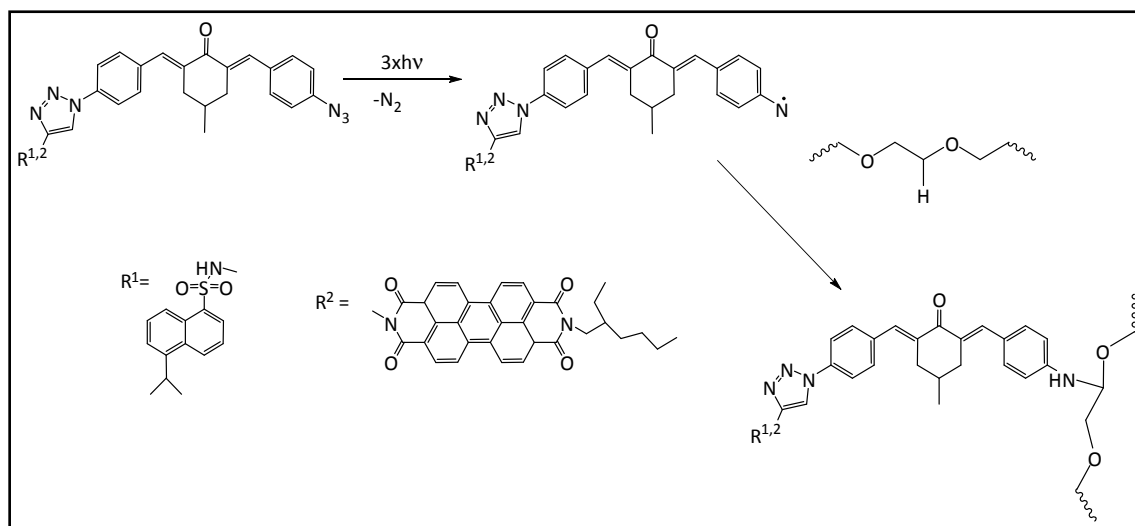


Figure 34: Sample processing and grafting procedure¹⁵⁸

Photolysis of the azide causes the dissociation of the N-N bond from the excited state, followed by the generation of nitrogen and highly reactive electron-deficient nitrene species.¹⁶⁷ This is followed by the direct immobilization of the short lived nitrene intermediate on the PEG network by insertion into a C-H bond. This step is applicable to a wide variety of matrices containing C-H or N-H bonds.

¹⁶⁶ Schuster, G.B.; Platz, M.S. „*Advances in Photochemistry*”, (Eds: D.H. Volman, G.S.Hammond, D.C. Neckers), John Wiley&Sons, Inc., Hoboken, N. **1992**, 69-143.

¹⁶⁷ Pinard, R.; Heckman, J.E.; Burke, J.M. *J.Mol.Biol.* **1999**, *287*, 239-251.



Scheme 21: Photolysis of aryl azide followed by insertion of the PEG sample¹⁵⁸

In our grafting experiment with the dansyl-derivative a fixed array was created. As it can be seen in Figure 35 the power of the laser was varied between 40 and 290 mW and the range of the inscribing speed was between 1 and 5 mm/s. The grafted patterns can be directly observed via laser-scanning microscopy (LSM). This integrated laser excites at 488 nm but within this wavelength only the excitation of the BAC-M can be observed.

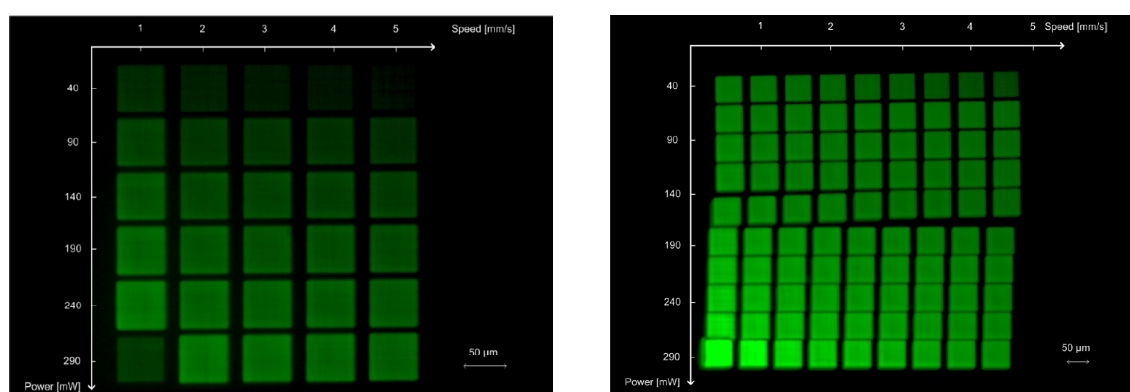


Figure 35: Grafting experiment with the dansyl dye (left) and the BAC-M (right)¹³⁴

The left picture in Figure 35 is the result of the grafting experiment with the dansyl functionalized BAC-M. The time changes are plotted against the x-axis and the laser-intensity along the y-axis. Because of initiation problems of the femto second laser the spot in the left bottom corner is not the brightest as it should be. However, it can be seen that the faster the inscribing speed and the lower the laser power, the spots darker the squares in the picture get. It is worth mentioning that the green color is not the real fluorescence color of BAC-M, but the filter of the LSM changes every color to green. In contrast to our experiment on the right picture a grafting experiment with the non functionalized BAC-M is shown. The spots show more brightness which is due to the excitation rate of the LSM laser. Unfortunately the wavelength of the laser

cannot be varied in this experiment, so it is not possible to measure the brightness/excitation of the dansyl dye.

The series with the perylene derivative was performed in a similar way like the dansyl-functionalized BAC-M. Also here the weight% of the product were varied and more product was used, not 2 but about 4 weight%. However, the reaction with the perylene did not generate the desired results. A combustion of the polymer matrix was observed when the spot was irradiated with the laser beam. As in the experimental setup for the grafting experiment shown, a CCD camera is installed so the combustion could be clearly observed.

Due to this results, for a better understanding also the TPA cross section was measured. These measurements were also performed in Vienna, by Zhiquan Li.

For the Z-scan measurements usually 10 mL solution with a concentration of 2-10 mol/L are required. The solubility of the products in DMF was not that good so a different solvent has to be found. However, strong enough signals for TPA cross section measurement with a concentration of 10^{-3} mol/L in chloroform could be afforded. The mono-substituted perylene compound (KG98) exhibit a large TPA cross section, but the tests could not make sure if this value only derives from the attached dye or from the whole molecule. The conjugation length of the perylene is not long and therefore these molecules are no good donors for the whole π -system anyway. The perylene with the triple bond has TPA cross section of 55 GM and the mono-substituted BAC-M of about 72 GM. Since both compounds have strong UV absorption at about 400 nm, the cross section value should belong to two-photon absorption. Attachments are the corresponding graphics.

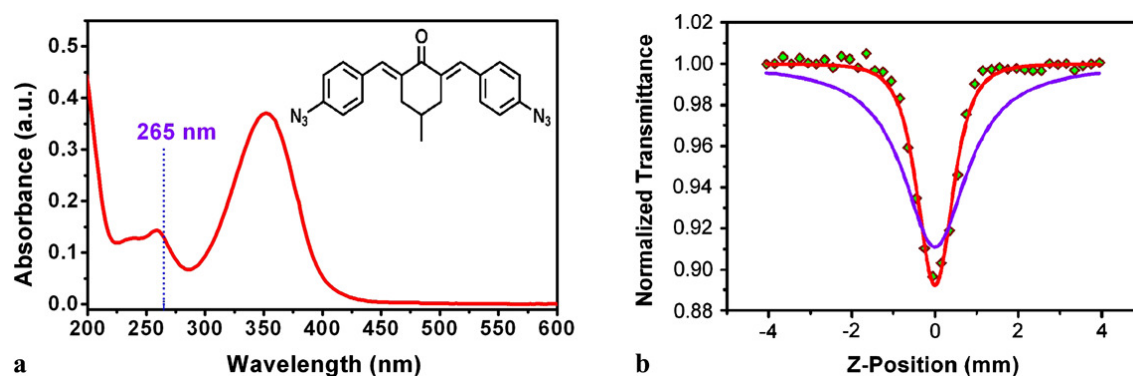


Figure 36: (a) UV-Vis absorption spectra of the BAC-M. (b) Results of the Z-scan characterization of BAC-M solution. Red solid line is the fit curve assuming the 3PA process and blue solid line is the fit curve assuming 2PA¹⁶⁸

The TPA cross section is measured with 100 fs pulses and the same concentration of the probes during the whole measurement, otherwise variation in the Z-scan curve can

¹⁶⁸ Ovsianikov, A.; Li, Z.; Ajami, A.; Torgersen, J.; Husinsky, W.; Stampfl, J.; Liska, R. *Appl. Phys. A*. **2012**, *108*, 29-34.

occur. Z-scans for KG98 performed at different pulse energies from 75 nJ to 135 nJ are compared in the left picture in Figure 37. The relative absorption is linear with the laser intensity, which indicates that the TPA is the predominant nonlinear absorption.¹⁶⁸ The Z-scans were started from low energies at which no nonlinear absorption occurs and increased the pulse energy for absorption to appear. Global fitting was used for processing the data measured with different pulse energies together.¹⁶⁹

The right picture in Figure 37 shows the result for q_0 versus pulse energy. A linear behavior is shown, which is a clear indication for pure TPA and nonexistence of ESA (excited state absorption) or any higher order absorption.¹⁷⁹ By fitting to the experimental data with different equations the TPA coefficient is extracted and the TPA cross section is calculated. As mentioned before the cross section here is 72 GM. The TPA cross section of the dansyl compound is 100 GM.

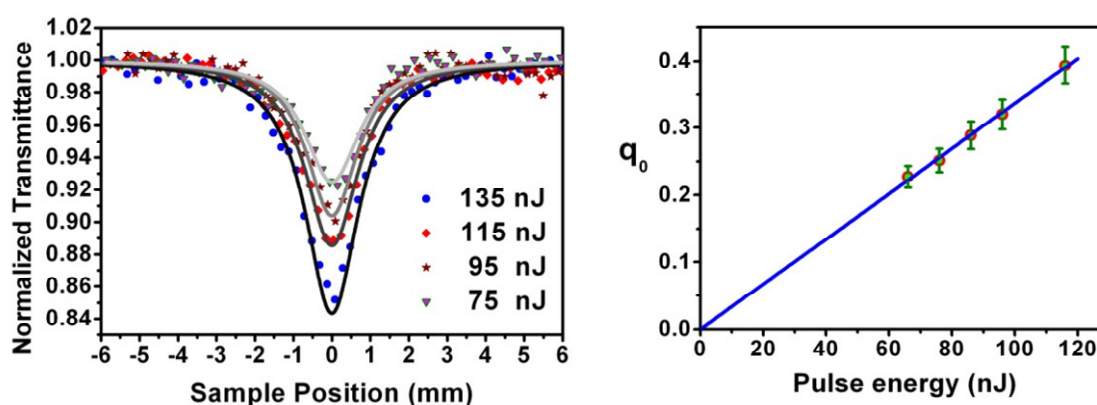


Figure 37: Z-scans for the mono-substituted perylene BAC-M. The pulse energy was determined for the sample and then Z-scans for KG98 were performed with different pulse energies (left picture)

In literature the TPA cross section is the most common value to evaluate TPA chromophores.¹⁷⁰ There are many different possibilities to measure the TPA cross section, such as nonlinear transmission,¹⁷¹ up-converted fluorescence emission,¹⁷² transient absorption,¹⁷³ and Z-scan analysis.¹⁷⁴ The advantages of Z-scan measurements are the sensitivity, relatively low costs, and ease in performance. On the other hand there are also some drawbacks, because this method is rather time consuming and a precise laser setup is indispensable for achieving reliable results as an

¹⁶⁹ Antonov, L.; Kamada, K.; Ohta, K. *Appl. Spectrosc.*, **2002**, *56*, 1508-1511.

¹⁷⁰ Oucher, N.; Rosspeintner, A.; Satzinger, V.; Schmidt, V.; Gescheidt, G.; Stampfl, J.; Liska, R. *Macromolecules*, **2009**, *42*, 6519.

¹⁷¹ Clay, G.O.; Schaffer, C.B.; Kleinfeld, D. *J. Chem. Phys.*, **2007**, 126.

¹⁷² Xu, C.; Webb, W.W. *J. Opt. Soc. Am.*, **1996**, *13*, 481.

¹⁷³ Bhawalkar, J.D.; He, G.S.; Prasad, P.N. *Rep. Prog. Phys.*, **1996**, *59*, 1041.

¹⁷⁴ Ajami, A.; Husinsky, W.; Liska, R.; Pucher, N. *J. Opt. Soc. Am.*, **2010**, *27*, 2290.

outcome of the fitting calculations.¹⁷⁵ Several modifications of the classic Z-scan setup are existing but no one can compensate the major drawback of this method.

There is no correlation of absorption and efficiency of the photoinitiator. The TPA cross section indicates the amount of absorbed energy of the initiator molecule by a two photon process. If the cross section is large the amount of absorbed energy is also large but nevertheless large energy absorption is not necessarily an indication of an efficient initiation of radicals. The energy can lead to fluorescence or it can be converted to thermal energy, which means in both cases that energy is lost and does not generate radicals.¹⁷⁵ So these measurements do not explain the efficiency of two-photon initiators, information on the formed radicals would be essential. To identify the radical species a time resolved ESR measurement or chemically induced dynamic nuclear polarization (CIDNP) would be needed.

Conclusion

In this work we focused on the development of functional molecules. The two photon absorption of the functionalized 2,6-bis(4-azidobenzylidene)-4-methylcyclohexanone with perylene or dansyl side groups via click chemistry was the main aspect of this project. Two ideas were pursued. One was to selectively graft the BAC-M on a polymer matrix and functionalize it on the reactive sites via click chemistry, and the second was the functionalization of the BAC-M and subsequent grafting on the polymer matrix.

However the BAC-M molecule is a bad acceptor in thiol-ene click chemistry and also not preferred in azide alkyne chemistry, therefore any post functionalization on the grafted polymer can be performed. The second problem was that according to the results of Ovsianikov et al. there are no more azide groups left after grafting the BAC-M on the polymer matrix.¹⁵⁸ Hence, the assumption that the residual groups of such already grafted bisazides can be used for the formation of 1,2,3-triazole rings was confuted.¹³⁴

For the second approach a copper catalyzed 1,3-dipolar cycloaddition of the crosslinking agent BAC-M and the two fluorescent dyes dansyl-alkyne and perylene-alkyne was performed. The reaction conditions of the azide-alkyne click reaction were optimized using different copper/solvent systems. In addition also propargyl alcohol, 5-hexyn-1-ol and hex-1-yne were added to the BAC-M to use it for comparative measurements due to the results of the TPA cross section measurements.

The molecules were synthesized and characterized with different analyses methods. The grafting of the molecules, as well as LSM and Z-scan measurements were performed at TU Vienna. The grafting of the dansyl dye was possible with good results however the perylene dye could not be inscribed into the polymer matrix. During

¹⁷⁵ Cicha, K.; Li, Z.; Stadlmann, K.; Ovsianikov, A.; Markut-Kohl, R. *J. Appl. Phys.* **2011**, *110*.

grafting the combustion of the polymer matrix was observed. Due to the grafting and the TPA-cross section results further measurements to uncover the uncertainties are required. A reliable statement concerning the nonfunctioning of the perylene-BAC-M system can only be taken after the results of the last Z-scans are completed.

Experimental

Materials

All chemicals used for this work were purchased from commercial sources (Fluka, Sigma Aldrich, Lancaster, Merck or ABCR) and unless mentioned otherwise, applied without further purification. BAC-M (2,6-bis(4-azidobenzylidene)-4-methylcyclohexanone) was obtained from TCI chemicals. All reactions were performed under an inert atmosphere of nitrogen using Schlenk techniques of not mentioned otherwise.

Methods

NMR spectroscopy (^1H , ^{13}C , COSY, HSQC and HMBC) was done on a Bruker Avance 300 MHz spectrometer (75 MHz for ^{13}C). Deuterated solvents were obtained from Cambridge Isotope Laboratories Inc. For FT-IR spectroscopy a Bruker ALPHA FT-IR Spectrometer was used. Measurements were performed in ATR mode. For liquid measurement solvents such as CH_2Cl_2 , Acetone and Nujol were purchased from Aldrich. UV/VIS absorption spectra were recorded with a Cary 50 UV/VIS Spectrophotometer from Varian. The measurements were done with a silica glass bulb applicative for a spectral range from 300 to 800 nm from Hellma. In all spectra the absorption was measured. For fluorescence analyses a Hitachi F-7000 was taken. Measurements were performed in a silica glass bulb and dichloromethane was used as solvent. In all spectra excitation and emission was recorded. MALDI-TOF mass spectrometry was performed on a Micromass ToFSpec 2E Time-of-Flight Mass Spectrometer using DCTB as a matrix. Thin layer chromatography was performed with aluminium sheets with silica gel 60 F_{254} from Merck. Via UV light irradiation at 365 nm and a 0.5 % dip solution of KMnO_4 the spots were visualized.

Two photon absorption was measured at the Technical University of Vienna, the basic setup can be seen in Figure 38. The femto-second laser beam is passed through an acousto-optic-modulator. This shutter diffracts the laser beam so that only the first order waves can be used for grafting reactions. The intensity is adjusted by a $\lambda/2$ waveplate and with a polarizing dependant beam-splitter. Before the beam exposes into the resin it is focused through a microscope objective. The motion along x- and y-axes of the laser beam is observed by high precision air bearing axes. The motion along z-axis which carries the resin container is also observed by a similar process. The mirror system ensures that the movements along x- and y-axes are parallel to the direction of the laser beam, so that the line of beam remains stable throughout the whole structuring process. For this inline process observation, a camera views the laser

beam and particularly focuses on the grafting spot. The axes are mounted on a hard stone frame, which is designed to damp vibrations. The base of whole setup is an optical table with an air friction damping which again suppresses vibrations. For the control of the machine, the axes and the laser intensity power meter is plugged to an electronic device, which processes the commands given by the control computer. The sample is illuminated using a red LED lamp to prevent premature polymerization.¹⁷⁶

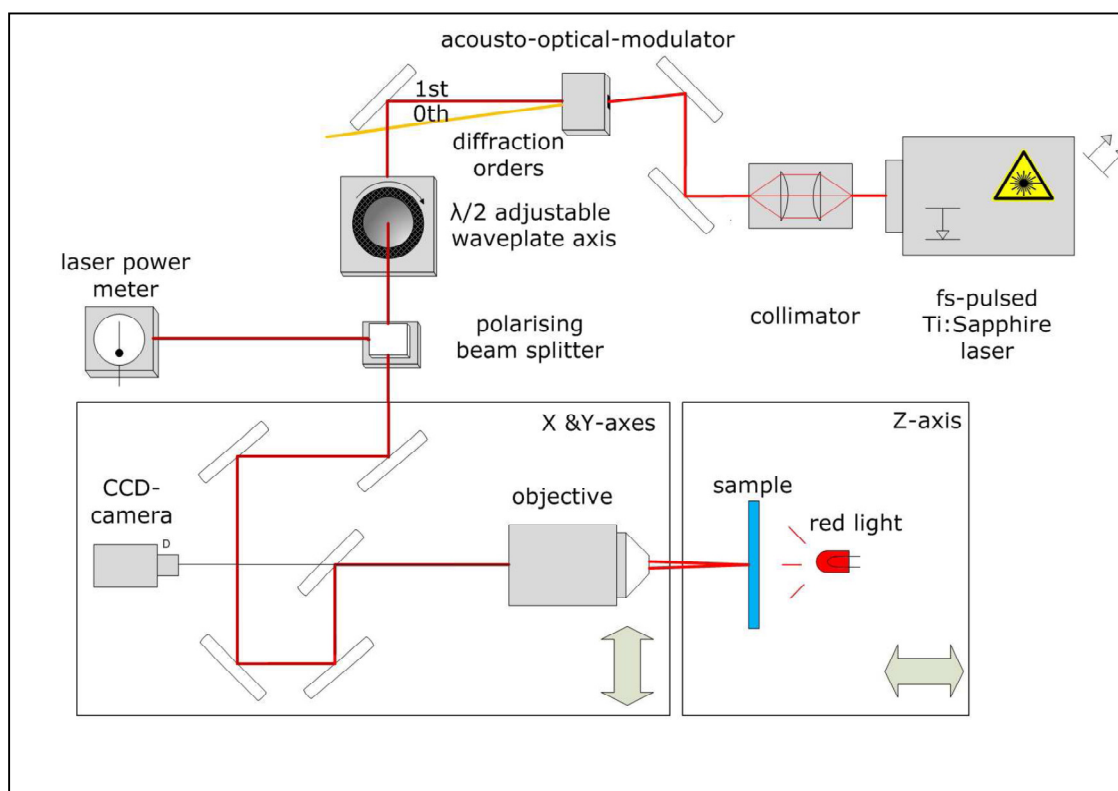


Figure 38: Schematic picture of the TPA experimental setup¹³⁴

For the evaluation of the order of the multiphoton process and the absorption cross-section the Z-scan technique was employed.¹⁷⁷ Z-scan can be performed in two ways. With the open-aperture (OA) Z-Scan method, which is sensitive to nonlinear absorption and the closed aperture (CA) Z-scan version, which is sensitive to nonlinear absorption as well as the nonlinear refractive index.¹⁷⁸ This technique involves the sample scanning along the beam propagation direction (z-axis) through the focal plane of a focused laser beam. As the sample approaches the focal plane, the nonlinear absorption increases, due to its dependence on the intensity of light. The two-photon absorption (2PA) probability is proportional to the square of light intensity; the three-photon absorption (3PA) is proportional to the third order of light intensity and so on. The light transmitted through the sample is collected using a large diameter convex

¹⁷⁶ Torgersen, J. master thesis; **2010**.

¹⁷⁷ Sheik-Bahae, M.; Said, A.A.; Wei, T.H.; Hagan, D.J.; Van Stryland, E.W. *IEEE J. Quantum Electron.* **1990**, *26*, 760-769.

¹⁷⁸ Ajami, A.; Rafique, M.S.; Pucher, N.; Bashir, S.; Husinsky, W.; Liska, R.; Inführ, R.; Lichtenegger, H.; Stampfl, J.; Lüftenegger, S. *Proc. SPIE*, **2008**, 70271H, 7027.

lens and then directed to a detector. The scanning result is a symmetric V-shaped signal showing higher absorption at the focal plane and less absorption at the sample position away from the focus. The order of nonlinear absorption can be determined fitting the theoretical equations for different order of nonlinear absorption to the experimental Z-scan data. From the fitting process, in addition to the nonlinear absorption coefficient, the value of the Rayleigh length can be extracted. If the appropriate equation is fitted to the experimental Z-scan data, this extracted Rayleigh length value should match the value measured experimentally. In this way, the Z-scan technique provides a way to determine the order of nonlinearity. After determining the order of nonlinear absorption, the multiphoton absorption cross-section can be extracted from the fitting of the respective equation to the experimental Z-scan data. Assuming that 2PA is the predominant nonlinear absorption process the theoretical equation is given as:

$$T(z) = \sum_{n=0}^{\infty} \frac{(-q_0)^n}{(n+1)^{3/2}(1+x^2)^n} \quad (1)$$

where $q_0 = N_A \rho \times 10^{-3} L I_0 \sigma_2 \lambda / hc$, N_A is the Avogadro number, ρ is the concentration, L is the thickness of the sample, I_0 is the maximum on axis intensity at the focus, which is calculated from $I_0 = 4V \ln 2 / \pi E p / (\pi w_0^2 \tau)$ ($E p$ is the pulse energy, w_0 is the beam waist radius, and τ is the pulse duration), λ is the wavelength of the laser radiation, σ_2 is the 2PA cross-section, h is the Planck constant, c is the speed of light in free space, x is a unit less variable defined as z/z_0 , z is the sample position measured with respect to the focal point and z_0 is the Rayleigh length. An ultra short laser system (FEMTOPOWER compact PRO) was used which delivers laser pulses with a maximum of 800 mW at a repetition rate of 1 kHz. The minimum pulse duration is typically 25 fs and can be stretched to a few hundreds of femto seconds. The full width at half-maximum is 41 nm and the spectrum is centered at 796 nm. The incident laser power was measured using a digital power meter prior to each measurement before the sample. It is necessary to use the same solvent in spectroscopic grade for the samples because a different polarity of the solvent causes a change in activity of the molecules. The experimental setup is shown in Figure 39. The transient laser beam through a attenuator is split in two orthogonal directions using a beam splitter and the lower intensity part is used as a reference detected by diode D_r . The other beam is directed to the focusing lens and then through the sample. A 0.2 mm thick one-time flow cell connected to a syringe pump for variable flow rates is used for test solutions. This cell is mounted on a translating stage, which can move the sample for a distance of 25 mm through the focus. This allows detecting any small change in nonlinear absorption. The transmitted energy is collected by a large diameter short focal length lens to ensure the whole energy transmitted through the sample is collected. A Si- diode with a 1 cm^2 detector was used to measure the transmitted energy. The computer software analyzes the intensity of individual laser pulses (including averaging over several laser

shots) and also handles the movement of the translation stage as well as the entire data acquisition process.¹⁷⁹

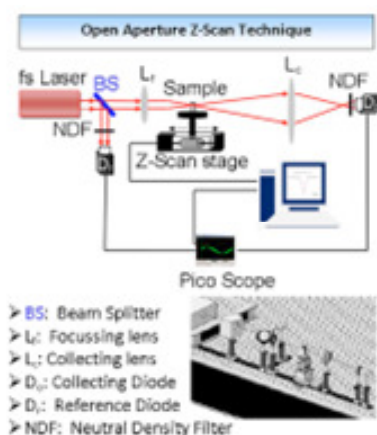
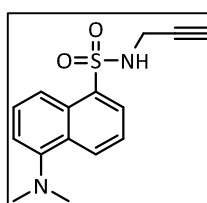


Figure 39: Schematic of the OA Z-scan setup.¹⁷⁹

Alkynes, Thiols and Click-Reactions

5-(dimethylamino)-*N*-(prop-2-yn-1-yl)naphthalene-1-sulfonamide

Dansyl chloride (0.5 g, 1.86 mmol, 1eq) and propargylamine (0.119 mL, 1.86 mmol, 1eq) were dissolved in 7 mL dry dichloromethane. After 15 minutes triethylamine (0.258 mL, 1.86 mmol, 1 eq) was added to the stirred solution. The reaction immediately turned from a dark yellow emulsion to a fluorescent clear solution. Reaction progress was monitored via TLC in CH/EA = 1:1. After 24 hours, it was quenched with water (pH 7) and extracted with DCM. The organic phase was dried over Na₂SO₄ and the solvent removed under reduced pressure. Yield: 478 mg (89%) yellow powder.



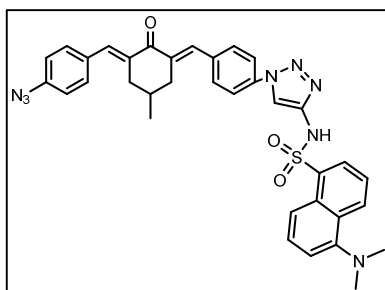
¹H-NMR (δ , 20°C, CDCl₃, 300.36 MHz): 8.55 (d, 1H, J = 7.76 Hz), 8.27 (t, 2H, J = 7.76 Hz), 7.56 (quintet, 2H, J = 7.31 Hz), 7.21 (d, 1H, J = 7.48 Hz), 4.82 (s, 1H, NH), 3.77 (d, 2H, J = 2.52 Hz, N-CH₂), 2.89 (s, 6H, N-(CH₃)₂), 1.92 (t, 1H, J = 2.50 Hz, CCH)

¹³C-NMR (δ , 20°C, CDCl₃, 75.53 MHz): 152.0 (1C, naph), 144.1 (1C, naph), 134.1 (1C, naph), 130.8 (1C, naph), 129.8 (1C, naph), 128.5 (1C, naph), 126.1 (1C, naph), 123.1 (1C, naph), 118.5 (1C, naph), 115.2 (1C, naph), 77.6 (1C, CCH), 72.6 (1H, CCH), 45.4 (2C, N-(CH₃)₂), 32.9 (1C, N-CH₂)

¹⁷⁹ Ajami, A.; Husinsky, W.; Liska, R.; Pucher, N. *J. Opt. Soc. Am. B*, **2010**, *27*, 2290-2297.

***N*-((1-4-((*E*)-3-(4-azidobenzylidene)-5-methyl-2-oxocyclohexylidene)-methyl)-phenyl)-1*H*-1,2,3-triazol-4-yl)methyl)-5-(dimethyl-amino)naphthalene-1-sulfonamide**

2,6-bis(4-azidobenzylidene)-4-methylcyclohexanone (2.3 g, 7.24 mmol, 5 eq) and dansyl-propargylamine (400 mg, 1.45 mmol, 1 eq) were dissolved in 10mL dichloromethane and stirred for 15 minutes at room temperature. Subsequently copper(I)iodide (220 mg, 1.16 mmol, 0.8 eq) was added to the yellow solution and heated to about 35°C. The mixture was stirred for 48 hours, the reaction progress was monitored via TLC (CH/EA = 1:1). For work-up it was quenched with water and extracted with dichloromethane and five times with H₂O dest. The organic phase was dried over Na₂SO₄ and the solvent was removed under reduced pressure. For purification a column chromatography with CH/EA 5:1 with a gradient to 1:1 was performed. Yield: 782mg (88%) yellow powder.



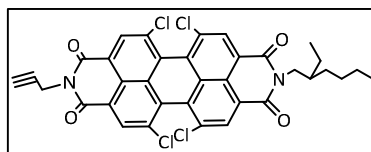
¹H-NMR (δ, 20°C, CDCl₃, 300.36 MHz): 8.49 (d, 1H, naph), 8.30 (d, 2H, naph), 7.75 (s, 2H, (ph)CH(cy)), 7.52 (m, 9H, ph, 1,2,3-triazole, naph), 7.15 (d, 1H, ph), 7.08 (d, 1H, ph), 5.86 (t, 1H, NH), 4.33 (d, 2H, NHCH₂-triazole), 3.02 (d, 2H, cy), 2.82 (s, 6H, N(CH₃)₃), 2.52 (m, 2H, cy), 2.04 (bs, 1H, cy), 1.11 (d, 3H, cy-CH₃)

¹³C-NMR (δ, 20°C, CDCl₃, 75.53 MHz): 189.73 (1C, cy CO), 144.83 (1C, naphCN(CH₃)₂), 140.66 (1C, naphCSO₂), 136.87 (2C, naph), 136.64 (2C, cyCCH), 136.25 (1C, phC-triazole), 135.35 (2C, CH), 134.85 (2C, phCCH), 134.76 (1C, naph), 132.69 (1C, triazole-CH₂), 132.25 (2C, ph), 131.68 (2C, ph), 130.82 (1C, naph), 129.99 (1C, naph), 128.80 (1C, naph), 123.45 (1C, CH triazole), 120.19 (2C, ph), 119.24 (2C, ph), 118.43 (1C, naph), 115.58 (1C, naph), 114.35 (1C, phC-N₃), 45.58 (2C, C(CH₃)₂), 38.90 (1C, NHCH₂), 36.65 (2C, cyCH₂), 29.83 (1C, cyCCH₃), 21.78 (1C, CCH₃)

1,6,7,12-tetrachloroperylene-3,4,9,10-tetracarboxylic-2-(2-ethylhexyl)-8-(prop-2-yn-1-yl)-diamine

1,6,7,12-tetrachloroperylene-3,4,9,10-tetracarboxylicbis-anhydride (430 mg, 0.811 mmol, 1 eq) was weighed into a Schlenk tube and about 5 mL of toluene were added. Then the two amines, 2-ethyl-hexylamine (0.146mL, 0.892mmol, 1.2 eq) and propargylamine (0.057mL, 0.892mmol, 1.2 eq), were added simultaneously. The reaction got dark red and was stirred for 24 hours at 110°C (refluxed). After that, dichloromethane was added and the solvent mixture was transferred into another flask to remove the solvent under vacuum. For further purification a column

chromatography with silica gel was done. It was started with DCM/pentane 1:3 with a gradient to DCM after color change acetic acid was added to remove the rest. TLC in DCM. Yield: 170mg product (31%).

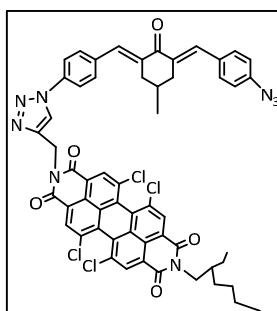


¹H-NMR (δ , 20°C, CDCl₃, 300.36 MHz): 8.70 (d, 4H), 4.99 (s, 2H), 4.15 (q, 2H), 2.23 (s, 1H), 1.76 (t, 1H), 1.5-1.25 (m, 8H), 0.98-0.75 (m, 6H)

¹³C-NMR (δ , 20°C, CDCl₃, 75.53 MHz): 162.59, 162.51, 135.62, 135.37, 133.29, 133.07, 131.55, 131.41, 129.07, 128.44, 123.40, 122.80, 77.82, 71.26, 44.66, 38.02, 30.71, 29.88, 28.67, 24.01, 23.08, 14.13, 10.60

1,6,7,12-tetrachloroperylene-3,4,9,10-tetracarboxylic 2-(2-ethylhexyl)amine-8 ((1-(4-(4-azidobenzylidene)-5-methyl-2-oxocyclohexylidene)methyl)phenyl)-1H-1,2,3-triazol-4-yl) (2.4)

1,6,7,12-tetrachloroperylene-3,4,9,10-tetracarboxylic-2-(2-ethylhexyl)-8-(prop-2-yn-1-yl)-diamine (100 mg, 0.148 mmol, 1 eq) and 2,6-Bis(4-azidobenzylidene)-4-methylcyclohexanone (stabilized with 30-40% water) (220 mg, 0.592 mmol, 4 eq) were weight into a Schlenk tube and about 7 mL of DCM were added. They were stirred together for about 15 minutes and then the Cu(I) salt was added. The reaction was stirred for 72 hours under reflux and monitored via TLC (DCM or DCM/MeOH 20:1). For the removal of copper iodide the reaction was extracted with much water, dried with Na₂SO₄ and the solvent was removed under reduced pressure. For further purification a column chromatography with silica gel was performed. It was started with DCM/Pentan 3:1 → DCM → DCM/MeOH 20:1. TLC in DCM/MeOH 20:1. Yield: 80mg product (52%).



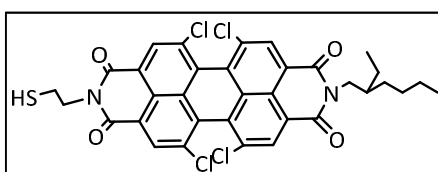
¹H-NMR (δ , 20°C, CDCl₃, 300.36 MHz): 8.70 (d, 4H) 8.16 (s 1H) 7.76 (d 4H) 7.56 (d 2H) 7.46 (d, 2H) 7.06 (d, 2H) 5.63 (s, 2H), 4.12 (m 2H), 3.03 (d, 2H), 2.52 (t, 2H) 1.94 (s, 2H), 1.50-1.27 (m 8H) 1.10 (d, 3H), 0.98-0.88 (m, 6H).

¹³C-NMR (δ , 20°C, CDCl₃, 75.53 MHz): 188.46, 161.54, 161.41, 142.69, 139.46, 134.51, 134.29, 134.22, 133.69, 131.06, 130.44, 129.86, 127.91, 127.41, 122.32, 122.26,

121.88, 120.45, 119.25, 118.05, 43.60, 37.71, 36.96, 35.49, 35.38, 34.47, 29.66, 29.33, 28.67, 28.23, 27.90, 27.62, 22.95, 22.04, 20.61, 13.10, 9.94, 9.56

1,6,7,12-tetrachloroperylene-3,4,9,10-tetracarboxylic-2-(2-ethylhexyl)-8-(2-aminoethanethiol)-diamine (2.5)

1,6,7,12-tetrachloroperylene-3,4,9,10-tetracarboxylicbis-anhydride (200 mg, 0.38 mmol, 1 eq) were weighed into a Schlenk tube and about 5 mL of toluene were added. Then the two amines, 2-ethyl-hexylamine (0.068 mL, 0.42 mmol, 1.2 eq) and 2-aminoethanethiol (0.032 g, 0.42 mmol, 1.2 eq), were added simultaneously. The reaction got dark red and was stirred for 24 hours at 110°C (refluxed). Afterwards dichloromethane was added and the whole solution was transferred into another flask to remove the solvent under vacuum. For further purification a column chromatography with silica gel was performed. The gradient used here started from DCM/pentane 1:3 to DCM and acetic acid. TLC in DCM. Yield: 82mg product (31%).

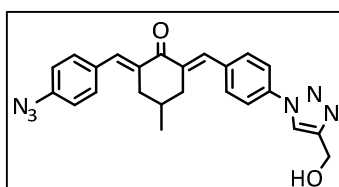


¹H-NMR (δ, 20°C, CDCl₃, 300.36 MHz): 8.65 (dd, 4H), 4.60 (q, 2H), 4.12 (q, 2H), 3.17 (s, 2H), 1.92 (d, 1H), 1.59 (s, 1H), 1.5-1.25 (m, 8H), 0.98-0.75 (m, 6H)

¹³C-NMR (δ, 20°C, CDCl₃, 75.53 MHz): 162.6, 162.25, 135.5, 135.32, 133.08, 133.03, 128.86, 128.46, 123.33, 122.96, 44.64, 39.91, 38.02, 35.95, 30.72, 28.66, 24.02, 23.08, 14.13, 10.61

2,6-bis(4-azidobenzylidene)-4-methylcyclohexanone-4-(4-(hydroxymethyl)-1H-1,2,3-triazol-1-yl)benzylidene)-4-methylcyclohexan-1-one

2,6-Bis(4-azidobenzylidene)-4-methylcyclohexanone (2.3 g, 6.2 mmol, 4 eq) and propargyl alcohol (0.088 mL, 1.55 mmol, 1 eq) were suspended in dichloromethane and stirred for 15 minutes, the mixture is a turbid suspension but gets clearer the longer it got stirred. Cu(II)sulphate, sodium ascorbate and TBTA were added to the reaction and it was stirred overnight at room temperature. The reaction progress was monitored via TLC (CH/EA 1:5). After 48 hours, for work up more DCM was added and the precipitate was filtered through a paper filter (doublesubstituted BAC-M). The rest was purified via column chromatography with DCM and a gradient to DCM/MeOH 10:1. Yield: 504mg (76%)

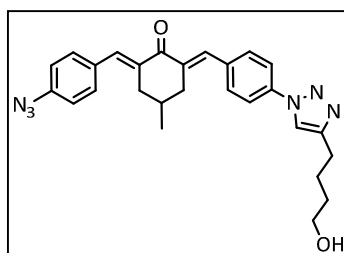


¹H-NMR (δ, 20°C, (CD₃)₂SO, 300.36 MHz): 8.83 (s, 1H, triazole), 7.98 (d, 2H, Benzol 4,6), 7.72 (d, 2H, Benzol 1,3) 7.66 (s, 1H, doublebond to azide 7), 7.59 (d, 3H, Benzol 21,19 and double bond to triazole 16), 7.17 (d, 2H, Benzol 22,18), 5.37 (t, 1H, OH), 4.64 (d, 2H, CH₂-OH), 3.96 (t, 2H, CH₂-CH-CH₂), 2.60(t, 2H, CH₂-CH-CH₂, 9,11), 1.80 (bs, 1H, CH₃-CH, 10), 1.02 (d, 3H, CH₃-CH, 15)

¹³C-NMR (δ, 20°C, (CD₃)₂SO, 75.53 MHz): 188.35, 136.36, 136.15, 135.36, 135.31, 134.91, 134.58, 132.17 (2C), 132.12, 131.76 (2C), 119.71 (2C), 119.26 (2C), 54.97, 35.70, 35.59, 28.57, 21.22

2-4-azidobenzylidene)-6-4-(4-(4-hydroxybutyl)-1H-1,2,3-triazol-1-yl)benzylidene)-4-methylcyclohexan-1-one

2,6-Bis(4-azidobenzylidene)-4-methylcyclohexanone (1 g, 2.69 mmol, 3 eq) and 5-hexyn-1-ol (0.099 mL, 0.89 mmol, 1 eq) were suspended in dichloromethane and stirred for 15 minutes, the mixture is a turbid suspension but gets clearer the longer it got stirred. Cu(I)I (86mg, 0.45mmol, 0.5 eq) was added to the reaction and it was stirred over night at room temperature and the reaction progress was monitored via TLC (CH/EA 1:5). After 48 hours for work up more dichloromethane was added and the precipitate was filtered through a paper filter. The rest was purified with a column chromatography with DCM and a gradient to DCM/MeOH 10:1. Yield: 420mg (60%)



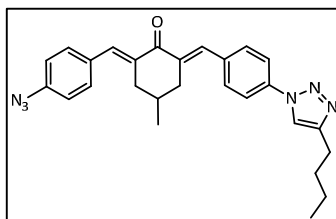
¹H-NMR (δ, 20°C, (CD₃)₂SO, 300.36 MHz): 8.64 (s, 1H, triazole), 7.98 (d, 2H, Benzol 4,6), 7.75 (d, 2H, Benzol 1,3) 7.67 (s, 1H, doublebond to azide 7), 7.61 (d, 3H, Benzol 21,19 and double bond to triazole 16), 7.28 (d, 2H, Benzol 22,18), 4.40 (t, 1H, OH), 3.44 (q, 2H, OH-CH₂-), 3.13-2.96 (m, 2H, CH₂-CH-CH₂, 9,11), 2.72 (t, 2H, OH-(CH₂)₃-CH₂, 28), 2.74-2.62 (m, 2H, CH₂-CH-CH₂, 9,11), 1.83 (bs, 1H, CH₃-CH, 10), 1.73 (quintet, 2H, OH-(CH₂)₂-CH₂-CH₂, 29), 1.51 (quintet, 2H, OH-CH₂-CH₂-(CH₂)₂, 30), 1.04 (d, 3H, CH₃-CH, 15)

¹³C-NMR (δ, 20°C, (CD₃)₂SO, 75.53 MHz): 188.45, 139.9, 136.44, 136.18, 135.35, 135.01, 134.62, 132.2, 131.78, 119.58 (2C), 119.32 (2C), 60.39, 35.71, 35.59, 31.96, 28.6, 25.36, 24.85, 21.24

2-4-azidobenzylidene)-6-4-(4-butyl-1H-1,2,3-triazol-1-yl)benzylidene)-4-methylcyclohexan-1-one

2,6-Bis(4-azidobenzylidene)-4-methylcyclohexanone (700mg, 1.89mmol, 5eq) and hex-1-yne (0.043 mL, 0.38 mmol, 1 eq) were suspended in DCM/H₂O dest. 1:1 and stirred for 15 minutes, the mixture is a turbid suspension but gets clearer the longer it got

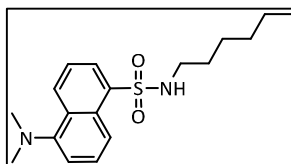
stirred. $\text{Cu}_2\text{SO}_4 \cdot \text{H}_2\text{O}$ (5 mg, 5 mol%) and sodium ascorbate (15 mg, 15 mol%) were added to the reaction and it was stirred very fast over night at room temperature and the reaction progress was monitored via TLC (CH/EA 1:5). After 48 hours for work up more dichloromethane and H_2O dest. were added and it was extracted three times. The rest was purified with a column chromatography with DCM and a gradient to DCM/MeOH 10:1. Yield: 160mg (94%).



$^1\text{H-NMR}$ (δ , 20°C, $(\text{CD}_3)_2\text{SO}$, 300.36 MHz): 7.82-7.75 (m, 5H, triazole, 4H arom.), 7.61 (q, 2H, arom.), 7.78 (d, 2H, doublebond), 7.08 (d, 2H, arom.-azide), 3.08 (q, 2H, CH_2 BAC-M), 2.82 (t, 2H, triazole- CH_2), 2.53 (q, 2H, CH_2 , BAC-M), 1.74 ($\text{CH}_2\text{-CH}_2\text{-CH}_2$), 1.71 (s, 1H, CH, BAC-M), 1.12 (t, 3H, $\text{CH}_2\text{-CH}_3$), 0.99 (t, 3H, $\text{CH}_3\text{-BAC-M}$)

5-(dimethylamino)-*N*-hexylnaphthalene-1-sulfonamide

Dansyl chloride (500 mg, 1.85 mmol, 1 eq) and hexylamine (245 μL , 1.85 mmol, 1 eq) were suspended in dry dichloromethane and stirred for 15 minutes, the mixture is a turbid suspension but after adding the triethylamine (275 μL , 1.85 mmol, 1 eq) it got clear and fluorescent. The whole reaction was stirred over night at room temperature and the reaction progress was monitored via TLC (CH/EA 1:1). For work up water was added as quencher and it was extracted with dichloromethane five times. No further work up was needed because NMR showed a pure product. Yield: 605mg (98%).



$^1\text{H-NMR}$ (δ , 20°C, CDCl_3 , 300.36 MHz): 0.74 (t, 3H, $\text{CH}_2\text{-CH}_3$), 1.16-0.95 (m, 6H, $\text{CH}_2\text{-(CH}_2)_3$), 1.38-1.26 (m, 2H, $\text{CH}_2\text{-(CH}_2)_3\text{-CH}_3$), 2.91-2.86 (m, 8H, $\text{NH-CH}_2\text{-CH}_2$, $\text{N-(CH}_3)_2$), 4.90 (bs, NH), 7.16 (d, 1H, aromatic CH *ortho* to aniline), 7.51 (q, 2H, aromatic CH *meta* to aniline and *meta* to sulfone group), 8.24 (d, 1H, CH *para* to aniline), 8.34 (d, 1H, CH *para* to sulfone group), 8.52 (d, 1H, aromatic CH *ortho* to sulfone group)

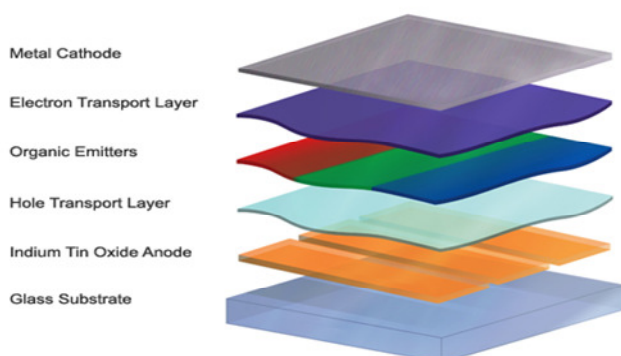
$^{13}\text{C-NMR}$ (δ , 20°C, CDCl_3 , 75.53 MHz): 152.0, 135.04, 130.34, 129.95, 129.74, 129.54, 128.39, 123.21, 118.95, 115.22, 45.44, 43.33, 31.15, 29.47, 26.10, 22.39, 13.93

Chapter 3

Triphenylamine Studies; Literature, Syntheses and Computational work

Introduction

Amine-oxide



Organic Light Emitting Diode Diagram



Figure 40: Modular design of an OLED and Sony's world's first 16.7 million color flexible OLED¹⁸⁰

Tertiary amine-oxides are basic, hygroscopic and thermic labile substances. The N→O group is very polar, hydrophilic and likely to build a strong interaction in the form of hydrogen bridge linkage. With long chained aliphatic rests, tertiary amines are used as tensides. As they are basic molecules, amino-oxides form salts which are more thermally stable than the free *N*-oxide, because of that they often get isolated as hydrochlorides. In the manufacture of triorganic-amine oxides for the oxidation mostly peroxides or peroxy-acids are used. Hydrogen peroxide or *m*CPBA are the most commonly used reagents for the preparation of amine-oxides. A different way would be oxidation under high oxygen pressure or with organo-hydroperoxides under metal-catalysis; here titanium, vanadium and molybdate are the most efficient ones.

When searching for proved scientific results for the synthetic oxidation of triphenylamine, different opinions of different areas have to take into consideration. It seems a bit like there are grey areas in scientific literature and opinions differ. At the end of the 19th and the beginning of the 20th century Piccard and Larsen¹⁸¹ wrote that there is only one mono-nitro derivative of triphenylamine known, which was prepared

¹⁸⁰ <http://www.engadget.com/2007/05/24/sonys-worlds-first-16-7-million-color-flexible-oled/>

¹⁸¹ Piccard, J.; Larsen, L.M. *J. Am. Chem. Soc.*, **1917**, 39, 2006-2009.

by Herz¹⁸² in the year 1890 by the treatment with nitric acid. Piccard and Kharasch needed the *p*-nitrotriphenylamine and tried to prepare it by introduction of phenyl groups into *p*-nitraniline. Irma Goldberg¹⁸³ introduced the use of phenyl iodide for the preparation of triphenylamine and some of its derivatives; she heated phenyl iodide with diphenylamine and potassium carbonate in presence of some copper powder.

After the first uses of triphenylamine there is a long time nothing to hear about it. In the 21st century triphenylamine and its derivatives were found to have useful properties in electrical conductivity and electroluminescence, and they are used in OLEDs as hole-transporters.¹⁸⁴ In contrast to other conducting organic materials the charge transport of triphenylamines is relatively fast, furthermore they build stable cations which make them less air sensitive than conjugated conducting materials like PPV (Poly(*p*-phenylene vinylene)). In the last years a lot of research has been done in developing semiconducting triphenylamine systems. Hereby the polymer systems are much more stable and easier to handle and to process than their low molecular counterparts. A.V. Grib¹⁸⁵ mentioned the conversion of triphenylamine derivatives into their oxidized corresponding derivatives. This reaction was only detected as general in the case of substituted triarylamines, on the contrary, unsubstituted triphenylamine is converted to a complex mixture of products, among which only traces of nitrobenzene were detected by the chromatograph. The oxidation of triphenylamine under the action of hydrogen peroxide in acetic anhydride was described earlier.¹⁸⁶ In Russian journals oxidation of triphenylamine is mentioned but never proved with analytical methods. Adams et al. discussed the electrochemical study on the anodic oxidation of triphenylamine in acetonitrile. It is oxidized at about 0.98v vs. SCE to an unstable monocation radical TPA⁺. The cation dimerizes or reacts with parent rapidly to form tetraphenylbenzidine (TPB). This reaction is accompanied by the loss of two protons per dimer, TPB is more easily oxidized than the starting TPA and undergoes further oxidation. This occurs in two, discrete one electron steps to give the TPB⁺ and finally the dication TPB²⁺.¹⁸⁷ The reaction is shown in Scheme 22.

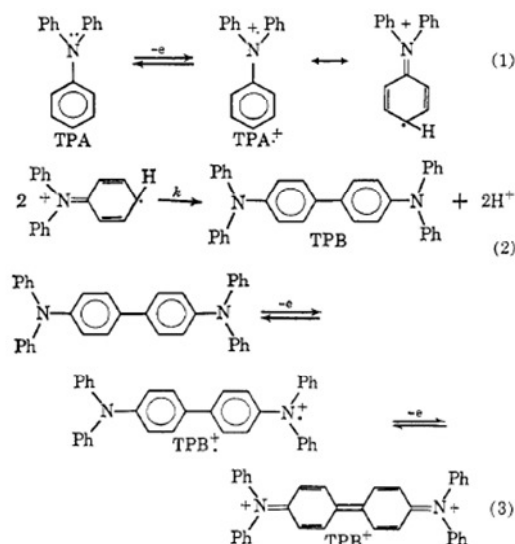
¹⁸² Herz, *Berichte*, **1890**, *23*, 2537.

¹⁸³ Goldberg, I. *Berichte*, **1907**, *40*, 4542.

¹⁸⁴ Shi, W.; Fan, S.; Huang, F.; Yang, W.; Liu, R.; Yong, C. *J. Mater. Chem.*, **2006**, *16*, 2387-2394.

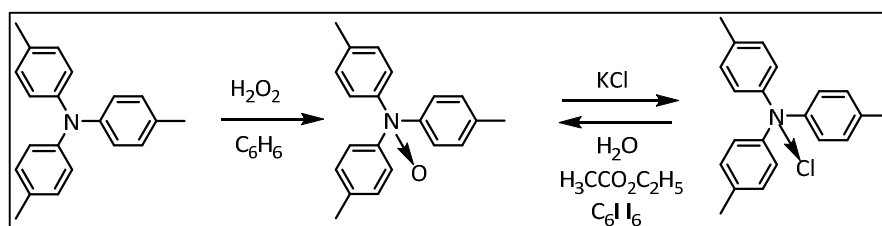
¹⁸⁵ Grib, A.V. *Seriya Khimicheskaya*, **1967**, *2*, 446-447.

¹⁸⁶ Belov, V.N.; Savich, K.K. *Zh. Obshch. Khimii*, **1947**, *17*, 257.



Scheme 22: Over all reaction scheme from TPA to TPB¹⁸⁷

In the 1970s Craig et al. proved that the stability of the TPA oxide is really low compared to other tertiary amine oxides.¹⁸⁸ In 2000 again a Russian group¹⁸⁹ discussed the stability of triarylamine-*N*-oxides. They mentioned the erroneous papers and also that till the present time no synthetic procedure for such triarylamines is described. They present a procedure for the, in their opinion, relatively stable (4,4',4''-trimethyl)triphenylamine-*N*-oxide. But also here no analytical data or proof is presented. In 2001 Zhao et al.¹⁹⁰ established that incorporation of electron-donating substituents at the *para*-position of triarylamines affords stable, often isolable, radical cations. Therefore they designed trarylamines where the *para*-position is blocked with electron donating groups. They particularly targeted electron-donating *para*-substituents that lack benzylic hydrogens. Thus, this design obviates not only the dimerization pathways through the *para*-position but also possible dimerization through a benzylic position. It is conceivable that all of these features can be incorporated into a tri-substituted triphenylamine.¹⁹¹



Scheme 23: Oxidation of (4,4',4''-trimethyl)-triphenylamine¹⁸⁹

¹⁸⁷ Seo, E.T.; Nelson, R.F.; Fritsch, J.M.; Marcoux, L.S.; Leedy, D.W.; Adams, R.N. *J. Am. Chem. Soc.*, **1996**, 3498-3503.

¹⁸⁸ Craig, J.C.; Purushoth, K.K. *J. Org. Chem.*, **1970**, 35, 1721-1722.

¹⁸⁹ Bulavka, V.N.; Gekhman, A.E.; Koshelev, K.K. at *ECSOC-4*, **2000**, *Triarylamine-N-oxides. I. The First Attempt of (4,4',4''-Trimethyl)triphenylamine-N-oxide Synthesis and Direct Proof of Its Formation*.

¹⁹⁰ Zhao, H.; Tanjutco, C.; Thayumanavan, S. *Tetrahedron Lett.*, **2001**, 42, 4421-4424.

¹⁹¹ Anderson, J.D.; Thayumanavan, S.; Barlow, S.; Lee, P.A.; Gruhn, N.; Carter, C.; Dodelet, J.P.; Marder, S.R.; Armstrong, N.R.

After 2000 many different oxidation procedures with e.g. different metal catalysts like gold,¹⁹² iron,¹⁹³ vanadium¹⁹⁴ or again uncatalyzed processes using activated H₂O₂, H₂O₂ with a catalyst like ascorbic acid, Caro's acid, dioxiranes or peracids and electrochemical oxidation¹⁹⁵ were tried.

Results and Discussion

Together with Pawel Cias who did the ab-initio studies of TPA derivatives the aim of this work was to prove or not prove the ability of triphenylamine to oxidize and build a stable oxidized form. Literature research, synthetic work with analytical methods and computational studies should give an overall picture of this question.

The literature study was discussed in the introduction of this chapter. In the synthetic part the interest was directed to the different synthetic pathways, the catalyzed and non-catalyzed ways to synthesize oxidized triphenylamine. The idea was to follow old synthetic ideas as well as new catalytic and electrochemical aspects. Although there is no real proof of an amine-oxide of triphenylamine in old papers the first attempts were to follow these procedures and afterwards try some newer ones and also include aspects which declare that the oxidized form is not stable enough.

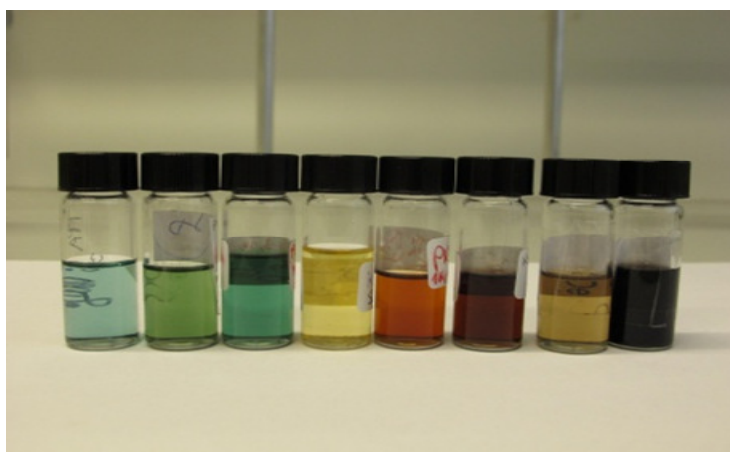


Figure 41: Different colors in maybe oxidized triphenylamine

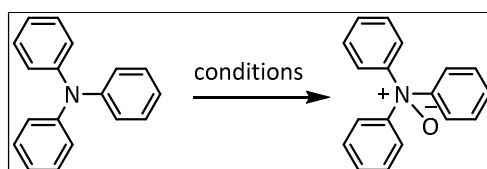
Herein the different reaction conditions which gave the best results are listed. At first a reaction scheme and the used conditions are listed.

¹⁹² Della Pina, C.; Falletta, E.; Rossi, M. *Topics in Catalysis*, **2007**, 44, 325-329.

¹⁹³ Wörl, S.; Hellwinkel, D.; Pritzkow, H.; Krämer, R. *Chem. Comm.*, **2003**, 2506-2507.

¹⁹⁴ Rout, L.; Punniyamurthy, T. *Adv. Synth. Catal.* **2005**, 347, 1958-1960.

¹⁹⁵ Yeh, S.J.; Tsai, C.Y.; Huang, C.Y.; Liou, G.S.; Cheng, S.H. *Electrochem. Comm.*, **2003**, 5, 373-377.



- 3.3 eq H_2O_2 (30%) in DCM, 8 h – 5 d, rt – 50°C
- 2.8 eq *m*CPBA (55%) in DCM, 2 h – 1 d, 0 – 50°C
- 3 eq H_2O_2 (30%), 3.7 mol% vanadium-catalyst in CH_3CN , 4 h, rt – 80°C
- 3.6 eq H_2O_2 (30%), 2 mol% ascorbic acid in DCM, 6 h, 40°C

Scheme 24: Scheme of oxidized TPA with different reaction conditions

In none of the tests a real stable amine-oxide could be received. After purification and analytical procedures there were only reaction mixtures or the non-reacted triphenylamine in a different color. Also heating under oxygen atmosphere and high pressure only provides a different colored product. As it can be seen in Figure 42, the NMR characterization could not obtain a clear result. The TPA-structure clearly changed not only to one reaction product but to a complex mixture of different products in different stages of oxidation which are so similar that it is not possible to separate them with common purification methods. Products were also analyzed with FT-IR measurements and UV-Vis spectroscopy but also these methods were not able to show clear results.

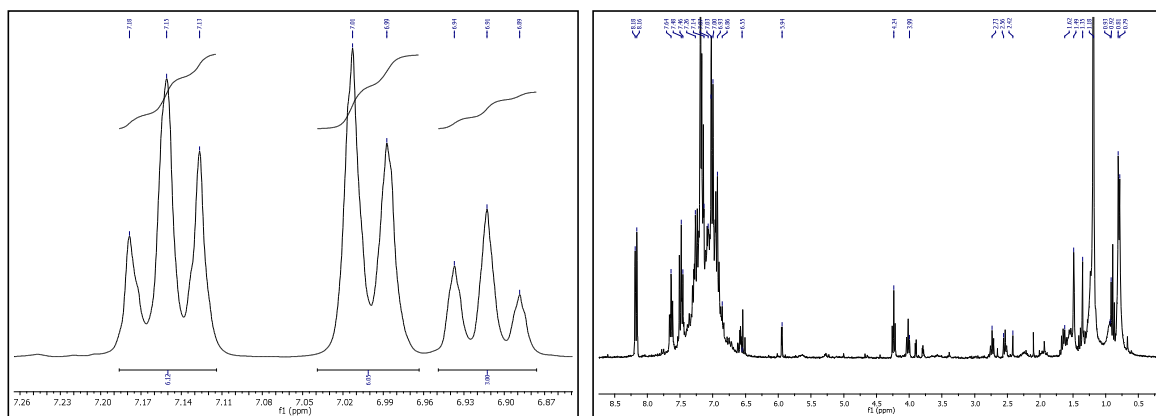
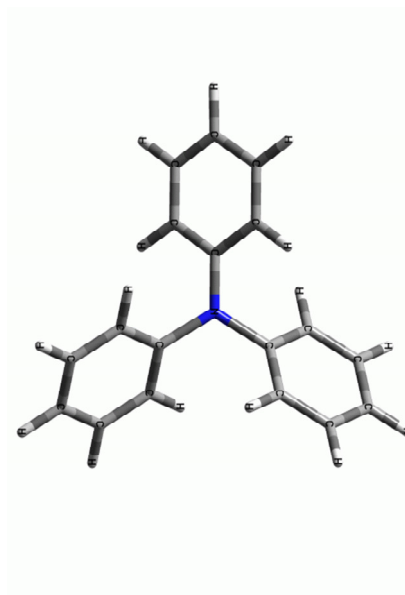
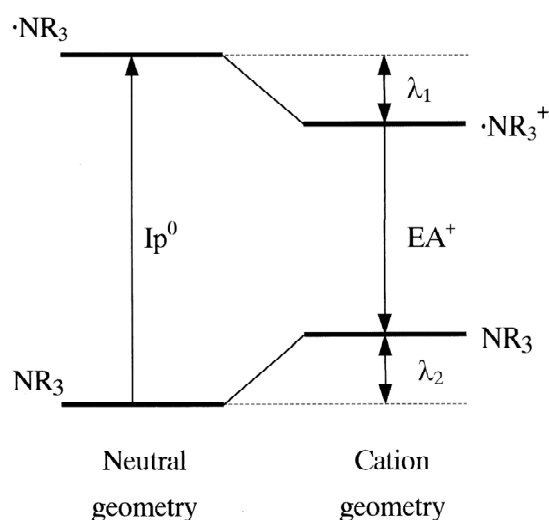


Figure 42: ^1H NMR of TPA in CDCl_3 and complex product mixture after oxidation and chromatographic purification

The ab-initio studies were made because the relationship between the molecular structure and the hole transport properties is vital in the process of device design, TPA is very helpful in these studies.

The requirement for a hole transport layer is an effective hole-generation with a low ionization potential and a high hole mobility. It should have a chemical reversibility and sufficient thermal stability with appropriate HOMO/LUMO levels and a good stability under atmospheric conditions e.g. toward oxygen. For improving the performance of

such a layer the knowledge of charge carrier energy levels and their mobility in organic thin films is essential. Furthermore an understanding of oxygen influence on organic layers and determination of oxidation products is important. In this regard the term ionization energy (E_i) is important. It is the minimum energy required to remove (to infinity) an electron from the atom or molecule isolated in free space and in its ground electronic state. This quantity was formerly called ionization potential, and was at one stage measured in volts. The ionization potential and the reorganization energies were estimated via DFT (density functional theory). Malagoli et al. made a density functional theory study of the geometric structure and energetic of triphenylamine-based hole-transporting molecules.¹⁹⁶ Compared with their results our ionization potential and the reorganization energy fit well.



Ip^0 : Vertical ionization potential of neutral molecule

EA^+ : Vertical electron affinity of cation radical

λ_1 : Reorganization energy of cation radical

λ_2 : Reorganization energy of neutral molecule

Figure 43: Scheme of the energy levels of the cation vs. the neutral form; DFT theory and TPA molecule

Table 8: DFT calculations with experimental comparison

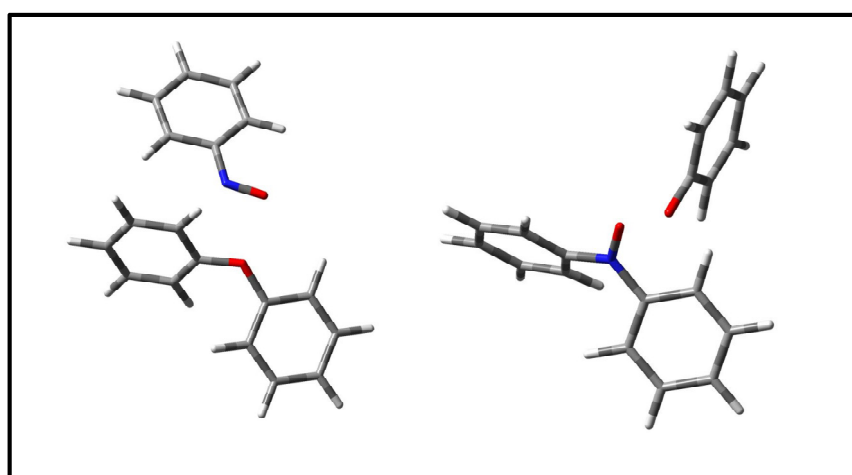
source	I_p (eV)	I (eV)
Malagoli, Bredas ¹⁹⁶	6.42	0.12
Cias et al.	6.55	0.11

¹⁹⁶ Malagoli, M.; Bredas, J.L. *Chem. Phys. Lett.*, **2000**, 327, 13-17.

experimental	6.75 ¹⁹⁷ 6.88 ¹⁹⁸	-
--------------	---	---

Table 9: Ionization potentials, HOMO-LUMO levels and reorganization energies in tri substituted TPAs

	I_p [eV] (exp.)	I_p [eV] (calc.)	HOMO [eV]	LUMO [eV]	HOMO- LUMO gap [eV]	λ_+ [eV]
TPA	6.75	6.55	-5.118	-0.719	4.399	0.11
TPA-(F) ₃	6.19	6.76	-5.443	-1.232	4.211	0.20
TPA-(Br) ₃	-	6.79	-5.595	-1.307	4.288	0.14
TPA-(NO ₂) ₃	-	7.97	-6.740	-3.228	3.512	0.13
TPA-(CH ₃) ₃	5.81	6.19	-4.925	-0.629	4.296	0.12
TPA-(OCH ₃) ₃	-	5.82	-4.649	-0.644	4.005	0.27
TPA-(NH ₂) ₃	4.84	5.32	-4.246	-0.451	3.795	0.49

Figure 44: TPA⁺ + O₂ reaction product – DFT calculations B3LYP/TZVP level. Structure of the expected products¹⁹⁷ Debies, T.P.; Rabalais, J.W. *Inorg. Chem.*, **1974**, *13*, 308.¹⁹⁸ Meijer, G.; Berden, G.; Meerts, W.L.; Hunziker, H.E.; de Vries, M.S.; Wendt, H.R. *Chemical Physics* **1992**, *163*, 209-222.

The last calculations were made about the spin distribution of TPA^+ and TPAO^+ . In Figure 45 we have on the left side the triphenylamine dimer radical cation which is straight in the middle and not twisted and on the right side the twisted middle of the oxidized TPA dimer radical cation.

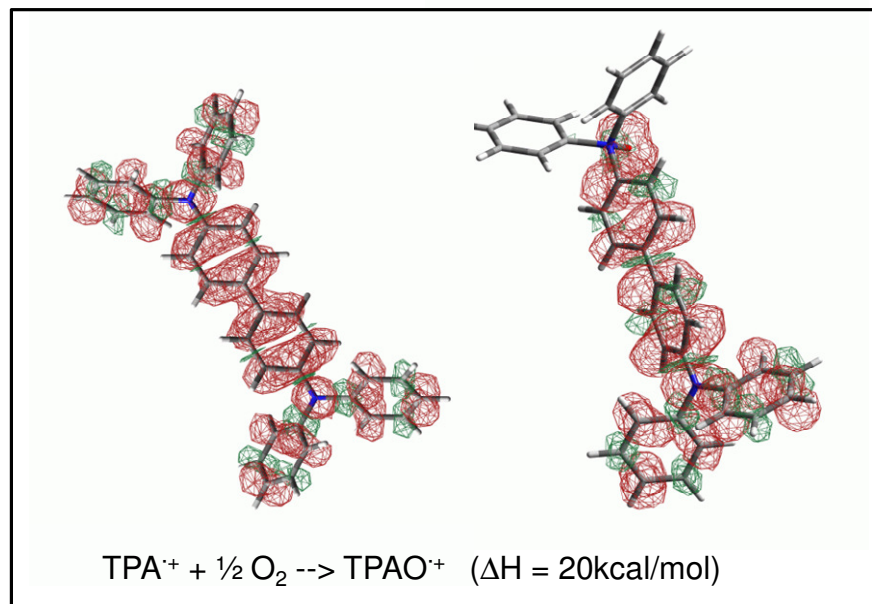


Figure 45: Spin distribution of TPA derivatives

With these studies and calculations the overall picture of experimental and theoretical work can be seen. In my opinion the oxidation of unsubstituted triphenylamine is not possible and the experimental and theoretical work of us and many other groups show a good overview of the possibilities in triarylamine oxidation and the possible results. Also different experimental methods were highlighted and the calculations allow a good overview over possible substituents and their use for fine tuning of the ionization potential, the HOMO-LUMO levels as a hole transport material and the mobility (reorganization energies).

Chapter 4

Organic Radical Batteries

Introduction

Organic Molecular Radicals

An organic molecular radical is a molecular entity which posses an unpaired electron. These radicals often appear as intermediates in photochemical or thermal reactions and they are also known to initiate and propagate polymerization and combustion reactions. Usually they are short lived and highly reactive but through dimerization or redox reactions with other molecules they can be converted into stable molecules. Thus the organic molecular radicals had been hitherto classified as unstable and intractable materials.¹⁹⁹ However, there are some radicals, whose stabilization is achieved via sterically protected structures around the radical centers or the unpaired electrons and also by resonance structures involving the unpaired electrons. Based on these chemical modifications, hundreds of stable organic radicals are now known.²⁰⁰

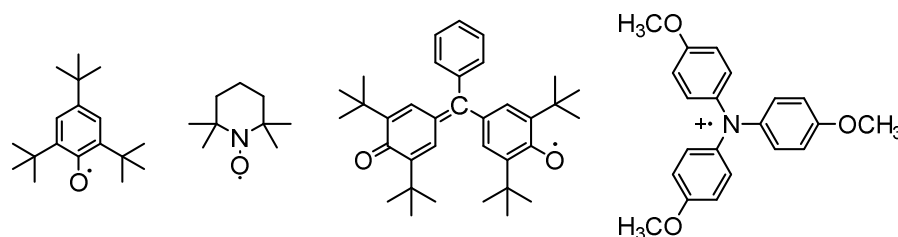


Figure 46: Stable radical molecules: 2,6-di-tert-butylphenoxide, TEMPO, galvinoxyl, triphenylamine-derivative

Some stable radicals such as TEMPO and its derivatives are commercially available and they have been extended to their polymeric radical analogs as well.

Organic derived electrode active materials have been studied since the 1980s and MacInnes et al., reported in 1981 an electrically conductive polyacetylene as potential application of p- and n-doping processes in polyacetylene to a rechargeable battery in an all organic device design.²⁰¹ Commercialization of this new technology was prevented because of the relatively slow electrochemical kinetics during the doping/de-doping of the polyacetylene, this affected the whole battery performance and also the cell voltage was not constant. Poly(acrylic-acid)-combined TEMPOs were

¹⁹⁹ Nishide, H.; Suga, T. *ECS Interface*, **2005**, Winter, p.32

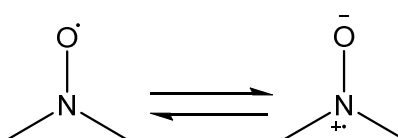
²⁰⁰ Walters, W.A., *Oxford University Press*, **1948**.

²⁰¹ MacInnes, D.; Druy, M.A., Nigrey, P.J.; Nairns, D.P.; MacDiarmid, A.G.; Heeger, A.J. *Chem. Commun.*, **1981**, 317.

synthesized and also polyaniline and polypyrroles, which both do not lead to efficient device performances because of their poor capacities, chemical instability, self discharge and polymer degradation have been studied. In the late 1980s disulfide compounds were investigated intensively as a cathode material.²⁰²

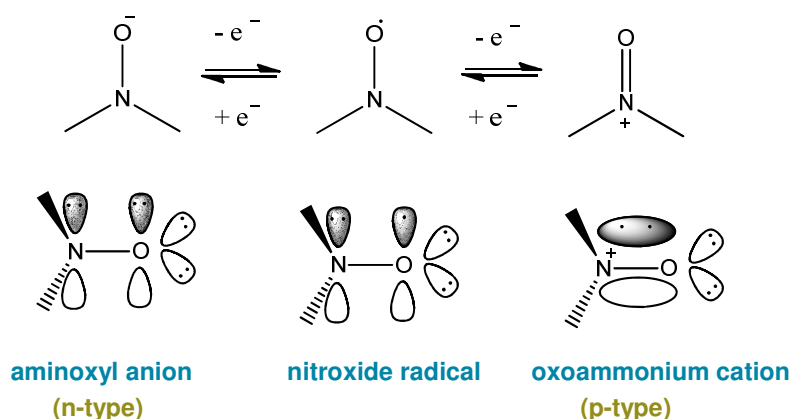
Organic radical based or metal-free redox reagents are examined due to the perspective of green and environmentally compatible chemical reaction processes. Organic radical polymers, especially the nitroxide polymers display reversible redox behavior. Oxidation of the nitroxide radical and reduction of the corresponding oxoammonium form is observed and therefore radical polymers have been utilized as the electrode active or charge-storage component for a secondary battery.²⁰³

Nitroxides



Scheme 25: Resonance structures of a nitroxide

Nitroxide radical polymers were chosen due to their small molecular weight per radical unit. The repeating unit structure provides a high density of unpaired electrons which is an almost quantitative doped state. A nitroxide radical is a stable radical with the spin-density centered on the oxygen atom. It has two resonance structures which offer a high stability to the radical. The redox couples presented in Scheme 26 show that on the anodic side the radical is oxidized to form the corresponding oxoammonium cation, this process is reversible and leads to p-type doping of the radical material. On the cathodic side the nitroxide radical is reduced to the aminoxy anion leading to n-type doping of the material. These redox couples should be applicable to the cathode and anode reaction of a secondary lithium ion battery, respectively.¹⁹⁹



Scheme 26: Redox couples of the nitroxide radical.¹⁹⁹

²⁰² Visco, S.J.; Mailhe, C.C.; DeJonghe, L.C. *J. Electrochem. Soc.*, **1989**, *136*, 661.

²⁰³ Nishide, H.; Iwasa, S.; Ou, Y.J.; Suga, T.; Nakahara, K.; Satoh, M. *Electrochim. Acta*, **2004**, *50*, 827.

Also based on results obtained by Nishide and Suga Figure 47 shows the charging and discharging mechanism of a prototype organic radical based lithium-ion battery where the p-type nitroxide radical polymer forms a cathode operated in conjunction with a carbon anode. During the charging process, the p-type radical polymer in the cathode is oxidized to the oxoammonium form. The discharging process, leads to a regeneration of the nitroxide radical by reduction of the oxoammonium form.

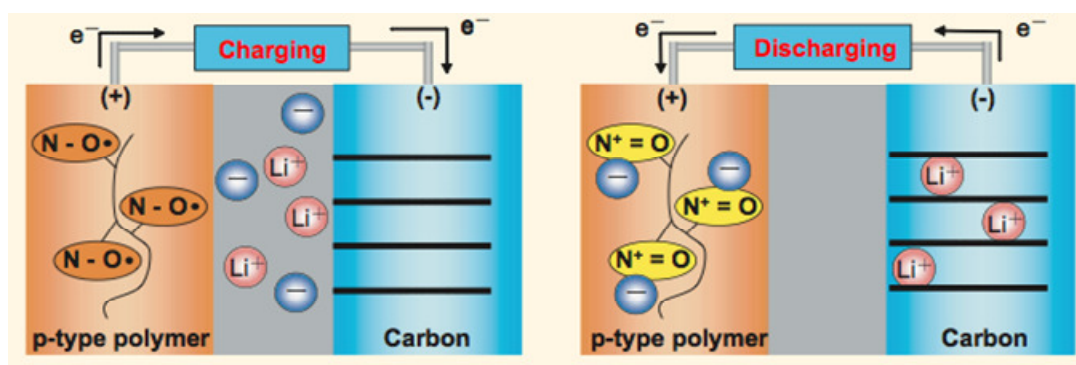


Figure 47: A lithium-ion battery based on a radical polymer cathode¹⁹⁹

Transfer rates and electron hopping

The electron-transfer rate constant for the nitroxide radical in solution is estimated to be in the order of $>10^{-1}$ cm/s⁸. Compared to the slow rates for other organic redox couples (10^{-8} cm/s disulfide redox) this is the most important feature of the nitroxides.¹⁹⁹

When the radical polymer is placed on a current collector and equilibrated in electrolyte solutions charge propagation within the polymer layer is accomplished, leading to high-density charge storage because the redox sites are so populated that electron self-exchange reactions are completed within a finite distance of the polymer layer.²⁰⁴ The redox gradient driven charge propagation is based on successive electron self exchange reactions. The apparent diffusion coefficient D , of the charge produced at the surface of the current collector is determined by the bimolecular rate constant k_{ex} , for the self exchange reaction.²⁰⁴ When the sites are immobilized in the layer, allowing only diffusional collision of the neighboring sites to undergo an electron self-exchange reaction the charge propagation process involves an electron hopping mechanism with a diffusion coefficient formulated by $D = k_{ex}\delta^2C/6$, where k_{ex} is the bimolecular rate constant, δ is the site distance and C is the site concentration in the polymer layer.²⁰⁵ The diffusion-limited outer-sphere redox reactions of radicals lead to the fast electron self-exchange reaction, resulting in the efficient transfer of charge produced at the surface of the current collector (*cf.* Figure 48).²⁰⁴

²⁰⁴ Oyaizu, K.; Nishide, H. *Adv. Mat.*, **2009**, *21*, 2339-2344.

²⁰⁵ Murray, R.W., *Molecular Design of Electrode Surfaces*, Wiley-Interscience, New York USA, **1992**.

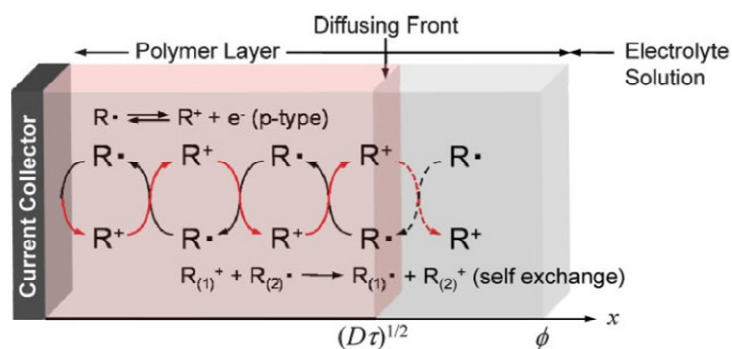


Figure 48: Electron hopping process in an ORB.²⁰⁴

Comparison with other battery systems

Organic radical batteries are not really comparable with lithium ion batteries. Lithium ion batteries are rechargeable via an intercalation process. Lithium ions move from anode to cathode during discharge, the positive ion is extracted from the anode (usually graphite) and inserts into the cathode (lithium containing compound). The reversible intercalation into graphite²⁰⁶ and intercalation into cathodic oxides²⁰⁷ was discovered in the 1970s by J.O.Besenhard, he also proposed the application in lithium cells.²⁰⁸ Secondary lithium ion batteries (LIBs) have a high storage capacity, the charge and discharge mechanism works through an intercalation mechanism of the lithium, which is a charge and mass transport because of diffusion of Li^+ ions. Due to that they suffer from limitations in the charge and discharge rates. Another big problem is the always recurring safety issues because of the metallic lithium.

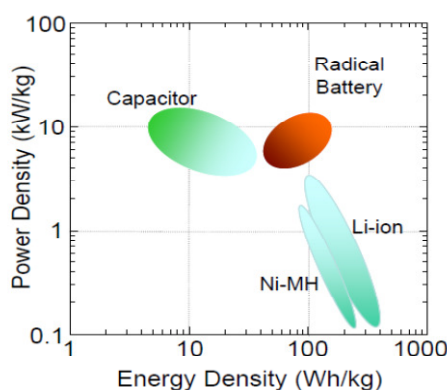


Figure 49: Ragone plot comparison between capacitors, radical batteries and Li-ion batteries²⁰⁹

In the Ragone plot a comparison between the state of the art storage possibilities is shown. ORBs have a better charge and discharge characteristic than LIBs and a higher energy density than capacitors but they are overall more comparable with their

²⁰⁶ Besenhard, J. O.; Fritz, H.P. *J. Electroanal. Chem.* **1974**, *53*, 329.

²⁰⁷ Besenhard, J. O.; Schöllhorn, R. *Journal of Power Sources*, **1976**, *1*, 267.

²⁰⁸ Besenhard, J. O.; Eichinger, G. *J. Electroanal. Chem. Interfacial. Electrochem.* **1976**, *68*, 1.

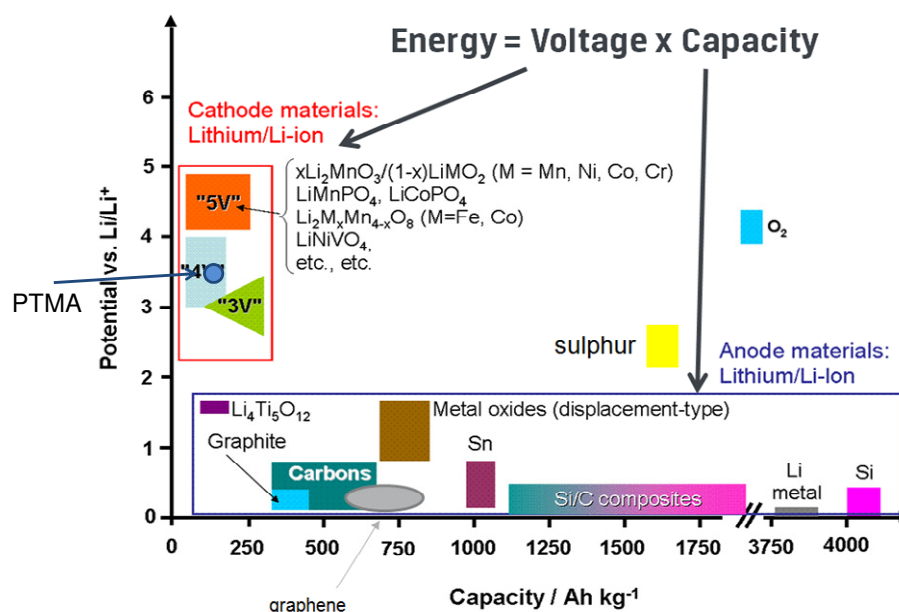
²⁰⁹ Knall, A.C.; Fast, D.E.; Gallas, K.; Schinagl, C.; Kren, H.; Koller, S.; Saf, R.; Stelzer, F. *ORB*, Polymer Symposium Leoben, **2012**.

features to the capacitors than to other secondary batteries. The performance of the radical battery is characterized by high power and high energy density and they are almost comparable to those of capacitors and conventional secondary batteries. The high capacity can be used for example as a power supply system for the backup or shutdown of personal computers during power failure. Other advantages of organic batteries are a thin profile which is also flexible. The high retainability of the charge/discharge capacity matches lithium ion batteries at 75% of their initial charge after 500 cycles.²¹⁰

The most important thing is the green and environmental friendly chemistry without heavy metals, they are non toxic and non flammable and do not require additional care for their handling. The reversible redox reactions of stable organic radicals do not cause structural changes and there is no mass transport between the electrodes, due to the earlier described electron hopping mechanism.

The main disadvantage of organic radical batteries is their low capacity compared to other battery systems. They only have minimal storage space for energy due to their lower theoretical capacities compared with lithium and also because of the not perfectly working slurry system, where only about a maximum of 50% of the mass derives from the active material.

In Figure 50 the differences and disadvantages of ORBs can be clearly seen. In the picture some cathode and anode materials of LIBs are shown. In comparison with the cathode Li-ion materials the commonly used radical battery material PTMA is somewhere in the middle. Most of the polymer materials have good potentials but the capacity values are so much lower than that of the commercially used LIBs.



²¹⁰ Foley, D. "NEC Develops New Ultra-Thin, Flexible, Rechargeable Battery Boasting Super-Fast Charging Capability", *NEC Corporation*, 2012.

Figure 50: ORB materials in comparison with LIBs²¹¹

State of the Art

An ongoing issue with the ORBs is the enhancement of the energy density or capacity. The capacity of conventional cathode materials for Li-ion batteries is in the range of 150-170 mAh/g. The theoretical capacity of for example PTMA as a radical battery cathode material is about 111 mAh/g. Therefore the challenge lies in designing new structures for nitroxide derivatives, to get higher theoretical capacities. Due to the properties of the nitroxide radical which has a low molecular weight per radical unit one design requirement is that the smaller these molecules get the higher are the capacities. New designs are coming for example from Nishide and his co-workers and some are shown in Figure 51.¹⁹⁹

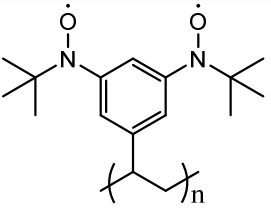
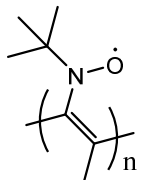
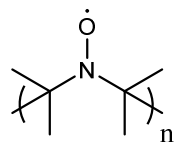
			p-type
138	127	114	MW
194	211	224	theoretical capacity (mAh/g)

Figure 51: Example of p-type radical polymers and their theoretical capacities

For application and testing the radical polymers, which work as cathode materials of a battery, a slurry is prepared. The mixture consists largely of an electrically conductive material like carbon black or carbon nano tubes. Also a binder material is used to connect the conductive material with the active polymer material. This mixture is coated with a doctor knife on a current collector (aluminum foil) and then incorporated in a Swagelok half cell with lithium as counter electrode. The schematic setup and the setup of the Swagelok cell are shown in Figure 52.

²¹¹ Courtesy of Varta Micro Innovation, 2012.

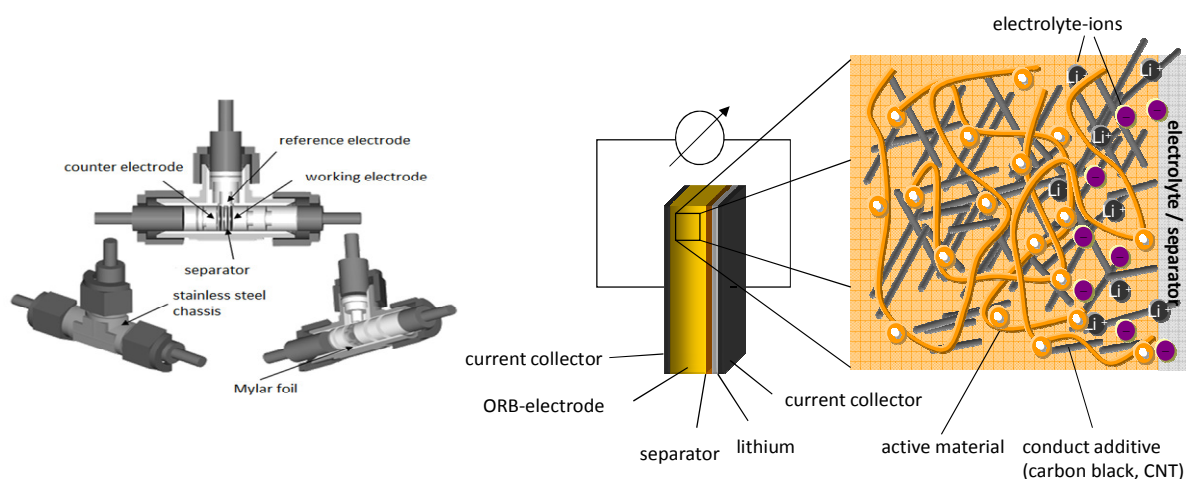


Figure 52: Schematic setup of an ORB half cell made in a Swagelok-half cell

Toward flexible Batteries – NEC

The design of soft portable electronic equipment, like roll up displays and wearable devices, requires the development of flexible batteries. Active radio-frequency identification tags and integrated circuit smart cards also require bendable or flexible batteries for durability in daily use.²¹² Transport rates at inorganic electrodes are limited by slow kinetics of ion intercalation and migration in these materials.²¹³ An approach of radical polymers is that an electrolyte layer is between two thin polymer layers, which have low conductivity but incorporate redox-active groups with the view to increase the overall redox capacity. In this case the polymer backbones provide a conducting path to interconnect the redox sites for a hopping of electrons by a self exchange mechanism resulting in a storage and charge in a homogenous solid.²¹²

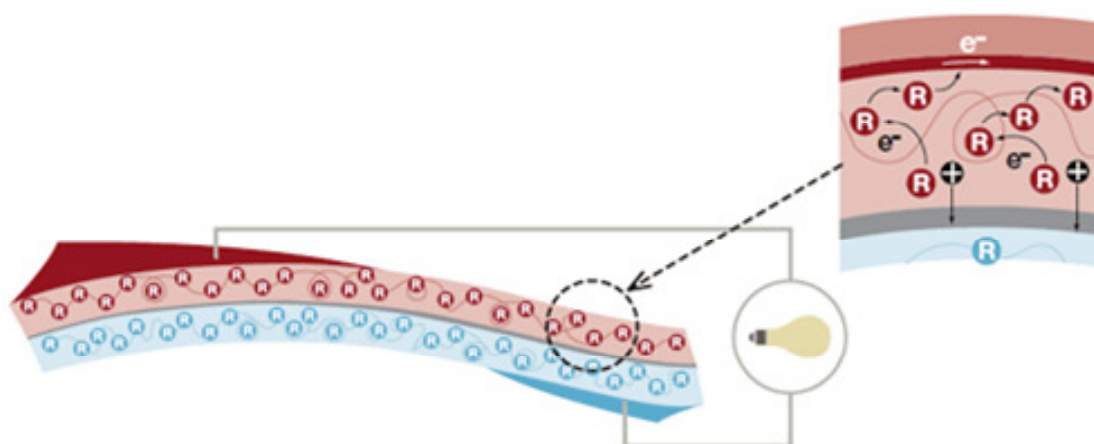


Figure 53: Example of electron hopping. The R-groups have different redox potentials. During charging, the charge is stored by oxidizing groups at the cathode and reducing groups at the anode. The output voltage of the battery corresponds to the gap between the redox potentials. The curves connecting the R groups are polymer chains, which give flexibility. Many R groups are attached to the polymer chain, so electrons can hop between neighboring R groups to produce the output current.²¹²

²¹² Nishide, H.; Oyaizu, K. *Science*, **2008**, *319*, 737-739.

²¹³ Aricó, A.S. *Nat. Mater.*, **2005**, *4*, 366.

NEC developed in 2012 an ultra-thin Organic Radical Battery compatible with IC cards with a thickness of 0.3 mm. Battery prototypes feature a 0.3 mm edge, 3 cm thickness, 3mAh capacity and 5 kW/L (kW/L is a battery's possible electrical power output per unit volume) high-output power density per unit volume. Prototypes are capable of 2.000 display screen updates, 360 consecutive flash firings and 35 location transmissions on a single charge. Furthermore, charge-discharge tests indicate that the batteries maintain 75% of their initial charge-discharge capacity after 500 cycles, equivalent to the performance of lithium-ion batteries for mobile phones.²¹⁴

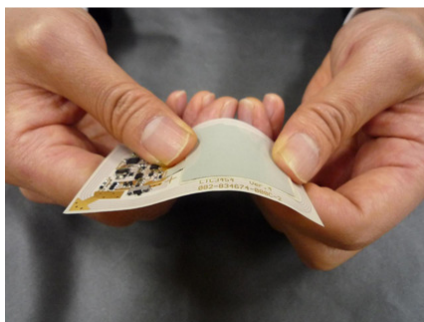


Figure 54: Ultrathin ORB prototype developed by NEC²¹⁴

For the production process a screen printing process was used as the method for electrode fabrication. Waseda University presented the idea of simply printing the electrodes for ORB applications. This was also the main industrial goal in the Austrian ORB project. In Figure 55 the schematic setup of this printable process is shown.

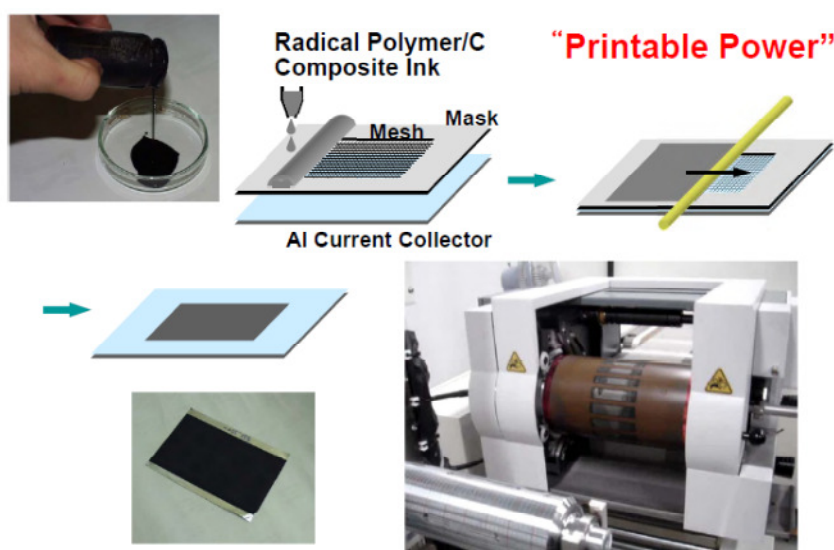


Figure 55: Schematic setup of the screen printing process for electrode fabrication²¹⁵

Tetramethyl-*p*-phenylenediamine (TMPD)

²¹⁴ http://www.nec.com/en/press/201203/global_20120305_04.html#02

²¹⁵ http://www.etp.eseia.eu/files/attachments/10760/163354_6th_business_seminar-Prof_Nishide.pdf

N,N,N',N'-tetramethyl-*p*-phenylenediamine is also known under the name Wurster's blue. Some of the substituted *para*-phenylenediamines show in their oxidized form different colors. This effect is caused by their organic ion radicals, which possess a really long lifetime because of the numerous mesomeric resonance structures. The reversible oxidation leads at first to a semichinondiimine and as the second step to a chinondiimine. They are sensitive against oxygen and the auto-oxidation in aqueous media is very common.²¹⁶ The unusual stability of *p*-phenylenediamine radical cations (e.g., Wurster's blue) has attracted much attention, and their intriguing electronic properties such as magnetic susceptibility,²¹⁷ high-spin activity,²¹⁸ electron and energy transfer behavior,²¹⁹ fluorescence,²²⁰ and electrostatic interactions²²¹ have been reported. The photochemistry and electrochemistry of TMPD has received considerable attention.²²² TMPD is often used as a one-electron reducing agent in the investigation of biologically important compounds.²²³

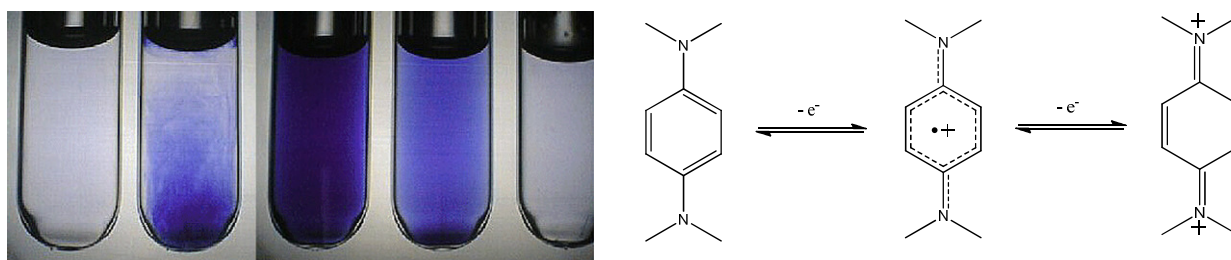


Figure 56: The oxidation process of Wurster's blue with the derived color states

Cyclic Voltammetry

Cyclic voltammetry or CV is a potentiodynamic electrochemical measurement. The working electrode potential is ramped linearly versus time till it reaches a set potential. When it reaches the set potential the ramp is inverted which can happen multiple times during a single experiment. The current at the working electrode is plotted versus the applied voltage to give the cyclic voltammogram trace. Cyclic voltammetry is generally used to study the electrochemical properties of an analyte in solution.²²⁴

For these measurements a three electrode setup is used which consists of the working electrode, a reference electrode and a counter electrode. Common materials for working electrodes are glassy carbon, platinum or gold. The reference electrode is Ag/AgCl or a standard hydrogen electrode. The setup includes an electrolyte which is

²¹⁶ Nickel, U. *Chemie in unserer Zeit*, **1978**, *12*, 89-98.

²¹⁷ Yamauchi, J.; Fujitha, H. *Bull. Chem. Soc. Jpn.* **1990**, *63*, 2928-2932.

²¹⁸ Sakamaki, D.; Ito, A.; Furukawa, K.; Kato, T.; Tanaka, K. *Chem. Commun.* **2009**, 4524-4526.

²¹⁹ Tsuchiya, T.; Wielopolski, M.; Sakuma, N.; Mizorogi, N.; Akasaka, T.; Kato, T.; Guldi, D.M.; Nagase, S. *J. Am. Chem. Soc.*, **2011**, *133*, 13280-13283.

²²⁰ Grilj, J.; Laricheva, E.N.; Olivucci, M.; Vauthey, E. *Angew. Chem. Int. Edt.*, **2011**, *50*, 4496-4498.

²²¹ Backer, M.D.; Hureau, M.; Depriester, M.; Deletoille, A.; Sargent, A.L.; Forshee, P.B.; Silbert, J.W. *J. Electroanal. Chem.*, **2008**, *612*, 97-104.

²²² Hazra, D.K.; Steenken, S. *J. Am. Chem. Soc.*, **1983**, *105*, 4380

²²³ Fujita, S.; Steenken, S. *J. Am. Chem. Soc.*, **1981**, *103*, 2540

²²⁴ Heinze, J. *Angew. Chem. Int. Edt.*, **1984**, *23*, 831-847.

added to ensure sufficient conductivity. The used solution is unstirred during the measurement which results in characteristic diffusion controlled peaks.²²⁵

Cyclic voltammetry has become an important and widely used electroanalytical technique in many areas of chemistry and is widely used to study a variety of redox processes. It is used for obtaining stability of reaction products, the presence of intermediates in oxidation-reduction reactions,²²⁶ electron transfer kinetics,²²⁷ the reversibility of a reaction²²⁸ and many other applications.

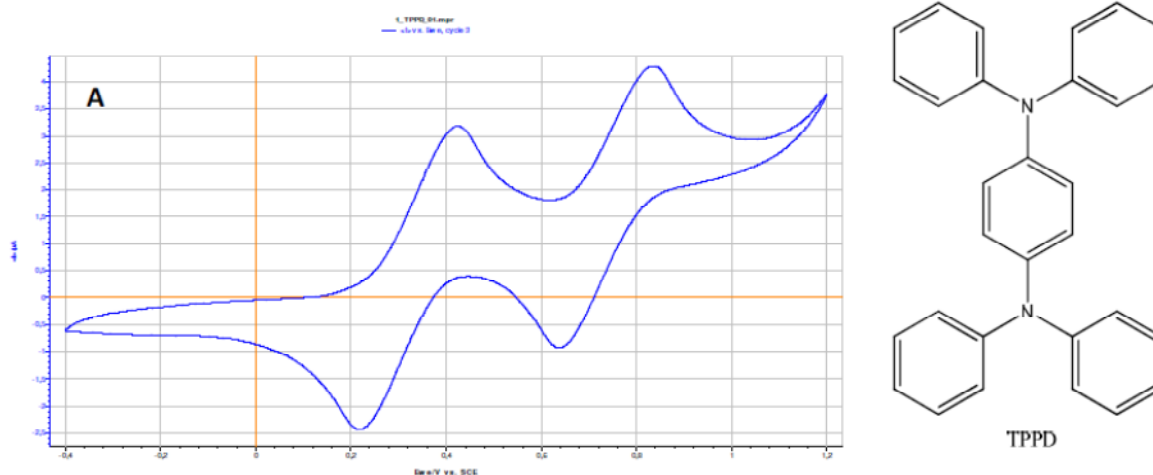


Figure 57: CV of tetraphenyl-*p*-phenylenediamine in solution (working and counter electrode Pt, reference-electrode Ag/AgNO₃, with 0.1M tetrabutylammoniumperchlorate, 1 mM in chloroform)

Results and Discussion

The ORB project, which was cooperation between the Polymer Competence Center in Leoben (PCCL), Varta Micro Innovation (VMI) and the Institute of Chemistry and Technology of Materials at TU Graz (ICTM), was focused on the synthesis and characterization of polyradicals as active material in organic radical batteries.

First steps and overview

The first step was the synthesis and characterization of a system known from literature. Poly-TEMPO-methacrylate (PTMA) as well as a TEMPO-substituted polynorbornene were synthesized, attached to Swagelok-cells and then CV-measurements and measurements at a constant current were performed. Furthermore, the polynorbornene was characterized via IR, ESR, susceptibility measurements, TGA/DSC and GPC. During the work with already known organic radical battery materials the tetrasubstituted *p*-phenylenediamine (TPPD) was identified as interesting building block for radical polymers. This molecule undergoes two reversible

²²⁵ Nicholson, R. S.; Irving, S. *Anal. Chem.* **1964**, *36*, 706–723.

²²⁶ Nicholson, R.S. *Anal. Chem.*, **1965**, *37*, 1351–1355.

²²⁷ DuVall, S.; McCreery, R. *Anal. Chem.*, **1999**, *71*, 4594–4602.

²²⁸ Bond, A. M.; Feldberg, S. *J. Phys. Chem.* **1998**, *102*, 9966–9974.

oxidation steps and is compatible with the reversible oxidation of TEMPO. Until now, this molecule and its derivatives were only used for photochemical or electrochemical applications but not as battery materials. TPPD possesses a high potential for different molecule structures with a high theoretical capacity and a wide range of possible polymerization techniques. One of the first steps during our work was to synthesize a model compound with the Wurster blue and TEMPO units to characterize the specific peaks in the cyclic voltammety spectrum. The model compound shows three distinct redox couples which can be referred to the oxidation peaks of the anodic scan as followed:

- the formation of the radical cationic species at 0.3 V
- the oxidation of the two TEMPO-units at around 0.7 V
- the second oxidation of the *p*-phenylenediamine moiety to the di-cationic species at 0.9 V

This finally results in the formation of a tetra-cationic species. Further cycling shows high reversibility, indicating the electrochemical compatibility of the two different redox-active groups.

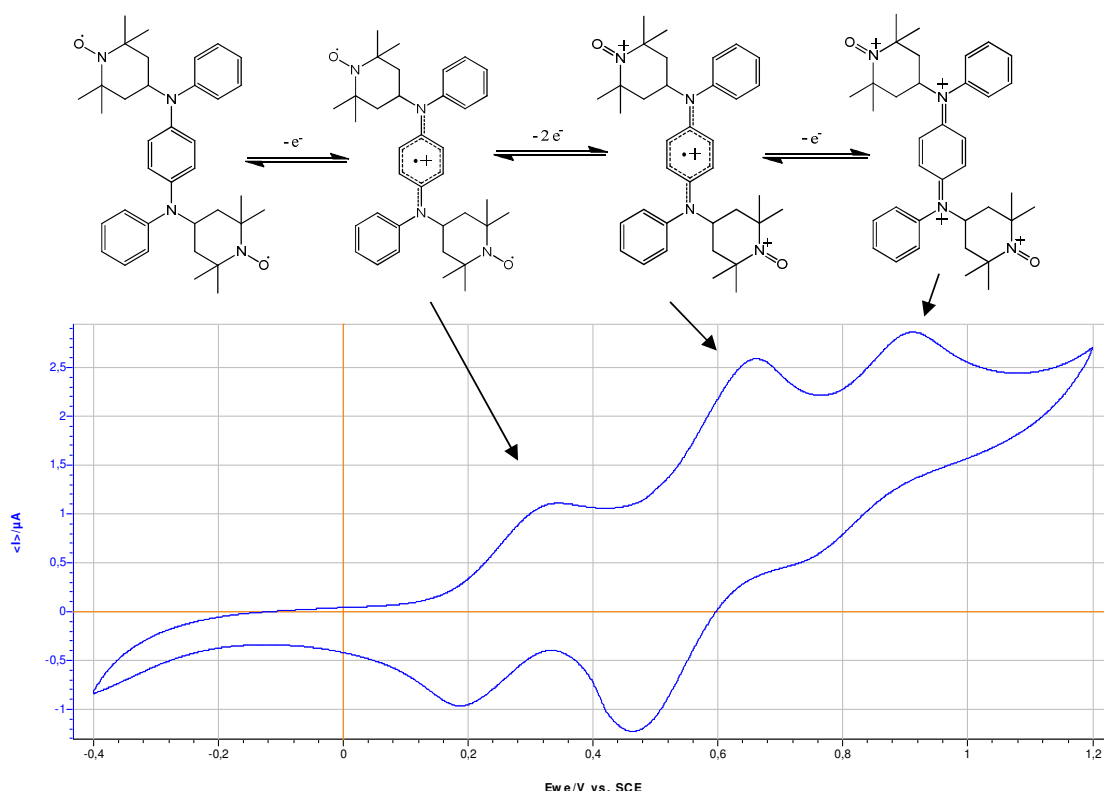


Figure 58: Cyclic voltammogram of the model compound in solution

Different people were involved in this project: in brainstorming, conceptualization, the development of new derivatives and their best synthesis ways and also in the characterization and analytical and electrochemical evaluations. Therefore not only my

results are presented here mainly due to the assistance of Astrid Knall and David Fast. Most of the work presented here is also regarded to the work of David Fast, who deserves my special thanks as lab colleague and quasi-supervisor.

The overview in Figure 59 shows the different ideas connected with the organic radical battery topic. In the beginning of the project, different monomer and polymer architectures were thought through according to theoretical capacities and examples already known in literature. Due to these findings our goals and ideas were modified.

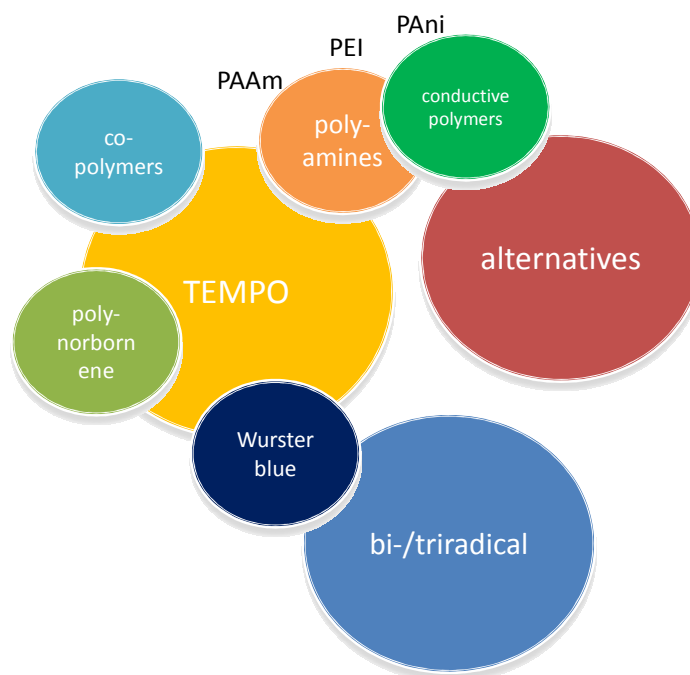


Figure 59: Overview of possible structures for organic radical batteries

Between 2010 and 2013 different types of cathode materials were synthesized in Graz, which can roughly be divided into the class of TEMPO-based materials with different polymer backbones, Wurster-blue based materials with different polymer backbones and the redox-active unit either in the polymer backbone or in the side chain and a mixture of both species.

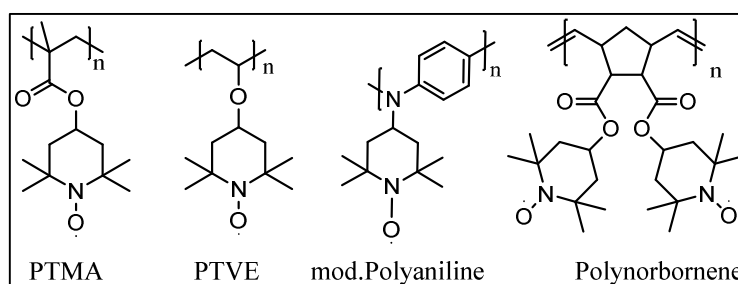


Figure 60: TEMPO-derived derivatives (theoretical capacities?)

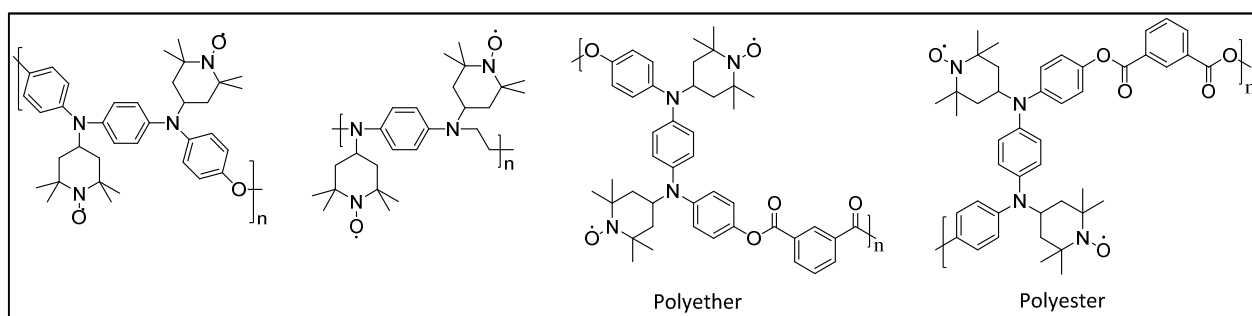


Figure 61: TEMPO-Wurster blue combination derivatives

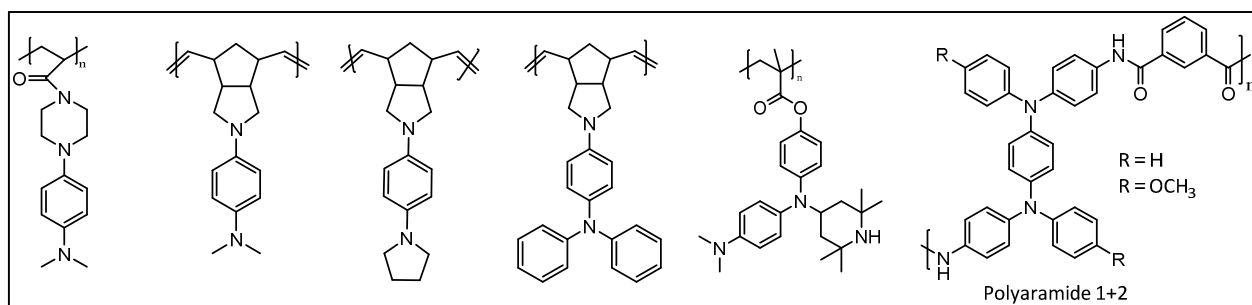


Figure 62: Wurster blue derived derivatives

The first attempts towards cathode materials were made with derivatives known from literature as for example the PTMA, PTVE and the polynorbornene with two TEMPO units. Results, analysis and evaluation of these three compounds were consistent with the literature results and that was a good start for studying characterization methods and the handling of radicals, which is sometimes really challenging.

C-N bond formation

One important step in the synthesis of most of the compounds was the C-N bond formation. For this step we mostly used the Buchwald-Hartwig reaction as well as a reductive amination reaction. Both of these synthetic strategies are really complex and they need long time studies for the right treatment strategies of the substrates.

Buchwald-Hartwig reaction

The Buchwald-Hartwig reaction is used for the synthesis of carbon-nitrogen bonds via the palladium catalyzed cross coupling of amines with aryl-halides. The synthetic use of this reaction is to shorten the parts of the synthesis of aromatic C-N bonds (nucleophilic substitution, reductive amination etc.) and also preserve chiral informations. The problem with such reactions is often the functional group tolerance and due to that the low yields.²²⁹ The development of the Buchwald-Hartwig reaction favored the facile synthesis of aryl amines, replacing to an extent harsher methods

²²⁹ Wolfe, J.P.; Wagaw, S.; Marcoux, J.F.; Buchwald, S.L. *Acc. Chem. Res.*, **1998**, *31*, 805–818.

(Goldberg reaction, nucleophilic aromatic substitution) while significantly expanding the repertoire of possible C-N bond formation.²³⁰

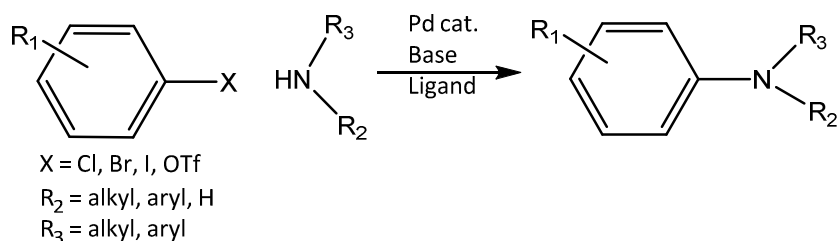


Figure 63: Principle of the Buchwald-Hartwig reaction

Stephen L. Buchwald and John F. Hartwig independently created a new approach toward aryl-amines via metal catalysts between 1994 and the late 2000s. During the development several generations of catalyst systems have been invented and with each of these systems greater scopes in terms of the coupling partners, milder conditions with a wider variety of aryl coupling partners were introduced.²³¹

The reaction mechanism for this reaction proceeds through steps known for palladium catalyzed C-C coupling reactions, namely oxidative addition, palladium amide formation (rather than transmetalation) and finally reductive elimination. Side reactions can compete with the reductive elimination wherein the amide undergoes β -hydride elimination to yield the hydrohalogenated arene and an imine product.²³²

One of the most important things during the development of this reaction was to determine the palladium species responsible for each of the steps, with several mechanistic revisions because more and more data occurred during the years.

Catalyst systems

There are two reaction pathways proposed, dependent on the type of ligand. A distinction must be drawn between monodentate and chelating phosphine ligands, and also other influences have been revealed especially concerning the alkybiarylphosphine developed by Buchwald.²³³

²³⁰ Hartwig, J.F. *Angew. Chem. Int. Edt.*, 1998, 37, 2046–2067.

²³¹ Hartwig, J.F. *Synlett*, 1997, 4, 329–340.

²³² Muci, A.R.; Buchwald, S.L. *Topics in Curr. Chem.*, 2002, 219, 131–209.

²³³ Wolfe, J.P.; Buchwald, S.L. *J. Org. Chem.*, 1996, 61, 1133–1135. b) Hartwig, J.F.; Richards, S.; Barañano, D.; Paul, F. *J. Am. Chem. Soc.*, 1996, 118, 3626–3633.

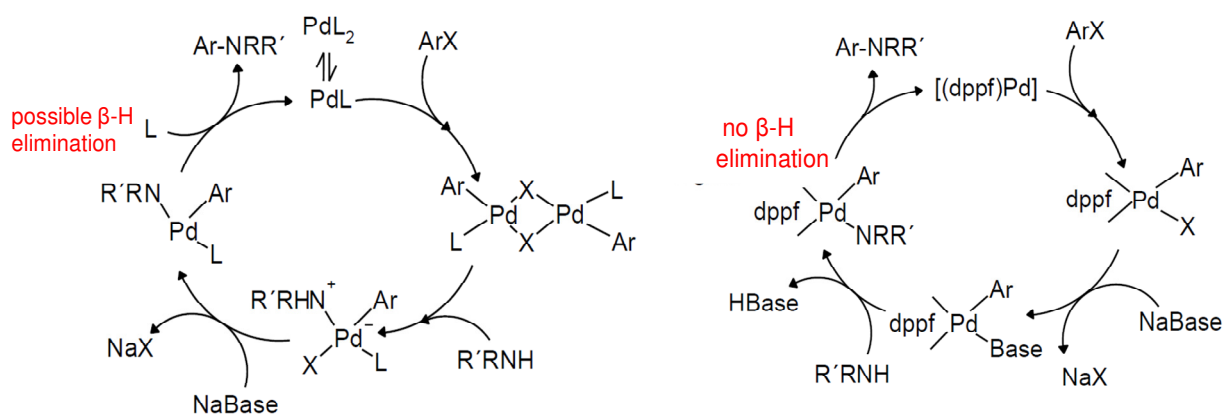


Figure 64: Catalytic cycles for monodentate (left) and bidentate ligands (right)

For monodentate ligand systems, the monophosphine palladium (0) species is believed to form before oxidative addition, forming the palladium (II) species which is in equilibrium with the μ -halogen dimer. The stability of this dimer decreases in the order of $X = \text{I} > \text{Br} > \text{Cl}$ and is responsible for the slow reaction of aryl iodides with the first-generation catalyst system. The amine ligation is followed by protonation of base which produces the palladium amide. This key intermediate reductively eliminates to produce the product and regenerate the catalyst. For chelating ligands the monophosphine palladium species is not formed, the reductive elimination can occur from either a four coordinate bi-phosphine or three coordinate monophosphine arylpalladium amido complex.²³⁴ First generation catalyst systems were able to couple both, cyclic and acyclic secondary amines (not diarylamines). However, under these conditions a coupling of primary amines is not possible due to competitive hydrohalogenation of the arene.²³⁵

Second generation ligands (+/-)-2,2'-bis(diphenylphosphino)-1,1'-binaphthyl (BINAP) and 1,1'-bis(diphenylphosphino) ferrocene (dppf), which were also used in our studies, and really helpful relating to work with primary amines and also allow the coupling of aryl iodides. With these ligands also better yields and higher rates can be observed. The chelation is thought to suppress β -hydride elimination by preventing an open coordination site.²³⁶ More recently sterically hindered phosphine ligands have been shown to be remarkably active catalysts, able to couple nearly every amine.²³⁷ These new catalysts are bulky, electron-rich monophosphine ligands showing high activity for assisting the palladium catalyzed amination reaction of aryl halides.²³⁸ Also electron withdrawing amines and heterocyclic substrates can be coupled under these conditions, despite their tendency to deactivate the palladium catalyst.²³⁹

²³⁴ Hartwig, J.F. *Pure Appl. Chem.* 1999, 71, 1416–1423.

²³⁵ Louie, J.; Hartwig, J.F. *Tetrahedron Lett.* 1995, 36, 3609–3612.

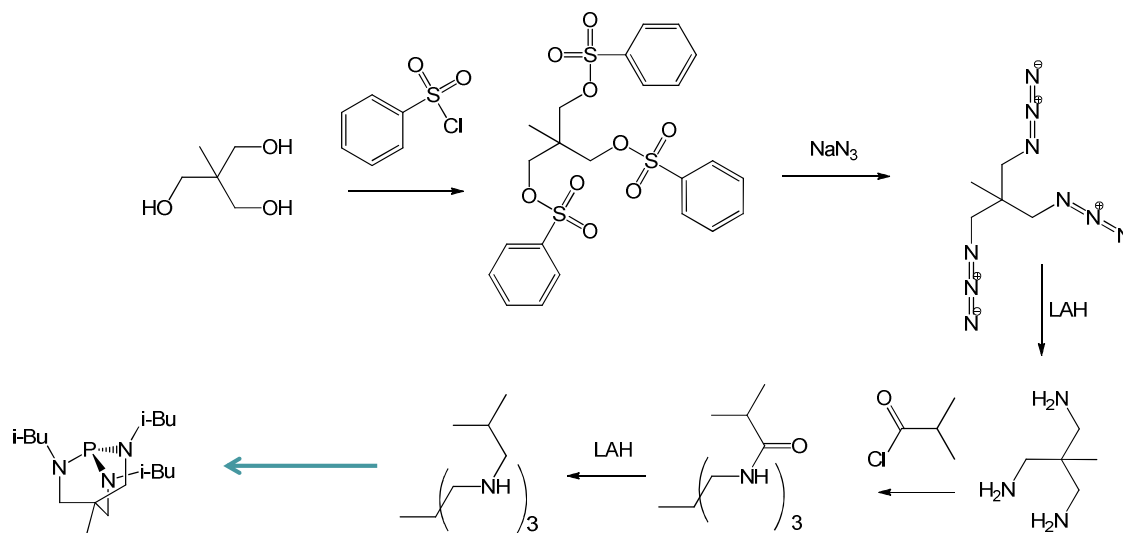
²³⁶ Driver, M.S.; Hartwig, J.F. *J. Am. Chem. Soc.* 1995, 118, 7217–7218.

²³⁷ Wolfe, J.P.; Tomori, H.; Sadighi, J.P.; Yin, J.; Buchwald, S.L. *J. Org. Chem.* 2000, 65, 1158–1174.

²³⁸ Xie, X; Zhang, T.Y.; Zhang, Z., *J. Org. Chem.*, 2006, 71, 6522–6529.

²³⁹ Ikawa, T.; Barder, T.E.; Biscoe, M.R.; Buchwald, S.L. *J. Am. Chem. Soc.* 2007, 129, 13001–13007.

Due to this information a catalyst known from literature was tried to synthesize. It is a catalyst for electron-poor, electron-neutral and electron rich aryl bromides, chlorides and iodides. The reactions encompassed aromatic amines (primary or secondary) and secondary amines (cyclic or acyclic). Also the weak base cesium carbonate can be used allowing a variety of functionalized substrates (esters, nitro groups). The ligand itself is not available for purchase and also the synthesis seemed in the end too time-consuming and also cost-extensive (over 200€).



Scheme 27: Reaction scheme for Buchwald Hartwig ligand

For future usage of the Buchwald Hartwig reaction for different derivatives (aryl, alkyl) with different halides (bromo, chloro, iodo) it is strongly recommended to synthesize such a ligand to overcome all the problematic issues of the C-N bond formation.

As mentioned before C-N coupling reactions for a given substrate are strongly dependent on the nature and the concentration of the catalytic system, as well as the nature of the base employed.²⁴⁰

Therefore, the big problem with the Buchwald-Hartwig reaction is the broad spectrum of possible solvents, bases, catalysts, ligands and temperatures (*cf.* Figure 65). Every component can be varied and if it is not possible to look up your special component in literature the process to find the right reaction conditions can be very long. With bidentate ligands, secondary amines are the preferred products whereas monodentate ligands lead to tertiary amines. Asymmetric substituted tertiary amines can be synthesized with arylbromides and arylchlorides, here the bromide reacts selectively before the chloride.

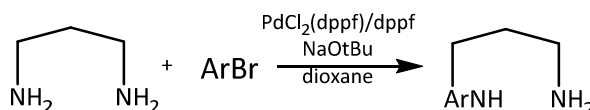
²⁴⁰ Beletskaya, I.P.; Bessmertnykh, A.G.; Averin, A.D.; Denat, F.; Guilard, R. *Eur. J. Org. Chem.*, **2005**, 261-280.

Chelating Biarylphosphines				Table 2. Overview of published single examples from 01/1999 to 01/2004 for the coupling of amines with halo or sulfonic acid ester aromatics.								
				1	2	3	4	5	6	7		
air-stability/handling commercial availability ease of preparation/costs temperature range versatility	+++ +++ ++ 80 - 110 °C +++	+++ +++ ++ 80 - 110 °C +++	+++ +++ ++ 80 - 110 °C +++	90	106	18	A = Tol: 2 A = CF ₃ : 3 A = C ₆ F ₅ : 12	4	20	39		
Ferrocene-based Phosphines				A								
				B	C							
air-stability/handling commercial availability ease of preparation/costs temperature range versatility	+++ +++ ++ 80 - 110 °C +++	+++ +++ ++ 80 - 110 °C +++	+++ +++ ++ 80 - 110 °C +++	46	23	8	A = CF ₃ : 5 A = C ₆ F ₅ : 3			11		
Carbenes/Imidazolium salts				B								
air-stability/handling commercial availability ease of preparation/costs temperature range versatility	+++ +++ ++ 25 - 110 °C +++	+++ +++ ++ 25 - 110 °C +++	+++ +++ ++ 25 - 110 °C +++	3	5	1	A = CF ₃ : 8			29		
Biphenyl-based phosphines (Buchwald's ligands)				C								
air-stability/handling commercial availability ease of synthesis/costs temperature range versatility	+++ +++ ++ 25 - 110 °C +++	+++ +++ ++ 70 - 110 °C +++	+++ +++ ++ 70 - 110 °C +++	+++ +++ ++ 70 - 110 °C +++	+++ +++ ++ 70 - 110 °C +++	+++ +++ ++ 25 - 110 °C +++	A = Tol: 4 A = CF ₃ : 3 A = C ₆ F ₅ : 10	A = Tol: 1 A = CF ₃ : 1 A = C ₆ F ₅ : 1	A = Tol: 1 A = CF ₃ : 4 A = C ₆ F ₅ : 13	13	15	9
				costs of bases								
				MW								
				€/mol base*								
				Cs ₂ CO ₃ 325.82 110-120								
				LHMDS 167.33 90-100								
				t-AmONa 110.13 30-40								
				t-BuONa 96.11 20-30								
				t-BuOK 112.22 15-25								
				K ₃ PO ₄ 212.28 6-8								
				NaOMe 54.02 4-5								
				K ₂ CO ₃ 138.21 4-5								
				KOH 56.10 1-2								
				NaOH 40.00 1-2								

Figure 5. Standard ligands used in C-N coupling chemistry with abbreviations for reference; plus signs indicate relative quality judged by the published literature, most often used ligands are boxed.

Figure 65: Variable conditions and components for the Buchwald-Hartwig reaction

The primary amino groups are favoured and the reaction of dihalobenzenes with polyamines gives the monoamination products in good yields, without formation of diamino compounds. Direct nucleophilic substitution only works with substrates containing electron withdrawing groups, including perfluorinated compounds.



Scheme 28: Buchwald Hartwig reaction with possible reaction conditions for these substrates

As example the reaction with a diamine was made in presence of 0.5-2 mol% of [PdCl₂(dppf)] and twice as much free dppf ligand. Sodium-butoxide was employed as a base (2 eq.) and the reaction mixture was refluxed in dioxane. Products were monoarylated diamines. The presence of electron withdrawing groups in *para* position of the benzene ring gives higher yields, with lower catalyst loadings. On the other hand the presence of other electron withdrawing groups led to lower yields. The presence of donor methoxy-groups in *ortho* position seems to be more favourable. The bromo derivatives were selectively substituted over the chloro substituents and surprisingly the iodides did not result in a substantial advantage over the bromides. The coupling of arylbromides with α - and β -carbon substituted primary diamines was also investigated with the results that β -substitution did not change anything but the α -substitution leads to lower yields. The reaction of diamination with dibromoarenes resulted mainly in monoaminated or reduced products. For the *ortho* and *meta* substituted dibromobenzene also a small amount of disubstituted product was found

with higher catalyst loadings and prolonged heating which also accelerates the reduction reaction.²⁴⁰

Ligands (BINAP and DPPF)

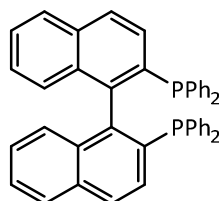


Figure 66: Structure of the bidentate BINAP ligand

Mixtures of $\text{Pd}_2(\text{dba})_3$ or $\text{Pd}(\text{OAc})_2$ and BINAP catalyze the cross coupling of amines with a variety of aryl bromides. Primary amines are arylated in high yield and certain classes of secondary amines are also effectively transformed.²⁴¹ The Pd-ligand complex is built in situ, by treating the $\text{Pd}_2(\text{dba})_3$ with two times the molar amount of BINAP. The process tolerates functional groups (ketones, esters) and the catalytic process proceeds over bis(phosphine)palladium complexes as intermediates, which are not likely to undergo undesirable side reactions. The general catalytic cycle for bidentate ligands is shown in Figure 64. The BINAP system is the most active and general system for coupling of arylbromides with primary amines. It also works with the weak base cesium carbonate allowing a high functional group tolerance. Electron rich aryl bromides gave poor results unless the aryl bromide also contained an ortho substituent. For cyclic amine the phosphinligand dppf is more effective.²⁴² Other ligands examined provided larger amounts of diarylated side products than BINAP. Also some secondary amines can be arylated with the Pd/BINAP system. However acyclic secondary amines are problematic substrates.

Base (NaO-*t*-Bu and cesium carbonate)

The first attempts for a organotin-free coupling reaction were made through the coupling of free amines in the presence of a bulky base like $\text{KO}t\text{-Bu}$ in Buchwald publications²⁴³ and LiHMDS in Hartwig publications.²⁴⁴

The use of the strong base $\text{NaO}t\text{-Bu}$ or $\text{KO}t\text{-Bu}$ in catalytic amination reactions leads to a relatively low level of functional group tolerance.²³⁰

However, sodium *tert*-butoxide provides the fastest reactions with the lowest catalyst loadings. But due to the low functional group tolerance methyl or ethyl esters form amides and nitroarenes decompose. As mentioned before cesium carbonate has a

²⁴¹ Wolfe, J.P.; Buchwald, S.L. *J. Org. Chem.*, **2000**, *65*, 1144-1157.

²⁴² Driver, M.S.; Hartwig, J.F. *J. Am. Chem. Soc.*, **1996**, *118*, 7217-7218.

²⁴³ Louie, J.; Hartwig, J.F. *Tetrahedron Lett.* **1995**, *21*, 3609-3612.

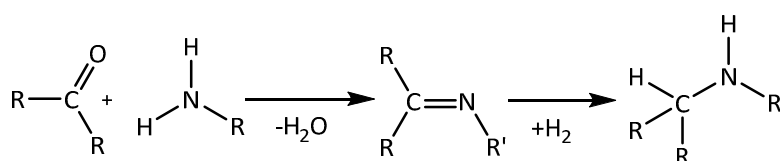
²⁴⁴ Guram, A.S.; Rennels, R.A.; Buchwald, S.L. *Angew. Chem. Int. Ed.*, **1995**, *34*, 1348-1350.

much higher functional group tolerance and can be used with the BINAP catalyst system. Lower catalyst loadings and higher temperatures lead to lower yields.

However the ligand/base system has to be chosen individually for each reaction. By considering advantages and disadvantages of both parts; low yields or high functional group tolerance and many other points, its often really time consuming and also expensive to try all the given systems.

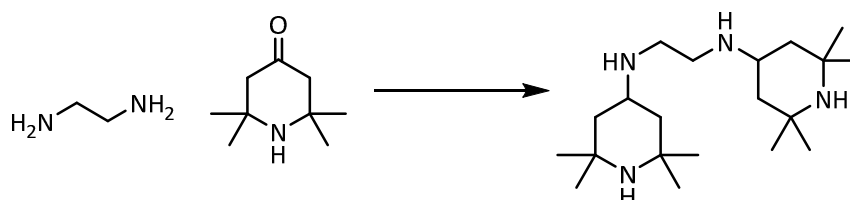
Reductive amination

The reductive amination which involves the conversion of a carbonyl group to an amine via an intermediate imine was one of the biggest challenges.



Scheme 29: Principle of the reductive amination

In our case the carbonyl group was a 2,2,6,6-tetramethylpiperidin-4-one, a ketone and TEMPO derivative. In Scheme 30 the two educts and the desired product are shown and in the table below all of the different reaction conditions we tried for this synthesis are listed.



Scheme 30: Reaction pathway of a desired product

Table 10: Reaction conditions for the reductive amination

reducing agent	solvent	pH	eq amine/salt
sodium triacetoxyborohydride	dry THF	7	1
Pd/C H ₂	MeOH	4	1.1
2-picoline borane	MeOH/AcOH 10:1	4-2	1
sodium triacetoxyborohydride	dry THF	4	1
sodium triacetoxyborohydride	dry MeOH	8	3.5/salt
sodium	dichloroethane	9	1/salt

triacetoxyborohydride			
sodium triacetoxyborohydride	dry THF	5	1.2 /salt
Pd/C H ₂	10 w% H ₂ O (neat)	7	1
sodium borohydride	MeOH/IR 120H ⁺	5	1
sodium cyano borohydride	dry MeOH	7	2/salt (monosubst)
sodium triacetoxyborohydride	dry THF	7	2/salt first imide formation
sodium cyano borohydride	dry MeOH	7	1/salt first imide formation

Also different work-up conditions were tested and reactions were repeated with different amounts of the compounds and purified via chromatographic and crystallographic methods.

The listed reaction conditions are known from literature. Because of this knowledge we tried the direct and stepwise amination.

Direct or stepwise formation

These two different approaches were compared with each other. In the direct way the carbonyl compound and the amine are mixed with the proper reducing agent without prior formation of the intermediate imine or iminium salt. The stepwise formation involves the intermediate imine step followed by the reduction.²⁴⁵ For the direct synthesis we used the catalytic hydrogenation with Pd/C and the amination with sodium cyanoborohydride. The reaction with the Pd/C is normally really effective but it leads also to low yields, product mixtures and maybe no turnover due to the molecular structure. It is also not useable with nitro or cyano groups and carbon-carbon multiple bonds. In our case the usage would be possible but only product mixtures or even no turnover could be observed. As second method sodium cyanoborohydride was used within acidic solutions (pH = 3) and it is soluble in hydroxylic solvents like methanol. At a pH of 3-4 it reduces aldehydes and ketones effectively but the reduction becomes slower at higher pH-values. At pH 6-8 the more basic imines are protonated preferentially and reduced faster than aldehydes and ketones.²⁴⁶ Limitations are that the reaction may require a fivefold excess of the amine and is slow with aromatic ketones and with weakly basic amines.²⁴⁷ The problem in the recommended synthesis is the basic nature of the amine and also the low amount of the amine. However the

²⁴⁵ Abdel-Magit, A.; Carson, K.G.; Harris, B.D.; Maryanoff, C.A., Shah, R.D. *J. Org. Chem.*, **1996**, *61*, 3849-3862.

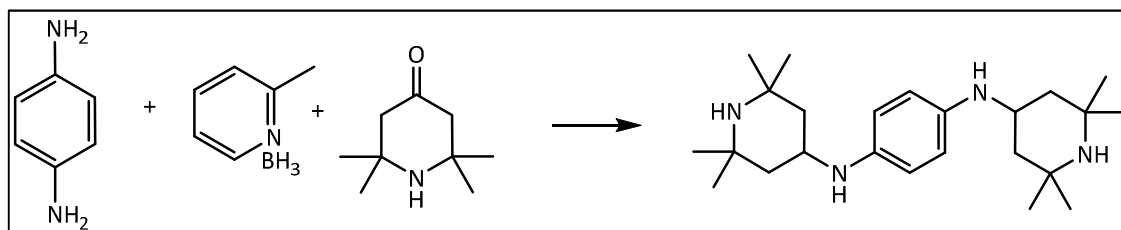
²⁴⁶ Borch, R.F., Bernstein, M.D.; Durst, H.D. *J. Am. Chem. Soc.*, **1971**, *93*, 2897.

²⁴⁷ Borch, R.F.; Durst, H.D., *J. Am. Chem. Soc.*, **1969**, *91*, 3996.

problem was that we need a double substituted amine, so due to this we needed an excess of the ketone, which is not a preferred reaction condition. Maybe this is the explanation to the problems with the direct reductive amination with sodium cyanoborohydride. Sodium triacetoxyborohydride was used for direct reductive amination with solvents like DCE and THF. These reactions should be performed under nitrogen atmosphere at room temperature mostly with acetic acid. The amination results were in literature as good or better than most comparable reported results. Unfortunately the standard conditions of Abdel Magit et al did not work that good with our substrates.²⁴⁵ Therefore we tried also the stepwise amination which is usually only performed with aldehydes. Here an imine is preformed; this formation is reversible and requires long reaction times and also the use of a dehydrating agent. The stepwise one pot procedure was carried out in methanol followed by in situ reduction with sodium borohydride. In these attempts we missed the usage of a dehydrating agent, the small amounts of our test-reactions did not give us the reason to worry about the water formation but that maybe was the reason for the reaction failure.

α -Picoline borane (pic-BH₃) is a cheap and commercially available alternative to NaBH₃CN or pyr-BH₃ for reductive amination reactions. The direct amination reactions were carried out in MeOH/AcOH (10:1) using pic-BH₃ as a reducing agent.²⁴⁸ Equimolar amounts of the amine, carbonyl and pic-BH₃ were used. Generally, anhydrous conditions should be used to generate imines, which are then reduced, therefore molecular sieves or Na₂SO₄ were employed under these reaction conditions. To keep the anhydrous conditions is often troublesome, especially with the use of acetic acid. Sato et al. added for testing conditions a small amount of water to their reactions and could only observe slightly lower yields.²⁴⁸ So we also tried to synthesize the product without molecular sieves but in none of the reactions a double-substituted product could be observed.

Here I have to mention that the reaction with pic-BH₃ in MeOH/AcOH with the *p*-phenylenediamine worked out as it is pictured in Scheme 31.



Scheme 31: Reductive amination with pic-BH₃ to the desired aryl-compound

Due to this successful synthesis we tried again the reaction conditions with the sodium triacetoxyborohydride with a 1:2 ratio of the amine to the TEMPO compound at a pH around 5. It was stirred for three days at room temperature and for work up it was

²⁴⁸ Sato, S.; Sakamoto, T.; Miyazawa, E.; Kikugawa, Y. *Tetrahedron*, **2004**, 60, 7899-7906.

extracted with acid and base and also with two different solvents (ether and dichloromethane), for further purification it was covered with ether and slowly crystallized. The crystals are the desired product.

Polymer Limitations

Palladium mediated aminations can generate donor-acceptor triarylamine copolymers in high yields and moderate molecular weight²⁴⁹ and poly-*N*-arylaniline materials with molecular weights near 5000 (around 15-20 monomer units).²⁵⁰ These polymerizations go through three molecular weight limiting events. First, CH-activation of the tolyl groups on the tri(*o*-tolyl)phosphine ligands used in amination reaction resulted in incorporation of phosphorus atoms into the polymer chains and most likely led to end-capping of the chains by phosphines and by hydrogen atoms. Cyclization of the oligomers competed with the chain growth. Because of these problems it was not possible to generate polymers with the desired chain length. In the paper of Hartwig et al. some new catalytic systems are presented and we also tried some of them but nothing led to the polymer length which we need for our polymer batteries.²⁵¹

Guey-Sheng Polymer, a working system

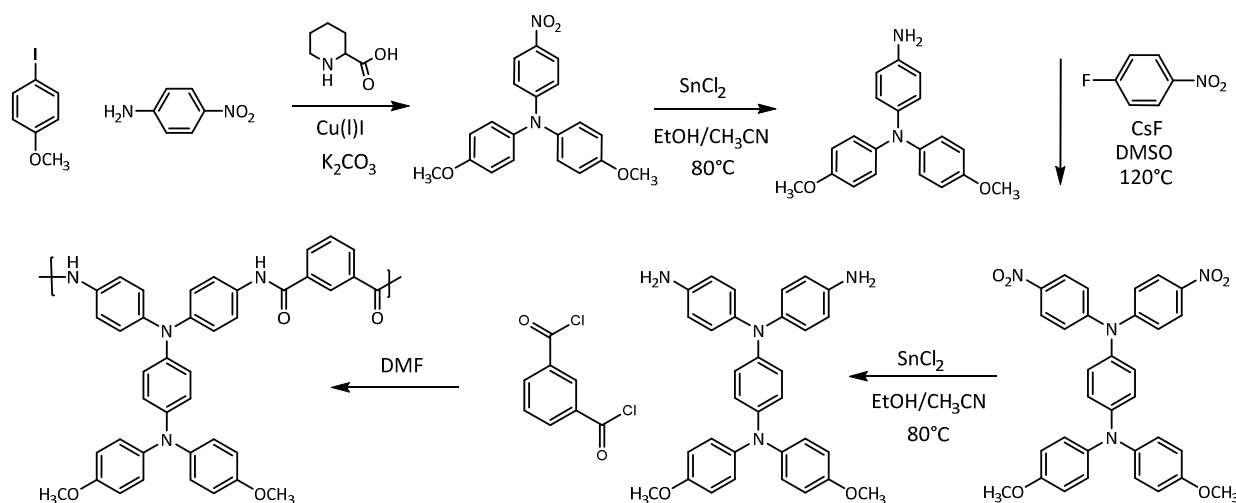


Figure 67: Reaction scheme for the preparation of the Guey-Sheng Polymer, a number of improvements over the original have been incorporated

To mention one of our reaction pathways from the idea to the polymer, I want to mention a polymer first introduced by Guey-Sheng Liou et al. with electrochromic properties.²⁵²

²⁴⁹ Goodson, F.E.; Hartwig, J.F. *Macromolecules*, **1998**, *31*, 1700.

²⁵⁰ Hartwig, J.F. *Angew. Chem. Int. Ed.*, **1998**, *37*, 2046-2067.

²⁵¹ Goodson, F.E.; Hauck, S.I.; Hartwig, J.F. *J. Am. Chem. Soc.*, **1999**, *121*, 7527-7539.

²⁵² Chang, C.W.; Liou, G.S. *J. Mater. Chem.*, **2008**, *18*, 5638-5646.

Poly(amine-imide)s

They also used the structural architecture of the *N,N,N',N'*-tetraphenyl-*p*-phenylenediamine for their research. The structure with some changes in the substituents and also in the polymerization technique is shown under the light of its electrochromic performance and not as a material for organic radical batteries. Due to this aspect we tried to synthesize two of these polymers and apply them into our batteries to test the electrochemical properties as well.

The redox properties, ion transfer process, electrochromism and photo-electrochemical behavior of *N,N,N',N'*-tetrasubstituted-1,4-phenylenediamines are of importance for technical applications.²⁵³ However the technological applications of most polyimides are limited by processing difficulties because of high melting and glass transition temperatures and limited solubility in most organic solvents.²⁵⁴ Tests with poly(amine-imide)s bearing pendent triphenylamine groups based on a new diamine *N,N*-bis(4-aminophenyl)-*N',N'*-diphenyl-1,4-phenylenediamine showed that the introduction of the bulky, intrinsically electron donating TPA group could decrease the HOMO energy levels and disrupt the coplanarity of aromatic units in chain packing which increases the between-chain spacing or free volume, thus enhancing solubility of the formed poly(amine-imide)s.²⁵⁴ Properties like solubility and the thermal and mechanical properties of this structure and its derivatives are generally much better than in other poly(amine-imide)s. These reports also lead us on the way of this compound and in my case the dimethoxy substituted derivative.

David Fast synthesized the unsubstituted polyaramide derivative and characterized it also with the known electrochemical tests. CVs and C-rate tests were performed.

C-rate

In the late 1700s, Charles-Augustin de Coulomb ruled that a battery that receives a charge current of one ampere (1 A) passes one coulomb (1 C) of charge every second. In 10 seconds, 10 coulombs pass into the battery, and so on. On discharge, the process reverses. Today, the battery industry uses C-rate to scale the charge and discharge current of a battery.²⁵⁵ Most portable batteries are rated at 1 C, meaning that a 1,000 mAh battery that is discharged at 1 C rate should under ideal conditions provide a current of 1,000 mA for one hour. The same battery discharging at 0.5 C would provide 500mA for two hours, and at 2 C, the 1,000 mAh battery would deliver 2,000 mA for 30 minutes. 1 C is also known as a one-hour discharge; a 0.5 C is a two-hour, and a 2 C is a half-hour discharge.²⁵⁶

²⁵³ Marken, F.; Hayman, C.M.; Bulman Page, P.C. *Electrochem. Commun.*, **2002**, *4*, 462.

²⁵⁴ Cheng, S.H.; Hsiao, S.H.; Su, T.H.; Liou, G.S. *Macromolecules*, **2005**, *38*, 307-316.

²⁵⁵ http://batteryuniversity.com/learn/article/what_is_the_c_rate, October **2013**

²⁵⁶ <http://www.buchmann.ca/chap5-page1.asp>, October **2013**

A battery analyzer discharges the battery at a defined current while measuring the time to reach it takes to reach the end of discharge voltage. A higher C-rate will produce a lower capacity reading and vice versa.

In reality, internal resistance turns some of the energy into heat and lowers the resulting capacity to about 95 percent or less.

Our system

For the unsubstituted polyaramide all the test CVs and characterizations were made and also constant current cyclization measurements at different C-rates were performed. The material shows here very good charging and discharging rates. 100 C corresponds approximately to 30 seconds of charging and discharging which is way more than a LIB can bring, here rates of about 5 C are about the highest you are able to obtain. This ability makes an ORB more comparable with a super capacitor and also the cycle stability and efficiency is comparable. The C-rate test leads after the 100 C cycling to an efficiency of more than 90% but here the low active material loading of only 10% has to be mentioned. About 92% of the theoretical capacity could be recovered.

With the *para*-methoxy substituted derivative expectations were even higher because the substituent should bring a higher stability to the system. CVs in solution were good as it is shown in Figure 68 but the cycle stability and also the recovery rate after the constant current cyclization unfortunately led to worse results (*cf.* Figure 69).

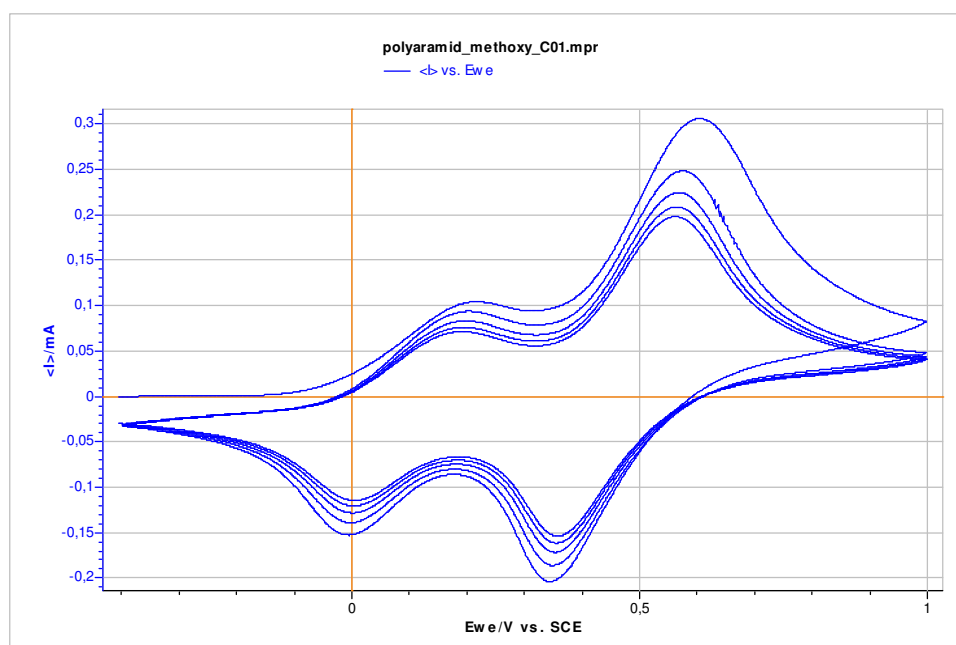


Figure 68: CV in solution, substituted polyaramid dissolved in DMF and spin-coated on ITO, Counter and working electrode: Pt; reference-electrode: Ag/AgNO₃; 0.1 M TBAP; acetonitrile, scan rate: 50 mV/s

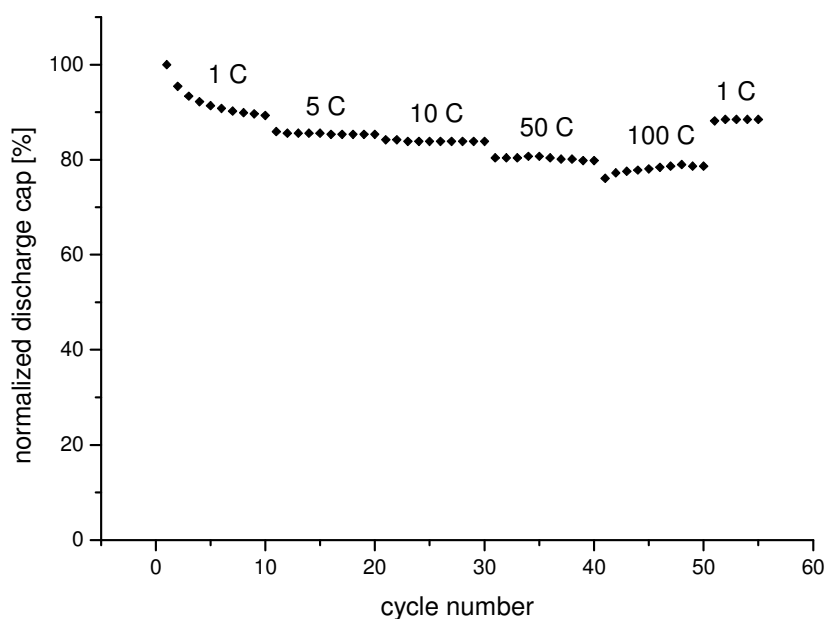


Figure 69: Constant current cyclization from 1C to 100C and back

The efficiency after more cycles was only at about 50%, with 20% of active material in the slurry mixture (*cf.* Figure 70). These results were unexplainable at first but a cyclization to lower voltages show a big reduction peak at about 2.75 Volt which indicates a decomposition of the material (*cf.* Figure 71). This problem may result from a filthy monomer but purity here was proven by IR and NMR measurements, therefore also a mass spectrometry should be performed.

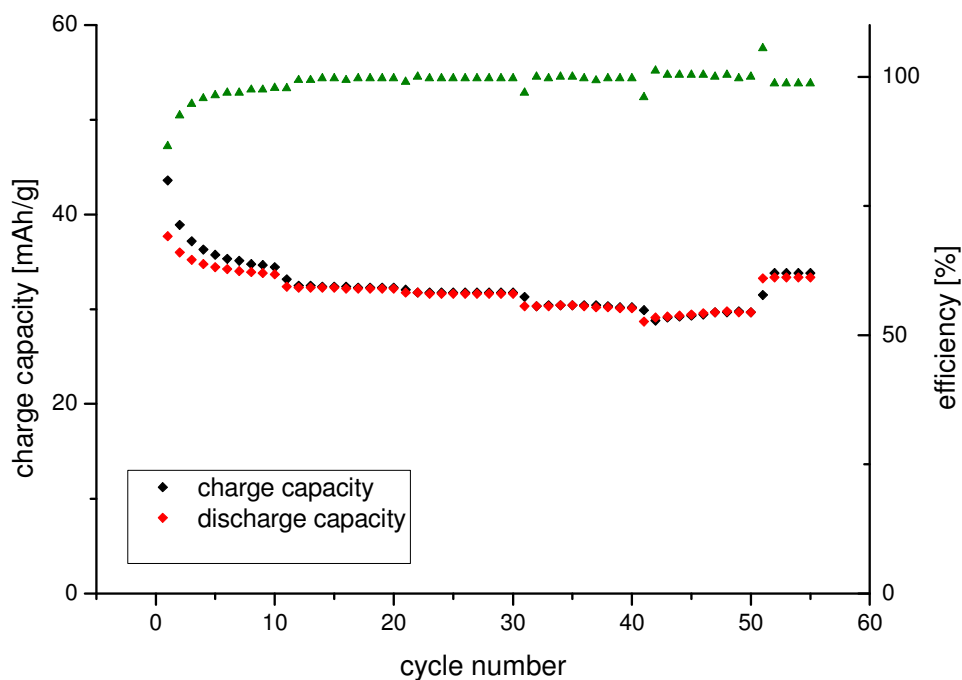


Figure 70: Charge/discharge capacity and efficiency

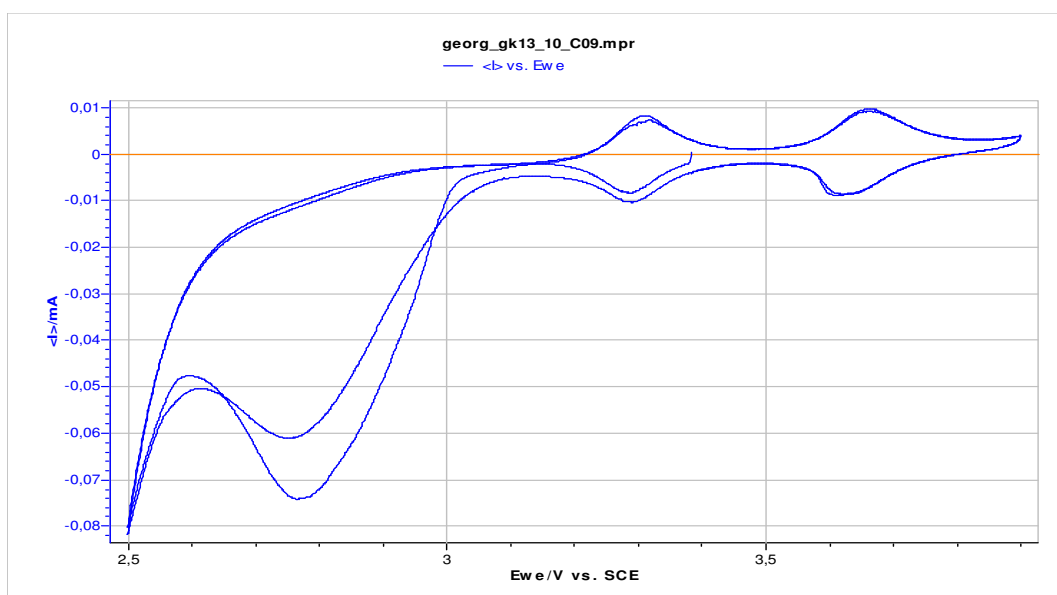


Figure 71: CV in halfcell after rate testing, proof decomposition at 2.75 Volt

Despite the decomposition problem the double substituted product should be more stable and provide the same to better results than the unsubstituted product.

The next steps are the testing for a better slurry composition with more active material and a more efficient system for the half cell. The future for this material seems to be really promising. High and low temperature testings are currently being conducted. This leads us to different applications for the polyaramid material in batteries and to a different market than that of lithium ion batteries.

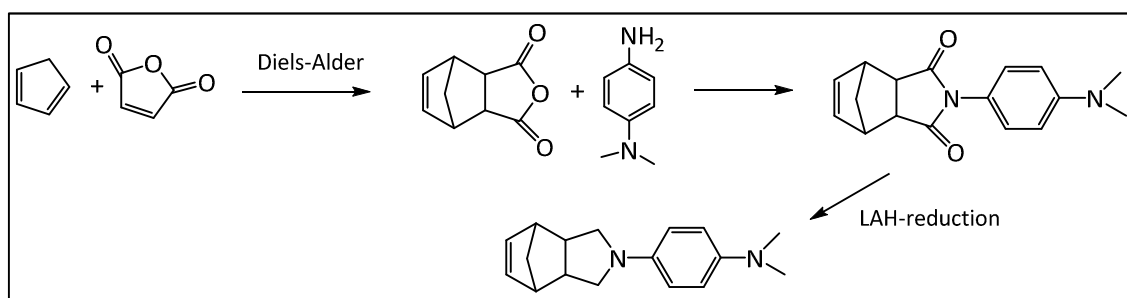
Norbornene-systems

Due to my former work with different norbornene derivatives and the also known TEMPO-norbornene derivatives already used in organic radical batteries, my part of worked also focused on ideas which include these compounds.

As the TEMPO-norbornene ester was used as model compound for characterization and preparation techniques and there are also many other kinds of poly (TEMPO-substituted norbornenes) known and described in literature,²⁵⁷ we decided to use our second structure, the Wurster blue moiety together with a norbornene backbone.

The first proposed synthesis has a theoretical capacity of 210 mAh/g and should be stable but also a good soluble polymeric compound (synthetic strategy in Scheme 32).

²⁵⁷ a) Katsumata, T.; Qu, J.; Shiotsuki, M.; Satoh, M.; Wada, J.; Igarashi, J.; Mizoguchi, K.; Masuda, T. *Macromolecules*, **2008**, *41*, 1175-1183. b) Sukegawa, T.; Kai, A.; Oyaizu, K.; Nishide, H. *Macromolecules*, **2013**, *46*, 1361-1367.



Scheme 32: One synthesis path to the norbornene-monomer 1

Monomer 1, a photochromic derivative? Analysis and characterization

One of our norbornene derivatives showed some photochromic properties which we had to proof due to the use for new applications. The photochromic effect became obvious during the synthesis and polymerization of monomer 1.

Photochromism is defined as a reversible phototransformation of a chemical species between two forms having different absorption spectra.²⁵⁸ It can also be described as a reversible change of color upon exposure to light, absorption bands in the visible part of the electromagnetic spectrum changes dramatically in strength or wavelength.²⁵⁹ Photochromism is just a special case of a photochemical reaction, most common processes here are pericyclic reactions, cis-trans isomerizations, intramolecular hydrogen transfer, intramolecular group transfers, dissociation processes and electron transfers. Another requirement of photochromism is that two states of the molecule should be thermally stable under ambient conditions for a reasonable time.²⁵⁸ All photochromic molecules back-isomerize to their more stable form at some rate what is accelerated by heating. For example spiropyrans are a class of photochromic material and their lifetime can be affected by UV light. Like most organic dyes they are susceptible to degradation by oxygen and free radicals; their colored form is the radical form of the molecule. Moreover, molecules with a similar phenylenediamine motif are known to be unstable in chloroform under light. It is proposed that these phenomena are related to carbon-chlorine single bond cleavages and the generation of free radicals.²⁶⁰

An application for our material would be a see through battery like proposed by Suga et al.²⁶¹ Here in a flexible battery a radical thin film on ITO-coated glass or a PET substrate a color change from blue (charged) and yellow (discharged) can be seen accompanied by redox reactions it can be used as indicator for the charging level what is more an electrochromic property than a photochrome effect.

²⁵⁸ Irie, M., *Chemical Reviews*, **2000**, *100*, 1683.

²⁵⁹ Durr, H.; Bouas-Laurent, H. *Photochromism: Molecules and Systems*, ISBN 978-0-444-51322-9.

²⁶⁰ Lian, W.R.; Wang, K.L.; Jiang, J.C.; Liaw, D.J.; Lee, K.R.; Lai, J.Y., *J. Polym. Sci. Part A: Polym. Chem.*, **2011**, *15*, 3248-3259.

²⁶¹ Suga, T.; Ohshiro, H.; Sugita, S.; Oyaizu, K.; Nishide, H. *Adv. Mater.* **2009**, *21*, 1627-1630.

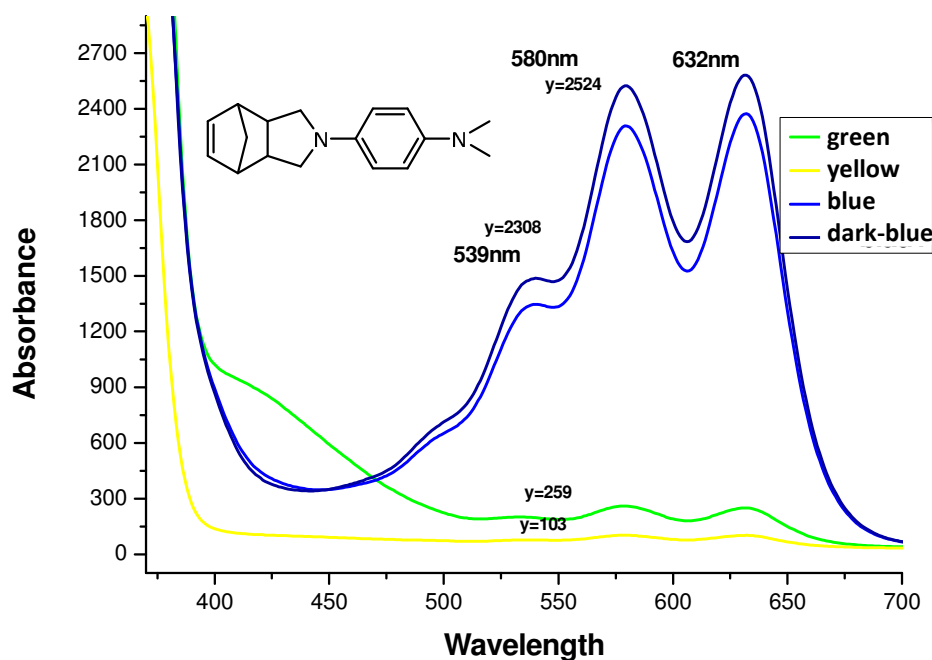


Figure 72: UV-Vis spectra of the norbornene monomer in the blue and the yellow state

In the absorbance spectra there is clearly a difference between the oxidized and unoxidized form visible. The curves are presented in the actual colors of the samples, whereby the substance exposed to light is blue, the sample in its transition state is green and the yellow curve derives from the sample stored in darkness (*cf.* Figure 72). The spectra were recorded in toluene and in chloroform but here no different behavior could be observed. As mentioned before it is possible to see a reversible photo-transformation between the two forms which show different absorption spectra.

The IR-spectra were also recorded in toluene but the solvent peaks were removed (*cf.* Figure 73). The mono-blue form is a freshly prepared solution and mono-yellow is a solution which was switched between light and darkness about 50 times and then recorded in the darkness. The two spectra look nearly the same and seem to be totally comparable.

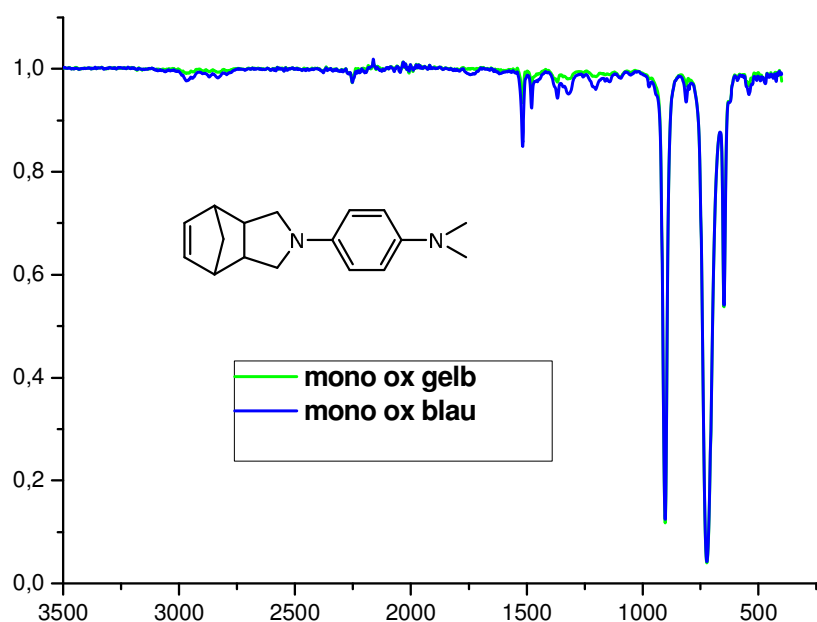


Figure 73: IR spectra before and after exposure to light

It was not possible to record a NMR spectrum of the solution because the product was not stable in solution whether in CDCl_3 , DMSO-d_6 , nor in toluene- d_8 not even when the solution is stored in the dark and just for a few minutes. Therefore the theory is that the color is not the only indicator of the oxidation or the change to the paramagnetic form. The molecule is only stable or measurable for about 20 minutes in the dissolved form, no matter if it is colored blue or yellow. Maybe by the full exclusion of water and oxygen the storage and stability time would be much longer. However on the basis of the existing resources, samples were prepared under nitrogen atmosphere with nearly fresh NMR solvents but not in the glove box under full oxygen and water exclusion, it was not possible to obtain a completely unoxidized product in solution.

The ^1H -NMR was recorded on the Bruker Avance 500 (*cf.* Figure 74) but a full detection of also Cosy, HSQC and ^{13}C NMR was not possible, because after about 20 minutes peaks start to disappear and the results of the correlation spectra and the ^{13}C were affected by that and the comparability was not yet given. These circumstances also infect the characterization of the polymer. No NMR spectrum could be recorded but polymerization was confirmed via IR because GPC-characterization was also not possible due to bad solubility of the material.

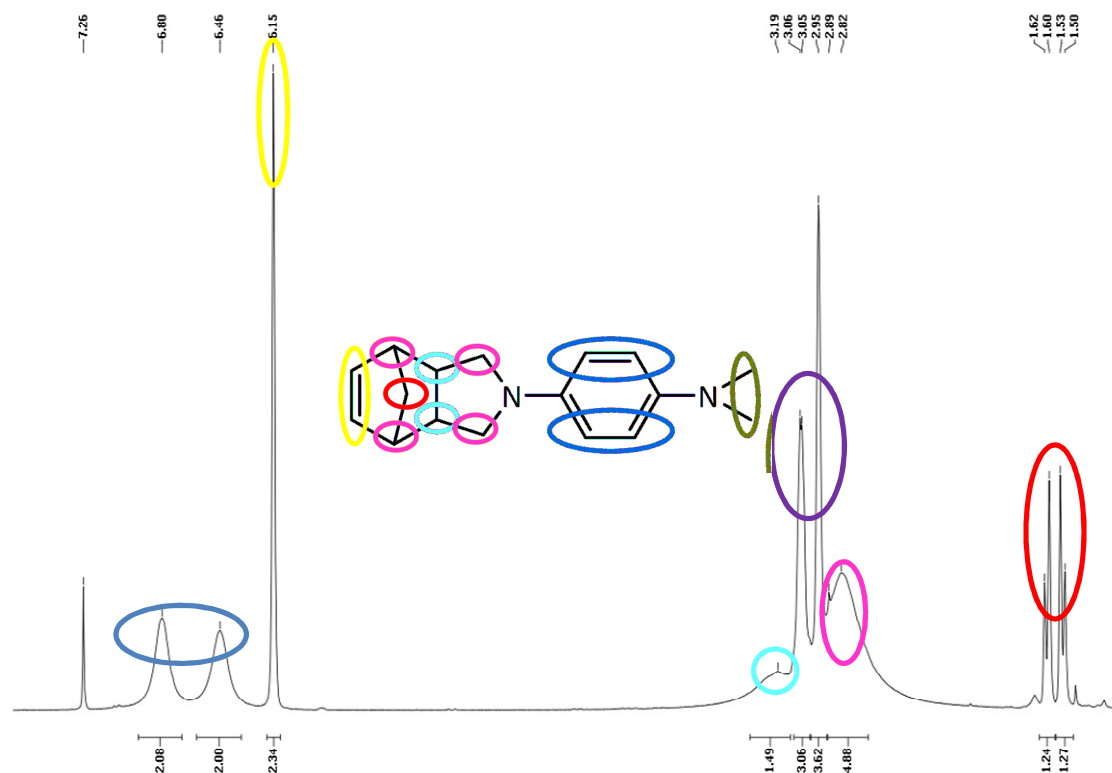


Figure 74: NMR of the unstable norbornene-monomer (paramagnetic)

The last indication for a photochrome molecule is that the molecular structure did not change at all, but this question should be answered by the measurement of a GC-MS. No changes could be observed but the full assurance is not possible because higher molecular parts cannot be detected. Unfortunately, the last method MALDI-TOF (*cf.* Figure 75) confirmed the presence of dimer and also trimer units. After 50 light cycles the dimer seems to be the main component but also monomer units could be detected. However this result leads to the conclusion that the molecule gives the impression of a photochrome substance but after full characterization unfortunately the conversion to higher molecular building blocks was detected which is also a disadvantage in the further usage of this molecule.

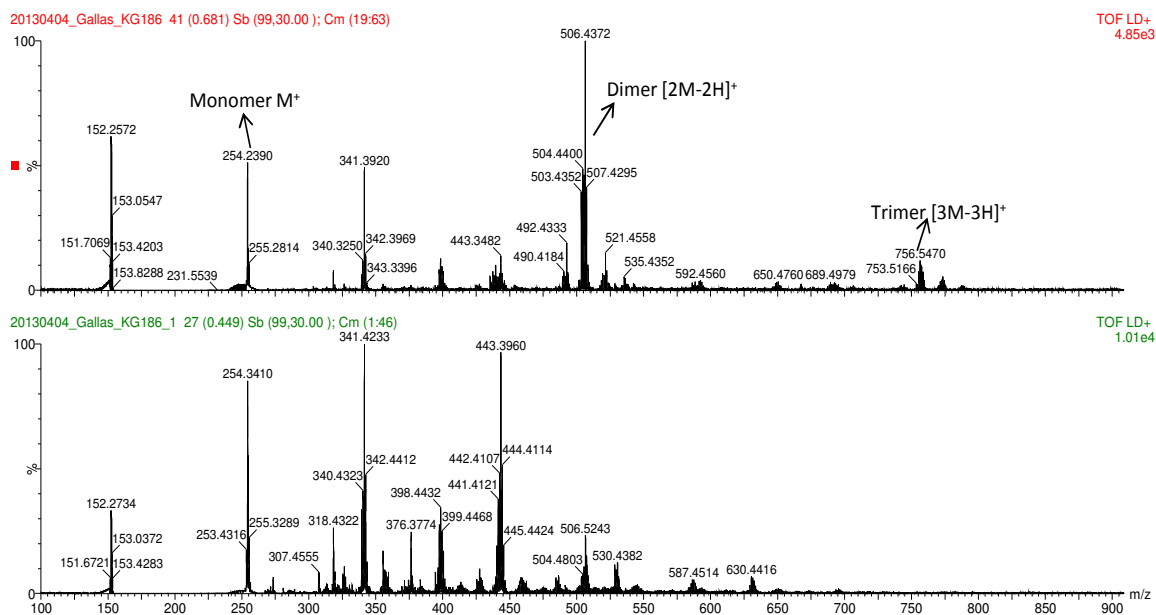


Figure 75: MALDI-TOF of the monomer before and after 50 blue/yellow cycles

Electrochemical measurements

The electrochemical measurements are presented here for completion regarding the use of the polynorbornene as a material for ORBs. The CVs in solution of the monomer 1 showed promising results.

However the measurements of the polymers were always more challenging due to the soluble or insoluble nature of the polymer in different solvents and furthermore the polymers seemed to be much more sensitive against oxidation.

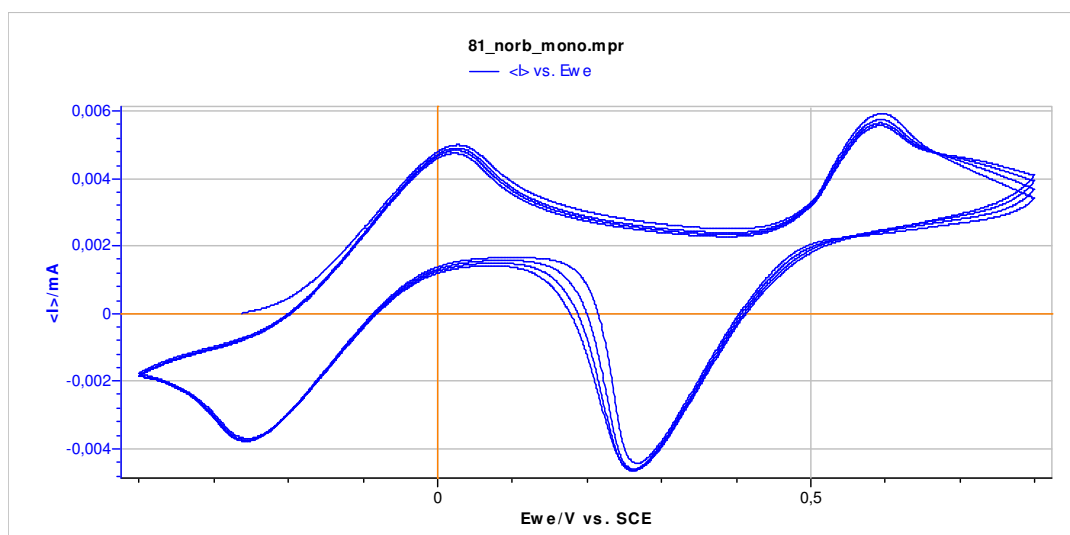


Figure 76: CV in solution of the norbornene-monomer in acetonitrile, counter and working electrode: Pt; reference-electrode: Ag/AgNO₃; 0.1 M TBAP, scan rate: 50 mV/s

The CV in solution showed the typical oxidation and reduction peaks of the Wurster-blue unit. For the polymer this setup could not be realized because the solubility of this

material was not good enough. The peaks of the polymer shifted a bit to the left to lower voltages, also the first reduction peak is not that clear and the second seems to show some decomposition. At this point we decided to use the half cell setup to exclude possible influences of the solvent, oxidation processes and solubility problems.

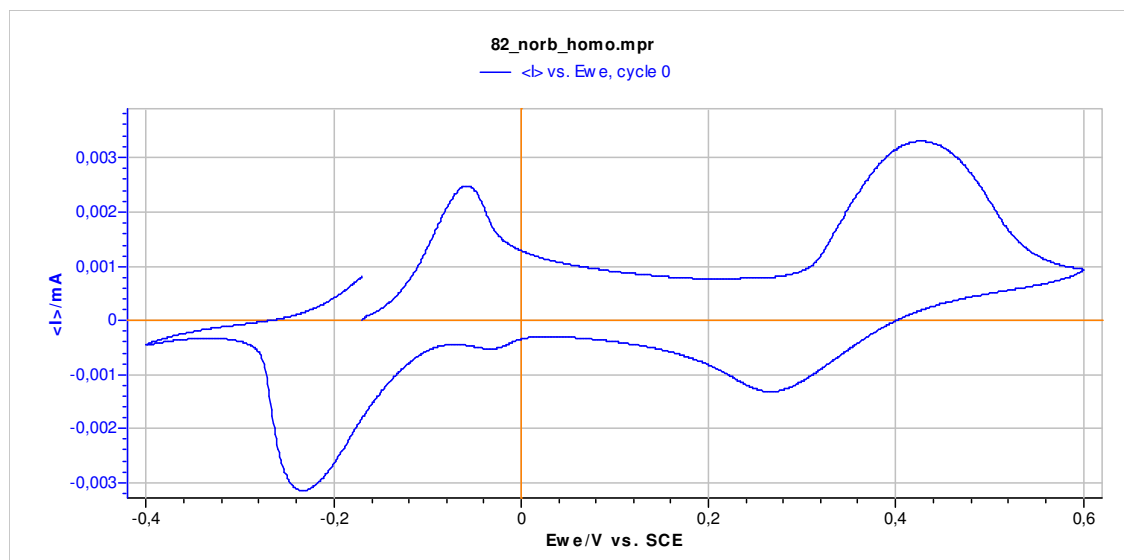


Figure 77: CV in solution of the norbornene-polymer in acetonitrile, counter and working electrode: Pt; reference-electrode: Ag/AgNO₃; 0.1 M TBAP, scan rate: 50 mV/s

Another problem with the setup in solution was the unknown amount of deposition processes at the electrodes.

With the copolymer setup of TEMPO and Wurster blue, where all three oxidation and reduction peaks should be visible, a test cycling was performed to identify possible depositions at the electrodes. The blue curve in Figure 78 is the decrease of the peak-hightness due to deposition of the solved polymer. After cleaning of the electrodes the same picture was visible by cycling it again in the same solvent.

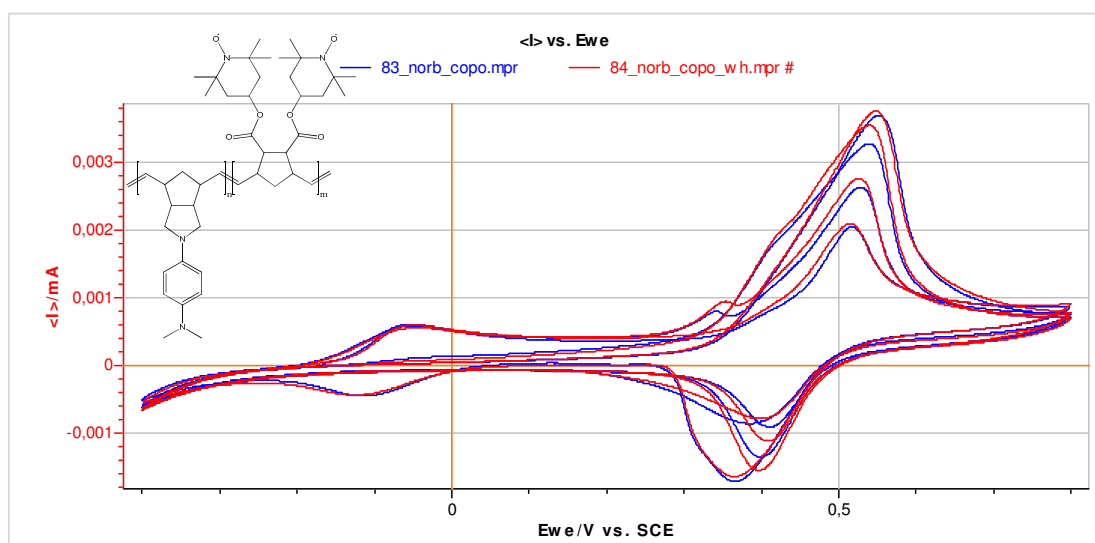


Figure 78: CV in solution of the norbornene-TEMPO copolymer in chloroform, counter and working electrode: Pt; reference-electrode: Ag/AgNO₃; 0.1 M TBAP, scan rate: 50 mV/s

So also deposition of the material is an unknown factor by further cycling of the material in solution. Due to that it was decided to adjust the voltage range (potential window) with the CV in solution but all further measurements were made with the half cell setup.

The situation for halfcell measurements was totally different (*cf.* Figure 79). With this system only one real charge and discharge cycle could be obtained. The big second reduction peaks relies on a decomposition of the material. Maybe the slurry composition is removed from the current collector or the active material is soluble in the electrolyte solution. In the first cycle 80% of the theoretical capacity could be reached which would be about 170 mAh/g and therefore nearly half of that of LIBs but unfortunately the stability of the material is not good enough.

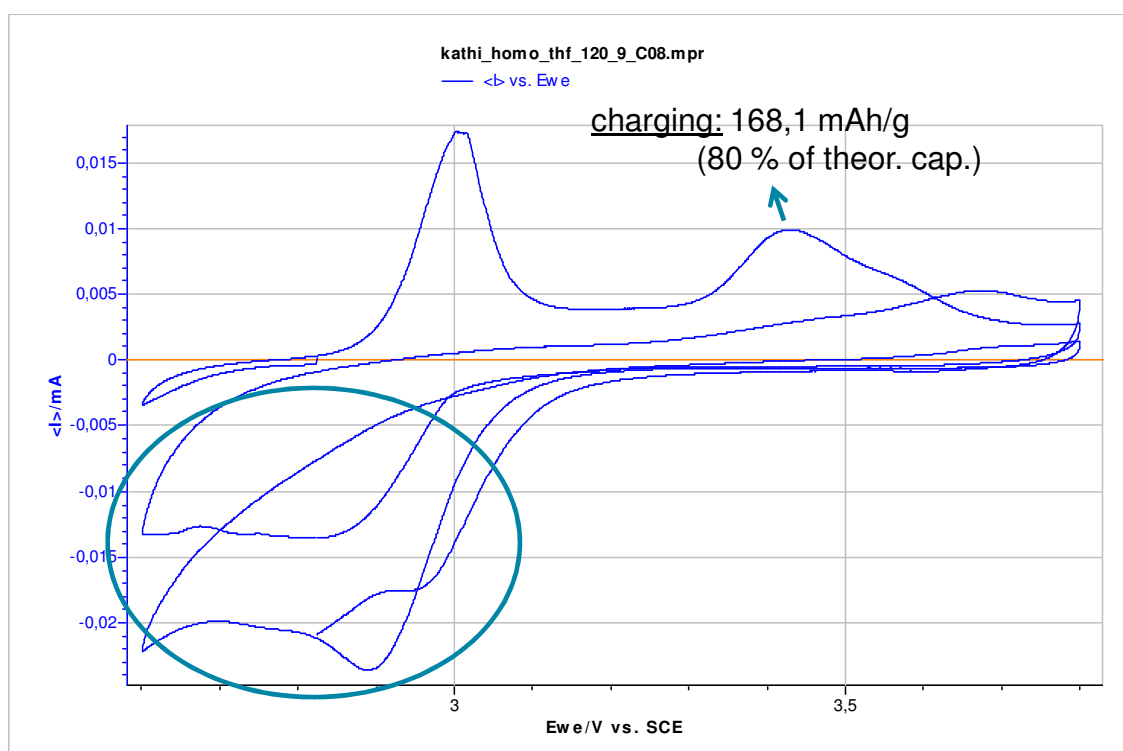


Figure 79: CV in half-cell, 10% active material, 10%PVdF, 10%Super P, scan rate 10 mV/s

A further approach was to increase the amount of active material either by increasing it in the slurry mixture or by spin coating the active material without further conductive material on the current collector.

Spin coating of the dissolved polymer solution was the method of choice. It was dissolved in toluene or DMF and spin coated as a very thin but closed film on the current collector foil. The film has to be thin enough (a few microns) to ensure electron hopping as a electron conducting process but thick enough to bring a high enough amount of material on the collector foil. The amount of active material is only 0.05 mg

per half cell but the film is thin enough for electron hopping processes. Figure 80 shows the CV in the halfcell but here only 13.6 mAh/g of the theoretical capacity could be reached what is not even 10% of the theoretical capacity.

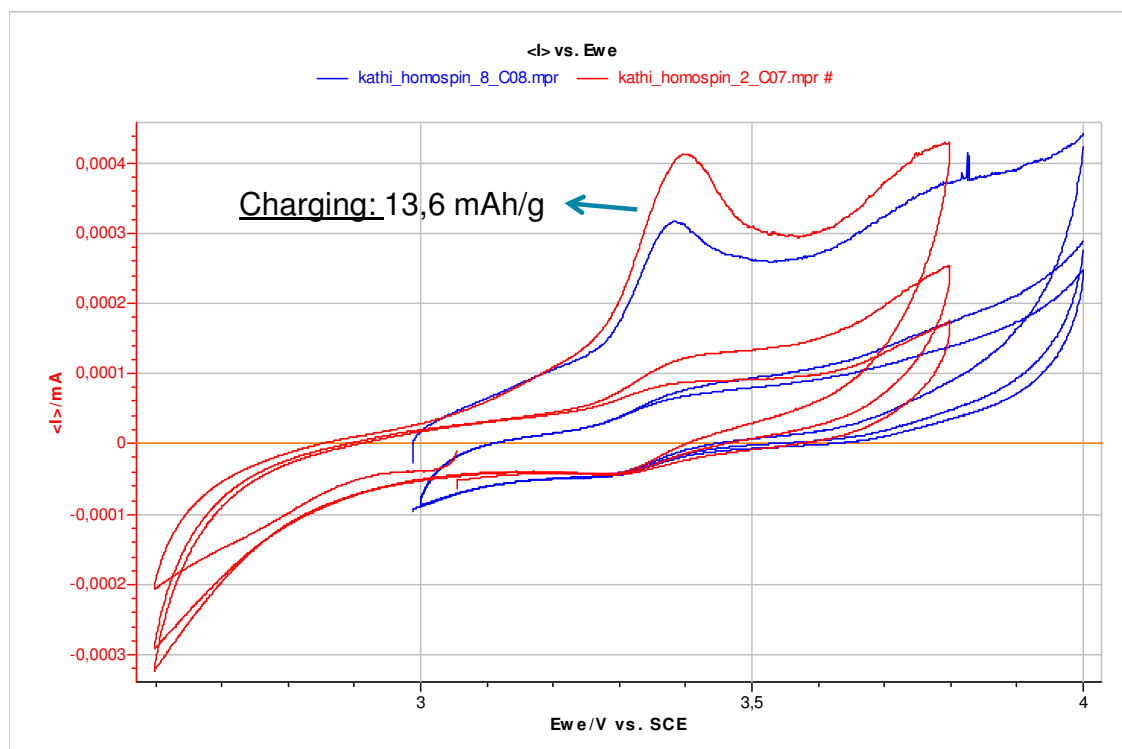


Figure 80: CV in half cell with spincoated active material, scan-rate 0.1mV/s

The stability of monomer 1 was not given and so a second norbornene-monomer stabilized through two phenyl rings was synthesized. Unfortunately this composition was even more unstable and so no CV in solution could be measured. The embedding into the half cell was not realized due to better working systems. Monomer 3 with the pyrrolidine ring was harder to synthesize but also not very stable. This might be due to the fact that it was not possible to get neither a pure monomer nor a long-chained polymer.

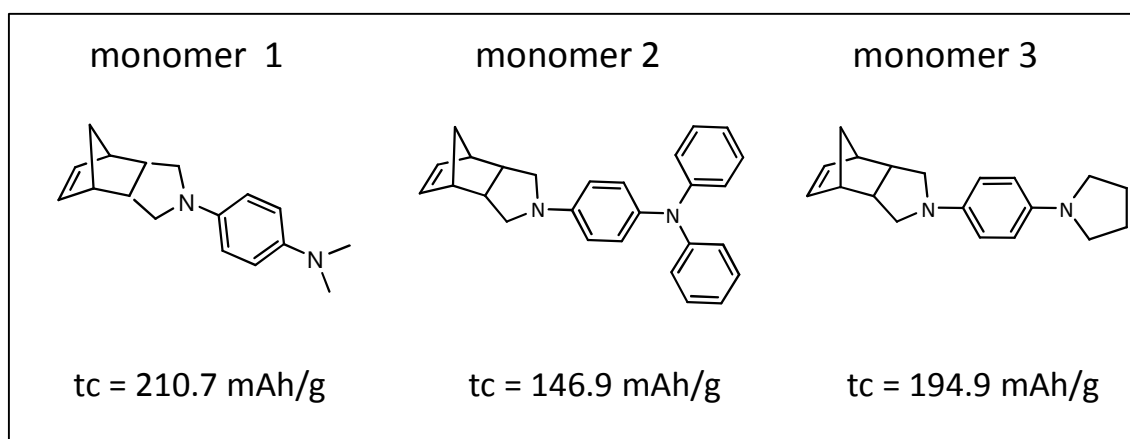
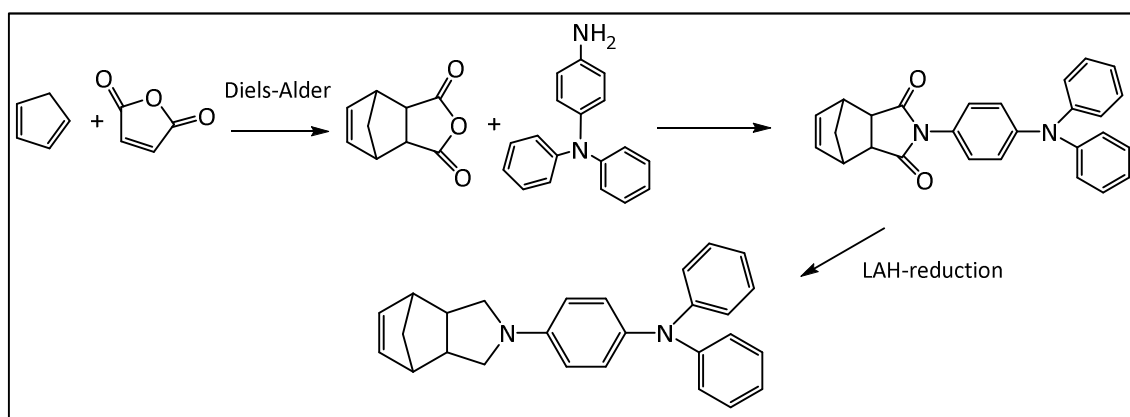
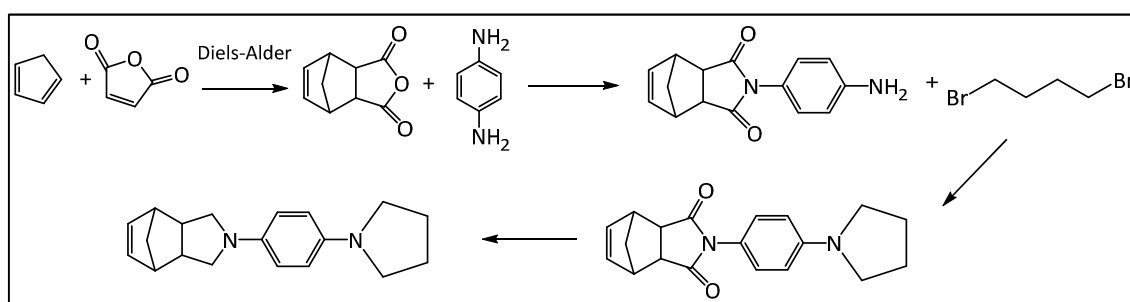


Figure 81: Three possible Norbornene-Wurster blue compositions



Scheme 33: Synthesis of norbornene-monomer 2



Scheme 34: Synthesis of norbornene-monomer 3

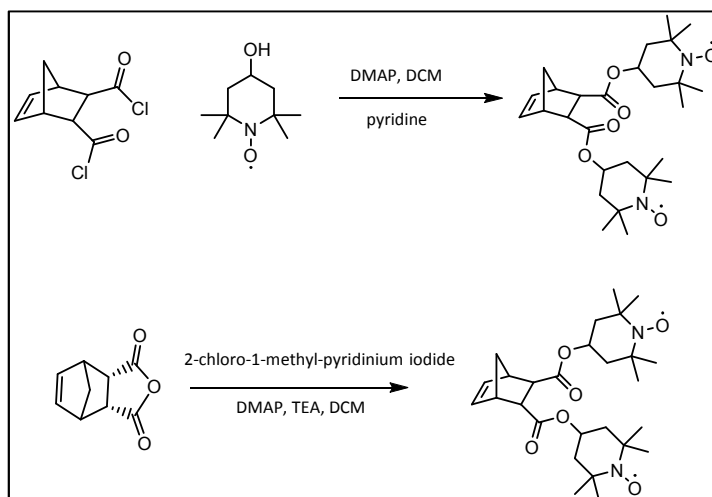
Summarizing the above, it can be said, that the theoretical capacities, especially that of monomer 1 were really promising and also the polymer backbone was a better base for longer polymer chains due to the high functional group tolerance of the ROMP technique and the good molecular weight distribution. Unfortunately with our generally used system, it was not possible to derive good results in the electrochemical measurements. For this purpose we would require a wider knowledge of electrochemical methods and maybe also a system which can be used in an oxygen free environment.

As a last point, different characterization methods of polyradicals used for battery applications are presented.

Therefore a model compound which was also used for different copolymerization reactions and electrochemical tests was synthesized.

TEMPO

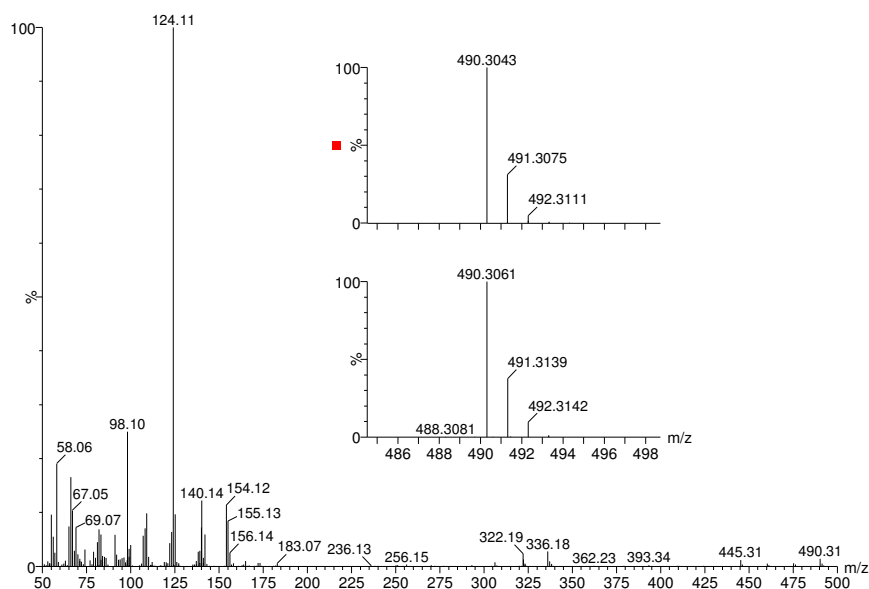
The TEMPO-norbornene was prepared via two different synthetic strategies. One attempt was to use the trans-5-norbornene-2,3-dicarbonyl chloride which provided the \pm endo,exo-Bicyclo[2.2.1]hept-5-ene-2,3-dicarboxylic acid bis[4-(2,2,6,6-tetramethylpiperidine-1-oxyl)] ester. And for the other one the cis-5-norbornene-endo-2,3-dicarboxylic anhydride was used which provided a mixture of isomers.²⁵⁷



Different characterization-methods through the example of the polynorbornene with TEMPO-radicals

Mass spectrometry

One of the challenges in characterizing paramagnetic substances, like radicals, is that it is impossible to make NMR studies. Therefore mass spectrometry was applied to investigate the structure of the monomers with TEMPO-units.



ESR

The ESR (electron spin resonance) spectroscopy is a technique for studying materials with unpaired electrons. It is analogous to NMR spectroscopy but here the electron spins get excited instead of the spins of atomic nuclei. It is a versatile, nondestructive analytical technique which can be used for a variety of applications including: oxidation and reduction processes, bi-radicals and triplet state molecules, reaction kinetics, as

well as numerous additional applications in biology, medicine and physics. However, this technique can only be applied to samples having one or more unpaired electrons.²⁶²

The basis of EPR (electron paramagnetic resonance) spectroscopy lies in the spin of an electron and its associated magnetic moment. When an electron is placed within an applied magnetic field, B_o , the two possible spin states of the electron have different energies. This energy difference is a result of the Zeeman Effect. The lower energy state occurs when the magnetic moment of the electron, μ , is aligned with the magnetic field and a higher energy state occurs where μ is aligned against the magnetic field. The two states are labeled by the projection of the electron spin, MS , on the direction of the magnetic field, where $MS = -1/2$ is the parallel state, and $MS = +1/2$ is the antiparallel state.²⁶³

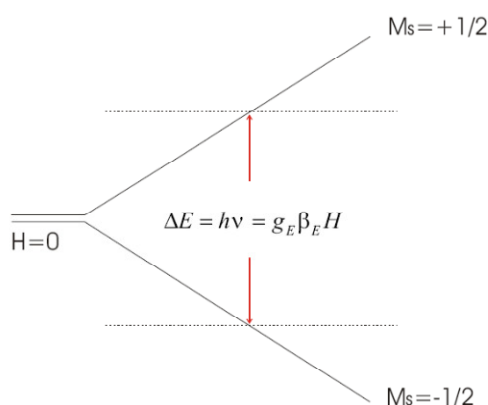


Figure 82: The Zeeman effect²⁶³

So for a molecule with one unpaired electron in a magnetic field, the energy states of the electron can be defined as: $E = g\mu_B B_o MS = \pm 1/2 g\mu_B B_o$ where g is the proportionality factor (or g -factor), μ_B is the Bohr magneton, B_o is the magnetic field, and MS is the electron spin quantum number. From this relationship, there are two important factors to note: the two spin states have the same energy when there is no applied magnetic field and the energy difference between the two spin states increases linearly with increasing magnetic field strength. As mentioned earlier, an EPR spectrum is obtained by holding the frequency of radiation constant and varying the magnetic field. Absorption occurs when the magnetic field “tunes” the two spin states so that their energy difference is equal to the radiation. This is known as the field for resonance. As spectra can be obtained at a variety of frequencies, the field for resonance does not provide unique identification of compounds.²⁶²

²⁶² University of Austin Texas, epr.cm.utexas.edu/WhatIsEPR.html.

²⁶³ Rupp, B., Saf, R., Fast, D.E., Stelzer, F. *Project Meeting ORB*, 24.01.2011.

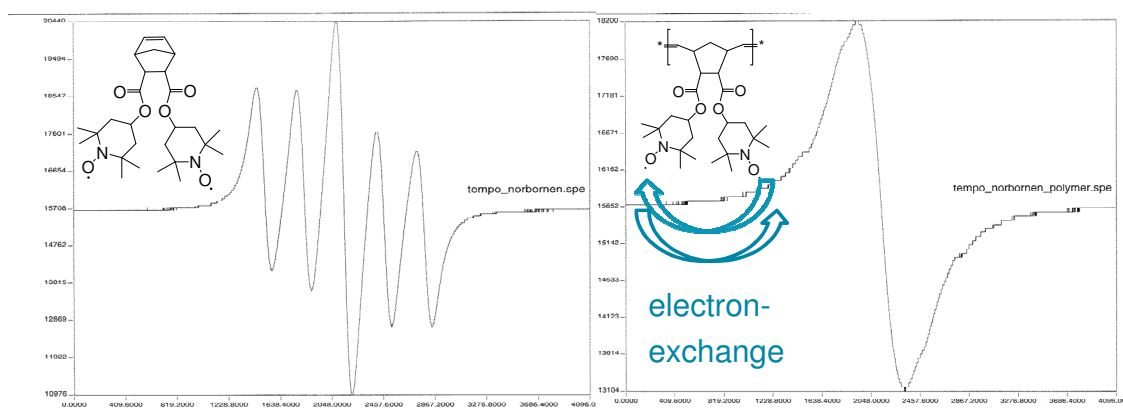


Figure 83: ESR-spectra of the monomer and the polymer

GPC

Gel permeation chromatography or size exclusion chromatography is a very important characterization method for polymers. Here important parameters like the molar mass distribution and different weight averages can be calculated. The solution of the polymer is pumped through a stationary porous phase, resulting in different retention times. The mole fraction (number average of molar mass M_n) and the weight fraction (mass average of the molar mass M_w) and the PDI (polydispersity index), the ratio between M_w and M_n gets determined. Also information about the nature of the polymerization and structural insights are processable properties.

Magnetic susceptibility

A useful method to determine the spin density, the quantity of radical groups and thus the capacity of a given poly-radical is the measurement of the magnetic susceptibility χ . This measurement gives us information about the magnetic centers incorporated in a material, as well as the interactions between unpaired spins. Ideal paramagnets comply with Curie's law $\chi=C/T$ (T is temperature in Kelvin, C is Curie constant) and show a horizontal line when χT is plotted vs. T . The red line in Figure 84 indicates the calculated value of the Curie constant for the TEMPO modified monomer and polymer. The experimental values coincide almost perfectly with this line and a spin density of 97% can be deduced considering an accuracy of the measurement of $\pm 3\%$. As a consequence, at least 97% of the radical groups can be considered active and will contribute to the capacity of the material.

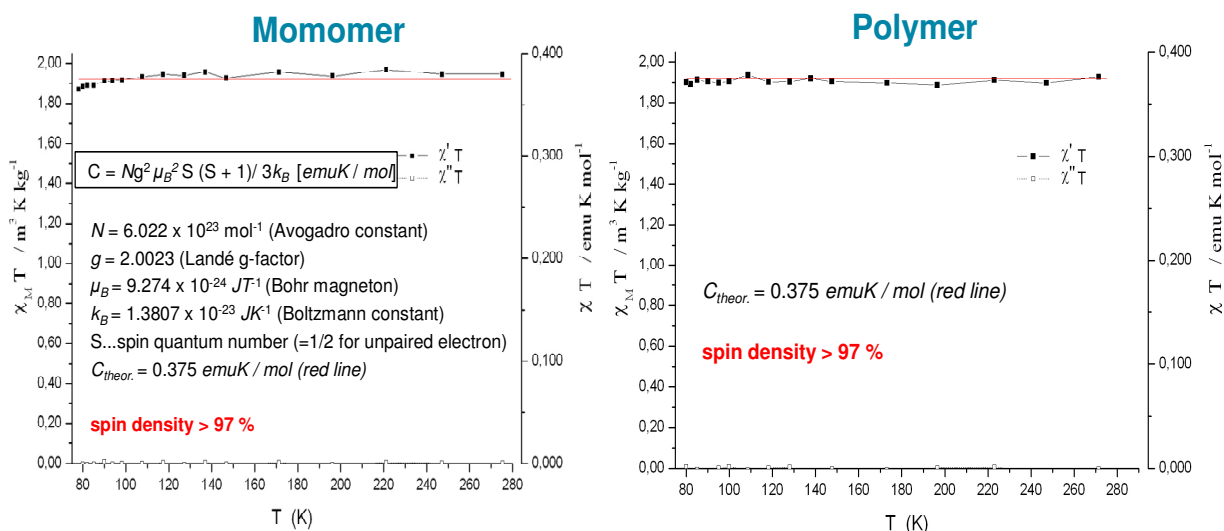


Figure 84: Magnetic susceptibility measurements for the TEMPO-modified norbornene monomer and polymer and the correspondent values for the Curie constant and spin density

IR-spectroscopy and cyclic voltammetry

These two are very quick and easy useable characterization methods. The cyclic voltammetry was explained before and demonstrated with an example. IR-spectroscopy is mostly used for monomers which lose their specific functionalities during polymerization. For example the C=C stretch signal in PTMA is no longer present in the polymer. In polymers like TEMPO where we have a nitroxide moiety this band is also often used for characterization. Our model compound shows strong absorption maxima at 1364 cm^{-1} which comes from the stretching bond of the N-O, which indicates the incorporation of the TEMPO moiety into the polymer.

Conclusion

The ORB project was a wide experience in different fields of chemistry. The first steps were to propose possible structures and molecules for the synthetic work. In this part of the work we tried many different approaches through different polymer backbones and polymerization techniques to different radical moieties and also the theoretical capacity of the substances was also in our focus. The focus was also on easy, cheap and not very time consuming synthesis, due to the collaboration of an industrial partner. The system should be comparable with the state of the art work of other groups or even better than that. Due to this reason we focused on the Wurster blue structure. Tetrasubstituted *para*-phenyldiamines are widely known and well studied compounds but has not yet integrated in organic radical batteries. The focus on the work with these compounds was on different electrochmic properties and applications.

Different characterization methods for polyradicals as well as the electrochemical analysis methods were studied with the help of already known model compounds

based on TEMPO-norbornenes. For my part of the project I further worked on norbornene-derivatives due to my experiences in this field. The synthesis of one compound the norbornene-monomer **1** is discussed in detail in the results and discussion part but unfortunately did not lead to a promising product for organic radical battery applications.

Special interest was also paid to the Buchwald-Hartwig reaction and the reductive amination which both lead in mostly simple ways to promising monomers or polymers for our research work. Both reactions but in particular the Buchwald-Hartwig reaction possess many different reaction conditions with different ligand/base systems. These systems have to be studied in literature but the optimum adjustment can only be found by trying a particular adjustment setting and by practice. Therefore we tried different systems for different substrates and were able to synthesize more or less successful different kind of monomer and polymer structures. But also these tests were finally cancelled due to the unstable or insoluble products which we derived.

As a last step a already known product from the group of Guey-Sheng Liou was synthesized and used for further electrochemical investigations. This polymer was till now not used as a material for organic radical battery but it includes the Wurster blue unit and due to that it was the appropriate candidate for our work.

With two derivatives of the polyaramides promising C-rate tests and long term measurements were realized. The next steps are the testing for a better slurry composition with more active material and a more efficient system for the half cell. The future for this material seems to be really promising. High and low temperature testings are currently being conducted. This leads us to different applications for the polyaramid material in batteries and to a different market other than of lithium ion batteries.

Experimental

Materials

Initiator **M31** ([1,3-bis(2,4,6-trimethylphenyl)-2-imidazolidinylidene]dichloro(3-phenyl-1H-inden-1-ylidene)(pyridyl)ruthenium(II)) was obtained from UMICORE AG&Co.KG. Other materials were obtained from commercial sources (Aldrich, Fluka or Lancaster). All reactions were performed under an inert atmosphere of nitrogen using Schlenk techniques. The synthesis of *±endo,exo*-Bicyclo[2.2.1]hept-5-ene-2,3-dicarboxylic acid bis[4-(2,2,6,6-tetramethylpiperidine-1-oxyl)] ester was already described in chapter 2 part 1.

Methods

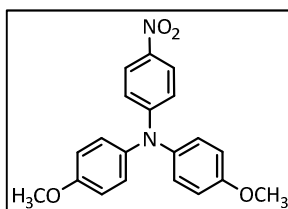
TR-EPR experiments were performed without modulation of the external magnetic field on a Bruker ESP 300E spectrometer equipped with a micro-wave amplifier, a TE

102 microwave cavity (microwave power 9 mW, response time 40 ns). The response of the EPR spectrometer after a laser pulse at a fixed value of the static magnetic field was stored in a LeCroy 9400 dual 125 MHz digital oscilloscope. The central control unit consists of a PC computer with a Debian Linux operating system and a GPIB interface board. The experiment is controlled by the program fsc2 (J. T. Toerring, Institut für Experimentalphysik, Freie Universität Berlin). A Continuum Surelite II, Nd:YAG laser with a fixed repetition frequency of 20 Hz (4-6 ns pulse width, frequency-tripled, 355 nm) was used as the light source. Polydispersity indices (PDI) and molecular weight data were determined by gel permeation chromatography (GPC) using THF as eluent, if not stated otherwise. The device setup comprises a Merck Hitachi L6000 pump (delivery volume 1 mL/min), separation columns from Polymer Standards Service (5 μ m grade size) and a refractive index detector from Wyatt Technology. For calibration polystyrene standards from Polymer Standards Service were used. NMR spectroscopy (^1H , ^{13}C , COSY, HSQC and HMBC) was done on a Bruker Avance 300 MHz spectrometer (75 MHz for ^{13}C). Deuterated solvents were obtained from Cambridge Isotope Laboratories Inc. For FT-IR spectroscopy a Bruker ALPHA FT-IR Spectrometer was used. Measurements were performed in ATR mode. UV/VIS absorption spectra were recorded with a Cary 50 UV/VIS Spectrophotometer from Varian. Electron impact (EI, 70 eV) mass spectra were recorded on a Waters GCT Premier equipped with direct insertion (DI). MALDI-TOF mass spectrometry was performed on a Micromass ToFSpec 2E Time-of-Flight Mass Spectrometer using DCTB as a matrix. Cyclovoltammetry was performed on a Bio-Logic VMP3 (in solution and in the Swagelok halfcell). For the constant current cyclization as electrolyte: 1M LiPF_6 in EC/DEC = 3:7 (v/v), with counter and reference el.: Lithium was performed on a Maccor Series 4000 battery tester.

Syntheses

4-Nitro-4', 4''-dimethoxytriphenylamine

Iodoanisole (2 g, 85.4 mmol, 4 eq) and nitroaniline (295 mg, 2.14 mmol, 1 eq) were dissolved in 8 mL DMF abs. in a Schlenk tube. Pipecolinic acid (221 mg, 1.71 mmol, 0.8 eq), copper(I)iodide (163 mg, 0.86 mmol, 0.4 eq) and potassiumcarbonate (2.4 g, 0.22 mol, 8 eq) were put together in another but bigger and broader Schlenk tube and the dissolved mixture of iodoanisole and nitroaniline were added drop wise. The whole mixture was heated to 120°C for 48 hours and the reaction progress was monitored via TLC in CH/Ea (4:1). After confirmation of full conversion the mixture was extracted with ethylacetate and NaOH. The organic phase was dried with Na_2SO_4 and the solvent was removed under reduced pressure. For further purification a column chromatography was performed in CH/Ea (1:1). Yield: 487mg (65%)

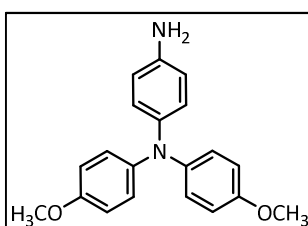


¹H-NMR (δ , 20°C, CDCl₃, 300.36 MHz): 8.00 (d, $J_3=9.2$ Hz, 2H) 7.13 (d, $J_3= 8.9$ Hz, 4H), 6.91 (d, $J_3=9.0$ Hz, 4H), 6.75 (d, $J_3=9.4$ Hz, 2H), 3.82 (s, 6H, OCH₃)

¹³C-NMR (δ , 20°C, CDCl₃, 75.53 MHz): 157.7, 154.1, 139.0, 138.3, 128.1, 125.6, 115.7, 115.2, 55.5 (OCH₃)

4-Amino-4', 4''-dimethoxytriphenylamine

The 4-Nitro-4', 4''-dimethoxytriphenylamine (0.3 g, 0.86 mmol, 1 eq) was dissolved in 14 mL acetonitrile and 12 mL ethanol. Afterwards the tin(II)chloride (1.8 g, 9.64 mmol, 11 eq) was added and the mixture was stirred at around 80°C (reflux) over night. The next day it was cooled down to room temperature, ethylacetate was added and then extracted with NaHCO₃ and NaCl. (strawberrymilk like emulsion). As an emulsion the two phases are hard to separate from each other, 5-10 times extraction. The organic phase was dried over Na₂SO₄, filtered and then the solvent was removed under reduced pressure. Yield: 240mg (88%)



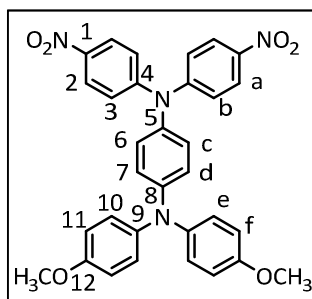
¹H-NMR (δ , 20°C, CDCl₃, 300.36 MHz): 6.81 (d, 4H, Hc), 6.77 (d, 4H, Hd), 6.72 (d, 2H, Hb), 6.53 (d, 2H, Ha), 4.90 (s, 2H, NH₂), 3.67 (s, 6H, OCH₃)

¹³C-NMR (δ , 20°C, CDCl₃, 75.53 MHz): 154.1 (C8), 145.1 (C1), 142.2 (C5), 137.1 (C4), 126.6 (C3), 123.4 (C6), 115.1 (C2), 114.7 (C7), 55.3 (OCH₃)

IR: 3455, 3371 cm⁻¹ (N-H stretch), 2966, 2920, 2845 cm⁻¹ (OCH₃, C-H stretch).

N,N-Bis(4-nitrophenyl)-*N',N'*-di(4-methoxyphenyl)-1,4-phenylenediamine

A mixture of cesium fluoride (247 mg, 1.62 mmol, 2.2 eq) in 4 mL DMSO was stirred at room temperature. To this mixture 4-amino-4', 4''-dimethoxytriphenylamine (240 mg, 0.75 mmol, 1.1 eq) and 4-fluoronitrobenzene (165 μ L = 220 mg, 1.56 mmol, 2 eq) were added in sequence. The mixture was heated with stirring at 120°C for 24 hours. After confirmation of full conversion via TLC in CH/EA (1:5) the mixture was slowly poured into 50 mL of stirred H₂O and the precipitation was filtered. The rest solvent was removed and it was recrystallized from DMF/MeOH. Yield: 315mg (75%)



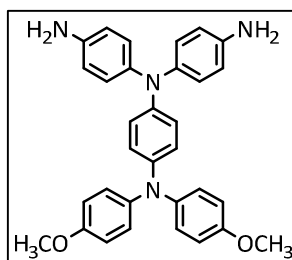
$^1\text{H-NMR}$ (δ , 20°C, DMSO- d_6 , 300.36 MHz): 8.16 (d, 4H, H^a), 7.19 (d, 4H, H^b), 7.11 (d, 4H, H^e), 7.04 (d, 2H, H^d), 6.93 (d, 4H, H^f), 6.77 (d, 2H, H^c), 3.73 (s, 6H, OCH_3)

$^{13}\text{C-NMR}$ (δ , 20°C, DMSO- d_6 , 75.53 MHz): 156.5 (C12), 151.9 (C4), 147.8 (C8), 141.8 (C1), 139.6 (C9), 135.5 (C5), 128.8 (C7), 127.7 (C10), 125.8 (C2), 122.0 (C3), 119.4 (C6), 115.3 (C11), 55.5 (OCH_3)

IR: 2934, 2834 (OCH_3), 1581, 1311 (NO_2)

***N,N*-Bis(4-aminophenyl)-*N',N'*-di(4-methoxyphenyl)-1,4-phenylenediamine**

N,N-Bis(4-nitrophenyl)-*N',N'*-di(4-methoxyphenyl)-1,4-phenylenediamine (1.6 g, 2.84 mmol, 1 eq) was dissolved in 45 mL acetonitrile and 50 mL ethanol and tin(II)dichloride (14.1 g, 62.6 mmol, 22 eq) was added. The reaction was heated to reflux over night. Via TLC monitoring completeness of the reaction was proved in CH/EA (1:2). It was extracted with ethyl acetate, brine and NaHCO_3 and afterwards the organic phase was dried, filtered and the solvent was removed under reduced pressure. For further purification a column chromatography with CH/EA 10:1 was performed. Yield: 1.4g (70%)



$^1\text{H-NMR}$ (δ , 20°C, DMSO- d_6 , 300.36 MHz): 6.85 (d, 4H, H^c), 6.80 (d, 4H, H^f), 6.77 (d, 4H, H^b), 6.70 (d, 2H, H^d), 6.56 (d, 2H, H^e), 6.50 (d, 4H, H^a), 4.50 (bs, 4H, NH_2), 3.73 (s, 6H, OCH_3)

$^{13}\text{C-NMR}$ (δ , 20°C, DMSO- d_6 , 75.53 MHz): 154.6 (C12), 145.3 (C1), 144.9 (C8), 141.8 (C9), 139.6 (C5), 136.6 (C4), 127.7 (C3), 124.6 (C7), 124.4 (C10), 118.9 (C6), 115.0 (C2), 114.9 (C11), 55.4 (OCH_3)

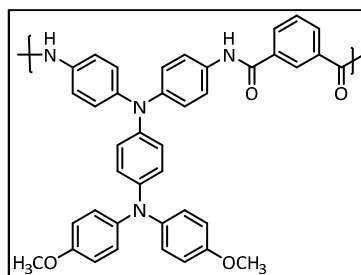
IR: 3434, 3360 cm^{-1} (N-H stretch), 2947, 2832 cm^{-1} (OCH_3 , C-H stretch)

Polyamide 1,3

N, N-Bis(4-aminophenyl)-*N',N'*-di(4-methoxyphenyl)-1,4-phenylenediamine (50 mg, 0.1 mmol, 1 eq) was dissolved in NMP (1 mL) and isophthaloylchloride (20 mg, 0.1 mmol, 1 eq) was also dissolved in NMP (0.5 mL). They were but together in a Schlenk tube and the mixture was heated to 100°C for one hour. Full conversion after this time was proved by TLC (CH/EE 1:5). After cooling down it was dropped into chilled methanol. The gluey polymer could not be separated from the solvent so the yield could not be verified. Another approach was dropped into chilled n-pentane which gave a yield of 51 mg (72%).

The second approach was performed with 90 mg (0.17 mmol, 1 eq) monomer and isophthalic acid (34 mg, 0.17 mmol, 1 eq). They were put together with lithium chloride (17 mg, 0.4 mmol, 2.4 eq) and 85 μ L pyridine in a Schlenk tube. TPP (0.48 mL, 0.17 mmol, 1 eq) was added drop wise and the reaction was stirred for three hours at 100°C. Full conversion was proven by TLC in CH/EA 1:1. The reaction was cooled down and then added to cold methanol. Yield: 78 mg (63%).

The third approach was done with 83 mg (0.165 mmol, 1eq) of the monomer and isophthalic acid (28 mg, 0.165 mmol, 1 eq) together with calcium chloride (20 mg, 0.18 mmol, 1.1 eq) in NMP (0.18 mL) was put into a Schlenk tube and dried in vacuum. After that, pyridine (0.08 mL) was added slowly and the reaction was heated to about 100°C. To the hot solution 0.16 mL TPP were added. After three hours of stirring full conversion was confirmed via TLC and the solution was dropped into cold methanol. The transfer of the polymer into a vial is a bit tricky and so only 76 mg product could be received. Yield: 76mg (76%)



$^1\text{H-NMR}$ (δ , 20°C, DMSO- d_6 , 300.36 MHz): 10.34 (s, 2H, NH-CO), 8.08 (d, 4H, H^g), 7.71 (d, 4H, H^a), 7.01 (d, 8H, H^b , H^c) 6.90 (d, 6H, H^f , H^d) 6.80 (d, 2H, H^e) 3.73 (s, 6H, OCH_3)

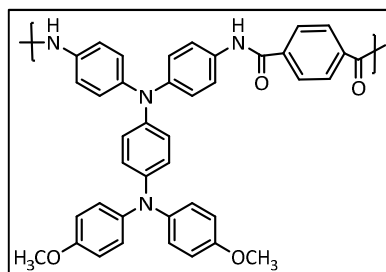
$^{13}\text{C-NMR}$ (δ , 20°C, DMSO- d_6 , 75.53 MHz): 164.7 (C=O), 155.5, 144.0, 143.7, 140.8, 137.6, 133.8, 127.8, 126.1, 125.3, 123.3, 122.0, 115.1, 55.4 (OCH_3)

IR: 3297 cm^{-1} (N-H stretch), 3040 cm^{-1} (aromatic C-H stretch), 2935, 2835 cm^{-1} (OCH_3 C-H stretch), 1655 cm^{-1} (amide carbonyl), 1235 cm^{-1} (asymmetric stretch C-O-C), 1034 cm^{-1} (symmetrical stretch C-O-C).

Polyamide 1,4

First approach with terephthalic acid. *N,N*-Bis(4-aminophenyl)-*N',N'*-di(4-methoxyphenyl)-1,4-phenylenediamine (0.1 g, 0.2 mmol, 1 eq) terephthalic acid (33 mg, 0.2 mmol, 1 eq), calcium chloride (24 mg, 0.21 mmol, 1 eq), NMP (0.19 mL, 2.1 mmol, 10.5 eq) were put in a Schlenk tube and evacuated while stirring. Pyridine (0.1 mL, 1.24 mmol, 6 eq) were added and the mixture was heated to 100°C. At this temperature triphenylphosphite (0.17 g, 0.77 mmol, 3.6 eq) was added and it was stirred for four hours. After the confirmation of full conversion the suspension was dropped into cold methanol. Yield: 129mg (97%).

Second approach with terephthaloylchloride. *N,N*-Bis(4-aminophenyl)-*N',N'*-di(4-methoxyphenyl)-1,4-phenylenediamine (50 mg, 0.1 mmol, 1 eq) and terephthaloyl chloride (20 mg, 0.1 mmol, 1 eq) were put together in a Schlenk tube with 1.5 mL of NMP and stirred for one hour. The conversion was confirmed via TLC CH/EA(1:5) and so the polymer was precipitated in methanol which worked not that good due to the high dilution. Yield: 54 mg (77%). Theoretical capacity: 84.7 mAh/g



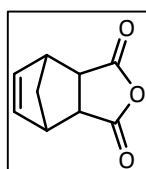
$^1\text{H-NMR}$ (δ , 20°C, DMSO- d_6 , 300.36 MHz): 10.40 (s, 2H, NH-CO), 8.11 (s, 4H, H^b), 7.70 (d, 4H, H^a), 7.00 (d, 8H, H^b, H^c), 6.88 (d, 6H, H^f, H^d), 6.77 (d, 2H, H^c), 3.72 (s, 6H, OCH₃)

$^{13}\text{C-NMR}$ (δ , 20°C, DMSO- d_6 , 75.53 MHz): 164.7 (C=O), 155.5, 144.0, 143.7, 140.8, 137.6, 133.8, 127.8, 126.1, 125.3, 123.3, 122.0, 115.1, 55.4 (OCH₃)

IR: 3312 cm⁻¹ (N-H stretch), 3037 cm⁻¹ (aromatic C-H stretch), 2932, 2833 cm⁻¹ (OCH₃, C-H stretch), 1654 cm⁻¹ (amide carbonyl), 1239cm⁻¹ (asymmetric stretch C-O-C), 1034 cm⁻¹ (symmetric stretch C-O-C).

***Endo*-5-norbornene-2,3-dicarboxylic anhydride (Carbic anhydride)**

Maleic anhydride (12 g, 0.12 mol, 1 eq) was dissolved in ethyl acetate and the same amount of cyclohexane with freshly distilled cyclopentadiene (10 mL, 0.12 mol, 1 eq) was added. After a short time a white precipitation of the product was filtered and again solved in hot toluene. The further addition of cyclohexane accelerated the precipitation. The product precipitated in the form of white crystals. Yield: 16.20 g (80%)

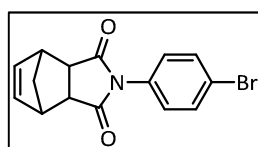


$^1\text{H-NMR}$ (δ , 20°C, CDCl_3 , 300.36 MHz): 6.31 (s, 2H), 3.62 (d, 4H), 1.83 (d, 1H), 1.60 (d, 1H)

$^{13}\text{C-NMR}$ (δ , 20°C, CDCl_3 , 75.53 MHz): 172.2 (C=O), 135.7 (2C, C=C), 47.9, 46.8, 46.6

2-(4-bromophenyl)-3a,4,7,7a-tetrahydro-1H-4,7-methanoisindole-1,3-dione

Carbic anhydride (2.58 g, 16 mmol, 1 eq) and 4-bromoaniline (2.7 g, 16 mmol, 1 eq) were dissolved in acetic acid and stirred under reflux for about four hours. Complete conversion was monitored via TLC in CH/EA (1:1) and for purification the reaction was convicted into 200 mL of H_2O dest.. It was extracted with dichloromethane and NaHCO_3 , dried over Na_2SO_4 , filtered and the solvent was removed under reduced pressure. Yield: 5.03 g (96%)

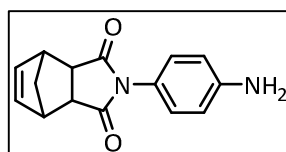


$^1\text{H-NMR}$ (δ , 20°C, CDCl_3 , 300.36 MHz): 7.55 (d, 2H, arom.), 7.05 (d, 2H, arom.), 6.35 (s, 2H, C=C), 3.55 (s, 2H), 3.45 (s, 2H), 1.82 (d, 1H), 1.63 (d, 1H)

$^{13}\text{C-NMR}$ (δ , 20°C, CDCl_3 , 75.53 MHz): 176.2 (2C, C=O), 135.9 (2C, C=C), 131.2, 130.7 (2C), 127.4 (2C), 120.1, 55.4, 48.2 (2C), 45.1 (2C)

2-(4-aminophenyl)-3a,4,7,7a-tetrahydro-1H-4,7-methanoisindole-1,3-dione

Carbic anhydride (1.5 g, 9.1 mmol, 1 eq) and *p*-phenylenediamine (0.98 g, 9.1 mmol, 1 eq) were dissolved in acetic acid and stirred under reflux for about six hours. Complete conversion was monitored via TLC in CH/EA (1:1). For purification the reaction mixture was poured into H_2O dest. and then extracted with dichloromethane and NaHCO_3 . The organic phase was dried over Na_2SO_4 , filtered and the solvent was removed. Yield: 1.8 g (78%).

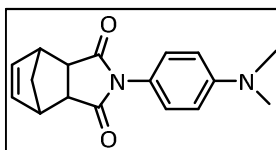


$^1\text{H-NMR}$ (δ , 20°C, CDCl_3 , 300.36 MHz): 7.02 (s, 2H, arom.), 6.45 (d, 2H, arom.), 6.33 (s, 2H, nb^{5,6}), 4.55 (s, 1H), 4.40 (bs, 2H, NH_2), 3.55 (s, 2H, nb^{1,4}), 3.45 (s, 2H, nb^{2,3}), 1.80 (d, 1H, nb⁷), 1.60 (d, 1H, nb⁷)

2-(4-(dimethylamino)phenyl)-3a,4,7,7a-tetrahydro-4,7-methanoisindole-1,3-dione

Endo-5-norbornene-2,3-dicarboxylic anhydride (2.91 g, 17.7 mmol, 1 eq) and *N,N*-dimethylbenzene-1,4-diamine (2.41 g, 17.7 mmol, 1 eq) were stirred in acetic acid under 120°C. After four hours the mixture was convicted into NaHCO_3 and a grey

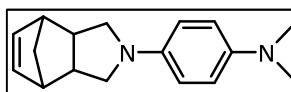
precipitation derived. The precipitation was filtered and re-crystallized from hot methanol, again filtered and dried under vacuum. Yield: 4.19 g (83%).



¹H-NMR (δ , 20°C, CDCl₃, 300.36 MHz): 6.93 (d, 2H, arom.), 6.68 (d, 2H, arom.), 6.22 (s, 2H, C=C), 3.46 (s, 2H), 3.36 (s, 2H), 2.93 (s, 6H, CH₃), 1.74, (d, 1H), 1.57 (d, 1H)

4-(1,3,3a,4,7,7a-hexahydro-2H-4,7-methanoisindol-2-yl)-N,N-dimethylaniline

A three-neck-flask was used with a dropping funnel, a drying tube and a reflux condenser; it should be worked water free. The flask is cooled with an ice bath and LAH (0.4 g, 10.6 mmol, 1.65 eq) was put into THF abs. Through the dropping funnel 2-(4-(dimethylamino)phenyl)-3a,4,7,7a-tetrahydro-1H-4,7-methanoisindole-1,3(2H)-dione (1.81 g, 6.4 mmol, 1 eq) also dissolved in dry THF was added drop wise. Hourly TLC monitoring in CH/Ea (1:1) was done till the conversion was complete. For quenching of the LAH, H₂O dest. was added drop wise. The THF was removed under reduced pressure and the reaction was extracted with ethyl acetate and NaHCO₃. The organic phase was dried over Na₂SO₄, filtered and the solvent was removed and afterwards it was re-crystallized from cyclohexane and ethyl acetate. Yield: 854 mg (53%). Theoretical capacity: 210.7mAh/g



¹H-NMR (δ , 20°C, CDCl₃, 300.36 MHz): 6.80 (s, 2H, arom), 6.46 (s, 2H, arom), 6.15 (s, 2H, C=C), 3.19 (s, 2H), 3.06 (s, 3H, CH₃), 2.95 (s, 3H, CH₃), 2.88-2.56 (m, 6H), 1.61 (d, 1H), 1.48 (d, 1H)

¹³C-NMR (δ , 20°C, CDCl₃, 75.53 MHz): not possible

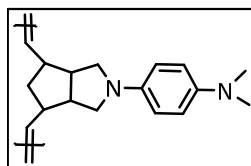
IR: 2979 (N-CH₃), 1345 (C-N), 1520 (C=C), 902, 730

GC-MS: experimental 254.1807; theoretical pattern: 254.1783

Polymerization of 4-(1,3,3a,4,7,7a-hexahydro-2H-4,7-methanoisindol-2-yl)-N,N-dimethylaniline

The monomer 1 (60 mg, 0.24 mmol, 100 eq) was dissolved in 1 mL of toluene in a Schlenk tube without light. The catalyst M31 (1.76 mg, 0.0024 mmol, 1 eq) was also dissolved in 0.5 mL of toluene and added with a syringe to the mixture. After 20 minutes it was stopped with ethyl vinyl ether (100 μ L) and the solvent was nearly removed. The sticky mixture was precipitated in chilled *n*-pentane under nitrogen

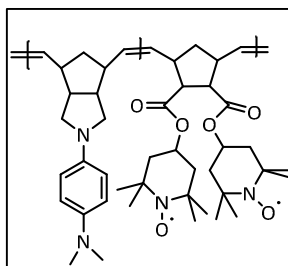
atmosphere. Product stays yellow, not blue and oxidized. Yield: 52mg (87%). No NMR characterization possible, due to the paramagnetic character of the compound.



GPC: not soluble

Copolymerization of 4-(1,3,3a,4,7,7a-hexahydro-2H-4,7-methanoisindol-2-yl)-*N,N*-dimethylaniline with the TEMPO diester

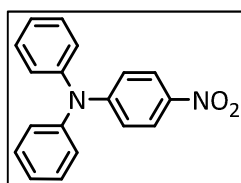
For the random copolymer the 4-(1,3,3a,4,7,7a-hexahydro-2H-4,7-methanoisindol-2-yl)-*N,N*-dimethylaniline (17 mg, 0.07 mmol, 50 eq) and the TEMPO-di-ester (33 mg, 0.07 mmol, 50 eq) were dissolved in 2 mL of degassed and dry dichloromethane. The catalyst M31 (1 mg, 0.0014 mmol, 1 eq) was dissolved in 0.5 mL of dichloromethane and added in one portion to the monomers. The reaction mixture was stirred for one hour, till it was yellow and then the solvent was narrowed and the gluey mixture was dropped into chilled *n*-pentane. Yield: 35 mg green precipitate (70%). No NMR characterization possible due to paramagnetic character of the compounds.



GPC: M_n : 66,000; M_w : 12,900, PDI: 1.9

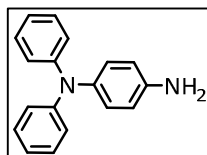
N-(4-nitrophenyl)-*N*-phenylbenzenamine

Diphenylamine (1.5 g, 8.86 mmol, 1 eq) and 1-fluoro-4-nitrobenzene (1.41 mL, 13.3 mmol, 1.5 eq) were dissolved in DMSO to a yellow reaction solution and then potassium *tert* butylate (1.69 g, 15 mmol, 1.7 eq) was added and the whole reaction got darkbrown. It was stirred over night at 80°C and on the next day the reaction progress was monitored via TLC in CH/EA (1:1). After full conversion of the educts the solution was added drop wise into NaCl sat. and filtered through a paper filter. Without further purification the precipitate was used for the reduction step.



N,N'-diphenylbenzene-1,4-diamine *N*-(4-nitrophenyl)-*N*-phenylbenzenamine

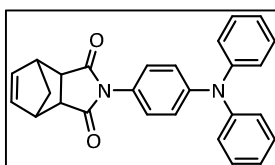
N-(4-nitrophenyl)-*N*-phenylbenzenamine (3 g, 10.8 mmol, 1 eq) was dissolved in ethanol (84 mL) and acetonitrile (70 mL) and tin(II)chloride (12 g, 54 mmol, 5 eq) was added and the reaction was stirred over night at 80°C. The TLC in CH/EA (1:1) showed full disappearance of the yellow nitro spot, so the reaction work up was done with extraction with ethyl acetate and NaHCO₃. The organic phase was dried over Na₂SO₄, filtered and the solvent was removed under reduced pressure. For further purification a re-crystallization with DCM/MeOH was performed and after that a column chromatography in CH/EA 10:1 with a gradient to EA was performed. Yield: 1.5 g (56%).



¹H-NMR (δ, 20°C, CDCl₃, 300.36 MHz): 7.10 (t, 5H, arom), 6.94 (d, 4H, arom), 6.82 (q, 4H, arom), 6.50 (d, 2H, arom.), 3.72 (bs, 2H, NH₂)

2-(4-(diphenylamino)-phenyl)-3a, 4,7,7a-tetrahydro-4,7-methanoisindole-1,3-dione

N,N'-diphenyl-1,4-phenylenediamine (406 mg, 1.56 mmol, 1 eq) was dissolved in 7 mL acetic acid and heated to 120°C in a Schlenk tube and then bicyclo[2.2.1]hept-5-ene-2,3-dicarboxylic anhydride (256 mg, 1.56 mmol, 1 eq) was added drop wise and the mixture was stirred for about one hour. For work up the reaction mixture was dropped into saturated NaHCO₃ solution and the grey-blue precipitate was filtered and dried. No further purification was made and the whole mixture was used for the next reaction step the reduction with LAH. Yield: crude about 500 mg (80%).

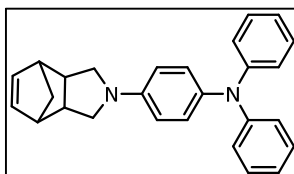


¹H-NMR (δ, 20°C, CDCl₃, 300.36 MHz): 7.19 (t, 5H, arom.), 7.02 (d, 4H, arom.), 6.97 (q, 4H, arom.), 6.87 (d, 2H, arom.), 6.17 (s, 2H, nb^{5,6}), 3.43 (s, 2H, nb^{1,4}), 3.34 (s, 2H, nb^{2,3}), 1.70 (d, 1H, nb⁷), 1.56 (d, 1H, nb⁷)

4-((3a,4,7,7a)-1,3,3a,4,7,7a-hexahydro-2H-4,7-methanoisindol-2-yl)-*N,N*-diphenylaniline (2-aza-1,2-dihydro-endo-dicyclopentadiene-2-*N,N*-diphenylaniline)

The reaction was performed in a three-neck-flask, which was evacuated and ventilated under inert atmosphere. The LAH (289 mg, 7.62 mmol, 3 eq) was put into 15 mL of dry THF. Then the 2-(4-(diphenylamino)phenyl)-3a,4,7,7a-tetrahydro-4,7-methanoisindole-1,3-dione (1 g, 2.54 mmol, 1 eq) was dissolved in 20 mL of dry THF and added drop wise through a dropping funnel. The reaction was heated to 80°C and stirred for about three hours. The reaction was monitored via hourly TLC in DCM/MeOH (10:1), it

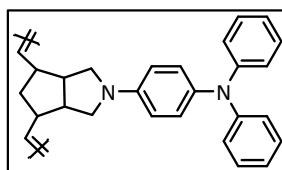
was not finished or even changed after three hours, so again LAH (2 eq, 192 mg) was added. Again after one hour of stirring the progress was monitored via TLC and again 192 mg LAH were added. For work up 10 mL of water were added slowly to the reaction to eliminate the excess of LAH and then the THF was removed under reduced pressure and it was extracted with NaHCO₃ and ethyl acetate. The organic phase was dried over Na₂SO₄, filtered and the solvent was removed under reduced pressure. For further purification a column chromatography was performed with CH/EE (10:1). Yield: 610mg (67%).



¹H-NMR (δ , 20°C, CDCl₃, 300.36 MHz): 7.18 (t, 5H, arom.), 7.02 (d, 4H, arom.), 6.97 (q, 4H, arom.), 6.87 (d, 2H, arom.), 6.17 (s, 2H, nb^{5,6}), 3.77 (q, 2H), 3.43 (s, 2H, nb^{1,4}), 3.34 (s, 2H, nb^{2,3}), 2.96 (q, 2H), 1.72 (d, 1H, nb⁷), 1.56 (d, 1H, nb⁷)

Polymerization of 4-((3a,4,7,7a)-1,3,3a,4,7,7a-hexahydro-2H-4,7-methanoisindol-2-yl)-N,N-diphenylaniline (2-aza-1,2-dihydro-endo-dicyclopentadiene-2-N,N-diphenylaniline)

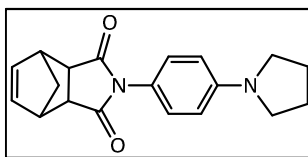
The monomer (80 mg, 0.24 mmol, 100 eq) was dissolved in 1.5 mL degassed and dry dichloromethane and the catalyst M31 (1.8 mg, 0.0024 mg, 1 eq) was dissolved in 0.5 mL dichloromethane and added subsequently. After one hour the conversion was confirmed via TLC CH/EE (1:1) and the reaction was stopped with ethyl vinyl ether (100 μ L). The solvent was nearly removed and the mixture was added drop wise to cold n-pentane. Yield: 58 mg (73%). Polymer is not soluble in any GPC nor NMR solvent. Electrochemical measurements were performed. (CV in solution).



2-(4-(pyrrolidin-1-yl)phenyl)-3a,4,7,7a-tetrahydro-1H-4,7-methanoisindole-1,3(2H)-dione

2-(4-aminophenyl)-3a,4,7,7a-tetrahydro-1H-4,7-methanoisindole-1,3-dione (50 mg, 0.2 mmol, 1 eq) was dissolved in a Schlenk tube in 1 mL dry DMF and subsequently dibromobutane (23 μ L, 0.2 mmol, 1 eq) and potassium carbonate (60 mg, 0.43 mmol, 2.2 eq) were added and stirred over night at room temperature. For work up the mixture was extracted with ethyl acetate and brine three times and the organic phase was dried over Na₂SO₄, filtered and the solvent was removed under reduced pressure.

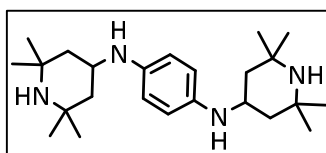
For further purification a column chromatography was performed with EA/MeOH 10:1.
Yield: 35 mg (48%)



$^1\text{H-NMR}$ (δ , 20°C, CDCl_3 , 300.36 MHz): 7.02 (s, 2H, arom.), 6.45 (d, 2H, arom.), 6.17 (s, 2H, nb^{5,6}), 3.45-3.30 (m, 8H, nb^{1,2,3,4}), 1.96 (t, 4H), 1.70 (d, 1H, nb⁷), 1.55 (d, 1H, nb⁷)

N^1, N^4 -bis(2,2,6,6-tetramethylpiperidin-4-yl)benzene-1,4-diamine

In a Schlenk tube *p*-phenylenediamine (250 mg, 2.31 mmol, 1 eq) was evacuated for one hour and after that a mixture of MeOH/AcOH (10:1) was added. Subsequently TEMPO (897 mg, 5.8 mmol, 2.5 eq) and picoline borane (494 mg, 4.6 mmol, 2 eq) were added and the mixture was stirred overnight. On the next day the conversion was controlled via TLC in EA/MeOH (1:1 with 1% triethylamine) and for staining HCl conc. was used. Through the vacuum line the methanol was removed and HCl (10%) was added. Then the mixture should be extracted with ethyl acetate but that just worked with a basic reaction mixture so NaOH was added. The organic phase was dried, filtered and the solvent was removed. Yield: 670 mg (75%), red crystals.



$^1\text{H-NMR}$ (δ , 20°C, CDCl_3 , 300.36 MHz): 8.50 (s, 4H), 3.60-3.50 (m, 2H), 2.00 (dd, 2H), 1.95 (d, 2H), 1.20 (s, 12H), 1.10 (s, 12H), 0.81 (dd, 5H)

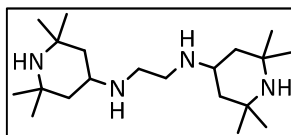
$^{13}\text{C-NMR}$ (δ , 20°C, CDCl_3 , 75.53 MHz): 139.42 (2C), 115.72 (4C), 51.40 (4C), 46.73 (4C), 46.38 (2C), 35.02 (4C), 28.61 (4C)

IR: 3364, 2956, 2923, 1731, 1513, 1460

TOF MS EI: calculated: $\text{C}_{24}\text{H}_{42}\text{N}_4$ 386.3409, detected 386.3404

N, N' -bis(2,2,6,6-tetramethylpiperidin-4-yl)methanediamine

2,2,6,6-tetramethylpiperidin-4-one (1 g, 6.44 mmol, 2 eq) and ethane-1,2-diaminium chloride (428 mg, 3.22 mmol, 1 eq) were dissolved in dry THF and stirred four hours at room temperature. After that sodium triacetoxyhydroborate (1.7 g, 8.05 mmol, 2.5 eq) was added with a further addition of THF. The mixture was stirred for a further 48 hours and the reaction progress was monitored via TLC in EA/MeOH (1:1). 0.5 mL HCl conc. were added and the reaction was extracted three times with dichloromethane and NaOH. For purification it was overlaid with diethyl ether for crystallization of the product. Yield: 460 mg (42%).

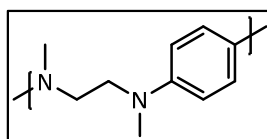


TOF MS EI: calculated: 338.3409 detected: 338.3404

¹H-NMR (δ, 20°C, CDCl₃, 300.36 MHz): 2.54 (q, 4H), 2.00 (dd, 2H), 1.95 (d, 2H), 1.20 (s, 12H), 1.10 (s, 12H), 0.81 (dd, 5H)

Buchwald Hartwig reaction: N¹,N¹,N²-trimethyl-N²-(*p*-tolyl)ethane-1,2-diamine

Dibromobenzene (110 mg, 0.48 mmol, 1 eq), *N,N*-dimethyl-1,2-ethane-diamine (50 μL, 0.48 mmol, 1 eq) and sodium *tert*-butylate (134 mg, 1.44 mmol, 3 eq) were put together in a Schlenk tube and evacuated. The palladium acetate (10 mg/mL in toluene, 104 μL, 1 mol%, 0.01 eq) and the palladium *tert* butylate (13.94 μL, 3 mol%, 0.03 eq) were mixed till the solution turned clear and added as a catalytic system to the other components. The reaction was heated at 110°C over night. Via TLC control in EA/MeOH (3:1, 1% TEA) complete conversion was proven. For work up it was extracted with NaOH and the organic phase was removed under reduced pressure. Yield: 40 mg. Theoretical capacity: 330mAh/g.



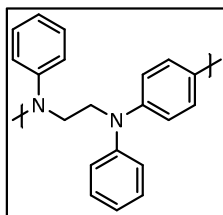
¹H-NMR (δ, 20°C, CDCl₃, 300.36 MHz): 7.22 (s, 1H), 6.62 (d, 3H), 3-45-3.27 (m, 4H), 2.97-2.62 (m, 6H), 2.39 (s, 3H)

IR: 3055, 1512, 1263, 750 cm⁻¹

GPC: only oligomer

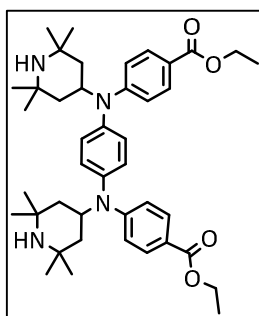
N¹-methyl-N¹,N²-diphenyl-N²-(*p*-tolyl)ethane-1,2-diamine

1,4-Dibromobenzene (111 mg, 0.47 mmol, 1 eq), *N,N*-diphenylethane-1,2-diamine (100 mg, 0.47 mmol, 1 eq) and sodium *tert* butylate (136 mg, 1.42 mmol, 3 eq) were put together in a Schlenk tube and evacuated. Diacetylpalladium (106 μL, 0.005 mmol, 0.01 eq) and tri-*tert*-butylphosphine (14 μL, 0.01 mmol, 0.03 eq) were stirred together till they are clear and then added subsequently to the other components with 4.5 mL toluene. The reaction was stirred over night at 110°C and the conversion was verified by TLC in EA/MeOH (3:1, 1%TEA). For work up it was extracted with NaOH and the organic phase was dried, filtered and the solvent was removed. Yield:



Diethyl 4,4'-(1,4-phenylenebis((2,2,6,6-tetramethylpiperidin-4-yl)azanediyl))-dibenzoate

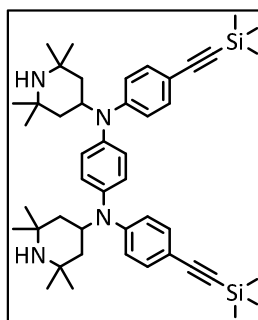
N,N-bis(2,2,6,6-tetramethylpiperidin-4-yl)benzene-1,4-diamine (50 mg, 0.13 mmol, 1 eq) and ethyl-4-bromobenzoate (42.2 μ L, 0.26 mmol, 2 eq) were put in a Schlenk tube and evacuated. Tris(dibenzylideneacetone)dipalladium(0) (118 μ L, 1.29 μ mol, 0.01 eq) and BINAP (2.4 mg, 3.9 μ mol, 0.03 eq) were put together in 1.3 mL of toluene and stirred for 20 minutes. Then the solvent were put together with the solid components and the base sodium *tert* butylate (31.1 mg, 0.32 mmol, 2.6 eq) was added. The reaction was stirred for 16 hours and conversion was proven via TLC in EA/MeOH (3:1). Ether was added and the precipitate was filtered and dried. Yield: 45 mg (51%).



$^1\text{H-NMR}$ (δ , 20°C, CDCl_3 , 300.36 MHz): 8.50 (s, 4H), 7.72 (s, 4H), 7.22 (s, 4H), 4.50 (q, 4H), 3.60-3.50 (m, 2H), 2.00 (dd, 2H), 1.95 (d, 2H), 1.45 (s, 6H), 1.20 (s, 12H), 1.10 (s, 12H), 0.81 (dd, 5H)

***N*¹,*N*⁴-bis(2,2,6,6-tetramethylpiperidin-4-yl)-*N*¹,*N*⁴-bis(4-((trimethylsilyl)ethynyl)phenyl)-benzene-1,4-diamine**

*N*¹,*N*⁴-bis(2,2,6,6-tetramethylpiperidin-4-yl)benzene-1,4-diamine (0.2 g, 0.52 mmol, 1 eq) and (4-bromophenylethynyl)-trimethylsilane (0.33 g, 1.3 mmol, 2.5 eq) were put together with sodium *tert*-butylate (0.17 g, 1.78 mmol, 3.4 eq). Palladium(II)acetate (conc. 10 mg/mL, 162 μ L, 0.01 eq) and tri-*tert*-butylphosphine (32 mg, 0.03 eq) were stirred in another Schlenk tube in dry and degassed toluene. The solvents were added to the solid components and stirred at 100°C over night. The reaction progress was monitored via TLC in EA/MeOH (3:1, 1%TEA). After full conversion for the work up 15 mL H_2O dest and 25 mL dichloromethane were added for quenching. The reaction was extracted with dichloromethane and the organic phase was dried over Na_2SO_4 , filtered and the solvent was removed. For further purification a column chromatography was performed in DCM/ H_2O /TEA 25:1:0.5. Yield: 0.25 g (69%)

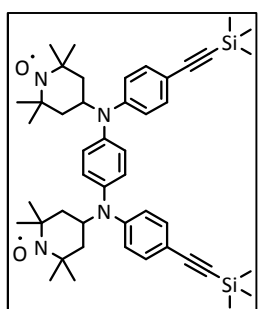


$^1\text{H-NMR}$ (δ , 20°C , CDCl_3 , 300.36 MHz): 7.2-7.52 (m, 12H), 3.00-3.10 (q, 2H), 1.70 (bs, 2H, NH), 1.60 (s, 24H), 1.30-1.45 (m, 8H), 0.25 (s, 18H)

TOF MS EI: calculated: 730.4826 detected: 730.4855

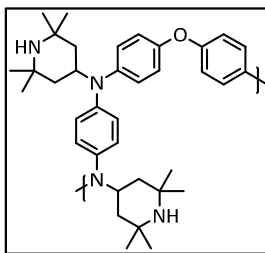
Oxidation of N^1,N^4 -bis(2,2,6,6-tetramethylpiperidin-4-yl)- N^1,N^4 -bis(4-((trimethylsilyl)ethynyl)-phenyl)-benzene-1,4-diamine

N^1,N^4 -bis(2,2,6,6-tetramethylpiperidin-4-yl)- N^1,N^4 -bis(4-((trimethylsilyl)ethynyl)-phenyl)-benzene-1,4-diamine (50 mg, 0.07 mmol, 1 eq) was dissolved in THF abs. and *m*CPBA (35 mg, 0.2 mmol, 3 eq) was added. After two hours of stirring the reaction was diluted with dichloromethane and extracted with NaHCO_3 . The organic phase was dried, filtered and the solvent was removed under reduced pressure. Yield: crude 60 mg (114%). The mass measurements showed that there is mono and di-oxidized product in the reaction which we were not able to separate from each other. No NMR possible due to the TEMPO radicals.



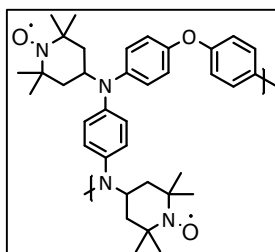
N^1 -methyl- N^1,N^4 -bis(2,2,6,6-tetramethylpiperidin-4-yl)- N^4 -(4-(*p*-tolylloxy)-phenyl)-benzene-1,4-diamine

Diacetoxypalladium (0.87 mg, 3.9 μmol , 0.01 eq) and tri-*tert*-butylphosphine (11.6 μL , 0.01 mmol, 0.03 eq) was stirred till the solution was clear in 1 mL of dry and degassed toluene. After that subsequently N,N -bis(2,2,6,6-tetramethylpiperidin-4-yl)benzene-1,4-diamine (150 mg, 0.39 mmol, 1 eq), 4,4'-oxybis(bromobenzene) (127 mg, 0.39 mmol, 1 eq) and sodium *tert* butylate (112 mg, 1.2 mmol, 3 eq) were added and stirred over night at 90°C . The mixture was extracted with dichloromethane and distilled water and NaHCO_3 . The organic phase was dried, filtered and the solvent was removed. No real polymer could be detected only oligomers. Yield: 204 mg (73%)



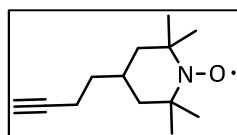
Oxidation of *N*¹-methyl-*N*¹,*N*⁴-bis(2,2,6,6-tetramethylpiperidin-4-yl)-*N*⁴-(4-(*p*-tolylloxy)-phenyl)-benzene-1,4-diamine

*N*¹-methyl-*N*¹,*N*⁴-bis(2,2,6,6-tetramethylpiperidin-4-yl)-*N*⁴-(4-(*p*-tolylloxy)-phenyl)-benzene-1,4-diamine (100 mg, 0.18 mmol, 1 eq) was dissolved in THF abs. and *m*CPBA (106 mg, 0.62 mmol, 3.4 eq) was added. It was stirred for five hours till the polymer precipitates and then it was diluted with dichloromethane and extracted with NaHCO₃. The organic phase was dried, filtered and the solvent was removed. Yield: 73 mg (69%). No NMR possible due to TEMPO radicals



4-(But-3-yn-1-yl)-2,2,6,6-tetramethylpiperidin-1-oxyl

4-Hydroxy-TEMPO (246 mg, 1.4 mmol, 1 eq), 3-bromoprop-1-yne (199 μ L, 1.8 mmol, 1.3 eq) and sodium hydride (71 mg, 1.8 mmol, 1.3 eq) were put together in 110 μ L of dry DMF. It was stirred for one hour and then the reaction was monitored via TLC in CH/Ea (5:1). For purification it was extracted with ethyl acetate and distilled H₂O. The organic phase was dried, filtered and the solvent was removed under reduced pressure. For further purification a column chromatography with CH/Ea (5:1) was performed. Yield: 179 μ L (60%)

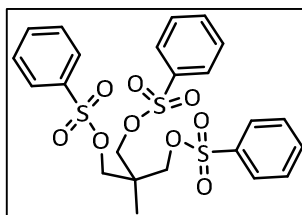


TOF MS EI: calculated: 208.1727 detected: 208.1730

2-Methyl-2-(((phenylsulfonyl)oxy)methyl)propane-1,3-diyl dibenzenesulfonate

In a flask with septum trishydroxymethylethane (2.44 g, 20.3 mmol, 1 eq) was dissolved in a mixture of dichloromethane and pyridine (20 mL each). The mixture was cooled with an ice bath and through the septum benzenesulfonylchloride (7.8 mL, 60.9 mmol, 3 eq) was added slowly. It was stirred over night without cooling and on the

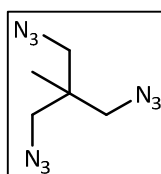
next day the reaction was precipitated in a mixture of 2M HCl and methanol. The white precipitate was filtered washed with methanol and re-crystallized in hot isopropyl alcohol. Yield: 8.83 g (80%)



$^1\text{H-NMR}$ (δ , 20°C, CDCl_3 , 300.36 MHz): 7.7 (m, 6H), 7.5 (t, 3H), 7.4 (t, 6H), 3.6 (s, 6H), 0.75 (s; 3.05 H)

1,3-Diazido-2-(azidomethyl)-2-methylpropane

2-Methyl-2-(((phenylsulfonyl)oxy)methyl)propane-1,3-diyl dibenzenesulfonate (4 g, 7.44 mmol, 1 eq) was dissolved in DMSO and sodium azide (1.44 g, 22.2 mmol, 3 eq) was added. The reaction was heated for five hours under reflux and then poured into 100 mL of distilled water. It was extracted with diethylether and the organic phase was dried, filtered and the solvent was removed under reduced pressure. The crude product was used for further LAH reduction. The LAH reduction did not give the desired product. Due to a time problem no further approaches were performed but due to literatures this reaction step should work out under standard LAH reaction conditions as described earlier in this work. From this reaction no NMR characterization was done due to the explosive nature of azides it was not possible to dry the product good enough to get a NMR result.



Appendix

Abbreviations

BAC-M = 2,6-bis(4-azidobenzylidene)-4-methylcyclohexanone

BINAP = (2,2'-bis(diphenylphosphino)-1,1'-binaphthyl)

CCD camera = charge-coupled device camera

CP = cyclopentadiene

CuAAC = Cu-catalyzed [3+2] alkyne-azide cycloaddition

CV = cyclovoltammogram

DCM = dichloromethane

DMAP = 4-dimethylaminopyridine

DTM-cell = differential turbidity measurement cell

DPPF = 1,1'-bis(diphenylphosphino)ferrocene

EA = Ethylacetate

ene = carbon-carbon double bond

ESR/EPR = electron spin resonance/ electron paramagnetic resonance

GC-MS = Gas chromatography–mass spectrometry

GM = Göppert Mayer

GPC = gel permeation chromatography

ΔG = Gibbs energy or free enthalpy

HOMO = highest occupied molecular orbital

ISC = inter system crossing

ITO = indium tin oxide

LAH = lithium-aluminum hydrate

LCST = lower critical solution temperature

LIB = lithium ion battery

LSM = laser scanning microscopy

LUMO = lowest unoccupied molecular orbital

Maldi-TOF = matrix assisted laser desorption ionization/ time of flight

M_n = number average molecular weight

MPA = multi photon absorption

Naph = naphthalene

NMR = nuclear magnetic resonance

OLED = organic light emitting diode

OPA = one photon absorption

ORB = organic radical battery

PAA = poly acrylic acid

PDI = poly dispersity index or perylene-3,4,9,10-tetracarboxdiimide

PEG = poly ethylene glycol

PEO = poly ethylene oxide

PPO = poly phenylene oxide

PTCDA = perylene-3,4,9,10-tetracarboxylic acid dianhydride

ROMP = ring opening metathesis polymerization

RT = room temperature

SOMO = single occupied molecular orbital

TCP = tetrachloroperylene

TPA = two photon absorption /triphenylamine

TLC = thin layer chromatography

TMPD = *N,N,N',N'*-tetramethyl-*p*-phenylenediamine

UCST = upper critical solution temperature

List of Figures

Figure 1: Set-up of a differential turbidity cell	11
Figure 2: Schematic ROMP	11
Figure 3: The ROMP mechanism at the example of a norbornene	12
Figure 4: ROMP catalyst M31 and monomers	14
Figure 5: Linear polymerization rate in the CH ₂ Cl ₂ /MeOH solvent	15
Figure 6: ¹ H-NMR of poly2-300	16
Figure 7: Lower critical solution temperatures at different pH-values with different polymer architectures	17
Figure 8: NMR of the aza norbornene product without further purification. Nearly no side products are visible	21
Figure 9: Starting materials for perylene syntheses	31
Figure 10: Effects of imide and bay substituents ⁷²	34
Figure 11: Three-dimensional structure of PDI with no substituents attached at the bay region (planar) on the left and three-dimensional structure with four substituents attached at the bay region	36
Figure 12: PET sensor concept with molecular orbital scheme ⁸⁷	38
Figure 13: UV-Vis spectrum of tetrachloroperylene	41
Figure 14: UV-Vis spectrum of the substituted bay area derivative. Replacement of the chlorine atoms led to a strong bathochromic shift.	44
Figure 15: NMR spectrum of the M3 copolymer in D ₂ O	48
Figure 16: NMR spectrum of the M3 copolymer in CDCl ₃ , with the perylene peaks	48
Figure 17: UV-Vis spectrum of TCP, 5, 3 (in chloroform c= ca. 10 ⁻⁵ M) and poly-1 (with fluorescence spectroscopy; c=0.2 mg mL ⁻¹ , inset)	49
Figure 18: Sigmoidal curve and PET measurements at different pH-values for the polymer blend	50
Figure 19: Sigmoidal curve and PET measurements at different pH-values for a random copolymer	51
Figure 20: Sigmoidal curve and PET measurements at different pH-values for a block copolymers	51
Figure 21: Fluorescence intensity as a function of pH (normalized, c(polymer)= 0.5 mg mL ⁻¹) ¹⁰⁰	52
Figure 22: Fluorescence intensity of poly-8 as a function of ascorbic acid concentration (inset: linear range, c(polymer)=0.5 mg mL ⁻¹) ¹⁰⁰	53
Figure 23: LCST effect in perylene PET probes at different pH-values	54
Figure 24: Jablonski diagram	61
Figure 25: Energy diagram for the essential states in centrosymmetric chromophores.	62
Figure 26: Two concepts for the design of TPA molecules according to Marder et al. ¹³⁴	63
Figure 27: Application of the TPA cross-section for the excitation wavelength for some chromophores, indicating the structure and measurement conditions	64
Figure 28: Spectra of the two functionalized perylenes for click-reactions ¹³²	69
Figure 29: ¹ H-NMR of the mono-substituted BAC-M ¹³²	72
Figure 30: ¹ H-NMR of the di-substituted BAC-M	72
Figure 31: FT-IR spectra of the two functionalized BAC-M perylene derivatives ¹³²	73
Figure 32: UV-Vis spectra of the BAC-M, perylene-alkyne and the mono- and di-functionalized derivatives ¹³²	74
Figure 33: Fluorescence spectra of the perylene and the dansyl derivatives ¹³²	74
Figure 34: Sample processing and grafting procedure ¹⁶⁰	75
Figure 35: Grafting experiment with the dansylic dye (left) and the BAC-M (right)	76
Figure 36: (a) UV-Vis absorption spectra of the BAC-M. (b) Results of the Z-scan characterization of BAC-M solution. Red solid line is the fit curve assuming the 3PA process and blue solid line is the fit curve assuming 2PA	77

Figure 37: Z-scans for the mono-substituted perylene BAC-M. The pulse energy was determined for the sample and then Z-scans for KG98 were performed with different pulse energies (left picture)	78
Figure 38: Schematic picture of the TPA experimental setup ¹³²	81
Figure 39: Schematic of the OA Z-scan setup. ¹⁸¹	83
Figure 40: Modular design of an OLED and Sony's world's first 16.7 million color flexible OLED	89
Figure 41: Different colors in maybe oxidized triphenylamine	92
Figure 42: ¹ H NMR of TPA in CDCl ₃ and complex product mixture after oxidation and chromatographic purification	93
Figure 43: Scheme of the energy levels of the cation vs. the neutral form; DFT theory and TPA molecule	94
Figure 44: TPA ⁺ + O ₂ reaction product – DFT calculations B3LYP/TZVP level. Structure of the expected products	95
Figure 45: Spin distribution of TPA derivatives	96
Figure 46: Stable radical molecules: 2,6-di-tert-butylphenoxide, TEMPO, galvinoxyl, triphenylamine-derivative	97
Figure 47: A lithium-ion battery based on a radical polymer cathode ¹⁹⁷	99
Figure 48: Electron hopping process in an ORB. ²⁰²	100
Figure 49: Ragone plot comparison between capacitors, radical batteries and Li-ion batteries	100
Figure 50: ORB materials in comparison with LIBs	102
Figure 51: Example of p-type radical polymers and their theoretical capacities	102
Figure 52: Schematic setup of an ORB half cell made in a Swagelok-half cell	103
Figure 53: Example of electron hopping. The R-groups have different redox potentials. During charging, the charge is stored by oxidizing groups at the cathode and reducing groups at the anode. The output voltage of the battery corresponds to the gap between the redox potentials. The curves connecting the R groups are polymer chains, which give flexibility. Many R groups are attached to the polymer chain, so electrons can hop between neighboring R groups to produce the output current. ²⁰⁹	103
Figure 54: Ultrathin ORB prototype developed by NEC ²¹¹	104
Figure 55: Schematic setup of the screen printing process for electrode fabrication	104
Figure 56: The oxidation process of Wurster's blue with the derived color states	105
Figure 57: CV of tetraphenyl- <i>p</i> -phenylenediamine in solution (working and counter electrode Pt, reference-electrode Ag/AgNO ₃ , with 0.1M tetrabutylammoniumperchlorate, 1 mM in chloroform)	106
Figure 58: Cyclic voltammogram of the model compound in solution	107
Figure 59: Overview of possible structures for organic radical batteries	108
Figure 60: TEMPO-derived derivatives (theoretical capacities?)	108
Figure 61: TEMPO-Wurster blue combination derivatives	109
Figure 62: Wurster blue derived derivatives	109
Figure 63: Principle of the Buchwald-Hartwig reaction	110
Figure 64: Catalytic cycles for monodentate (left) and bidentate ligands (right)	111
Figure 65: Variable conditions and components for the Buchwald-Hartwig reaction	113
Figure 66: Structure of the bidentate BINAP ligand	114
Figure 67: Reaction scheme for the preparation of the Guey-Sheng Polymer, a number of improvements over the original have been incorporated	118
Figure 68: CV in solution, substituted polyaramid dissolved in DMF and spin-coated on ITO, Counter and working electrode: Pt; reference-electrode: Ag/AgNO ₃ ; 0.1 M TBAP; acetonitrile, scan rate: 50 mV/s	120
Figure 69: Constant current cyclization from 1C to 100C and back	121
Figure 70: Charge/discharge capacity and efficiency	121
Figure 71: CV in halfcell after rate testing, proof decomposition at 2.75 Volt	122
	156

Figure 72: UV-Vis spectra of the norbornene monomer in the blue and the yellow state	124
Figure 73: IR spectra before and after exposure to light	125
Figure 74: NMR of the unstable norbornene-monomer (paramagnetic)	126
Figure 75: MALDI-TOF of the monomer before and after 50 blue/yellow cycles	127
Figure 76: CV in solution of the norbornene-monomer in acetonitrile, counter and working electrode: Pt; reference-electrode: Ag/AgNO ₃ ; 0.1 M TBAP, scan rate: 50 mV/s	127
Figure 77: CV in solution of the norbornene-polymer in acetonitrile, counter and working electrode: Pt; reference-electrode: Ag/AgNO ₃ ; 0.1 M TBAP, scan rate: 50 mV/s	128
Figure 78: CV in solution of the norbornene-TEMPO copolymer in chloroform, counter and working electrode: Pt; reference-electrode: Ag/AgNO ₃ ; 0.1 M TBAP, scan rate: 50 mV/s	129
Figure 79: CV in half-cell, 10% active material, 10%PVdF, 10%Super P, scan rate 10 mV/s	129
Figure 80: CV in half cell with spincoated active material, scan-rate 0.1mV/s	130
Figure 81: Three possible Norbornene-Wurster blue compositions	130
Figure 82: The Zeeman effect	133
Figure 83: ESR-spectra of the monomer and the polymer	134
Figure 84: Magnetic susceptibility measurements for the TEMPO-modified norbornene monomer and polymer and the correspondent values for the Curie constant and spin density	135

List of Schemes

Scheme 1: Scheme of the mannose-monomer preparation	18
Scheme 2: <i>O</i> -Glycosylation with different leaving groups and activators	19
Scheme 3: Aza norbornene building and subsequent Amadori-rearrangement	20
Scheme 4: Reaction scheme of the original aza norbornene reaction with the improved reaction conditions	20
Scheme 5: Different approach to the third monomer based on a carbohydrate structure with a more stable amide bond and the involvement of the Amadori rearrangement	23
Scheme 6: Possible reactions of perylene-3,4,9,10-tetracarboxylic acid dianhydride (PTCDA) ⁵⁶	33
Scheme 7: Overview of symmetrically and asymmetrically <i>N</i> -substituted perylene bisimides (PBIs) classified according to the nature of respective substituents	33
Scheme 8: Synthesis of water-soluble perylene diimides bearing polar substituents in the bay region ⁷³	35
Scheme 9: Cyclohexyl as solubilizing group	35
Scheme 10: Syntheses of asymmetric perylenes	37
Scheme 11: "Bad" synthetic route to asymmetric perylene derivatives, time consuming, bad yields	41
Scheme 12: "Good" synthetic route to asymmetric perylene derivatives, not time consuming but bad yield	42
Scheme 13: Best synthetic route to asymmetric perylene derivatives with good yields and easy purification	42
Scheme 14: Synthetic route to bay-position substituted perylenes (special case for <i>n</i> -butylamine)	44
Scheme 15: Synthesis of the perylene-based monomer M3.	45
Scheme 16: Synthesis of the different polymer architectures	45
Scheme 17: Thiol-ene reaction either with a free radical or the catalyzed thiol-Michael addition, which both lead to the same endproduct ¹³⁹	65
Scheme 18: Mechanism of the radical thiol-ene coupling at the above picture and of the thiol-Michael addition ¹⁴¹	66
Scheme 19: Products of thermal and catalyzed 1,3-cycloaddition	67
Scheme 20: Early proposed mechanism for the CuAAC ¹³²	67
Scheme 21: Photolysis of aryl azide followed by insertion of the PEG sample ¹⁵⁶	76
Scheme 22: Over all reaction scheme from TPA to TPB	91
Scheme 23: Oxidation of (4,4',4''-trimethyl)-triphenylamine ¹⁹¹	91
Scheme 24: Scheme of oxidized TPA with different reaction conditions	93
Scheme 25: Resonance structures of a nitroxide	98
Scheme 26: Redox couples of the nitroxide radical. ¹⁹⁷	98
Scheme 27: Reaction scheme for Buchwald Hartwig ligand	112
Scheme 28: Buchwald Hartwig reaction with possible reaction conditions for these substrates	113
Scheme 29: Principle of the reductive amination	115
Scheme 30: Reaction pathway of a desired product	115
Scheme 31: Reductive amination with pic-BH ₃ to the desired aryl-compound	117
Scheme 32: One synthesis path to the norbornene-monomer 1	123
Scheme 33: Synthesis of norbornene-monomer 2	131
Scheme 34: Synthesis of norbornene-monomer 3	131

List of Tables

Table 1: Solvents, M_n and PDI for the hydrochloride of monomer 2	15
Table 2: Polymer characterization of different random copolymers	17
Table 3: GPC Data	47
Table 4: pka app and PET efficiency	49
Table 5: LCST temperatures at different pH-values	53
Table 6: Different types of click reactions	64
Table 7: Different reaction conditions for test-reaction of BAC-M with 5-hexyn-1-ol	71
Table 8: DFT calculations with experimental comparison	94
Table 9: Ionization potentials, HOMO-LUMO levels and reorganization energies in tri substituted TPAs	95
Table 10: Reaction conditions for the reductive amination	115